TU Delft
Delft University of Technology

WL | Delft Hydraulics

HydroQual
(New York)

On the consolidation and erosion of cohesive sediments

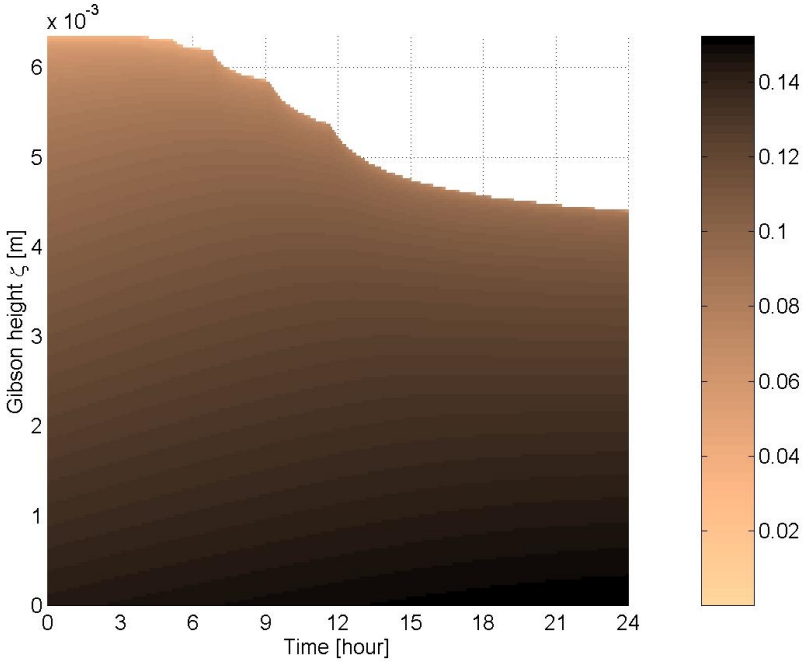

11 July, 2002

M.Sc. thesis of G.J. de Boer

Delft University of Technology
Civil Engineering and Geosciences
Division of Hydraulic and Geotechnical engineering
Section of Fluid Mechanics

On the consolidation and erosion of cohesive sediments

Supervisors:

Prof.dr.ir. F.B.J. Barends
Prof.dr.ir. J.A. Battjes
Dr. J.D. Pietrzak
Ir. L.Postma
Dr.ir. J.C. Winterwerp

11 July, 2002

M.Sc. thesis of G.J. de Boer

Delft University of Technology
Civil Engineering and Geosciences
Division of Hydraulic and Geotechnical engineering
Section of Fluid Mechanics

water, when you don't trouble it, becomes clear
- Tibetan proverb

Prologue

Water is the vital element of nature. But when water is too abundant, too scarce or too contaminated, life itself can be at stake. This thesis deals with the third aspect, that of contamination. When mankind does not live in harmony with the surrounding water, it can become a threat not only to nature, but also to mankind. At school we all learned that the ancient empire of Mesopotamia fell because poor irrigation made the land brackish. Nowadays mankind is still capable of disrupting the very ecosystems he lives in, and at a faster pace. The water quality in the *Aral Lake* for instance has plummeted to a life-threatening level in the short period of the existence of the USSR. For decades poisonous insecticides washed away from the cotton plantations in central Asia and ended up in the bed of this lake. Presently the lake is drying up and the bed sediments, with their adhered contaminants, can blow away freely with the wind. Consequently many children are born there nowadays with deformed limbs. Apparently mankind only learns from the past, that mankind does not learn from the past.

Although, fortunately, the need to deal with this planet's (water) assets in a sustainable way has been recognised by many nowadays, the ever-growing population, the lack of natural (water) resources and the social inequality make these kinds of problems very hard to tackle. Solutions to these problems will always be a mix of social, economical, ecological and technical measures[1]. The construction of an integral water management solution, comprising all these fields of expertise, can be compared with the building of a Roman arc bridge: every single stone has to be present to make the bridge complete. With one single stone missing the arc will not stand. A recognisable piece of this bridge is called the key-stone. Here the analogy of arc bridge building with the construction of integral solutions should end: no field of water quality management should be considered more important than another. But currently some aspects of integral water management do need more attention than they get. "Heavy metals and synthetic organics are also a growing problem, deserving far more attention than they've received. However, insufficient research has been done on them.."[2]. I hope my thesis fills in another tiny spot in this field.

In my thesis I constructed a new resuspension model for cohesive sediments and I also integrated it into the modelling environment of Delft3D-WAQ. Apart from the recognised need for greater understanding of the fundamental behaviour of heavy metals, I believe modelling will play a more dominant role in water management in the future than many suspect. Despite growing environmental awareness and sustainable development, mankind will continues to exploit nature. Among others, the ever-increasing population and the steady depletion of natural resources account for this. Accordingly the way in which we (will) exploit the earth will tend to the natural limits of this system. And once we are on the fringe of the natural limits, some mindless actions may lead to instability of it. If we want to prevent such events, we shall have to increase our awareness and knowledge of the natural system. Monitoring and simulating are indispensable tools for increasing our understanding. Even if the model simulations cannot be used to give predictions, due to the vast uncertainties in all the parameters, they can still be used to get a feeling for the system. This insight was one of my motives in dedicating myself to writing this thesis, apart from my liking for physical, mathematical and computational modelling off course.

[1] E.g. McCully, Patrick. *Silenced rivers : the ecology and politics of large dams*. Londen, Zed, 2001.

[2] Gleich, P.H., A. Singh and H. Shi 2001. *Emerging threats to the world's freshwater resources.* A report of the Pacific Institute in development, environment and security, Oakland, California.

Abstract

A new one dimensional vertical water bed model suitable for (long-term) water quality modelling in the Delft3D-WAQ software package is developed and tested. This model consists of a consolidation module and an erosion module (figure I). A new erosion formulation is proposed, allowing only erosion when the actual bed shear stress exceeds the actual yield strength. The bed shear stress is considered a stochastic variable with a Rayleigh distribution and the actual yield strength is related to the density and the cohesion as proposed by Merckelbach [2000]. The vertical distribution of the density can be computed by the consolidation module, which consists of a new, fast parameterisation of the finite strain consolidation equation of Gibson [1967] with the constitutive relations of Merckelbach [2000]. For the swelling due to erosion, other constitutive relations are proposed. The consolidation module has successfully been validated on a consolidation experiment by Kuijper et al. [1990]. A new method to determine a reproducible 'measure' of the physical consolidation parameters has been proposed. The total water bed model has successfully been validated on erosion experiments in a rotating annular flume by Kuijper et al. [1990]. We can conclude that the combination of a parameterised consolidation module and the new erosion formulation is very promising. Physical and numerical complications of the model are also discussed.

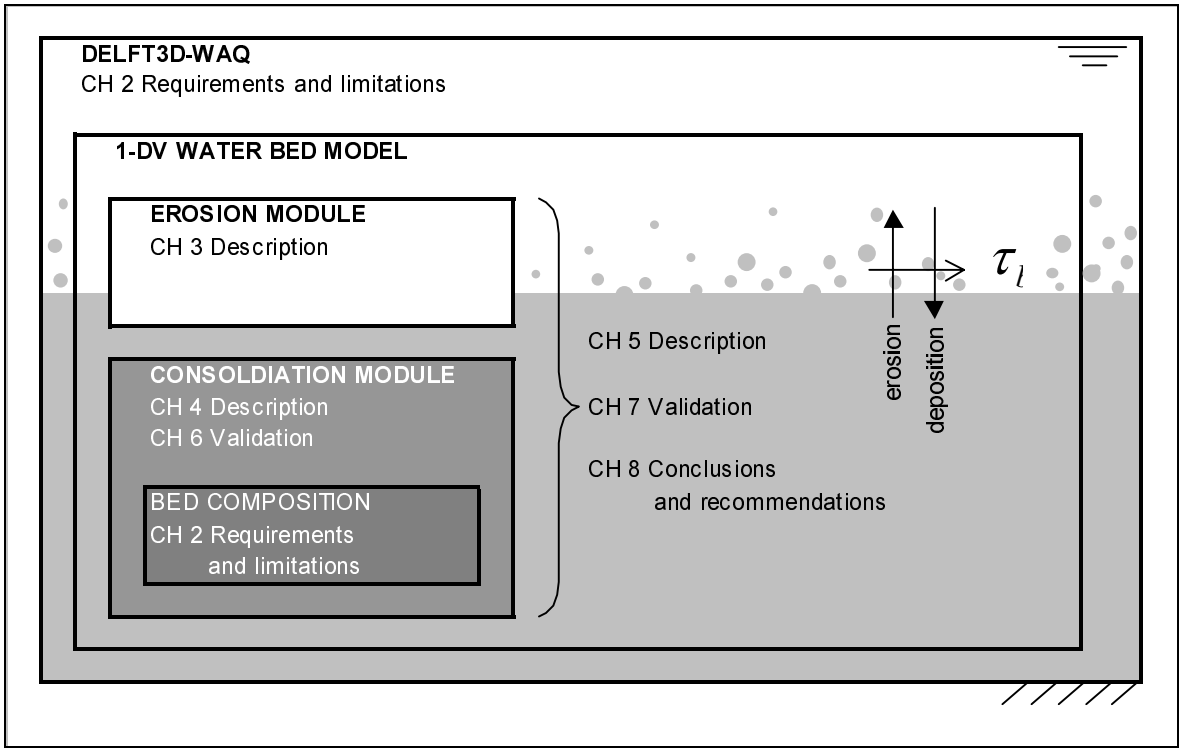

Figure I: Set-up of the study (report)

Summary

In water quality modelling, erosion and deposition of cohesive sediments are processes of paramount importance: (i) cohesive sediments control the light permissivity and (ii) they are the major carriers for heavy metals. The concentration of cohesive sediments in the water is to a large extent controlled by erosion and deposition behaviour. For instance, the opening of the Haringvliet Sluices in the Netherlands, which is currently considered, may lead to resuspension of severely polluted cohesive sediments deposited in the sixties after the closure of the tidal basin. The currently most widely used erosion models are poorly based on physical principles and lack the ability to describe erosion of the consolidated sediment bed at increased shear stresses e.g. during a storm. More advanced models exist, but these are too slow for long term water quality modelling. There is a need for a new modelling approach that is both fast and accurate.

The aim of this study is to develop and test a new one dimensional (1-DV)water bed model suitable for long term water quality modelling. This model is suitable for long-term water quality modelling. The model consists of (a) a new erosion formulation and (b) a new fast consolidation model. In order to use the new model for water quality modelling, it is implemented in the Delft3D-WAQ modelling software. Besides the new 1-DV water bed, the existing water bed model ECOM-SED of HydroQual is tested in this thesis.

The new water bed model will only deal with erosion of cohesive beds: the clay fraction is at least 10 % and is much larger than the sand fraction. The 1-DV water bed takes only into account surface erosion: entrainment of high concentrated mud suspensions (>100 mg/l) and mass erosion due to very high bed shear stresses will not be dealt with. Biological activity will not be taken into account.

A new erosion formulation is proposed that regards the bed shear stress as a stochastic variable and allows erosion only when the actual bed shear stress exceeds the actual yield strength at the interface. Merckelbach [2000] gives a formulation that relates the actual yield strength to the density and the cohesion. For the time and depth dependent cohesion no model is available, for the consolidation there is.

The vertical distribution of the density can be computed fast by the new consolidation module. This module is based on the finite strain consolidation equation of Gibson [1967]. This differential equation can describe the density, the effective stress and the permeability as a function of time and depth. To prevent moving boundary conditions, material coordinates are used. In order to solve this non-linear differential equation, constitutive relations relating the effective stress, the density and the permeability have to be substituted. In the virgin loading regime, the fractal relations of Merckelbach [2000] are be used. When erosion occurs however, the consolidated material experiences a stress relief and the bed swells. A separate constitutive relation is necessary for this reloading regime. A few simple relations for this regime are given based on literature.

The Gibson equation has been solved with a new, fast parameterisation, consisting of a Fourier series. It contains only the constitutive relations for virgin loading. The parameterisation does not take into account the non-linear advection terms of the differential equation, which are of the same order as the other terms. The effects of large strains are still present in the parameterisation, because the parameterisation is written in terms of the material coordinates. This model has been compared with numerical results for the case of consolidation experiment in a settling column. The parameterisation gives good results, but near the interface it underestimates the densities.

The parameterised consolidation model has successfully been validated on consolidation experiments performed in a settling column by Kuijper et al. [1990]. The three consolidation parameters can be obtained from the measurements by a method given by Merckelbach [2000]. An improved method is proposed, giving an objective, reproducible and physically based range of values of the consolidation parameters. With this whole range of combinations reasonable results of the density profiles and the lowering of the interface can be obtained. Accordingly, it is not possible to determine the value of a parameter. It is clear

though that the consolidation parameters should always be addressed as a set, not as individual values. To determine if a set can give good results, the settling column should be simulated with the parameterisation that gives results that are just as good as a numerical model. A sensitivity analysis has been performed on the consolidation model. The model is very sensitive to the fractal dimension. The parameterisation is less sensitive to the other empirical parameters.

The 1-DV water bed model has been implemented in Delft3D-WAQ. The 1DV-waterbed model consists of two modules with different time scales: an erosion module with the same time scale as Delft3D-WAQ, and a consolidation module with a larger time scale. The consolidation time step should be chosen as large as possible, because this module requires most of the computation time. A set-up of the 1-DV water bed model is proposed allowing the two modules to have different time steps. A temporary sediment cache is needed for this configuration, accounting for the erosion and deposition until the consolidation module is activated. The progression of the erosion is calculated by iteration at time steps of a few seconds. An exact but difficult method is also mentioned, but not implemented in the 1-DV water bed model yet.

The profiles of the bed properties as calculated by the consolidation, have to be sampled to store them in the computer. A few methods are treated. A sigma coordinate system is chosen, with a constant number of sampling points is in time. Every time material is removed by erosion or added by deposition, the bed profiles have to be redistributed, thereby interpolating the profiles linearly. This leads to small errors if the resolution is too low. The consolidation time step poses restrictions on the required number of Fourier components in the consolidation parameterisation. A conservative rule of thumb has been derived by examining a profile with steep density gradients.

The new 1-DV water bed model has been validated on short term erosion experiments performed in a rotating annular flume by Kuijper et al. [1990]. These erosion experiments have been performed on the same beds that were measured in the consolidation experiments used to validate the parameterisation. In the rotating annular flume two experiments have been performed: one after one day of consolidation and one after seven days of consolidation. The 1-DV water bed model can simulate the results from the annular flume experiment well: (i) the simulations show the same characteristic exponential decay evolution of the eroded material height, (ii) the model can be calibrated good in a qualitative sense and (iii) the decrease in the erodibility between one and seven days of consolidation can be simulated with the consolidation as the only strengthening process. No time dependent function for the cohesion is necessary. In the erosion models used currently, a time history of the bed sediment has to be ‘remembered’ to determine the erodibility. In the 1-DV water bed model the history is stored in the shape of the density profile which is calculated by the consolidation module. We can conclude that the combination of the parameterised consolidation module and the erosion module in the 1-DV water bed is promising. The model does also have some minor complications however, which can be divided in physical problems and numerical problems. A few solutions are proposed for the numerical problems.

The 1-DV water bed model needs eight physical input parameters. The three consolidation parameters can be determined from standard consolidation experiments in a settling column. The other five physical parameters have to be determined by means of numerical experiments (trial and error). No standardised laboratory tests are yet available. These five parameters govern swelling, cohesion, geotechnical coefficients, erosion rate, and the scale of the probability distribution of the bed shear stress. The model results are sensitive to four of these parameters. Accordingly more research is needed on these parameters. This makes the 1-DV water bed not yet fully applicable for engineering purposes.

The 1-DV water bed model has not yet been applied to long term water quality problems for which it is designed. A recommendation is to compare long term runs to field data and to results from old layer models.

In the short term validation simulations of the 1-DV water bed model, the erosion is governed by the tail of the Rayleigh probability distribution of the actual local bed shear stress. Accordingly the stochastic nature of bed shear stress governs erosion. These findings corroborate earlier findings mentioning that turbulent bursts govern the erosion.

Table of contents

1 Introduction

In water quality modelling, erosion and deposition of cohesive sediments are processes of paramount importance. The concentration of cohesive sediments in the water column has a very decisive influence on features that can directly be regarded as a measure for the water quality. The first important parameter is the light permissivity. An increased turbidity leads to a reduced biological activity, which in turn affects the nutrient-chain. Second, cohesive sediments are the major carriers for heavy metals [Mehta, 1989]. The electromagnetic nature of the sediments leads to a high adhesion of heavy metals to the clay particles or flocs. Thus the spreading of suspended cohesive sediments controls the dispersion of heavy metals.

The concentration of cohesive sediments, however, is not only controlled by erosion and deposition behaviour. Far from riverine sources and sinks of material, and in the absence of significant biological production, erosion is the major source for suspended particles in the water column [Sanford et al., 2001].

Erosion of cohesive sediments is one of the most studied aspects of fine sediment transport. Experiments include laboratory (flume) tests, in situ (flume) experiments and field observations. This research started over 40 years ago, when Einstein jr. encouraged his pupils Krone and Partheniades to initiate the study of the behaviour of eroding mud. Krone`s deposition formula and Partheniades' erosion formula are still widely used nowadays. Since then, a large amount of (experimental) research in the field of cohesive sediments has been carried out, but no universal erosion formula is known yet. Therefore, erosion modelling has still a strong empirical tradition. Accordingly, the currently most widely used erosion/ resuspension models give the erosion rate as a function of the excess bed shear stress and up to 3 empirical material coefficients [Mehta, 1989]. In this approach the excess bed shear stress is defined as the current (and wave) induced bottom shear stress minus a critical shear stress below which no erosion occurs. The empirical coefficients are determined by fitting the models to short-term erosion experiments. These formulations however are poorly based on physical principles. The current erosion and deposition models for cohesive sediments do not always give an accurate description of the exchange of cohesive sediment between the water column and the bed. These formulations lack especially the ability to describe erosion of cohesive sediments at the consolidated bed at increased shear stresses e.g. during a storm.

When it is the intention either to model erosion and sedimentation patterns, or to integrate these patterns in order to model morphological changes on the long term, the current approaches are satisfactory. Erosion and deposition alternate and therefore peaks in sediment fluxes are smoothed out in time. The effect of severe conditions is averaged out. Van Ledden [2001] shows that simple models are able to predict the long-term evolution of the bathymetry of estuaries and tidal basins fairly well in a qualitative way.

There is concern however, whether the current approaches are adequate for water quality problems, where modelling the seasonal variations in sediment concentrations in the water is important. When it is the intention to model the water quality, peaks in sediment fluxes are very important. High resuspension fluxes during a few days result in a reduced light permissivity or the resuspension of heavy metals and can subsequently result in severe starvation of plants and animals. For instance, the opening of the Haringvliet Sluices in the Netherlands, which is currently considered, may lead to resuspension of severely polluted cohesive sediments deposited in the seventies after the closure of the tidal basin. For water quality issues episodic events are more important than for morphology. To predict the implications of episodic events sufficiently, the models should account for the sediment balance more realistically. The bed behaviour should not only depend on the bed shear stress, but also on the history of the sediment. Incorporating a true dynamic bed requires a strength formulation by modelling both the formation and the evolution of the sediment layers on/in the bed as a function of time and depth.

It is possible to include some history of the consolidated waterbed by modelling the empirical coefficients as a function of either depth [Sanford et al., 2001] or time [HydroQual, 2001]. These

formulations, with varying coefficients, are able to describe erosion experiments. However, it has yet to be proven that they are able to give a good description of the sediment exchange fluxes over long periods of time, including some severe bed shear stress events. Moreover, the values assigned to the parameters in each layer lack a physical basis. Thus there is a need for a new modelling approach.

The time dependent evolution of a cohesive bed can be described by the Gibson finite strain consolidation equation [Gibson, 1980]. This model gives a full description of the density, the permeability and the effective stress in a sediment bed as a function of both depth and time. This consolidation model requires material functions that interrelate the density, the permeability and the effective stress. For the application considered in this thesis, these material functions should particularly be valid in the fluffy sediment layers that are formed by deposition on the waterbed. Merkelbach [2000] has derived and successfully tested a set of material functions based on a fractal description of mud. With this knowledge, it should be possible, at least in theory, to give a (full) process based description of the sediment exchange processes. This description should then replace the current empirical erosion models.

Aim: The aim of this study is to develop and test a new one dimensional vertical water bed model (hereafter referred to as 1-DV water bed model) suitable for (long-term) water quality modelling. The 1-DV water bed model should be based on a strengthening module, that will consist of a parameterisation of the exact consolidation equation, and a new erosion module (figure 1.1). The time scales of these two modules are different and a good interaction between these modules has to be constructed. The 1-DV water bed model will be incorporated in the water quality part (WAQ) in the Delft3D software environment. Herein the model should be able to make accurate predictions within a reasonable calculation time. By incorporating the 1-DV water bed model into Delft3D-WAQ, cohesive sediment can immediately be dealt with in a three dimensional way.

Besides the 1-DV water bed model, the water bed model ECOMSED of HydroQual is also tested.

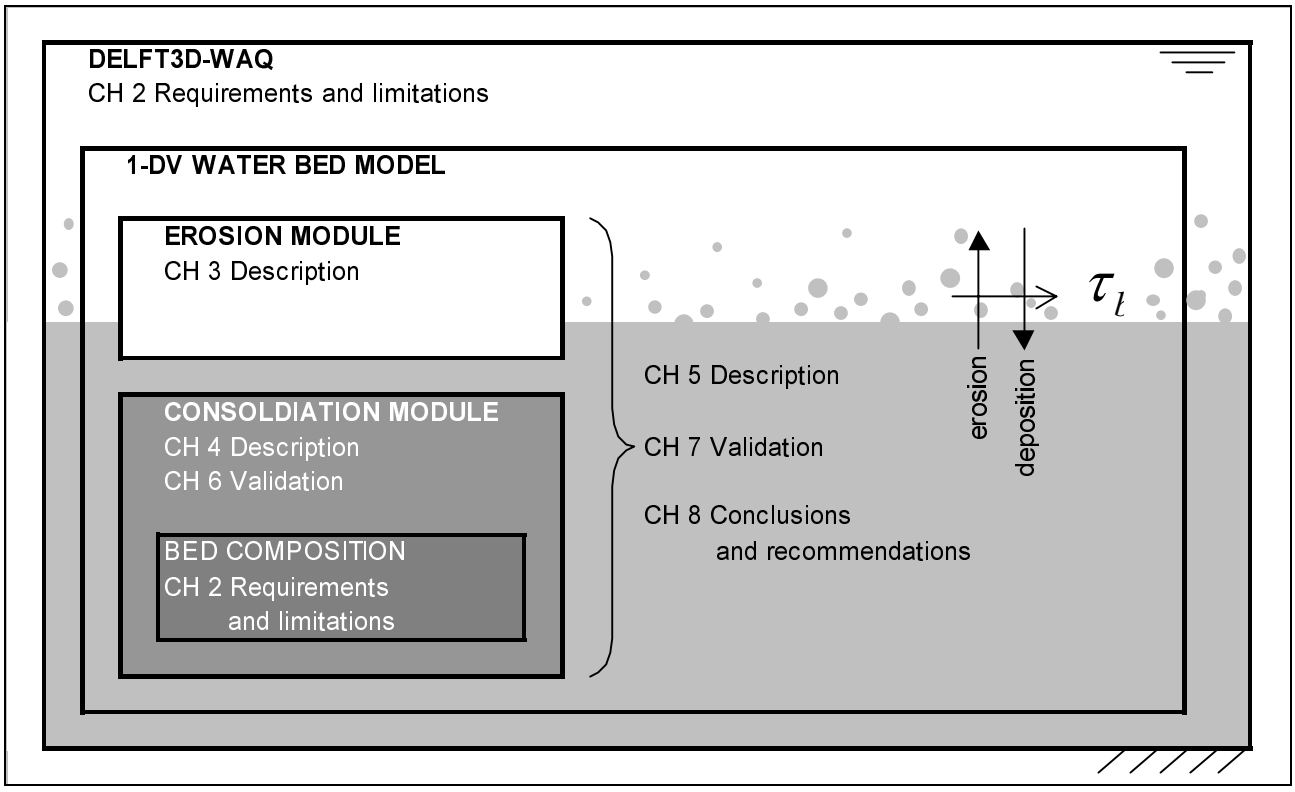

Figure 1.1. The 1-DV water bed model and its modules

Framework study: Alan Blumberg and Parmeshwar L. Shresta of Hydroqual in New York took the initiative for a joint study by HydroQual (New York) and WL | Delft Hydraulics to explore the most appropriate approach for a new cohesive sediment bed model, and if promising, to develop this new bed model. The water quality part WAQ of the Delft3D modelling environment (see chapter 2) of WL | Delft Hydraulics does not use a consolidation module at present. Simple empirical erosion formulations are used with a two-layer system allowing only small variation of the parameters in depth. At HydroQual, the computational modelling environment ECOM-SED is used. Currently a sediment module is implemented in this software package with a so-called bed armouring module (or consolidation module) with a time parameter that describes that the sediment becomes increasingly less erodable. Eventually the sediment forms part of the fully consolidated bed and is not erodable anymore under normal flow conditions.

This M.Sc. project is also a part of a larger WL | Delft Hydraulics project: SLIK. This WL project is called “development bed model” and is focussed on an improved understanding of the chemical, physical and biological processes in the waterbed. In the long run all these processes should be integrated in one bed model.

Set up of this report: Figure 1.2 shows a schematic representation of the set-up of this study. It also shows what information is gained from literature and what information is new. The requirements and the limitations of the model are treated in chapter 2. These requirements and limitations are due to the imbedding in Delft3D-WAQ and due to the bed composition. In chapter 3, a literature study is performed on erosion. Several existing models are described at increasing complexity. At the end of the chapter a new, appropriate formulation for the erosion formulation is derived. Chapter 4 deals with the Gibson finite strain consolidation equation, which describes the time and depth dependent behaviour of the effective stress, the permeability and the density in the mud bed. This non-linear differential equation can be solved using the constitutive relations of Merckelbach [2000], that relate the effective stress, the permeability and the density to each other. For the reloading regime other constitutive relations are necessary. A few simple constitutive relations for reloading will be given, based on similarity with results from literature. Next, a simple and fast parameterisation of this consolidation model is derived. This parameterisation is compared to numerical results for the case of a consolidation experiment in a settling column. Chapter 5 elaborates on the implementation of the erosion and consolidation modules of the 1-DV water bed model in the computer code and the numerical difficulties resulting from that. In chapter 6, the consolidation module of the 1-DV water bed model is validated using a consolidation experiment [Kuijper et al., 1990]. This experiment has been performed on the same bed that has been exposed to an erosion experiment in a rotating annular flume. The parameterisation is also compared to numerical results on the same data set. In chapter 7 the rotating annular flume erosion experiment of [Kuijper et al., 1990] is used to validate the entire 1-DV water bed model. Chapter 8 contains the conclusions and recommendations.

Last but not least a few remarks about the lay-out of this report. When I refer to an article which I consulted myself, I use square brackets [], but when I refer to an piece of literature I did not read myself, I use round brackets (). And, very important, this thesis contains quite a lot of pages. To remedy this shortcoming, note that every chapter contains a summary at the end.

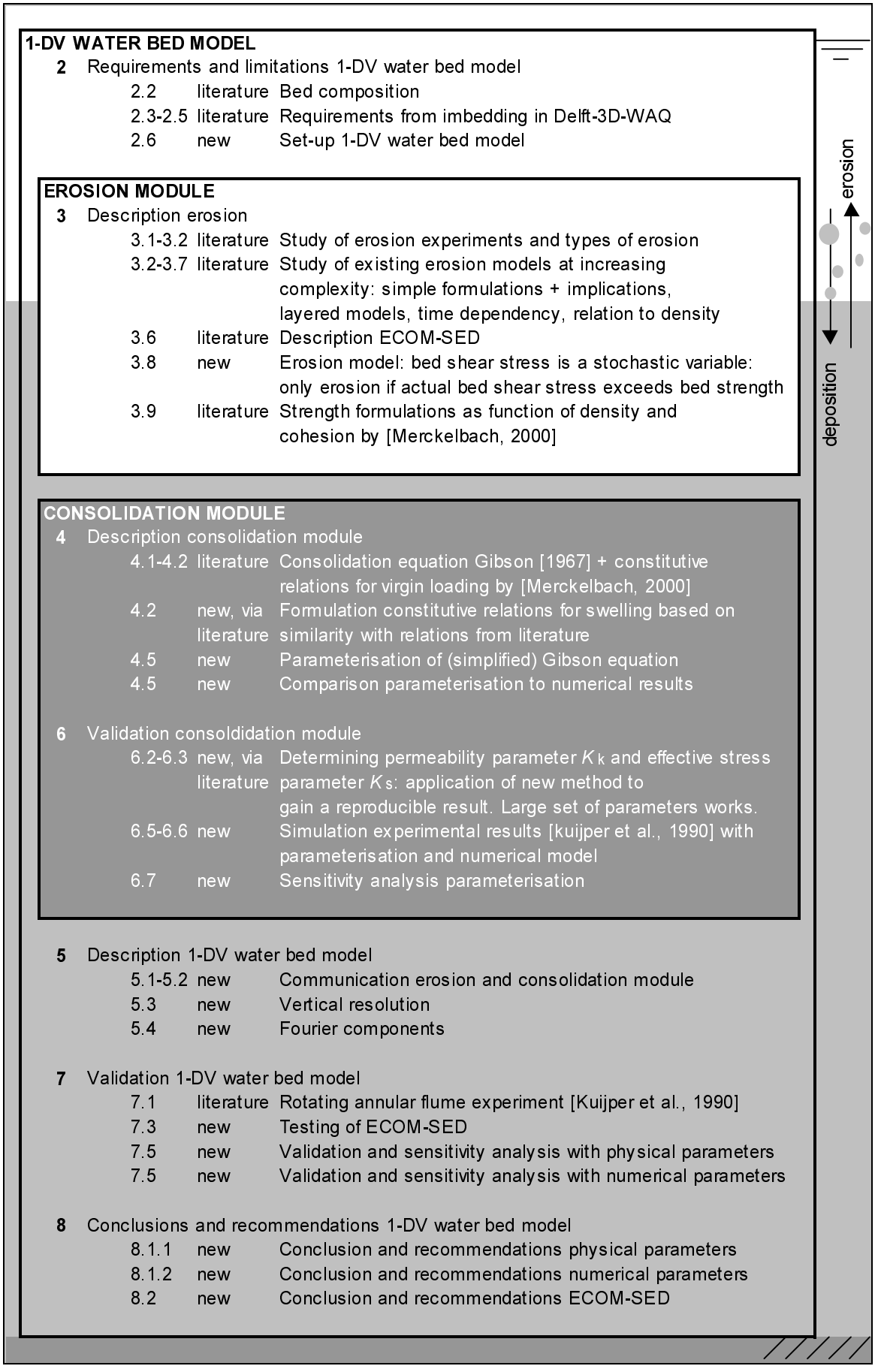

Figure 1.2. Schematic presentation of the contents of the present study.

2 Requirements and limitations

2.1 Introduction

With water quality issues, one has to deal with aggregation levels that range over several orders of magnitude: the behaviour of cohesive sediments with respect to heavy metals at nanometre scale affects policy decisions on a national and a global level (figure 2.1). For water quality modelling, one cannot take into account all the relevant processes on all the levels of aggregation, since this would lead to an enormous amount of computations. “A model is a simplification of a part of reality for a certain purpose.” [Battjes et al., 1997] The number of simplifications in the 1-DV water bed model depends on the purpose of the model. The goal of this thesis is to develop a model that can deal with seasonal variations in cohesive sediment concentrations in open water systems for water quality purposes. This chapter deals with the limitations of this model. The most important question arising is: is it possible to deal with all the cohesive sediment processes necessary for water quality engineering?

The processes necessary from the environmental engineers’ point of view should be retrieved from the environmental engineers themselves. Therefore a questionnaire has been sent to environmental engineers from HydroQual and WL | Delft Hydraulics, two world leaders in environmental modelling. On the basis of the responses to this questionnaire, originally enclosed in [Winterwerp, 2000], the requirements of the new bed model have been assembled. It turns out that it is not possible (yet) to deal with all the demands from the questionnaire, since the available knowledge and computer resources are not sufficient.

Winterwerp [1999] for instance has already developed a very sophisticated 1-DV water bed model. This model contains equations for the turbulent kinetic energy balance, flocculation, hindered settling and consolidation. This model can very well be applied to simulate the 1-DV behaviour of a bed for a period up to a few tidal cycles. For modelling seasonal variations however, it requires too much calculation time. Therefore the number of processes in the new 1-DV water bed model has to be smaller than in this model.

At present, water quality models already contain erosion models. These models are treated in chapter 3. They are very fast, but they contain too few physical processes to give an accurate description of the erosion behaviour. The number of processes in the new 1-DV water bed model has to larger than in these models.

Both the model of Winterwerp [1999] and the *currently used erosion formulations*, are not very useful for modelling seasonal variations. They are *either too slow or too inaccurate.* There is a need for a new 1-DV water bed model that contains more physics than the erosion models used at present, and is faster than the model of Winterwerp [1999]. Therefore, the 1-DV water bed model derived in this study will contain the minimum number of processes necessary to model seasonal variations: consolidation and erosion.

This chapter will treat the relation of the 1-DV water bed model to the aggregation levels of figure 2.1. First the limitations from the lower scale levels, the bed composition, will be treated in section 2.2. Then the requirements resulting from incorporation in the Delft3D-water quality modelling system will be discussed in section 2.3. This modelling framework poses some limitations with respect to the resolution in both time and space. The limitations from the lower and higher aggregation levels leave some remaining space for the 1-DV water bed model. In section 2.4 a set up for the 1-DV water bed model will be proposed. A summary concludes this chapter.

Figure 2.1. Aggregation levels water quality modelling.

2.2 Bed composition

The elements of the waterbed are: non cohesive sediments, gas, cohesive sediments, water and organic matter. Not all these elements will be modelled. In order to understand the implications of these simplifications, a brief description will be given of all bed elements before discarding some of them. The description of the cohesive sediment also explains why cohesive sediments are the major carriers for heavy metals.

2.2.1 Non-cohesive sediments

The non-cohesive sediments, sand and silt consist of relatively large particles. The size of silt ranges from 2 μm to 63 μm and sand is defined as the particles between 64 μm and 2 mm [Lambe, 1979]. The deposition and erosion of these particles for a given current condition is sensitive to the diameter of these particles. Large particles are only transported at severe current conditions, smaller particles are eroded at less severe conditions and settle more slowly. The clays and silts, the smallest particles, settle only in very quiescent conditions. This means that in open water systems *spatial segregation* occurs with respect to the diameter. This segregation is quite visible in lakes originating from damming a river (e.g Haringvliet in the Netherlands). Coarse sediments deposit near the river, the suspended sediments deposit near the dam. In tidal basins this segregation happens as well. The sands deposit near the entrance of the sea, the clays settle at the head [Van Ledden, 2001]. This means that when modelling the waterbed of a large area with a one-dimensional vertical model, different models should be applied to different areas in the river basin. This is a very important feature for the larger levels of aggregation. The 1-DV water bed model can only be applied in the muddy areas.

2.2.2 Gas

Gas in the bed (methane) results from decomposition of organic matter. The gas can be present in the bed both as bubbles and as individual molecules dissolved in the pore water. Chemical decomposition processes are responsible for the production of these gases. The mechanical behaviour of gas bubbles is not straightforward. Bubbles can absorb gas dissolved in the pore water and can merge with other bubbles. Bubbles can even explode and make the gas dissolve in the pore water again. The gas bubbles are responsible for delaying the consolidation of a mud bed. They introduce an extra resistance to the water fluxes, because they reduce the pore water volume. Second they lead to a smaller bulk weight of the bed, resulting in a smaller self-weight compaction. The bed may even rise when a large amount of gas is produced [Van Kesteren, pers. com.]. Thirdly it has a strong effect on the stress-strain behaviour of the bed. The compressibility of the pore water increases tremendously when it contains gas bubbles. Lick [2001] investigated the effects of the presence of gas on the erodibility. “For reconstructed sediments at approximately 20ºC the effects of gas were to decrease the density by up to 10%, to increase the erosion rate by as much as a factor 60, and to decrease the critical shear stress for erosion by as much as a factor 20 compared with sediments with no gas present.”

2.2.3 Cohesive sediments [3]

Cohesive sediments consist of clay particles (< 4 μm) and organic matter. The organic matter is degraded as time passes. “The boundary between cohesive and cohesionless sediment is, unfortunately, not clearly defined and generally varies with the type of material. However, dominance of inter-particle cohesion over

[3] All information on cohesive sediments without references is from [Lambe, 1979]

gravitational force increases with decreasing particle size. Thus the effects of cohesion on the behaviour of clays is much more pronounced than on silts, and, in fact, cohesion in clayey muds is primarily due to the presence of clay-sized sediment."[Mehta, 1989] A sand-mud mixture is cohesive when it consists of a blend of clay, silt and fine sand with a clay percentage > 5 -10%, while a non-cohesive mixture is comprised of clay, silt and sand with a clay percentage < 5% [Van Ledden, 2002].

The suspended clay particles can cluster into aggregates or flocs: this is called flocculation. Flocs are formed in the water column when cohesive particles collide repeatedly. Collision mechanisms include Brownian motion, differential settling and current shear. The size of the flocs can be up to a few 100 μm. The settling velocity of these flocs is several orders of magnitude larger than the settling velocity of the individual particles. The result of the flocculating behaviour is that the bed is build with aggregates as elementary pieces rather than individual particles. This influences the behaviour of the bed. Both the properties of the cohesive sediment and the water influence the rate and final degree of flocculation.

The clay particles contain minerals with a negative electromagnetic charge. A clay particle attracts ions to neutralise this net charge. Since these attracted ions (cations) are usually weakly held on the particle surface and can be readily replaced by other ions, they are called *exchangeable ions*. The ions can also be replaced with (poisonous) heavy metal ions. Clean flocs can slowly adsorb heavy metals from the surrounding water by diffusion exchange of the exchangeable ions. Likewise, contaminated flocs can also release the absorbed heavy metal ions to the surrounding clean water. This property of cohesive sediments accounts for the vital importance of cohesive sediments for water quality issues.

Both the clay mineral and the cations hydrate, pick up water. The exchangeable ions with their shells of water are too large to fit into a single layer on the surface of the minerals. So the ions with their surrounding water are forced to move away from the mineral surface to positions of equilibrium. This equilibrium situation is determined by the attraction of the ions to the mineral surface and tendency to move away from each other because of their thermal energies. This film of water attached to the particles in this fashion is called the *double layer*. Consequently the flocs (and soil) contain large percentages of water. The presence of this double layer prevents the clay particles from touching each other. Some types of clay particles can bind much water, some others, like kaolite, cannot. This means that at a certain volume fraction of clay some clay-water mixtures still behave as a fluid, whereas others behave as a gel already. The specific surface of the sediment, the surface area of a particle per unit mass, determines this property of sediment. The specific surface is a fairly good measure of the surface per unit charge that determines how much water a particle can hold in the double layer.

The clay particles (with their double layer) exert two counteracting forces on each other. Since the negative charge on a clay particle is balanced by the cations in the double layer, two advancing particles begin to repel each other when their double layers come in contact with each other. This repelling force is strongly dependent on the characteristics of the fluid. For the small particles and at short distances, these electromagnetic forces are of the same order as the Van der Waals forces. By the Van der Waals force, or the secondary binding force, that acts between all adjacent pieces of matter, the particles attract each other. This force is independent of the characteristics of the fluid between the particles. When the attractive force is larger than the repulsive force, the particles flocculate, otherwise they *disperse*. The result of these two antagonistic forces is that clay particles attract each other when they are very close, but they repel each other when they are less close, with the consequence that the particles are forced to cluster into aggregates when the suspension reaches a critical concentration.

The clay particles have the shape of small plates rather than spheres. Although the overall charge of the minerals is negative, the clay particles are charged positive near the tips of the plates. Hence the properties of aggregates, and accordingly the properties of the deposited bed, can change by a rearrangement of the particles. The water molecules, which are dipoles, can rearrange as well. When for instance a high concentrated mixture has been stirred and remains untouched for a period of time, the water molecules, the particles and aggregates rearrange and the electromagnetic forces can start to develop stronger mutual

bonds. As a result of this, the viscosity of the mixture increases. By shaking or stirring of the mixture these bonds are broken and the mixture becomes less viscous again. This effect is known as thixotropy.

2.2.4 Water [4]

The water in the pores fills up the space between the sediment particles. The substances dissolved in the water influence the double layer, therefore the characteristics of the water have a strong influence on the flocculating behaviour. The tendency towards flocculation is usually caused by an increase of the electrolyte (cation) concentrations, the ion valance and the temperature, or by decreasing the dielectric constant, size of hydrated ion, pH and anion adsorption.

The positive ions in the water responsible for flocculation can originate from dissolved salts or acids: acids contain H^+-ions and salts contain positive charged minerals. When for instance fresh riverine water, carrying suspended sediments, flows into an brackish estuary, the sediment deposits relatively quickly by formation of flocs as a result of the effects described above. The flocculation in waste water treatment plants is generated by addition of minerals.

The valence (amount of charge) of the minerals determines the thickness of the double layer necessary for the neutralising the charge, for instance Na^+ vs. Al^{3+}. This property is measured as *SAR* (Sodium Adsorption Ratio). When the double layer is thinner (due to ions with a larger charge), the particles attract each other faster when they are still in the suspension phase. Accordingly, the water has less time to escape when aggregates are formed and about the same amount of water can be enclosed inside the aggregate as when the double layer were thicker.

The lattice structure of a floc depends on the characteristics of the fluid as well. In fresh water the flocs are formed in the perpendicular 'edge-to-face' configuration. The positive charged tips of the plates attach to the negative charged surface area of the plates. This results in very low-weight flocs. In salt water the configuration shows much more parallelism between adjacent particles, so the flocs have a higher self-weight.

2.2.5 Biological activity

Biological activity has a heavy effect on the bed due to turbation, burrowing, excretion, and so forth. Recent research for instance by de Brouwer [2002] of the Dutch Institute for Ecological Research (NIOO) concludes that algae play a very crucial role in the sediment balance of a river delta. The top of a mud layer can team with diatoms, which have a large influence on the erodibility of the bed. Diatoms are monocellular algae with a silica coat. The conclusions are based on experiments on mud with diatoms in the laboratory and on field investigations in the Westerschelde, the Oosterschelde, the Eems-Dollard in the Netherlands, in the mouth of the British river Humber, and in the tidal areas at the coasts of Scotland and France. In all these locations mats of diatoms play the same crucial role. In the spring time they proliferate and become rampant. During the subsequent three to four months they cover up the tidal flats making erosion difficult. The biological algae mats form a very smooth or slippery sheet on top of the mud, that hardly allows the waves and the currents to get hold of the sediment. Moreover, the algae sheets trap suspended sediment from the water. Consequently, within a period of a year the bed can raise up to 6 centimetres.

At the start of the summer the sheet is disturbed by worms, snails, shrimps and shellfish that devour the algae and burrow into the sediment. These organisms also make cracks and holes in the bed. These irregularities are weak spots in the mud layer and lead to a distortion of the flow pattern. Accordingly they stimulate erosion. When the diatoms are almost gone, the same wave and current conditions that did not cause any erosion in the spring time, will result in severe resuspension. [Voormolen, 2002]

[4] All information on water without references is from [Lambe, 1979]

2.2.6 Engineering requirements

Environmental engineers have the following requirements for a new bed model. The model should be able to deal with both sand and mud beds. In river basins the sediment consists mainly of mud (clay and silt) and in the sediment in the Wadden Sea consists of sand-mud mixtures. Moreover, the sediments in the areas of application are rich in organic compounds. Engineers would also like to include the effects of chemistry (redoxprocesses and precipitation) and the above mentioned biological activity in the formulations for erosion and consolidation.

2.2.7 Limitations

With respect to the composition of the bed, the focus of the 1-DV water bed model is on cohesive sediment mixtures. This implies that the volume of the **clay fraction is at least 10 %** and can be very high, up to 80 % or so. The effects of **organic material, biological activity, chemical processes and gas** on the physical behaviour (consolidation and erosion) of the bed **will not be considered explicitly**, since the process knowledge and the available computer power are not sufficient yet.

2.3 Relation to Delft3D-WAQ

The 1-DV water bed model will be incorporated in a computational modelling system that can simulate the water motion and the associated spreading of substances. Such a modelling system is Delft3D (see annex 2.1). **Accordingly the 1-DV water bed model will be immediately applicable for three dimensional engineering purposes**. Delft3D is one of the few (four) most widely used engineering software environments for aquatic systems in the world. The US geological Survey recently took the initiative for an open source sediment model, to combine the leading models in the world.[5] If the 1-DV water bed model performs adequately in Delft3D-WAQ, it might be useful for this open source model as well.

2.3.1 Areas of Application Delft3D-WAQ

The model is to be applied in both low dynamic open water systems, such as lakes and reservoirs, and in high dynamic environments such as rivers, estuaries, bays, oceans and coastal areas. Examples of open water systems in the Netherlands are: estuarine and delta systems as the Rhine delta, coastal seas as the Wadden Sea, river sedimentation basins as Lake Ketel/IJssel and drainage water systems (polder bosom waters and brooks).

Typical values of the physical parameters in these applications are listed below. The new 1-DV water bed model is expected by environmental engineers to be able to handle these situations.

- Water column concentrations vary from tens of mg/l to thousands of mg/l.
- Water depths range from 1 m – 50 m
- Flow velocities range from 0.1 m/s – 1 m/s
- Maximum wave heights and periods are generally less than 2.5 m and 6 s
- Typical sedimentation rates range from 0.0001 $gcm^{-2}d^{-1}$ (lacustrine environments) to 0.05 $gcm^{-2}d^{-1}$ (estuarine and near shore environments)
- Erosion rates are of the order of 0.00005 $gcm^{-2}d^{-1}$ (mm-dm/year) to 0.03 $gcm^{-2}d^{-1}$. (gross mm-cm/day). When represented as an increase of the concentration in a 10 m water column, 1 mm of erosion equals about 10^{-3} m · 150 kg/m^3 / 10 m = 150 mg/l.

[5] http://woodshole.er.usgs.gov/project-pages/sediment-transport/

Observations in estuaries suggest the importance of *fluid mud layers*. "With continuous ADCP, CTD registration in a tidal area one observes a resuspension of material into the lower meter of the water column within half an hour, often right after the turn of the tide rather than at the highest water velocities. This resuspended material settles within half an hour at slack tides as well." [Postma, 2001]. 'As the spring neap tidal cycle progresses, the resuspension settles through the water column so that concentrations in the upper part of the water column decrease while concentrations near the bed increase. Thus the stratification in the suspension becomes more pronounced. At times when the currents are weak, the near-bed layers become stationary on the bed, but are redispersed on the succeeding tide. As neap tide approaches, stationary suspensions persist progressively longer into the succeeding tidal cycle, both as a result of the typically lower bed shear stress near neap tide and higher shear strength due to settling and consolidation. These observations (..) emphasise the critical need to detect and quantify the near-bed sediment transport governed by the motion of high density fluid mud layers. In the majority of estuarial and coastal environments in which measurable rates of cohesive sediment transport occur, it is not unusual to find that a significant portion of the transport is in fact confined to the near-bed region, particularly in areas of low current speeds or when the flow regime is wave dominated. The ratio β of the near bed concentration to depth-mean concentration is well above unity in these cases.' [Mehta, 1989]

The 1-DV water bed model will be **limited to applications with low-concentrated suspensions in the water column of a few 10 mg/l up to several 100 mg/l.** At higher concentrations sediment-turbulence interactions, the above mentioned sediment-driven density currents (turbidity currents), formation of (thick) layers of fluid mud and non-Newtonian effects start to play a role. These effects influence both the erosion process and the strengthening process. The extended model of Winterwerp [1999] mentioned in section 2.1 can deal with these processes.

2.3.2 Cohesive sediment features Delft3D-WAQ

A few features of Delft3D-WAQ with respect to cohesive sediments are:

- All algae are considered to be 100% cohesive sediment. Accordingly algae can be transported with the water flow as suspended sediments.
- Three size fractions or components, with independent flocculation and settling velocities, can be used to represent particulate inorganic matter.
- Particulate organic matter can be represented by four components, namely detritus carbon, other organic carbon, carbon in diatoms, carbon in non-diatom algae (Green).
- The seven particulate substances in the water column are used to calculate the light conditions which influence algae growth.
- The bed sediment is modelled as a two-layer system. Each layer is homogeneous (well mixed). The two layers can have different compositions of the seven substances. The density of a layer is variable depending on the sediment layer composition, which is also variable. The porosity within a given layer is constant (user defined).
- A third (deeper) layer exists (but is not explicitly modelled) which can supply sediment for upward sediment transport (digging).
- The erosion rate from the top layer of the bed is determined using the empirical erosion formula of Partheniades (see chapter 3). This erosion rate formulation will be replaced by the 1-DV water bed model.

2.3.3 Time resolution Delft3D-WAQ

The time resolution of the 1-DV water bed must be coupled to the time frame of Delft3D-WAQ in which the model will be incorporated. Typical time steps for the hydrodynamic simulations are in the order of seconds to minutes (20 s – 360 s). These time steps are necessary to account for the propagation of waves properly. The WAQ-module can use any time step that is an integer multiple or an integer divider of the hydrodynamic time step. However, a time step as small as the FLOW timestep is not meaningful in the process-based WAQ modelling environment, because the actual displacements of the water do not change as fast as the propagation of the waves. Often time steps in the order of 1 hour or even 1 day (Wadden Sea, Netherlands) are sufficient to model the problems to be solved. WAQ averages the high time-resolution output from FLOW to the smaller resolution of the WAQ time steps. The sedimentation and erosion are accounted for in this WAQ time frame.

The 1-DV water bed model consists of an erosion module and a consolidation module. The time frame of the erosion module has to be the same as the WAQ time frame. Resuspension and deposition will have to be accounted for in every WAQ time step. The time frame of the consolidation however still has to be defined in terms of the WAQ frame. The consolidation process has large time scales with respect to the exchange of sediment with the bed: time steps up to days may be sufficient. In chapter 6 the relation between these time scales will be dealt with.

The simulation time can amount to multiple years and sometimes even decades. Typical time scales that can occur in the 1-DV water bed model are intertidal (diurnal/semi-diurnal), spring-neap variations, seasonal variations and river floods and *drainage event.* Bed response (sedimentation and erosion) should be modelled throughout these cycles, and net effects should be accumulated for the simulation time.

2.3.4 Spatial resolution Delft3D-WAQ

The 1-DV water bed module will be incorporated in the Delft3D-system. The horizontal resolution of the Delft3D water motion ranges from 10 to 1000's of metres. The WAQ module can be used for any geographic area where the FLOW module is applied. The grids of Delft3D and WAQ do not have to be the same. The water motion requires small grid cells, where for the water quality (and accordingly the bed exchange processes) larger grid cells are sufficient. The waterbed can have the same erosion and consolidation properties over a large geographical area (a tidal flat for instance). So dealing with one single bed profile in a large area can be physically sufficient. Delft3D offers the option to cover the water motion grid with a WAQ grid with a coarser (and irregular) spatial resolution. This is called aggregation. These larger areas are called segments. In this way the time consuming calculations of the waterbed and the spreading of the substances are only carried out when it is really necessary.

The vertical resolution of the hydrodynamic motion in the water column is in the order 10 sigma-layers (boundary fitted layers). These water motion layers can be aggregated into a smaller number of water quality layers. Hence WAQ can also handle three-dimensional problems. Every water quality process-subroutine is called upon from every WAQ grid cell. A grid cell is one of the layers above a segment. A number of criteria attached to each cell makes a 'mask' possible to the application of the subroutines. The reaeration processes for instance are solely called upon from water surface cells. Likewise the consolidation module will only be called upon from bottom cells. The 1-DV water bed subroutine however is unaware of the number of grid cells from which it is called upon. Due to the one-dimensional nature of the equations this does not have any complications, nor should it have. So reduction of the WAQ model to the 1-D or 2-D case is an option. On the other hand, the incorporation of the 1-DV water bed model for each horizontal bed cell by WAQ, makes it automatically a three dimensional bed model.

The required vertical discretization of the bed is in the order of mm to dm.

2.4 Set-up 1-DV water bed model

2.4.1 Output required

Environmental engineers expect the model to provide the following parameters as a function of depth and time: distribution of dry density or similar parameters, erosion rate coefficients (e.g. critical shear stress for erosion and erosion rate parameter), permeability, pore water flows and sediment composition (clay, org. matter, etc.). Furthermore, the basic requirement of the 1-DV water bed module is that it is mass conserving.

2.4.2 Set-up 1-DV waterbed model

The bed model is based on two components: an erosion module and a consolidation module. Different processes with different time scales govern these two modules. The proposed set-up of the 1-DV waterbed model is shown in figure 2.1.

2.4.3 Erosion module

Erosion is initiated by the turbulence of the water near the bed and the shear stress due to the velocity gradient in the boundary layer. The turbulence level near the bed is also represented as a shear stress. When the total shear stress increases, the erosion increases. The rate of erosion depends furthermore on the type of constituent. Sand erodes particle by particle. General rules are available relating the rate of erosion to fluid and grain properties by means of the Shields parameter. The Shields parameter is a dimensionless relation between the submerged weight of a particle and the bed shear stress. The eroded sand can be transported either as bed load or as suspended load. The erosion of sand drops dramatically when a small percentage (order 5%) of cohesive sediments is added. Since sand is not considered in this model, in the following the erosion of mud will be described.

The behaviour of eroding mud differs from the behaviour of sand. Mud erodes either particle by particle, aggregate by aggregate or chunk by chunk [Partheniades, 1965]. The chunks travel a short time as bed load and meanwhile disintegrate. The small clay particles dissolve in the water above. That means that an eroding mudbed does not have a bedload layer. Only recently theoretical and experimental rules relating the rate of erosion to fluid and sediment properties have been derived [Van Kesteren, 1997], [Lick, 2001]. The behaviour of the bed can be considered as cohesive when it contains about 15 % clay or more.

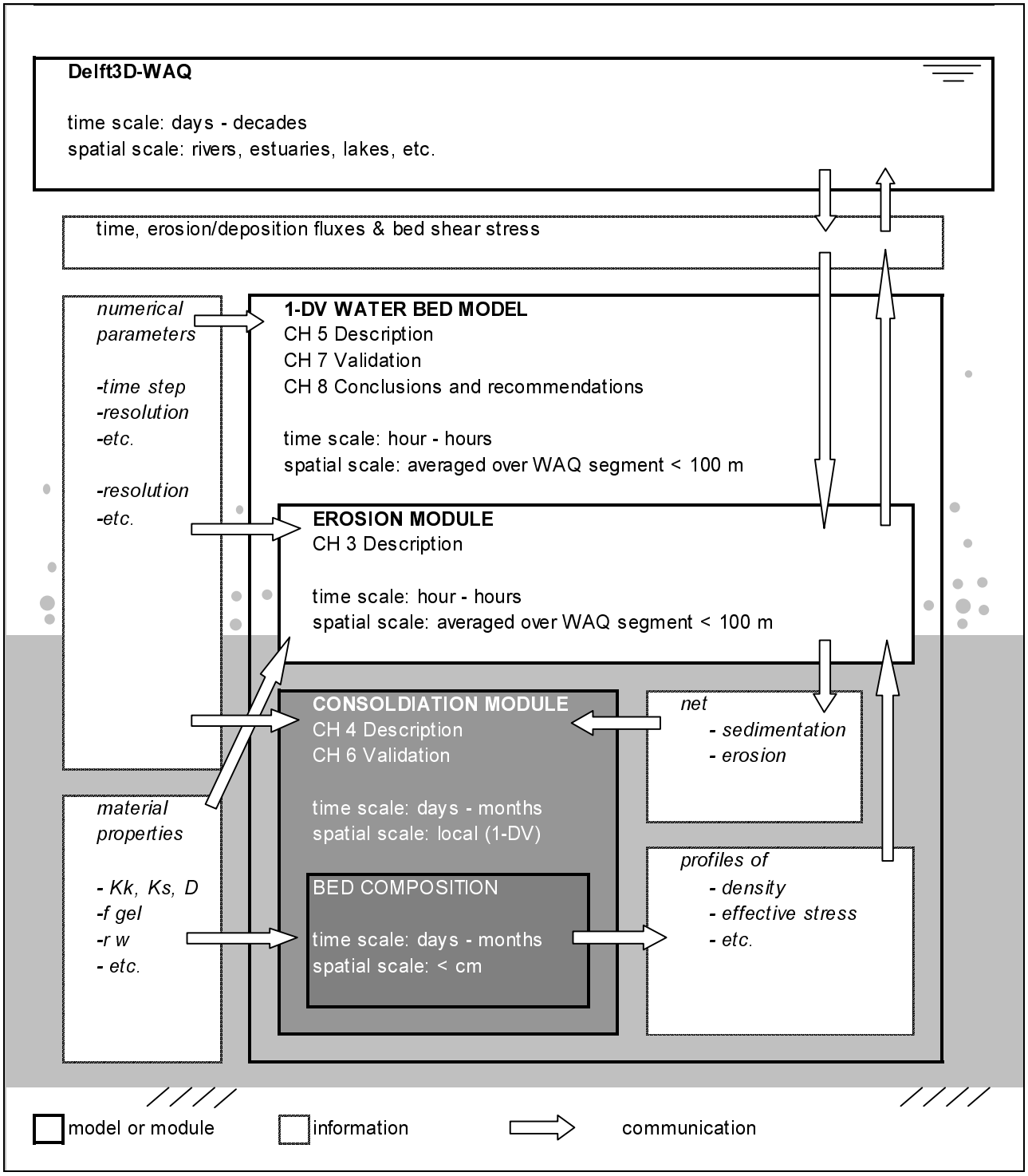

Figure 2.1. Set-up 1-DV water bed model with separate erosion and consolidation modules

Erosion by currents and waves is to be considered. The erosion mechanisms can be discriminated on the basis of the ratio of the time scale of the forcing and the time scale of the adaptation of the bed. When the forcing is quick with respect to the adaptation, the situation is called undrained. When the forcing is slow, that is when the bed has the time to compensate water pressure gradients, it is called drained. Muddy beds can be eroded by the following main mechanisms:

- Through drained surface erosion by the wave and current induced bed shear stresses. Note that when waves play a role, the wave-induced shear stresses are often at least one order of magnitude larger than flow-induced shear stresses. This kind of erosion is referred to as drained, because the material has time to adjust to the fluid forcing before it is eroded.
- Through liquefaction of the bed by the cyclical wave loads. This kind of erosion is referred to as undrained bulk erosion. It is a highly complicated process, which requires modelling of the stress history of the bed as well, because cyclical loading can also result in a strengthening of the bed (when stress levels are below the critical state line).
- By means of mass erosion of wave and current induced bed shear stresses. When the bed shear stresses are so large that they exceed the undrained yield strength of the material, whole chunks of bed material are loosened from the bed.

The model is to be applied for all open water systems. This implies low and high dynamic conditions with respect to flow and wave action. It is proposed however to **limit the 1-DV water bed model to flow- and wave-induced surface erosion processes,** because the liquefaction and mass erosion are not well understood yet. The erosion model will be dealt with in chapter 3.

2.4.4 Consolidation module

A bed can gain resistance against erosion by different strengthening mechanisms. General mechanisms include the presence of protecting sheets of algae and armouring (finer sediments erode, leaving the coarser sediments behind or coarser sediments deposit, thus protecting the underlying finer sediments). Because the 1-DV water bed model will only be dealing with muddy beds and the effects of biological activity are discarded, the above general effects can be neglected. For a muddy bed two additional strengthening processes are responsible.

- The muddy bed can consolidate. During consolidation, the water content decreases by self-weight compaction of the structure, thereby increasing the effective stresses and the densities. The Gibson finite strain consolidation equation can describe this process. Recent work of Merckelbach [2000] resulted in a set of constitutive equations that can be used to solve the Gibson equation.
- Even without consolidation the strength can increase [Merckelbach, 2000]. The true cohesion can develop by strengthening of the physico-chemical inter-particle or inter-aggregate bonds. This effect is known as thixotropy (see section 2.2.3). This can happen by decreasing the distance between the particles and thereby increasing the Van der Waals forces. Or this can happen by local restructuring along the surface of the aggregates so that the quality of the bonds between the surfaces increases. Bonds inactive with respect to the effective stress level can become active (this happens after unloading due to erosion).

For the strengthening due to consolidation a model exists, for the strengthening due to thixotropy no model exists yet. Therefore **the main strengthening in the 1-DV water bed model will be due to the consolidation equation**. Chapter 4 deals with the consolidation model. For the thixotropy an (estimated) empirical formula can be used to calibrate the 1-DV water bed model.

The Gibson equation of consolidation gives a continuum profile of the bed. In the bed no sorting occurs, since the bed is a volume-filling network. Accordingly, one size fraction is sufficient to describe the consolidation: therefore the 1-DV water bed model will only deal with one size fraction (of mud). The 1-DV water bed model can therefore not provide the sediment composition required by the environmental engineers. Therefore this composition has to be modelled with the current layer approach of WAQ. **The current layer model of WAQ has to be used next to the new 1-DV water bed model to model the composition of the bed**. The 1-DV water bed model will then only provide the erosion rates, the layer system will keep track of the sediment composition. WAQ can deal with three inorganic and four organic compounds. Therefore the deposition fluxes of the compounds have to be merged when going from the

water column to the 1-DV water bed module. And when erosion occurs, the total sediment flux has to be distributed over the various fractions again. WAQ already contains functions that can provide for this [Delft Hydraulics, 1999].

2.5 Summary

- The aim of the study is to develop and test a one dimensional (1-DV) water bed model, suitable for (long term) water quality modelling. The current erosion models have two major disadvantages. They are either too time consuming, because they contain too much physical processes or they are not accurate enough, because they contain too few physical processes. The new 1-DV water bed model will avoid the shortcomings of these two models. It contains the minimum number of processes necessary to model seasonal variations: erosion and consolidation.
- The 1-DV water bed model has the following limitations with respect to the composition: the effects of organic material, biological activity, chemical processes and gas on the physical behaviour (consolidation and erosion) of the bed will not be considered. These properties can have a large influence on the erosion characteristics however. Furthermore, the bed material is considered 100 % cohesive: at least 5-10 % of the volume is clay [Van Ledden, 2002].
- The applications are both low-dynamic environments (lakes, reservoirs) and high-dynamic environments (rivers, estuaries, oceans and coastal areas). The 1-DV water bed model is be limited to applications with low-concentrated suspensions of a few 10 mg/l up to several 100 mg/l. Hindered settling and fluid mud will not be taken into account.
- The 1-DV water bed model is incorporated in the Delft3D software environment that can be used in these areas. Accordingly the 1-DV water bed model is immediately applicable for three dimensional engineering problems. This software environment puts some restrictions on the spatial step and the time resolution.
- The output of the 1-DV waterbed module to Delft3D-WAQ should provide the following parameters as a function of depth and time: dry density or a similar variable, erosion rate coefficients (for instance critical shear stress for erosion and erosion rate parameter), size distribution and permeability. A very important requirement is that the bed model should be mass conserving.
- The 1-DV water bed model consists of an erosion module and a strengthening module. In the erosion module we limit ourselves to flow- and wave-induced surface erosion processes. Mass erosion and liquefaction are not considered.
- The governing processes for the strengthening module are consolidation and cohesion. The growth of true cohesion (thixotropy) cannot be modelled, but it can be incorporated by means of an empirical formula to calibrate the model. The consolidation can be incorporated as a process.
- The consolidation module can only handle one size fraction only, although environmental engineers consider the size-distribution of cohesive and non-cohesive fractions very important. The current WAQ layer formulation can used for this. Therefore the current layer model of WAQ has to be used together with the new 1-DV water bed model. In this combination, the new 1-DV water bed model provides for the erosion rate, while the layer model remembers the composition of the bed.

3 Erosion [6]

The aim of this chapter is to find or derive an erosion formulation that is capable of dealing with seasonal variations. To achieve this, a tour will be made of existing erosion models. It will deal with the models at increasing complexity, until an appropriate model is found.

Considering the importance of experiments, their methods and their characteristic results will be shortly dealt with in section 3.1. Section 3.2 gives the different erosion types that have been discerned. Section 3.3 lists the basic erosion models. The implications of these simple models will be dealt with in section 3.4. The layered approach is discussed in the section after that. In section 3.6 time dependency of the erosion parameters of the layers will be introduced to account for the shortcomings of the layered model. A more fundamental and physically based approach to deal with the time dependency of erosion is possible, however. Therefore, the erosion will have to be described as a function of the time dependent density and the time dependent cohesion. The time dependent behaviour of the density can be modelled with the Gibson equation of consolidation, which will be given in the next chapter. Some examples that relate erosion rate solely to density will follow in section 3.7. In section 3.8, the use of stochastic parameters, rather than the deterministic ones generally used, will be explored. A model with the bed shear stress as a stochastic variable is proposed. This model needs a description of the actual bed strength in terms of the density and the thixotropy, that will be given in the next to last section. A summary concludes this chapter.

3.1 Erosion experiments

All mathematical and computational erosion models have to be validated or calibrated on extensive experimental data. Experiments are and will be the very basis for all the cohesive sediment models. A few types of laboratory measurements exist. First there is the flume test (section 3.1.1). A simple but also widely used method is the shaker (section 3.1.2). A recent development is Sedflume (section 3.1.3). The erosion experiments have in common that they can only be used to investigate the erosive behaviour of natural and/or reconstructed mud beds on short time scales.

3.1.1 Regular flume test

Two types of regular flume tests are available: a rotating annular flume and a straight flume. A bed on the bottom of a flume (see annex 3.1) is exposed to a shear stress time series. This bed can be a deposited bed, obtained by allowing a well-mixed suspension with a high concentration to consolidate for a certain period of time, or a placed bed. The erosion rate and the total eroded mass can be determined from the concentration in the water, which is measured.

Often, a series of stepwise increments of bed shear stress is imposed on the bed. The erosion rate at a specific bed shear stress is very large just after application of a new shear stress, after which the erosion rate decreases to a constant value or becomes zero. By the time the erosion rate is constant or zero, the shear stress is again stepwise increased. The time scale of the erosion at a certain shear stress is 15 min [Sanford, 2001] to 1 hour [HydroQual, 2001]. The behaviour of the erosion rate at a single level of the bed shear stress can at first sight be described by an exponential decay function.

A similar instrument is the Sea Caroussel [Sanford et al., 2001]: a submersible rotating annular flume. It can be used to perform in situ erosion tests on the actual water bed.

[6] This chapter contains passages from Sanford et al. [2001], Mehta [1989] and Postma [2001] and some (fragments of) sentences of other work from the list of references.

3.1.2 Shaker

The Shaker (Tsai and Lick, 1986) is a portable device that can be used both in the laboratory and in the field (see annex 3.2). A cylinder is partially filled with sediment by reconstructing a sediment specimen, by allowing a well-mixed suspension with a high concentration to consolidate for a certain period of time or by inserting an in situ core. The lower part of the column is then filled with a sediment 'bed', the upper part with water. An oscillating grid oscillates up and down in the water in the upper part of the Shaker and creates turbulence. The turbulence generated, and therefore the amount of sediment resuspended, is a function of the speed at which the grid in the Shaker oscillates. The shaker apparatus is calibrated to laboratory annular flume experiments using the concept of 'equivalent shear stress'. The premise is that when the flume and the shaker produce the same concentrations under the same environmental conditions, the shear stresses needed to produce these concentrations are equivalent. Shaker studies have been conducted in at least twelve different aquatic systems and the results obtained from these studies have been used in a number of modelling efforts (see annex 3.3) [HydroQual, 2001]. The shaker studies indicate the presence of a so-called resuspension potential: the concept that at a certain shear stress only a finite amount of sediment can resuspend.

3.1.3 Sedflume

"Sedflume is essentially a straight flume that has a test section with an open bottom through which a coring tube containing sediment can be inserted. The coring tube has a rectangular cross-section, 10 cm by 15 cm, and is generally 20 to 100 cm in length (see annex 3.2). As the sediment at the water-interface is eroded by the flow through the test section, the sediments in the coring tube are moved upwards by the operator by means of a piston and a jack inside the coring tube. This is done at such a rate that the sediment water-interface is at the same level with the bottom of the test and inlet sections at all times. The shear stress at the sediment-water interface is a known function of the flow rate and can be varied by changing the flow rate. High shear stresses, up to 25 Pa, can be applied. In this manner, erosion rates can be measured as a function of depth in the sediments with shear stress as a parameter. For laboratory tests, sediments are poured into the core and then allowed to consolidate for various periods of time before erosion tests are initiated. In field tests, relatively undisturbed sediment cores can be obtained by means of a diver or by means of a long pole from a ship. Tests are initiated almost immediately after the cores are taken. For details of the apparatus, test procedure, or procedures for obtaining cores, see (McNeil et al.1996)." [Jones et al., 2001]

3.2 Erosion types

Despite the large amount of (experimental) research in the field of cohesive sediments, no universal erosion formula (framework) is known yet. There is general agreement however that the bed shear stress caused by waves and currents is the general factor causing erosion. Moreover, three main modes of erosion have been discerned. A distinction has been made between surface erosion (i.e. resuspension), mass erosion and re-entrainment [Mehta, 1989].

"The deposition of clay can be considered as the transition from a *dilute suspension* to *a high concentrated mud suspension (HCMS)* with Newtonian behaviour and increased viscosity (figure 3.1). Due to the self-weight of a HCMS-layer, water may be expelled if the flow conditions within the HCMS layer are sufficiently calm. At less calm conditions however the sediment can move to the dilute suspension again by re-entrainment. The HCMS-layer will compact until the *gelling point* is reached at which a volume-filling network is formed, and effective stresses start to develop. The layer consolidates and concurrently develops strength. Although being very soft and fluidlike, the behaviour of the consolidating layers changed from Newtonian to non-Newtonian. With the passage of time the *consolidating* (soft) *bed* turns into a stiff,

settled bed. Both beds may be eroded if the bed shear stresses are sufficiently high, so that the cohesive sediment is resuspended." [Merckelbach 2000]

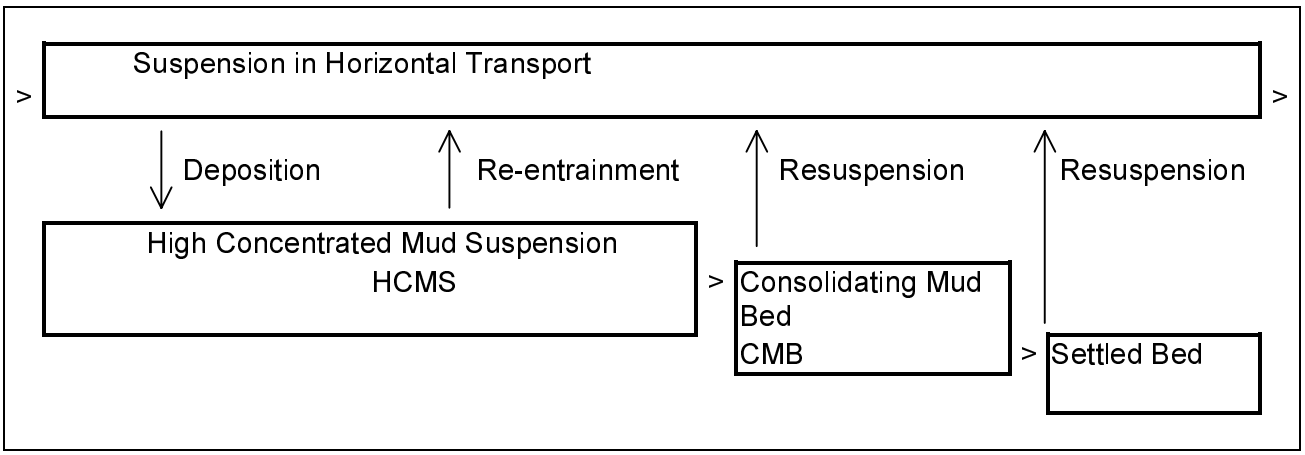

Figure 3.1. Physical states and processes governing estuarine cohesive sediment transport (after Mehta, 1982)

"When the bed shear stress becomes large, or when rapidly accelerating flows occur, the consolidating settled bed may fail at some plane below the surface and clumps of material are mass eroded. Mass erosion is dominant in areas of strong tidal currents and also under storm-generated flows." [Mehta, 1989] This type of erosion is strongly governed by the internal pressure fluctuations in the bed, and less by the bed shear stresses [De Wit, 1995]. This erosion type will not be dealt with in this thesis, as argued in chapter 2.

In the mass and surface erosion mode, the site-specific sediment characteristics, as well as the manner in which a deposit is formed, control the resistance to erosion. When re-entrainment occurs however, the erosion is not limited by the sediment properties. The carrying capacity of the fluid is the only limiting factor in the erosion process. This type of erosion dominates in very soft sediments, generally referred to as fluid mud. The presence of fluid mud can explain the large (β) factor between the concentrations in water column and the concentrations near the bed as mentioned in the observations above. Entrainment models have been developed that calculate the entrainment of a fluid mud layer by means of a turbulent kinetic energy balance [Winterwerp, 1997]. He predicts that a 10 cm thick fluid mud layer with a concentration of 150 to 250 kg/m^3 will be eroded within one hour. Consequently we can conclude that entrainment is a process with very short time scales. That means that entrainment models are not of particular interest for modelling seasonal variations. But entrainment does happen every tidal cycle, so it cannot be discarded. A very simple entrainment or erosion formulation for high concentrated mud suspensions will be used in the 1-DV waterbed model. In chapter 6 this choice will be elaborated on. The erosion model that will be searched in the remaining part of this chapter should provide formulations for the surface erosion.

Surface erosion (resuspension) typically occurs at low to moderate values of the excess shear stress and is prevalent in estuaries subject to currents of low to moderate strength. There are two types of surface erosion. "Laboratory experiments (Parchure and Mehta, 1985; Tsai and Lick, 1987; Graham et al., 1992) and field studies (Hawley, 1991; Amos et al., 1992) have revealed that only a finite amount of sediment can be resuspended from a cohesive bed exposed to a constant shear stress as a result of armouring (consolidation). The amount of fine-grained sediment resuspended from a cohesive sediment bed is given by (Gailani et al., 1991) the erosion potential ε." [HydroQual, 2001] (see annex 3.3). This behaviour is characteristic of erosion type I where the erosion is limited with respect to the eroded depth. In erosion type I the strength of the bed increases with depth. After some erosion has occurred, the resistance to erosion of the upper exposed layer becomes too large. Accordingly the erosion reduces dramatically or might even stop. Alternatively, the erosion can be unlimited with respect to the eroded depth (type II).

Sanford et al. [2001] have shown that the difference between erosion types I and II is related both to the time rate of change of the forcing (bed shear stress) and to the depth rate of change of a resistance (the

critical shear stress). The erosion is a balance between incremental increases in bottom shear stress and incremental increases in the resistance to erosion. Hence the same bed can exhibit type I erosion, type II erosion or something in between. If the interval over which each successive shear stress is applied is short compared to the sediment depletion time scale of the bed, the erosion will appear to be type I. If the interval is long, the erosion will appear to be type II. Accordingly, surface erosion type is not a physical property, but an apparent behaviour due to more fundamental physics behind the erosion process. This insight is a first step to a unified erosion theory.

A few examples of the erosion types I and II will be given. Sanford et al. [2001] predict that under tidal forcing, which is a slow change of the bed shear stress, the erosion is of type I and the erosion rate is maximal at the maximal acceleration of the tide, rather than during the maximal shear stresses. This is in accordance with the observations mentioned in section 3.1.4. Under a wave forcing, which is a fast change of the shear stress, the erosion is of type II and the erosion rate is maximal at the peak of the shear stresses. In the annular flume experiment of Kuijper [1990], where successive stepwise increments in the bed shear stress were applied, the in-between behaviour is shown (see chapter 7). The erosion rate is reducing for a certain period of time (order 1 hour), and then becomes constant with a low rate. It tends to a straight line, to a constant erosion rate. This suggests equilibrium between entrainment and softening of the bed.

3.3 Basic erosion models

The two erosion modes available for surface erosion, type I and type II, often are modelled with different, frequently incompatible formulations. For relatively dense, consolidated beds (water or moisture content well below 100%) with uniform properties a widely used formulation is the (adapted) Ariathurai-Partheniades erosion formulation:

$$E = M \cdot \left(\frac{\tau_b - \tau_{cr}}{\tau_{cr}} \right)^n H\left(\frac{\tau_b - \tau_{cr}}{\tau_{cr}} \right) \tag{3.1}$$

where E is the mass erosion flux [kg/m^2/s], M is an erosion coefficient [kg/m^2/s], τ_b is the bed shear stress, τ_{cr} is the critical shear strength, n is an exponent often set to 1 and H is the Heaviside step function [7]. This formula says that the erosion does not start until the critical value τ_{cr} of the bed shear stress is exceeded. When this threshold is exceeded, the erosion rate increases linearly with the shear stress surplus τ_b - τ_{cr}. The erosion parameter M has to be determined empirically. Its values range from 10^{-3} to 10^{-5} [kg/m^2/s] [Winterwerp, 1989]. Another commonly used formulation is an exponential form. This equation describes the net erosion of soft (water content well above 100% [8]) partially consolidated beds:

$$E = \varepsilon_f \cdot \exp\left(\alpha\left(\tau_b - \tau_{cr}\right)^\beta\right) H\left(\tau_b - \tau_{cr}\right) \tag{3.2}$$

where ε_f is the floc erosion rate and α and β are empirical coefficients [Mehta, 1989].

With constant parameters, the above equations describe erosion of type II. When the parameters are variable with depth or when the erosion is set to zero when a certain amount of material has been eroded (after the clean bed assumption), the equations can be used to model type I. Van Kesteren [1997] developed a model that gives the erosion rate in case of an equilibrium between entrainment and softening of the bed. It includes the time scale of the swelling of the bed, that is one of the two dominant time scales according to Sanford et al. [2000]. (The other important time scale is the time scale of the forcing.) The model of Van Kesteren describes the surface erosion type in between type I and type II behaviour and is valid for a homogenous mud layer with uniform density only.

---

[7] $H(x) = \begin{cases} 0 & x < 0 \\ 1 & x \geq 0 \end{cases}$

[8] The water content is defined by the weight of the water divided by weight of soil in a soil element [Lambe et al., 1979]

Example 1. The erosion formulation of Van Kesteren [1997] in steady state reads

$$E = M \cdot \frac{\tau_b - \tau_{cr}}{\tau_{cr}} = \rho_d \frac{c_v}{10 d_{50} e_{cr}} \frac{\tau_{cr}}{\tau_y - \tau_{cr}} \cdot \frac{\tau_b - \tau_{cr}}{\tau_{cr}} \tag{3.3}$$

where ρ_d is the dry bed density, c_v is the consolidation coefficient from the Gibson equation of consolidation, e_{cr} the critical water content of the sediment at which it can be entrained, d_{50} is the median floc size at deposition and τ_y is the actual undrained yield strength. This equation looks like equation 3.1. The erosion rate coefficient M is not constant, but is a function of depth because τ_y is a function of depth.

This expression is based on a few simple physical observations. First the progression x of a swelling front in the bed in m/s can be described by $x = \sqrt{\pi c_v t}$ on the basis of a simplification of the consolidation equation. This leads to a downward celerity of the swelling front of $dx/dt = \pi c_v / 2x \approx c_v / x$. The erosion rate is limited by the progression of this swelling front, because only aggregates in the dilated zone of the bed above the swelling front can be eroded. Moreover this relation is only valid when the swelling front has the time to penetrate into the bed. In the period of one wave for instance, this is not the case. Second, the erodable depth will be constrained by the aggregate size. The erodable depth is at least 10 times the median aggregate size plus intermediate water in order to apply a continuum approach: $\Delta z = 10 d_{50} e_{cr}$. And third, the erodable part of the bed above the swelling front can described by the linear relationship $\Delta z = x\left(\tau_b - \tau_{cr}\right) \Big/ \left(\tau_y - \tau_{cr}\right)$. For details see [Van Kesteren, 1997]

When we perform a *reductio ad absurdum* for the equations 3.1 and 3.2 , we see that the erosion rate continues to increase if the bed shear stresses increase. Obviously this cannot be true. The following reasons account for this. The limited permeability of the sediment does not allow the material to be taken away at any large rate. When a part of the bed erodes, the remaining bed will swell due to the reduction of the load. The swelling front of the plane where the effective stresses are zero, has a finite speed of penetrating into the bed. As long as the excess pore pressures due to the erosion have not dissipated yet, the sediments will be exposed to negative excess pore pressures: the sediment will be sucked (on)to the bed. This will result in an erosion rate increasingly smaller with increasing bed shear stress. Moreover, the entrainment rate of the fluid is limited. And third, another erosion mode will occur when the shear stresses become too large: mass erosion. Mass erosion can be described approximately by an expression of the form of equation 3.1 (but with other coefficients). Mass erosion falls beyond the scope of this study.

"All general erosion formulations above have parameters that typically are set empirically, through laboratory erosion tests, in situ tests or large scale observational data. However, interpretation of the data is often at least partially subjective, and frequently the results are specific to a physical configuration and time history of the procedure used. For example, some researches define τ_{cr} as the stress at which (the slightest) initiation of motion first occurs, some define it as the stress at which significant erosion first occurs (a specific erosion rate defined in advance), some define it by extrapolating erosion rate vs. stress data back to zero erosion and some define an entire depth sequence of increasing critical stresses.

Similarly, the erosion M or floc erosion rate ε_f at a given applied shear stress can be defined in many ways. Some define it as the initial erosion rate after application of a new stress, others as the erosion rate after some initial response period has passed, and others as the average erosion rate during the period of application. These differences can lead to significant differences between derived parameters, even when tests are performed with the same sediments."[Sanford et al., 2001].

The lack of consensus on a basic mathematical description, and on the way to obtain the empirical parameters, betrays a lack of understanding of the underlying physics. Not with standing these shortcomings, can these models be used in engineering practise? This will be dealt with in the next section.

3.4 Implication of basic models

When using the basic erosion models, as mentioned in the previous section, it is difficult to simulate seasonal variations. When a constant erosion coefficient and a constant critical shear stress are used, the potential resuspension is unlimited, and with common coefficients also pretty fast as soon as the critical shear stress is exceeded. Using the 'clean bottom assumption' may solve this. The waterbed in such a model starts as a 'rock' bottom. No erosion is possible at the start of a simulation. In the course of time, suspended sediment from the water column can settle on top of this rock bed. This deposited layer of erodable material is available for erosion. If in an area the critical shear stress is exceeded however, all the available material in this area is almost immediately eroded. When for instance in these clean bottom areas material is deposited during slack tide, all of this material may immediately be taken away in other phases of the tide. Hence the model results show only spatially net sedimentation areas and clean bottom areas. If the dominant forces responsible for erosion increase (the neap tide becomes spring tide or the weather becomes more windy) this results in a slight increase of the areas with resuspension. The instantaneous resuspension can be tempered by using very small coefficients (compared to literature). Being the only remedy, this is generally done in seasonal models.

In reality, in many areas there is an equilibrium between sedimentation and resuspension. Only part of the available sediment erodes when the shear stress exceeds the critical shear stress. These equilibrium areas will show some net sedimentation on neap tides and in quiet summer conditions and some net resuspension on spring tides and in more stormy winter conditions. Even when very high shear stresses act on these beds, not all sediment will be resuspended instantaneously. The deeper material might not be subject to erosion immediately. However, when this material lies on top for a while, it will swell and eventually becomes available to erosion. This secondary erosion rate is much smaller than the initial erosion rate however. When the basic models are used for these areas, the erosion cannot be predicted accurately. The resuspension will either be too high, because the deeper material is treated the same way as the more erodable younger material, or be too low because on a clear bottom no secondary erosion takes place. Hence the approach with constant parameters should be replaced by an approach with depth varying parameters.

When using the basic models for long term morphology, the results can be reasonable. The morphological behaviour of estuaries often depends on non-cohesive as well as cohesive sediments. Van Ledden [2001] created a model by simultaneously taking into account bed level changes due to sand and mud transport and by including spatial and temporal variations of the bed composition. In this model, the mud resuspension formulation is the adapted Partheniades erosion equation. The model results for a period of several decades show two propagating deposition waves for sand and mud, respectively. The results are compared qualitatively with field data from the Rhine-Meuse estuary in the Netherlands, an estuary in which the tide is strongly reduced due to human interference. The observations show similar morphological characteristics, which indicates that the model is a step forward on the way to a better understanding of the morphological behaviour of sand-mud estuaries.

Summarising: If one has a tidal area with a bed that largely consists of erodable material (except for e.g. some sandy, gravelly or rocky canals with high water velocities), then the only way at present of modelling seasonal variations and episodic events is to adjust the coefficients in such a way that the non-canal zones (areas with lowest velocities) are net sedimentation areas. For water quality issues, the current formulations are not sufficient to model the effects of episodic events and seasonal variations. For other purposes, e.g. long term morphology, episodic events have less effect and the current equations can be sufficient. Therefore a new modelling approach is necessary for water quality purposes.

3.5 Layered erosion models

The use of depth varying parameters can be introduced to remedy the shortcomings of the basic erosion models. The bed has to be discretized into several layers, where each deeper layer has a larger resistance against erosion. Such a model can account for an equilibrium bed where alternately deposition and resuspension takes place, without a clean bottom in the period in between. Different types of layers are possible: with an Eulerian coordinate system, with a Lagrange coordinate system and with a material coordinate system, see [Gibson, 1981]. Moreover, the description of the layers can be continuous or discrete.

Example 2. A layered approach is used in the bed model of Delft3D-WAQ. The system consists of two fully mixed independent layers (a multiple layer system is currently under construction). Each of these layers has to be assigned a critical shear stress and an erosion rate coefficient by the user. Moreover, each of these layers keeps track of its own composition of the three possible sediment fractions. Sediment can move from one layer to another depending on the thickness of the layers, on the user-defined inter-layer fluxes and on the layer mode. Two modes of the layer thickness are possible. If a fixed layer thickness is chosen, layer 1 is always exposed to the waterbed interface (Lagrange approach). A sediment flux from this top layer to the water column is equal to the sediment flux from the second layer to the first layer. Resuspension is only possible if layer 1 contains sediment. If a variable layer thickness is chosen, any layer can be exposed to the water (Eulerian approach). By definition there are no fluxes between the layers, unless the user specifies fluxes. Resuspension and deposition occur at the exposed layer. Resuspension is therefore only possible if at least one of the layers contains sediment.

In both modes of the layer thickness, a third (*n*th) *digging layer* can be used to bury sediment from the layers out of the WAQ-system or to dig sediment into the WAQ-system. This third layer is not modelled; only the fluxes with the other layers are are modelled. In the clear bottom assumption, the fluxes from these layer upwards are zero.

The major shortcoming of Delft3D-WAQ and similar systems is of course that the assignment of values of the parameters to the layers is rather subjective. A solution for this would be to measure the erodibility of the sediment (in the field) and use these data in the model.

Example 3. Jones and Lick [2001] have created a general multiple layer model. In their model there are no sediment fluxes between these layers. They can define the erosion rate of the various layers experimentally by means of the new experimental Sedflume instrument as described in section 3.1.2. The measurement results of this facility can be imported into the software directly. The properties of the numerical layers are assigned according to the measurements. This approach is very useful, and has been successfully applied to a real river (lower Fox River in the USA). It does not incorporate the consolidation of the bed however. Therefore the eroding behaviour of future deposits cannot be modelled in this approach. It is only equipped to calculate the erosion of an existing bed. It does have an armouring model though to account for the strengthening behaviour of future deposits of sediments coarser than mud.

The correspondence between the layered methods is that the parameters of each layer have to be determined either experimentally or subjectively. With these approaches it is possible to give a good description of the erosion of the material present in the bed at the moment a simulation starts. However, despite the fact that these models with empirically determined parameters can describe erosion experiments accurately, they still are not able to describe the erosional behaviour of future deposits. Alternating erosion and deposition therefore cannot be accounted for, because the assignment of the parameters to new layers cannot be

performed on a physical basis. Some way or another a time parameter has to be included that accounts for the decrease in erodibility of (future) deposits in time. In the next section this requirement will be explored.

3.6 Layered erosion models with time dependency

How can we include the time dependency of the erosional behaviour of the sediment? The first option to deal with the time dependency would be to find out how the erosion parameters themselves change in the course of time. Some have tried to create a model this way. In these approaches, the erosion parameter M generally decreases and the critical shear stress increases with increasing site exposure. An example of such a model is found in ECOMSED[9], [HydroQual, 2001].

Example 4. [10] In the bed model of Lick et al. [HydroQual, 2000] which is incorporated in the ECOM-SED model, the erosion parameter M is a function of time. Experiments suggest that the resuspension potential into the water column is not resuspended instantaneously but over a time interval approximately one hour (Tsai en Lick, 1987; MacIntyre,1990). The resuspension rate (per unit time) is thus given by

$$E = \frac{\varepsilon}{T_\varepsilon} = \frac{a_0}{T_\varepsilon Z}\left(\frac{\tau_b - \tau_{cr}}{\tau_{cr}}\right)^n \quad for \quad \int_0^t E\left(\tau\left(t^*\right)\right)dt^* < \varepsilon \tag{3.5}$$

where ε is the resuspension potential (kg/m^2); a_0 is an empirical sediment yield coefficient; T_ε is the period over which the erosion potential is eroded (≈3600 sec), Z is an empirical sediment age coefficient to express the effects of armouring and consolidation of the sediment; τ_b is bed shear stress (Pa); τ_{cr} is critical shear stress for erosion (Pa); and n is a coefficient depending upon the depositional environment ($n \approx 2$ to 3). Once the amount ε has been resuspended, E is set to zero until additional sediment is deposited and available for resuspension or until the shear stress increases (Gailani et el., 1991). Formulation 3.5 looks like the Partheniades formulation 3.1 when the erosion rate coefficient M equals $a_0 / T_\varepsilon / Z$.

To simulate the effects of sequential deposition and erosion realistically, and the subsequent change in bed properties such as thickness and erodibility characteristics, a vertically segmented model of the cohesive sediment bed is constructed as shown in Annex 3.4. This is achieved by discretizing the sediment into seven layers. Each layer of the bed is characterised by a unique dry bed density (ρ_d), a critical shear stress for erosion (τ_{cr}) and an initial thickness. The time after deposition for each layer increases linearly from one day at the surface, which is composed of freshly deposited material, to seven days in the bottom layer. After each day, the amount of sediment from a certain layer moves to the layer beneath. During this process, the sediment becomes older. Previous laboratory results (Tsai en Lick, 1987; MacIntyre et el.,1990) have indicated that consolidation effects on resuspension are minimal after seven days of deposition, hence deposited sediments more than seven days old are assumed to be seven days old. The sediments in the 7th layer do not shift to a lower layer. The sediment age coefficient Z in the resuspension potential equation (3.5) increases with time according to [HydroQual, 2001]:

$$Z = Z_0 T_d^m \tag{3.6}$$

where T_d is time after deposition and with $m \approx 0.5$ for quiet conditions and $m \approx 2$ for dynamic conditions. Another formulation, used by [Velleux, 2001] is

$$Z = Z_0 \exp\left(\alpha T_d^m\right) \tag{3.7}$$

[9] http://www.hydroqual.com/Hydro/ecomsed/index.htm

[10] This section contains passages from *A primer for Ecomsed,* HydroQual 2001.

When Z is an exponential function of the time after deposition as in (3.7), it can vary from 0.1 to 50. The erosion potential equation contains a coefficient Z_0 or α without straightforward dimensions: the dimensions change when the power m over T_d changes. This kind of behaviour of coefficients is always due to a lack of physical background and should be prevented.

In ECOM-SED the erosion coefficient a_0 and the age T_d of the material in the layer determine the erosion rate coefficient M. The coefficient a_0 is the same for every layer, but the age T_d can be adjusted for each layer separately by the user. In the model, every day the material shifts from one layer to the next. The actual age of the material given by these shifts is not related to the age T_d that governs the erosion coefficient M. The age T_d of every layer can be assigned any value, it is not related to the actual age of the material. This way any depth variable distribution of the value of erosion potential can be used.

The layered bed model conserves mass, with resuspension and deposition fluxes occurring only at exposed bed level. During the course of the simulation, the bed model accounts for changes in thickness, the mass of cohesive and non-cohesive sediments in each layer, resulting from resuspension and deposition at the sediment-water interface. When the erosion depletes one layer in a certain time step, no other layer can be eroded in that timestep. ECOM-SED accounts for deposition and erosion at time steps of about 1 hour.

The ECOM-SED approach is still not able to predict seasonal variations in the suspended sediment concentrations. With 7 layers it is possible to simulate the behaviour of the bed during a single tide as mentioned in the observations above. “However, spring neap tide cycles last 14 days. The 7 neap days will result in net sedimentation on the bed. Due to the 7-day history in ECOMSED, all this sediment has the same properties after 7 days. Consequently, for the spring tide part the bottom will act as a clear bottom. Only by expanding the ECOM-SED approach to a history of 14 days, a spring–neap tide cycle behaviour for sediment towards and from the bottom can be obtained. The same holds for seasons. Only by expanding the history to 365 days, a year cycle can be modelled with respect to transport to and from the bottom. Without such a 365 days history the only seasonal effect is that at seasons with higher shear stresses a larger percentage of river input remains in suspension like with the basic models described in section 3.4. ECOM-SED may lack the instantaneous resuspension of the small areas that become clean at high shear stresses in the Partheniades approach. That depends on the setting of the coefficients of the 7-days or over layer”, analogous to the digging layer in Delft3D-WAQ [Postma, 2001]

To predict long term variations, one needs a layer configuration that accounts for the age of the sediments as long as the simulations. An option is to use a separate layer for each deposition interval, as by [Shresta et al. 1996] in the next example. However, this obviously leads to an enormous amount of layers.

Example 5. “During each succeeding timestep of the simulation, either erosion or deposition occurs, depending on the shear stress on the bed. If deposition occurs, then sediment is deposited in layers of new material for each interval, each layer characterised by unique bulk density, shear strength, erodibility characteristics and thickness (see annex 3.5). When the shear stress is imposed on the bed surface exceeds the shear strength of the exposed deposited layers, erosion occurs, either as mass erosion of an entire layer (or layers) or surface erosion of a part of a layer. In the model, mass erosion is defined as bulk erosion en masse, of the sediment from the topmost layer, downward to the next to last layer of newly deposited material. The last layer of the newly deposited material is then subject to surface erosion, defined as particle by particle resuspension from the bed. This process proceeds downward though layers of the original bed, so long as the shear stress imposed exceeds the critical shear stress at each erodable layers until the cessation of the erosion. During each timestep, if the erosion depth is computed to be greater than the depth of the layer, then surface erosion for the next layer becomes a function of the local critical shear stresses and the fraction of time remaining in a given

simulation step. If the erosion depth is less than the depth of the layer, then surface erosion stops, and the new thickness of the partially eroded layer is computed. (..) After application to South San Francisco Bay he concludes that 'the comparison of predicted and observed values of some key variables indicate reasonable performance of the model, but also suggest a need to evaluate certain limitations considerations inherent in modelling realistic environmental situations. (..) The process of mass and surface erosion need to be further investigated in the laboratory for different sediment types and shear strengths. Such tests can provide the data needed to describe soil erodibility characteristics such as erosion rate coefficients and critical shear stresses for sediments that are representative of specific surface water systems."

Two remarks will be made with respect to this example. First, a suggestion to improve the above model with a layer for each deposition interval would be a new kind of layer-system. One could for instance use layers respectively containing the sediment deposited during the last 1,2,4,8,16,32 etc. days.[11] A small problem has to be accounted for however: a good redistribution of the material over the layers during every timestep has to be formulated. (For instance when dealing with a 2 day layer on top of an 4 day layer: move 50% of the 2 day layer to the 4 day layer every day, or move the 2 day layer as a whole to the 4 day layer every 2 days). The number of layers is reduced drastically this way.

Second, even with this sophisticated layer model, the erosion parameters of the layers cannot be assigned values in a physically based manner. The approach still lacks physical background. This is also remarked by [Shresta et al. 1996]. This shortcoming is inherent to the fact that the erosion parameters are not fundamental coefficients, but merely apparent properties of the bed. What are the options to solve this problem of the current erosion models? This will be dealt with in the next section.

3.7 Fundamental time dependency

The basic important notion for a set-up of a new erosion model with a physical basis is that any model on any level of aggregation will need the empirical parameters. The parameters are a function of processes on a smaller level of aggregation (see figure 2.1). The coefficients in the current erosion models (e.g. M, τ_{cr}, a_0) are (but) apparent properties of the sediment. A description of the current erosion parameters in terms of the underlying physics is necessary to give a better description of the erosion. The parameters in the current models should be seen as a parameterisation of these processes on a smaller scale. But currently there is no connection between the erosion parameters and the governing physics on a smaller level of aggregation. The erosion parameters are determined empirically. Therefore the current erosion models are actually merely 'behaviour based models'. The parameters are tuned to describe what is happening, rather than explaining it. Therefore the forecasting value of the models should not be valued too high. They will have to be replaced by models that give a more fundamental description of the bed: 'process based models'.

These process based models deal with this physics on smaller scales of time and space, on a smaller level of aggregation. "From field tests as well as from laboratory tests with Sedflume, it has been determined that erosion rates depend on at least the following parameters (besides the applied bed shear stress): bulk density, average particle size, particle size distribution, mineralogy, organic content, volume of gas contained in the sediment, salinity of pore water and time after deposition" [Lick, 2001]. Other fundamental bed properties might be: effective stress, cohesiveness (thixotropy), cracks per unit of surface, unremolded yield strength and biological disturbance/activity.

One should realise that the 'fundamental' parameters that are necessary to describe the bed, are apparent properties on their turn as well. These bed properties can be described as a function of processes on an even

11 In case even this results in too large a number of layers, a series with a larger base number can be used: e.g. 1,3,9,27,81,... or 1,4,16,64,... days.

smaller level of aggregation. The description on these smaller levels of aggregation deals with individual flocs and individual cracks. These very small levels will not be dealt with currently. The process on these small levels are parameterised in the 'fundamental' bed properties at a larger scale level.

Using the concept of aggregation levels, there two steps are required to describe the erosive behaviour of the bed. The first is to find out the relation between the fundamental bed properties and the erodibility. The second step is to describe these bed properties as functions of time and depth. It is expected to be easier to determine the time and depth dependence of these fundamental parameters than of the dependence of the erosion parameters.

The process based models require a description of both the consolidation process and the time development of thixotropy (cohesion): "For bentonite, 5 μm quartz (not cohesive!) and probably other fine-grained, very cohesive sediments, the effects of gellation (=thixotropy) are significant and need to be considered. For these sediments, the parameters are dependent on the time after deposition and, more generally, on the strain rate history of the sediments. As with soils, this is a complex process and needs further investigation" [Lick, 2001]. However, it is already possible to describe the time dependent behaviour of a few of the strain rate history properties as a function of time and depth. The Gibson finite strain consolidation equation (see the next chapter) is able to describe the effective stress, the density and the permeability as a function of time. The main investigation of this chapter is to derive an erosion model that has this strain rate history as input for the erosion. Three examples will be given of research that relates the erosion coefficients to the density. But Lick also mentions that cohesion is another very important parameter. The influence of cohesion is not known yet, nor its time dependency. An assumption has to be made for this cohesion so that it can be used to calibrate the 1DV-waterbed model.

Example 6. Govindaraju et al. [1999] use the following formulation

$$E = M\left(\frac{\tau_b - \tau_{cr}}{\tau_{cr}}\right) \quad with \quad \tau_{cr} = \alpha\rho_d^{\beta} \tag{3.10}$$

where ρ_d is the dry density and α and β are empirical coefficients that have been obtained from laboratory experiments (Migniot 1968). Owen (1970) found $\alpha = 6.85\cdot10^{-6}$ and β=2.44 and Thorn and Parsons (1980) found $\alpha = 8.42\cdot10^{-6}$ and $\beta = 2.28$ [Mehta 1989]. The erosion coefficient M is still present in this approach, but the critical shear stress is formulated as a function of a more fundamental bed property: the dry density. The number of coefficients has increased however from 2 to 3. However, α and β are a parameterisation of processes on a smaller level of aggregation. (Note that the dimensions of α change when β changes.)

Example 7. Sanford et al. [2001] have tried to determine the continuous depth variation of the erosion parameters by extensive analysis of the results of an erosion experiment in an annular flume. They try to reconstruct these continuous profiles without knowing the bed properties as a function of depth. They present an erosion formulation that they consider a first step towards a unified erosion theory for fine sediments. It reads:

$$E = \rho_s\phi_s(z)\beta\cdot\left(\tau_b - \tau_{cr}(z)\right)H\left(\tau_b - \tau_{cr}(z)\right) \quad with \quad \tau_{cr}(z) = \tau_{cr,0} + \gamma\cdot z \tag{3.4}$$

where γ is the rate of increase of the critical density for erosion τ_{cr} with depth, β is a local coefficient [m/s/Pa], ρ_s is the sediment density, ϕ_s is the volume fraction of sediment and τ_{cr} is the critical shear stress for erosion. In their model, the change in the erosion rate coefficient M is attributed solely to the changes in density. The critical shear stress is set equal to the applied bed shear stress when the erodable material has been depleted.

They reconstruct the erosion rate coefficient M and the critical shear stress as a function of the total eroded mass m, rather than the eroded depth z. Their results show a smooth consistent increase of τ_{cr} as the total eroded mass m increases. The rate of increase in $\tau_{cr}(m)$ is most rapid at low values of m, just

below the initial sediment surface. The critical shear stress profiles approach $\tau_{cr}=0$ for non-zero values of m. They believe that that anomaly is due to the presence of a 'floc' or 'fluff' layer.

M increases rapidly with increasing m just below the sediment surface, but then tends to level out or decrease. They assumed that the changes in M were due to changes in ϕ_s. This means that the relation $M(m)$ should be of the same form as the relation $\tau_{cr}(m)$. Using such a relation clearly overestimates the M at larger m though. Accordingly, they conclude that their assumption of a linear increase of M with ϕ_s was the weakest point of their model-data comparison and it needs further study. This may indicate a less than linear dependence, or it may signify that some other source of variability has been neglected. It can for instance signify that the coefficient β is not constant, but decreases with increasing τ_{cr}. Or that the multiple-grain sizes have an influence. Or the armouring due to non-negligible sand fraction in their experiments.

In the above example one attempts to relate the erosion coefficient to the density without measuring the density profiles. It is most likely that such an incomplete approach will not succeed. The number of unknown parameters is too high: one has to determine both the coefficients and the density distribution from only erosion experiments. Lick et al. do measure both the erosion behaviour and bed properties.

Example 8. [Lick et al. 2001] investigated the relation between the erosion rate and various sediment properties with laboratory and field tests with Sedflume. They also measured the density profiles of the samples they exposed to Sedflume. A graph of the results can be seen in figure 3.2. They report a relation between erosion and bulk properties of the form

$$E = A\tau_b^n \rho^m \tag{3.8}$$

where τ_b is the bottom shear stress, ρ is the bulk density (varying with time and depth) and A, n and m are empirical parameters. These coefficients are different for each different sediment and depend on the bulk properties particle size, organic content, volume of gas, salinity and time after deposition. In this approach the erosion rate coefficient M from equation 3.1 is subdivided into ρ^m and a coefficient A. Note that this approach does not contain a critical erosion coefficients τ_{cr}. Lick et al. do not believe in the existence of a critical shear stress: they define it as the bed shear stress at which an erosion rate of 10^{-4} cm/s occurs (approx. 1 mm in 15 minutes).

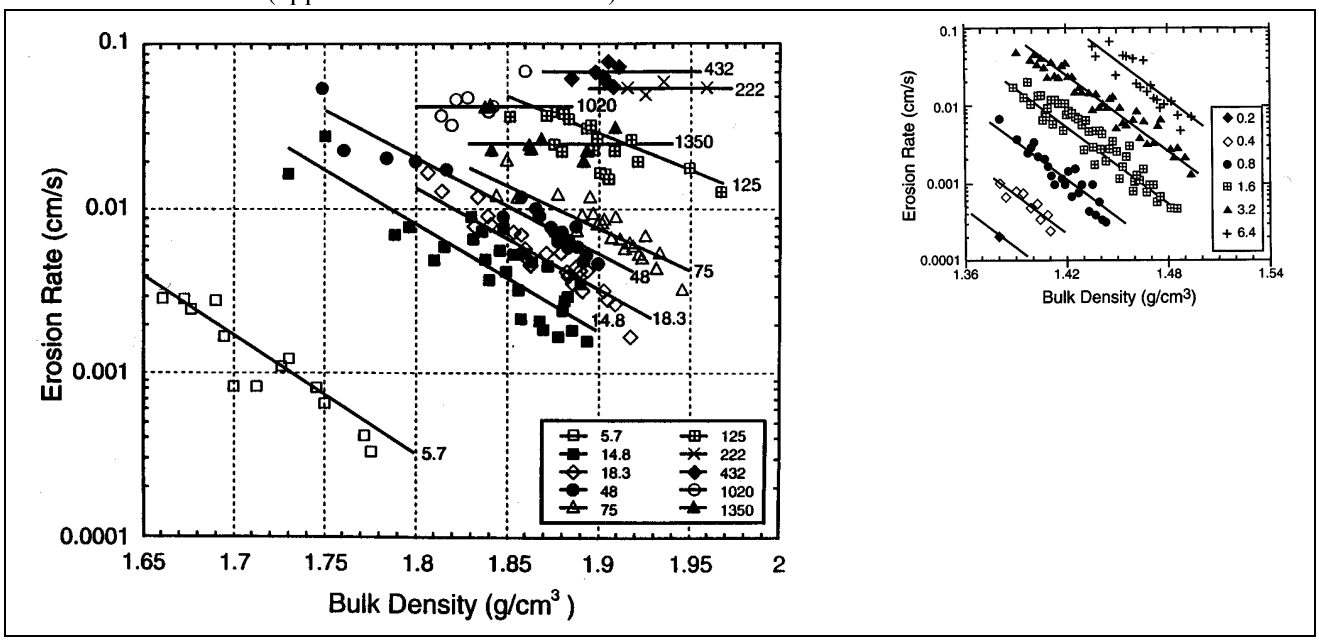

Figure 3.2. Erosion rates as a function of dry density measured with Sedflume. Left frame dependence on uniform particle size (μm) at shear stress of 1.6 N/m^2 and right frame dependence on bed shear stresses (N/m^2) and left. [Lick, 2001]

The relations between the erosion rate in [cm/s] and the bulk density in the semi-log plot of figure 3.2 are straight lines. The erosion rate is plotted in log scale, the bulk density on a linear scale. Lines that are straight in a semi-log plot can be described by an exponential function. When different bed shear stresses are applied the lines in the figure shift, but they keep the same slope. This indicates the presence of shear stress dependent factor. Accordingly, the formula for this behaviour is

$$E = A\tau_b^n \exp\left(\alpha\rho_b\right) \tag{3.9}$$

and not the power-law as given by Lick in equation 3.8. Probably the data are correct, and the formula is not. Anyway, the erosion rate can be related to the bulk density.

The research in the above examples yielded erosion tests on samples with known properties and relations between the erodibility and the density were derived (measured erosion test results + measured density profiles → erodibility relations). The above examples do not give a universal relation yet, but they do give hope in finding such a relation between the erosion coefficient and the fundamental bed properties in the near future. Since there are no better results known yet, these incomplete relations will have to be used. The goal of this thesis is to go the other way round. With the solution of the density profile by the consolidation equation, the bed shear strength profile can be constructed. This profile will be used in an attempt to simulate erosion experiments (calculated density profiles + assumption for erodibility relations → calculated erosion test results).

3.8 Stochastic parameters

3.8.1 Introduction stochastic nature of the bed shear stress

Most of the classical erosion formulations try to give a deterministic description of the erosion process. The bed shear stress however, the general factor causing erosion, is a stochastic variable. The bed shear stress is due to current shear and turbulence. For calculating the horizontal force on a current over a large area (as in Delft3D-flow), the local turbulence peaks can be averaged out. But when using bed shear stress to calculate the erosion of bed material, it is not correct to use one value of the bed shear stress by averaging out local peaks. The relation between the erosion and the bed shear stress is not necessarily linear. Therefore local peaks can be responsible for a more than average share of the erosion. “The stochastic behaviour of turbulence is probably an important aspect in the phenomenological description of erosion. The erosion process seems to be determined largely by burst-induced accelerations in the turbulent boundary layer. This effect, however, could not be quantified up till now [Winterwerp, 1989]” A few examples of cohesive sediment theories that take into consideration the probabilistic nature will be treated.

Example 9. Partheniades [1965] already recognised the probabilistic nature of erosion. He tried to give a description of the erosion rate by using a statistical distribution function of the bed shear. Therefore he assumed that the instantaneous, local shear stress τ_0 on the bed has a normal distribution with mean τ_b and standard deviation $\tau_b \cdot \eta_b$. He assumed the mean stress τ_b to be given by the common methods for the bed shear stress. The actual shear stress on the bed can become very large, but the very large shear stresses act only for a short period of time and on a small area.

The distribution of the inter-particle cohesive forces is narrow enough compared to the spread of the shear stress τ_b so that the strength can be considered as constant. The inter-particle forces C due to the cohesion were assumed constant and proportional to the cohesion c. The maximum tensile stress σ_{max} induced by flow at the joints of the clay particles or within the particles themselves, was taken proportional to the local shear stress τ_0. He used

$$\frac{\sigma_{\max}}{C} = k\frac{\tau_b}{c} > 1 \tag{3.11}$$

as a criterion for erosion, in which k is an overall proportionality factor. Assuming a normal distribution for the bed shear stress, the following general equation for the erosion rate was derived:

$$E = M \cdot p\left(\frac{\sigma_{\max}}{C} = k\frac{\tau_b}{c} > 1\right) = \frac{AD\rho_b}{t(\tau_0)}\left[1 - \frac{1}{\sqrt{2\pi}}\int_{-\frac{c}{k\tau_b\eta_b}-\frac{1}{\eta_b}}^{\frac{c}{k\tau_b\eta_b}-\frac{1}{\eta_b}} \exp\left(-\tfrac{1}{2}\omega^2\right)d\omega\right] \tag{3.12}$$

in which p is a probability, D is the average diameter of eroded particles or clay clusters, A is a dimensionless coefficient accounting for the shape of the eroded flocs, ρ_b is the bulk density of an individual eroded particle (!), $t(\tau_0)$ is the time required for a stress $\sigma_{\max} > C$ to act for the removal of a particle, ω is a dummy variable and E is the erosion rate in kg/m^2/s. The product M is a function of the soil properties while η_0 depends on the bed surface configuration and the flow conditions. Thus, the flow parameters and the soil properties have been distinctly separated. The integral in 3.12 (standard error function) is needed because the bed shear stress can be both positive and negative in a normal distribution while the failure at micro level is dependent on the absolute value of the bed shear stress only.

Example 10. The erosion formulation 3.2 is also based on a probabilistic approach. "The rate process theory, developed originally for chemical reaction rates, has since been interpreted heuristically to explain the dynamics of a variety of particulate systems undergoing time-dependent deformation including soil creep and erosion. With reference to erosion, flow-induced shear deforms the aggregates at the bed surface, and if due to this process, all the inter-particle bonds connecting an aggregate to its neighbours are ruptured, the aggregate will be entrained. A bond is broken when a certain minimum or threshold internal bond energy is exceeded. The shear stress and the bond strength are both stochastic variables, since the stress varies temporally at a given site, while the strength exhibits a spatial distribution at a given degree of consolidation. The threshold energy concept thus lends itself to a probabilistic description and the erosion rate expression relating the natural logarithm of the floc erosion rate ε_f to the excess shear stress ultimately results, the proportionality factor being temperature dependent due to the influence of temperature on electro-chemical bond strength. Analysis of the experimental results, after successful attempts to obtain a non-dimensional expression of the form of equation 3.1, yielded a best-fit relationship of the form $\ln \varepsilon / \varepsilon_f = \alpha \sqrt{(\tau - \tau_b)}$." [Parchure, 1985] As already mentioned, this relation is valid for very soft mud.

Example 11. The rate of deposition is generally described by [WL | Delft Hydraulics, 1999]

$$D = -w_s c P \tag{3.13}$$

where $w_s(c)$ is the (hindered) settling velocity, c is the concentration and P is the probability of deposition. P represents the fraction (of time) that the actual bed shear stress exceeds the critical shear stress for deposition. When there is no bed shear stress at all, in a lake for instance, all the sediment deposits (P=1). When the average bed shear stress is very large with respect to the critical shear strength for deposition τ_d, no sediment deposits at all (P=0). When assuming a linear relationship between P and the bed shear stres, in the interval $\tau_b < \tau_d$ (Krone, 1962)

$$P = \frac{\tau_b - \tau_d}{\tau_d} \tag{3.14}$$

this leads to

$$D = -w_s c\left(\frac{\tau_b - \tau_d}{\tau_d}\right)H\left(\frac{\tau_b}{\tau_d} - 1\right) \tag{3.15}$$

where H is the Heaviside function and D is the deposition rate in kg/m^2/s. For sediment particles larger than 200 μm Gessler (1967) showed that the probability function of distribution P could be described with a Gaussian distribution, or error function

$$P = erf\left(\frac{1}{2\sigma}\left(\frac{\tau_d - \tau_b}{\tau_b}\right)\right) \tag{3.16}$$

where σ is the standard deviation for the stress variation which Gessler determined to be about 0.57. To determine $P(\tau_b)$ the Gaussian distribution has to be integrated. An analytical formulation (error < 0.001%) of this integral is available, so the model is readily applicable for incorporation in computational models [Jones et al., may 2001].

3.8.2 Newly proposed erosion model with Rayleigh distribution of the bed shear stress

The above model of Partheniades (3.12) gave me the aspiration to construct a model with a similar, but simpler integral formulation. I assume a Rayleigh distribution for the actual bed shear stress τ_0 at one moment in time and at one infinitesimal area of the bed. An advantage of the Rayleigh distribution is that it does not allow negative bed shear stress to act. So we only have to deal with a probability of exceedence at one side of the bed shear stress spectrum. This makes the evaluation of the probability exceedence function easier. A property of the Rayleigh distribution is that it contains only one argument: the standard deviation is fully dependent on the average (fixed variance). A disadvantage of this is that the turbulence field might not be fitted accurately. An advantage of this is, however, that only one parameter has to be estimated when no data of the turbulence field are available. (This reduces the chance of large mistakes.)

In order to use the Rayleigh distribution, the regularly used bed shear stress τ_b is has to be related to the scale parameter (average μ) of the Rayleigh distribution. The regularly used bed shear stress τ_b is not necessarily equal to the average of the Rayleigh distribution (modal value or *rms*-value might also be possible). A coefficient α is proposed to relate the regularly used bed shear stress τ_b to the scale parameter μ of the Rayleigh distribution: $\mu = ½\cdot\tau_b\cdot\sqrt{(\pi/\alpha)}$, where μ is the average of the Rayleigh distribution.

The Rayleigh distribution can be used to formulate a failure criterion for the bed. This criterion reads as follows: erosion can only occur when the actual bed shear stress τ_0 (at one point at one moment in time) exceeds the actual strength τ_y of the bed. The actual strength τ_y is not the critical shear stress τ_{cr}, but it is the partially drained yield shear stress. This actual strength is at least equal to the critical shear stress and generally (much) higher. This unremolded yield strength can be calculated as a function of the density, the effective stress and the cohesion. The actual strength τ_y is considered a deterministic variable. The expectation is that the variation in the strength of the bed is much smaller than the variation in the local actual bed shear stress at one moment in time.

Once the above erosion criterion allows erosion, the bed is assumed to be eroded with erosion rate M. The erosion rate M is determined by the entrainment rate of the fluid and the permeability of the sediment. It describes how fast a particle can be loosened from the bed and abducted by the fluid, provided the local shear stress exceeds the local bed strength. M is a function of both the bed properties (permeability) and the fluid properties (entrainment rate). It should be possible to give a formulation of M in terms of these parameters. The argument of the Rayleigh function is also a function of both a fluid property (average bed shear stress) and a bed property (yield strength). The classical distinction between bed and fluid factors is not present in this model.

The resulting new erosion model reads:

$$E = M \cdot p\left(\tau_0 > \tau_y\right) = M \exp\left(-\alpha\left(\frac{\tau_y}{\tau_b}\right)^2\right) \tag{3.17}$$

where E is the erosion rate in kg/m^2/s, α is a scale parameter of the Rayleigh distribution, τ_b is the regularly used bed shear stress in Pa, M is the erosion rate in kg/m^2/s provided the local shear stress τ_0 (at one point at one monent in time in Pa) exceeds the local bed strength τ_y (in Pa). Figure 3.3 shows a graph of the Rayleigh distribution for α =0.5. In this case the regularly used bed shear stress τ_b equals the most probable

value (modal value) of the actual bed shear stress τ_0 (the value at the peak of the distribution) If α were equal to $\pi/4$, the regularly used bed shear stress τ_b would be equal to the average μ of the Rayleigh distribution. The parameters α and M have to be fitted on experimental data.

In an erosion test, where the bed shear stress is stepwise increased, the behaviour of this equation is as follows. As erosion progresses at a constant bed shear stress, the actual yield strength at the interface increases: accordingly p and the erosion rate become smaller. When the bed shear stress is stepwise increased again, p and the erosion rate suddenly increase again, after which it will slowly begin to decrease again.

The behaviour of 3.17 is fundamentally different from the formulations generally used. With equation 3.17 the erosion rate increases if the *deficit* bed shear stress *decreases*, while with the classical equations (3.1 to 3.3) the erosion rate increases if the *excess* bed shear stress *increases*. A second difference is that when we perform a *reduction ad absurdum* of 3.17, we see that the erosion rate is limited to M. With the classical equations, however, the erosion rate keeps on increasing if the bed shear stress increases and other formulations (bulk erosion) have to be used.

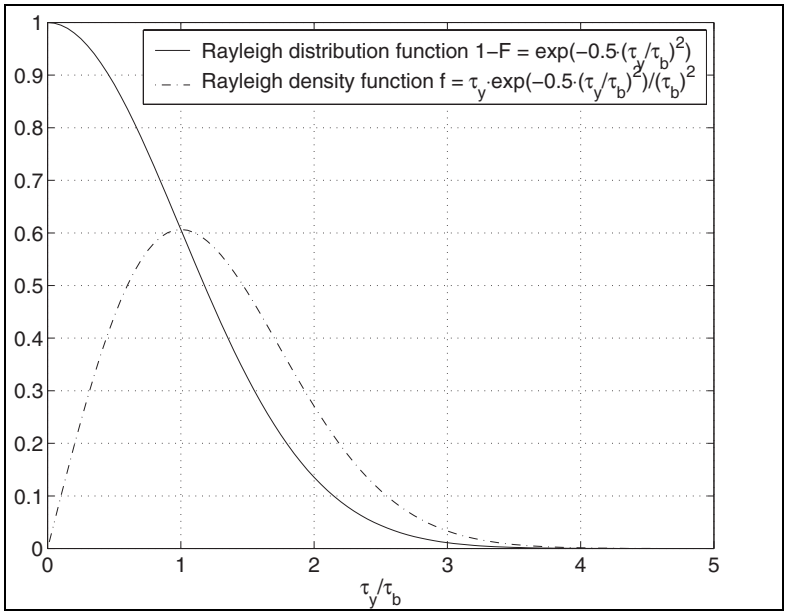

Figure 3.3. Erosion rates as a function of the actual yield strength τ_y and the regularly used bed shear stress τ_b with α=0.5

3.9 Bed yield shear stress

Merckelbach [2000] derived a relationship between the volume fraction of mud ϕ and the undrained principal yield shear stress τ_c in terms of microscopic properties (which will not be described here). The undrained principal yield stress τ_c is the yield stress in the failure layer (for which any orientation is possible), while the yield stress τ_y is the yield stress parallel to the bed. These two stresses are interrelated by the Mohr circle. This formulation of τ_c is based on a fractal description of the material at the micro-level. This yield stress τ_c acts in the failure plane and reads:

$$\tau_c = c_a'\phi + \tfrac{1}{3}\tan\varphi'\left(1+2K_o\right)K_{\sigma,0} + \tan\varphi'\sigma_0' \tag{3.18}$$

where c'_a is the true cohesion, ϕ is the volume fraction of mud, φ' is the angle of internal friction, K_0 is the coefficient of lateral stress, $K_{\sigma,0}$ is a empirical parameter describing creep and swell and σ'_0 is the effective stress. This formula looks similar to the Mohr-Coulomb failure criterion

$$\tau_c = c + w\sigma'_0 \tag{3.19}$$

where c is the cohesion and w is a coefficient. The first term in 3.18 is the cohesion due to thixotropy, the second term is the cohesion due to pre-stressing (overconsolidation) and the third term is the effective stress part. The first two terms account for the cohesion c in the Mohr-Coulomb criterion (3.19).

The first term in 3.18 represents the inter-aggregate strength. The other two terms describe the inter-particle bonds. Note that the first inter-particle bond term (the second term) is part of the cohesion, while the second inter-particle term (the third term) is the effective stress term in (3.19). Relation (3.18) may not be complete, since it is derived by simply adding the inter particle strength within the mud aggregates and the inter aggregate strength. Strengths however, cannot simply be added. We should first know the mode of failure at the micro level: do the inter-particle and the inter-aggregate strength act parallel or serial? Despite this objection, Merckelbach was able to describe measured strength profiles with (3.18) . The model is therefore considered applicable.

The term $c'_a\phi$ is a function of physico-chemical properties. Merckelbach assumed the effects of the inter-aggregate strength c'_a to be linear with the volume fraction of mud ϕ. Hence, there is also physical strengthening of the cohesion due to the increase in the volume fractions of mud ϕ. c'_a stands for the increase in true cohesion due to the development of bonds between the aggregates. The increase of the strength of the bonds c'_a in time is generally referred to as ageing or thixotropy. It can be seen as the chemical increase in strength (e.g. by electromagnetic forces, see section 2.2.3). The determination of the time dependent parameter $c'_a(t)$ describing the growth of the cohesion is hard to define and is therefore somewhat ambiguous. Determining the product $c'_a\phi$ on the long term is also complicated by the creep effect, which accounts for an increase of cohesion as well. In Merckelbach [2000] an increase of 1 Pa/day is mentioned for $c'_a\phi$ for periods up to 95 days.

The undrained principal yield stress τ_c acts in the plane of failure. The orientation of this failure plane depends on the ratios between the three stresses in the three independent directions. In a mud layer there is no distinction between the two stresses in the horizontal plane. That means that there are two options left. Merckelbach [2000] derived the relation between the yield stress τ_c in the plane of failure and the yield stress in the horizontal plane by means of the circle of Mohr. The following two options exist:

$$\tau_y = 2\frac{c_a'\phi_{clay}\cos\varphi' + \frac{1}{3}K_{\sigma,0}(1+2K_0)\sin\varphi'}{1+\sin\varphi'} + \left(K_0 - \frac{1-\sin\varphi'}{1+\sin\varphi'}\right)\sigma_v' \qquad (1-K_0)\sigma_v' > \tau_y \qquad (3.20)$$

and

$$\tau_y = c_a'\phi_{clay}\cos\varphi' + \tfrac{1}{3}K_{\sigma,0}(1+2K_0)\sin\varphi' + K_0\sin\varphi'\sigma_v' \qquad (1-K_0)\sigma_v' \le \tau_y \qquad (3.21)$$

where σ'_v is the vertical effective stress. The precise formulation depends on the ratio of the horizontal and the vertical plain stresses K_0. This ratio is not very well known in the field. This introduces a large uncertainty. A second source of uncertainty is that in equation 3.17 the bed shear stress τ_b will be compared to τ_y. The bed shear stress is not very well known either. For these reasons it is not considered necessary to perform a refinement to 3.18 as in 3.20 and 3.21 Therefore the main relation (3.18) will be used.

Some simplifications can be applied to equation 3.18. The model will be used to calculate the actual yield strength at the interface. At this level the effective stresses are almost zero (only the self-weight of one floc), so the effective stress term can be discarded. When substituting the constitutive relation of Merckelbach[2000] $\sigma'_v = K_\sigma\phi^n - K_{\sigma,0} \approx 0 \rightarrow K_{\sigma,0} = K_\sigma\phi^n$, (3.18) becomes:

$$\tau_c = c_a'\phi + \tfrac{1}{3}\tan\varphi'(1+2K_o)K_\sigma\phi^n \qquad (3.22)$$

where K_σ is an empirical effective stress coefficient. The angle of internal friction varies between 5° and 40° [Lambe, 1979], and K_0 varies between 0.3 and 3. That means that $\tan\varphi'(1+2K_0)/3$ is of order 1. Since $\sigma'_v = K_\sigma\phi^n$ in the virgin loading regime, the second yield strength term from 3.22 scales with the effective stress. Near the interface the effective stresses are zero, so the term $\sigma'_v = K_\sigma\phi^n$ is very small at the interface. The cohesion term $c'_a\phi$ dominates there. The yield strength near the interface is of paramount importance for the calculation of the erosion. That means that the undrained yield strength term with the largest uncertainty, the cohesion term, will have the dominant influence on the erosion characteristics. The term

$\sigma`_v = K_\sigma \phi^n$ can be calculated very well, but this term is not very important near the interface. Only when old layers with a high density are exposed to erosion at the top, can this term have a significant influence.

3.10 Summary

The aim of this chapter was to find or derive an erosion formula that is capable of dealing with seasonal variations. Despite lots of research, erosion of cohesive beds is not yet a well understood phenomenon. Erosion experiments are very important and a few types are discussed. A (literature) study has been made of the different erosion types. Very soft beds that have just been deposited, also known as fluid mud, can be re-entrained. The consolidating and settled bed can be subject to mass erosion when the bed shear stress becomes very large. However, mass erosion is not dealt with in this thesis, the bed will solely be exposed to surface erosion. Surface erosion can be limited (type I), or unlimited (type II) with respect to depth. Recent research states that the surface erosion type is dependent on the ratio between the characteristic time scale of the forcing and that of the bed. This insight makes it possible to merge surface erosion type I and II.

The basic erosion equations for surface erosion contain an erosion coefficient and a critical shear stress. It turns out that there is no general agreement on which formulation to use, nor on the way to determine the parameters required for these formulations. When the general erosion equations are nevertheless applied in order to model seasonal variations in sediment concentrations, it turns out that they are not able to describe an equilibrium bed. The model results show either a bed with net deposition, or a bed where the entire computational bed has been depleted (a clean bottom). In reality, equilibrium beds occur, where alternately erosion and deposition can occur without a clean rock bed in between. The model we are looking for should be able to deal with such a bed.

A widely used remedy for the inappropriate behaviour of the basic erosion models is to use a bed that consists of layers that become more resistant to erosion at larger depth. The number of layers is directly linked to the 'memory' of the model. So modelling seasonal variations with a regular approach will require the use of a huge number of layers. Using a set of layers in which each deeper layer covers a longer period of time (0-1, 2-4, 5-8, 9-16 days etc.) can remedy this. Moreover, the assignment of the erosion parameters to the layers can only be performed empirically or in a subjective manner. Even if such an approach can be used to simulate erosion tests, the erosive behaviour of future deposits cannot be modelled. A time parameter has to be included to account for this. The first option is to make the erosion parameters itself a function of time. Since the erosion parameters are not fundamental bed coefficients, this will not be a promising approach. A better approach is (i) to find out what the relation is between the erosion parameters and fundamental bed properties, and (ii) describe these fundamental bed properties as a function of time and depth.

With respect to (i), after a lot of experiments [Lick, 2001] concludes that the erosive behaviour of muds is largely dependent (among others) on (a) the bulk density and (b) the effects of gellation (thixotropy). With the Gibson equation of consolidation, it is possible to describe the bulk density profile as a function of time and depth. No model is (yet) available for the thixotropy however, so this effect has to be determined empirically. The thixotropy can be used to calibrate the 1DV-waterbed model however.

With respect to (ii), some erosion models that relate the erosion to the density already exist. These models do not have a physical basis however. Therefore, a new erosion formulation is proposed. This formulation regards the actual bed shear stress τ_o at one moment in time as a stochastic variable with a Rayleigh distribution, rather than the deterministic bed shear stress τ_b regularly used. In this formulation, erosion only occurs when the actual strength τ_y is smaller than the actual bed shear stress τ_0. The actual strength τ_y can be related to the density and the thixotropy with a model proposed by Merckelbach [2000]. Combining the Gibson equation of consolidation with this new erosion model, might lead to a new useful 1-DV water bed model. In the next chapter a consolidation model is developed for this aim.

4 Consolidation

In this chapter a consolidation model will be derived using finite strain consolidation theory of Gibson [1967 & 1981]. In section 4.1 the governing differential equation is described. This differential equation needs constitutive relations in order to be solved. These are treated in section 4.2. The constitutive relations of Merckelbach [2000] are used in the virgin loading regime. A few models will be presented for the reloading regime. The resulting model can calculate the density as function of time and depth. In section 4.3 the numerical solution is discussed. Fast parameterisation methods in general are described in section 4.4 One new, fast parameterisation, proposed by Merckelbach [2001], is dealt with in section 4.5. This parameterisation will be compared to the exact numerical solution. A summary is found at the end of this chapter.

4.1 Gibson equation for consolidation

Gibson [1967] derived a one-dimensional vertical (1-DV) consolidation equation in material coordinates time t and material depth ζ (with the rigid bottom of consolidating layer at ζ =0) and the void ratio e as the dependent variable. It gives a continuum description of the bed and is valid for one sediment fraction only. It contains an advection term and a diffusion term.

$$\frac{\partial e}{\partial t}+\Delta\frac{\partial}{\partial\zeta}\left[\frac{k}{1+e}\right]+\frac{1}{\rho_w g}\frac{\partial}{\partial\zeta}\left[\frac{k}{(1+e)}\frac{\partial\sigma_v^{'}}{\partial\zeta}\right]=0 \tag{4.1}$$

In this differential equation k represents the permeability, σ'_v the vertical effective stress (total stress minus water pressure), Δ the relative density of the sediment material and ρ_w the density of water. A few assumptions have been made to derive this equation. These are:

- The consolidation process is a one dimensional vertical process
- The pore water and the solids are incompressible and they are both homogeneous in composition.
- The consolidating layer is fully saturated
- The effective stress, i.e. the difference between the total stress and the pore water pressure, controls the strains
- Inertia effects are negligible
- The pore water flow relative to the particles can be modelled by Darcy's law.

Merckelbach [2000] showed that rewriting this equation using the volume fraction of mud

$$\phi=\frac{1}{1+e} \tag{4.2}$$

as the dependent variable rather than the void ratio e gives a simpler partial differential equation[12]:

$$\frac{\partial\phi}{\partial t}-\Delta\frac{\partial}{\partial z}\left[k\phi^2\right]-\frac{1}{\rho_w g}\frac{\partial}{\partial z}\left[k\phi\frac{\partial\sigma_v^{'}}{\partial z}\right]=0 \tag{4.3}$$

where z is the Eulerian coordinate. The Gibson equation can be obtained by using the following relationships.

Mass balance:

$$\frac{\partial\phi}{\partial t}+\frac{\partial\phi v_s}{\partial z}=0 \tag{4.4}$$

[12] Sills (1985) already expressed this equation in terms of the variable n, which is the same as ϕ.

with the effective 'settling velocity' v_s in the consolidating bed:

$$v_s = -k\left[\phi\Delta + \frac{1}{\rho_w g}\frac{\partial\sigma'_v}{\partial z}\right] \tag{4.5}$$

In order to solve the Gibson model, a relation between the effective stress σ'_v, the permeability k and the volume fraction of mud ϕ is necessary. These are called constitutive relations. These will be dealt with in the next section. The above 'settling velocity' v_s in the bed can be derived from the following relationships. The vertical force equilibrium (with ρ_s as the density of the sediment material and ρ_w as the density of water) reads:

$$g\left(\phi\rho_s + (1-\phi)\rho_w\right) + \frac{\partial\sigma_v}{\partial z} = 0 \tag{4.6}$$

The generalised Darcy law for pore water flow relative to the particles (with p_e as the excess pore pressure and v_f as the effective fluid velocity:) reads :

$$(1-\phi)\left(v_f - v_s\right) = -k\frac{1}{\rho_w g}\frac{\partial p_e}{\partial z} \tag{4.7}$$

Continuity:

$$v_s\phi + v_f(1-\phi) = 0 \tag{4.8}$$

Effective stress principle (with p_h as the hydrostatic water pressure):

$$\sigma_v = \sigma'_v + p = \sigma'_v + p_e + p_h \tag{4.9}$$

If it is assumed that the effective stresses are zero, then the diffusion term drops out of (4.5). If this is substituted in (4.4), the resulting equation (4.3) is similar to Kynch's sedimentation theory [1952], provided an appropriate formulation of the permeability k is chosen. Equation (4.3) without the diffusion term is a wave equation where the characteristic velocity is a function of the density. Only one boundary condition can be imposed at the upper boundary. To prevent sediment from settling through the rigid bottom and beyond in this model, the characteristic velocity has to approach zero near the rigid bottom. Kynch uses a relation of the form $v_s=\alpha(\phi-\phi_0)^\beta$ to account for this. This (implicit) formulation of $k(\phi)$ reduces v_s to zero if the concentration approaches ϕ_0. In the suspension phase the densities are still below the structural density. The clay particles do not form a volume-filling network there. For this phase Kynch's sedimentation theory has originally been developed.

The formulation of k used in the hindered settling regime (e.g. equation 4.22) is different than the formulation of k in the consolidating bed. In the formulations of k valid for the consolidating bed, v_s does not reduce to zero if the concentrations become high. Using such a formulation and discarding the effective stress term in (4.5) at the same time, would allow the sediment to settle through the rigid bottom and beyond. Consequently, when for k a formulation is used that is valid in the consolidating bed, the model cannot be used without the effective stress term in equation (4.5). When the diffusion is included, a second boundary condition can be imposed at the lower boundary of the bed. This boundary condition prevents sediment from settling through the rigid bottom and beyond.

It is also possible to combine mass balance (4.4) with two separate relations for k: one valid for the consolidating bed at levels where ϕ is larger than the structural volume (effective stresses present) and a hindered settling formulation at the levels where ϕ is smaller than ϕ_{gel} (no effective stresses present). Then one single model can be used from the interface water-air down to the rigid bottom of the waterbed. Merckelbach [2000] prepared a numerical model in Eulerian coordinates in this fashion. It can be used to simulate the settling behaviour in an entire settling column experiment. Winterwerp [2000] also prepared a model like this, including formulations for turbulence and flocculation, that can be used to simulate the behaviour of mud during a period up to a few tidal cycles.

However, high concentrated mud suspensions in which Kynch's theory is valid are not accounted for in the present 1-DV water bed model (chapter 2). Accordingly, a clear distinction is made between the bed and

the water, without any hindered settling above. One formulation for k can be used that is valid in the waterbed only. This equation will be described in the next section.

On the other hand, the 1-DV model reduces to Terzaghi's consolidation theory when cancelling the advection term and linearising the result. Terzaghi's consolidation theory describes infinitesimal strain consolidation, whereas Gibson's equation describes finite strain consolidation. Terzaghi's theory does not account for the effect of the reduced pore volume due to consolidation on the geometry and permeability of the bed. It assumes a constant permeability and can therefore handle only small strains. This theory is useful to describe the time dependent behaviour in consolidated clays. This theory is not suitable for freshly deposited mud beds, since large strains may occur. The more general consolidation model by Gibson is more appropriate.

When solving the Gibson equation in the Eulerian coordinate system, one is confronted with a moving water-mud interface. In a material (Lagrangian) coordinate system, the water-mud interface is fixed in time. The material coordinates (ζ,, t_m) relate to the Eulerian coordinates (z,t) as

$$\zeta = \int_0^z \phi\left(z^*,t\right)\, dz^* \text{ or vice versa } \frac{\partial \zeta}{\partial z} = \phi(z,t) \tag{4.10}$$

$$t_m = t \tag{4.11}$$

The associated transformation rules are:

$$\frac{\partial}{\partial z} = \frac{\partial}{\partial t_m}\frac{\partial t_m}{\partial z} + \frac{\partial}{\partial \zeta}\frac{\partial \zeta}{\partial z} = \phi\frac{\partial}{\partial \zeta} \tag{4.12}$$

and (using equation (4.4) for $\partial\zeta / \partial t$)

$$\frac{\partial}{\partial t} = \frac{\partial}{\partial t_m}\frac{\partial t_m}{\partial t} + \frac{\partial}{\partial \zeta}\frac{\partial \zeta}{\partial t} = \frac{\partial}{\partial t_m} - v_s\phi\frac{\partial}{\partial \zeta} \tag{4.13}$$

Notice that the real time t and the material time t_m are equal, but that their implication is quite different. In the partial derivative with respect to t_m in (4.13), not only the derivative with respect to the real time t is included, but also the rate of change due to the changing position of the 'observer'.

The result written in terms of the volume fraction of mud ϕ is:

$$\frac{\partial \phi}{\partial t_m} + \phi^2\frac{\partial v_s}{\partial \zeta} = 0 \tag{4.14}$$

with

$$v_s = -k\phi\left[\Delta + \frac{1}{\rho_w g}\frac{\partial \sigma'_v}{\partial \zeta}\right] \tag{4.15}$$

Combining these results (or transforming equation 4.3 directly) leads to equation (4.1) written in terms of ϕ:

$$\frac{\partial \phi}{\partial t_m} - \Delta\phi^2\frac{\partial}{\partial \zeta}[k\phi] - \frac{\phi^2}{\rho_w g}\frac{\partial}{\partial \zeta}\left[k\phi\frac{\partial \sigma'_v}{\partial \zeta}\right] = 0 \tag{4.16}$$

One needs initial and boundary conditions to solve this. The initial condition can be any density profile (or effective stress profile).

$$\phi(\zeta,0) = \phi(\zeta) \quad 0 < \zeta < \zeta_i \tag{4.17}$$

The first boundary condition is that the waterbed is assumed to have a rigid and impermeable bottom:

$$v_s(0,t) = 0 \Rightarrow \frac{\partial \sigma'_v(0,t)}{\partial z} = (\rho_s - \rho_w)g\phi \quad t > 0 \tag{4.18}$$

The second boundary condition is that the effective stresses are assumed to be zero at the interface:

$$\sigma'_v(0,t) = 0 \quad t > 0 \quad \zeta = \zeta_i \tag{4.19}$$

where ζ_i is the bed-water interface.

4.2 Constitutive relations

4.2.1 Virgin loading

Gibson's advection-diffusion-equation contains three dependent variables: ϕ, k and σ'_v. In order to solve the Gibson equation, relations for the effective stress σ'_v and the permeability k are necessary. Measured field and laboratory data in the virgin loading regime (see section 4.2.2) are known to be more or less adequately fitted by a wide variety of empirical relationships. These relations usually contain two and sometimes even more empirical parameters (dependent on the way of plotting: the offset, the slope and sometimes the curvature). For a summary of these relations see Den Haan (1992). A very common approach assumes a linear relation between the void ratio and the natural logarithm of the effective stress [Lambe , 1979]:

$$e = e_1 - C_c \log\left(\frac{\Delta\sigma`_{v,1}}{\sigma'_{v,1}}\right)^{-b} \tag{4.20}$$

where C_c is the compression index, e_1 is the reference void ratio, $\sigma`_{v,1}$ is the reference effective stress and $\Delta\sigma`_{v,1}$ is the effective stress with respect to this reference stress.

Kranenburg [1994] proposed a new approach to the constitutive relations, further elaborated by Merckelbach [2000]. On the basis of a fractal analysis of mud and of a series of experiments on soft muds, he derived a new set of constitutive equations that relate both the effective stress and the permeability to the volume fraction of mud ϕ. When solving the Gibson equation, one can use the following constitutive equations, where K_σ, K_k and D are empirical coefficients.[13]

$$\sigma'_v = K_\sigma \phi^{\frac{2}{3-D}} - K_{\sigma,0} = K_\sigma \phi^n - K_{\sigma,0} \tag{4.21}$$

$$k = K_k \phi^{-\frac{2}{3-D}} = K_k \phi^{-n} \tag{4.22}$$

where n=2/(3-D). These relations are simple power laws, but the parameters K_σ, K_k and D do have a better theoretical background. K_σ and K_k are a function of all kinds of microscopic properties of mud (e.g bond strength, viscosity) that cannot be determined themselves. These microscopic properties are lumped into the bulk variables K_σ and K_k that can be determined empirically. Hence they do give an insight in the nature of mud. Merckelbach [2000] also presents a way of determining these parameters by consolidation experiments with a suspension in a settling column. These methods will described and applied in chapter 7.

D is the fractal dimension of a mud and ranges theoretically from 2 to 3 (plate to sphere). In the water phase however, D has been observed to range from 1.7 to 2.3. Commonly observed fractal dimensions in the bed vary from 2.6 to 2.8 [Winterwerp, 1999] (making the power n range from 5 to 10). The fractal dimensions D for the permeability and the effective stress are theoretically the same, but in practice they can be different.

The variable $K_{\sigma,0}$ describes creep and relaxation processes. It accounts for the effect when effective stress decreases while the density (ϕ) does not, or, when the density increases, while the effective stress does not. However, $K_{\sigma,0}$ can also be applied to describe over-consolidation processes in fully plastic material. Then $K_{\sigma,0}$ stands for the pre-compression level (see next section): the effective stresses drop, but the density does not show a corresponding decrease.

Combining Gibson's advection-diffusion equation with the above constitutive equations, gives a non-linear partial differential equation with only ϕ (or σ'_v or k) as the dependent variable. The resulting equation is the staring point for the parameterisation, see section 4.4.

[13] Note that these constitutive relations are less advanced than the detailed consolidation process description given in section 4.1

4.2.2 History of loading: over-consolidation

The Gibson equation deals with the effects of the consolidation aspects of the bed, while the choice of a constitutive material model determines the computed consolidation behaviour of the bed. The fractal relations between the stress levels and the volume fraction of mud (equation 4.21 and 4.22) are only valid in the virgin loading regime. These fractal relations are normally called the VCL (Virgin Compression Line). In the virgin loading regime material has only been subject to stress levels increasing in time during its presence in the bed, never to a decrease in the stress level. A consolidation test can be modelled with the (virgin) fractal relation quite well. In the 1-DV waterbed however, erosion and deposition occur alternately. When erosion and deposition occur all the time, consolidation of the bed is alternated by swell. The fractal relations are not valid for swell. What happens when the bed swells?

Erosion of a top layer leads to total stress relief of the deeper layers of the bed. This results after some time in swelling or expansion of the bed (negative consolidation). This swelling does not happen immediately, since the flow of pore water is time-limited due to the resistance of the flow through the material. Initially, the pore pressures carry the full load and the effective stress does not change. In the case of erosion the 'load' is negative and hence the pore pressures are negative. Water flows into the bed due to the pressure gradient that results from the negative excess pore pressures. The excess pore pressures dissipate and after some time the excess pore pressures are gone. Consequently the effective stresses have decreased again to an equilibrium level and carry the full load. The structure however, does not change back to its original state: the density does not regain the value it had when it first experienced these effective stress levels.

This behaviour can be explained as follows. The deformations due to the consolidation are largely plastic: they occur due to rearrangement of the structure into a more compact state. The number of places where particles touch each other (bonds) per unit area increases this way. The difference of present stress level and historic stress level is 'remembered' by the number of these bonds. When a drop of the stress levels occurs, the number of bonds remains the same, whereas the fraction of effective bonds falls back. The particles will not come closer to each other until they experience stress levels higher than those met before. Only when the stress levels exceed the maximum historic stress level again, the consolidation proceeds and the density starts to increase again.

A graph of measurements of the effect of cyclic loading on the effective stress level and the density is given in figure 4.1. It is seen that there are different branches with different slopes in the e-log(σ'_v) state plane. These branches are called stress paths. The line BDF is the virgin loading curve. The lines AB, CD and EF are the reloading branches. In the three points B, D and F the reloading lines meet the virgin loading curve. If the e-log(σ'_v) state passes these points, the compressibility suddenly drops back from the reloading value (C_s) to the VCL value (C_c). When the load on material increases and decreases all the time, the (σ'_v, e) state in the bed moves up and down over the VCL line and the swell lines. At each stress level there are more values of the density possible. We can conclude that the relation between the void ratio and the effective stress levels in the case of swell is different from the relation at the VCL. The behaviour of the bed cannot be described with the relations (4.20) and (4.21) alone. A separate constitutive model for the reloading part of the regime is necessary to describe the behaviour of the bed.

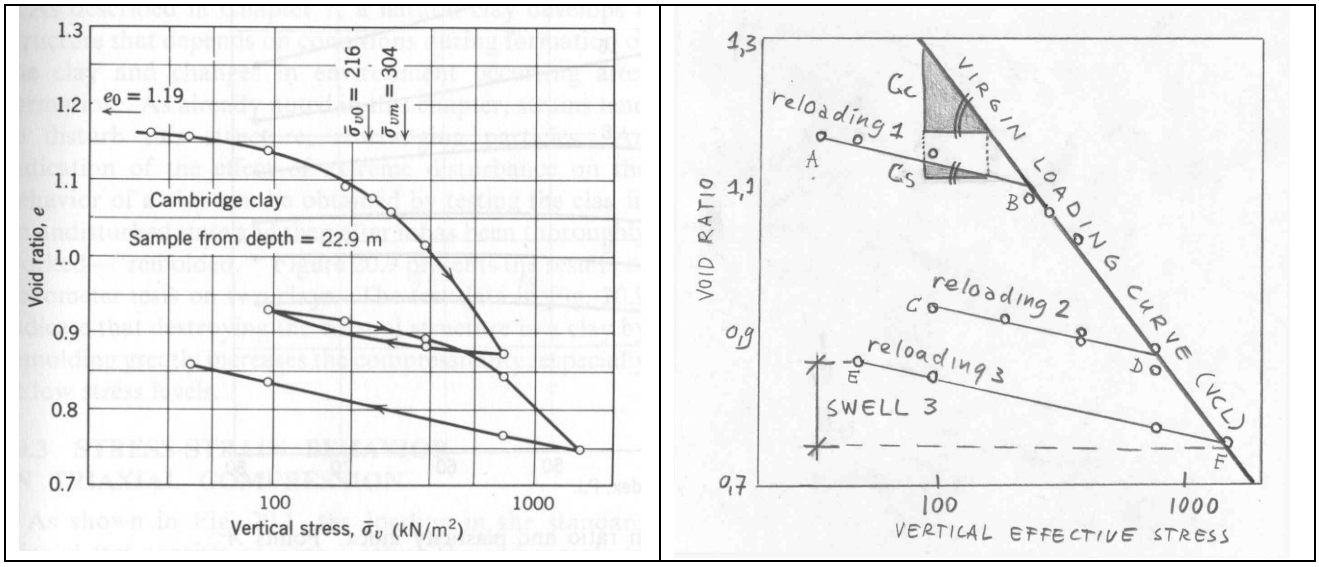

Figure 4.1. Cyclic loading of mud/clay [Lambe, 1979 p.299] (L) + explanation (R)

Material models for cyclic loading are diverse and the knowledge is less developed. Some knowledge is available however. Often the relation between the void ratio and the logarithm of the effective stress is linear according to equation (4.20) in the virgin loading regime. Often a linear relation is assumed between the void ratio and the logarithm of the effective stress in the reloading regime as well [Van Kesteren [1995]. In figure 4.1 one can see that both the virgin and the reloading branches are almost straight lines in the e-log(σ'_v) plane. The slope of the reloading line is called the swell index C_s. Generally C_c is a about factor 3 to 5 higher than C_s [Van Kesteren, pers. com.].

To describe the bed, a formulation of the two branches in the stress-density plane is necessary. Since fractal relation (4.21) is used, which is given in the ϕ-σ'_v plane, the relations valid for reloading will be given in these parameters as well. Different models are possible to describe the behaviour of the bed in the stiff reloading regime. Two extreme models are possible. They assume the material to be (i) fully elastic when the same constitutive relation is used for the virgin loading regime, or (ii) they assume it to be fully plastic, when the density is never allowed to decrease.

In reality the material will be neither fully plastic, nor fully elastic. The material will swell, but with a smaller stiffness than at first compression. The bed will not swell to it original density. The stiffness at swell is too small to assume an infinite $d\sigma'_v/d\phi$ and the difference between the stiffness at swell and the stiffness at compression is large enough to require a separate constitutive model for both the virgin loading and the unloading regime. Models that account for this will be chosen linear (on log scale) for reasons of simplicity, analogous to the material models for virgin loading. In these more linear material models two state variables are necessary, whereas for the two extreme models (i) and (ii) only one variable is necessary to describe the state of the bed (either σ'_v or ϕ, the other can be determined with 4.21). The models for the reloading curve require information of two kinds. First, the ratio between the stiffness of the virgin loading branch and the reloading branch is required. Second the swell state model has to include the point where it diverges from the virgin loading curve: the point $(\sigma'_{v,max}, \phi_{max})$, where $\sigma'_{v,max}$ and ϕ_{max} are respectively the effective stress and density at the intersection of the virgin loading curve and the swell curve. Since the point is on the virgin loading curve, $\sigma'_{v,max} = K_\sigma \phi^n_{max}$ holds, and one parameter is sufficient to describe this point. With the two parameters σ'_v and ϕ_{max}, the state of the bed is totally described, $\sigma'_{v,max}$ and ϕ can be determined with (4.21) and the formulation for the reloading branch.

A few useful descriptions are available for the linear swell models: (iii) the reloading branch is linear in the e-log(σ'_v) plane, (iv) in the log(ϕ)-log(σ'_v) plane or (v) in the ϕ-σ'_v plane. These descriptions lead to different models. All these models have the basic linear model concept that can be written as an explicit

function $\phi=(\sigma`_v,\phi_{max})$ where ϕ_{max} is the density at the intersection of the virgin loading curve and the swell curve and σ'_v is the effective stress.

A parameter generally used to 'remember' the load history, is the ratio of the effective *maximum past consolidation stress* at a certain material level to the current effective stresses. It is called the Over Consolidation Ratio (*OCR*). *OCR* is larger than one in the reloading regime and one in the virgin loading regime. [Lambe, 1979]

$$OCR = \sigma'_{v,max} / \sigma'_v \tag{4.23}$$

In figure 4.1 the effective stress on the sample in the field was 216 kN/m^2, while the maximum stress it ever experienced was 304 kN/m^2, so *OCR* = 304/216 = 1.45 (point B). When *OCR* and σ'_v are known, $\sigma'_{v,max}$ can be determined with (4.23) and ϕ_{max} can be determined with (4.21).

i) Fully elastic: The first model assumes that the stiffness at swell is the same as the stiffness at virgin compression. Fractal relation (4.21) is considered valid in both the virgin loading regime and in the swelling regime. The model will always result in the same equilibrium condition, irrespective if the initial condition is below or above this equilibrium profile. The bed does not have a memory of its historic loads. This can lead to very unrealistic results, of which one can see an example in figures 4.2 and 4.3.

In figures 4.2 and 4.3 the results are included of the behaviour of the consolidation with an artificial over-consolidated initial condition. This artificial initial condition is a uniform effective stress and a uniform density over the entire depth of the settling column. This strongly over-consolidated bed was allowed to consolidate with the same constitutive relation for virgin and reloading. One can see that the bed returns to the equilibrium condition associated with the consolidation of fresh deposited material. The interface height of the bed rises with 30%. A fully elastic model is obviously not appropriate.

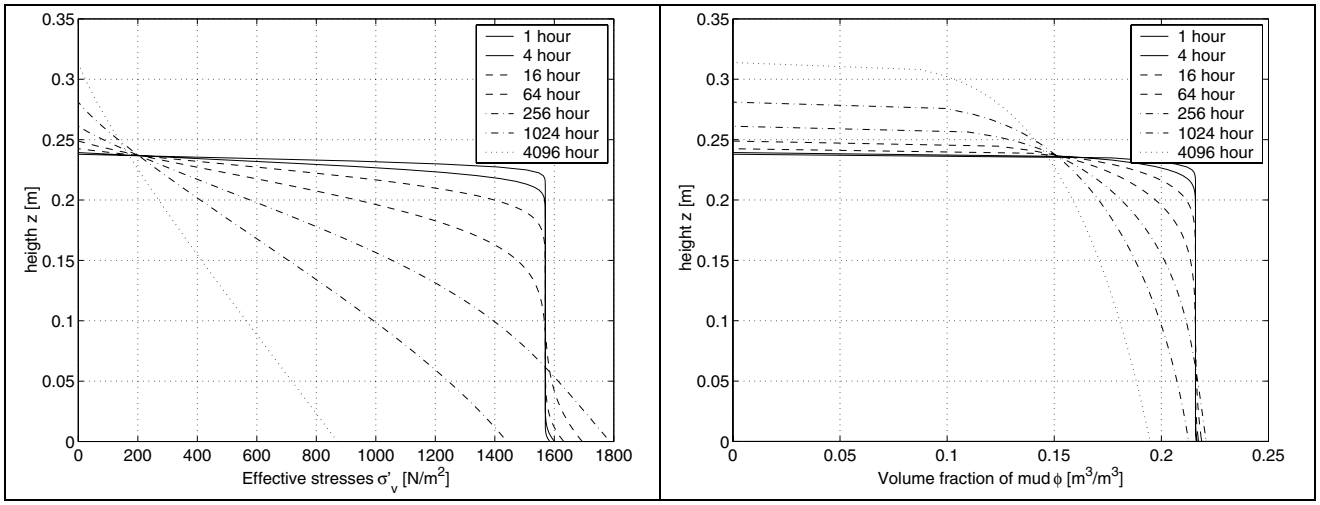

Figure 4.2 (L). The behaviour of the effective stress in a settling column with over-consolidated material without a 'memory' (elastic).

Figure 4.3 (R). The behaviour of the volume fraction of mud in a settling column with over-consolidated material without a 'memory' (elastic).

ii) Fully plastic: The stiffness of swell is much larger than the stiffness of compression. In figure 4.1 one can see results from experiments: the reloading curves (AB, CD and EF in figure 4.1) are much steeper ($\Delta\sigma'_v/\Delta e$ larger) than the virginal-loading curve (BDF in figure 4.1). This can be modelled by assuming an infinitely large $\Delta\sigma'_v/\Delta\phi$ (AB, CD and EF horizontal in figure 4.1). When we assume this, the compaction due to consolidation is 100 % plastic. In this case the level of compaction is a direct measure of historic stress levels. The neglect of this swell can be acceptable if the time scale of erosion is much smaller than that of the swelling (or if the erosion is small). This is the case when the bed does not have the time to

adjust to a new situation because the previous stress level is restored by sedimentation. When neglecting swell, the mud volume at a certain material level ζ never decreases, while the stress levels do decrease. Therefore accounting for the history is fairly simple. The volume fraction of mud only increases when the stress levels are high enough to compact it (higher than the maximum past historic stress). When the stress levels are too low, it simply keeps its old density: One can use the variable $K_{\sigma,0}$ for this purpose. In this approach $K_{\sigma,0} = OCR \cdot \sigma'_v$ is the level of pre-stressing: $K_{\sigma,0}$ remembers the difference between the present stress level and the maximal stress level in history. Constitutive relation (4.21) is still valid using the variable $K_{\sigma,0}$ only for over consolidation. This model contains the three state variables σ'_v, ϕ and $K_{\sigma,0}$. These three values are not independent: only 2 of these 3 variables have to be chosen to represent the bed, the third can be calculated. In terms of physics, σ'_v and ϕ are the most useful parameters. Therefore, in the model the stress and the volume of mud are used rather than the level of pre-stressing. The total fully plastic constitutive model becomes:

$$\phi(\zeta)_{new} = \max\left\{\phi(\zeta)_{old}, \left(\sigma'_{v,old}(\zeta)/K_\sigma\right)^{1/n}\right\} \tag{4.24}$$

In figure 4.4 and 4.5 one can see the behaviour of a suspension in a settling column with fully elastic (4.5) and fully plastic (4.4) behaviour. When relation (4.21) is used for both the virgin loading regime and the unloading regime, the density near the interface decreases to values below the structural density. In reality this does not happen. With the fully plastic model the interface between the initial profile (either suspension or consolidating mud bed) and the clear water above it is very sharp.

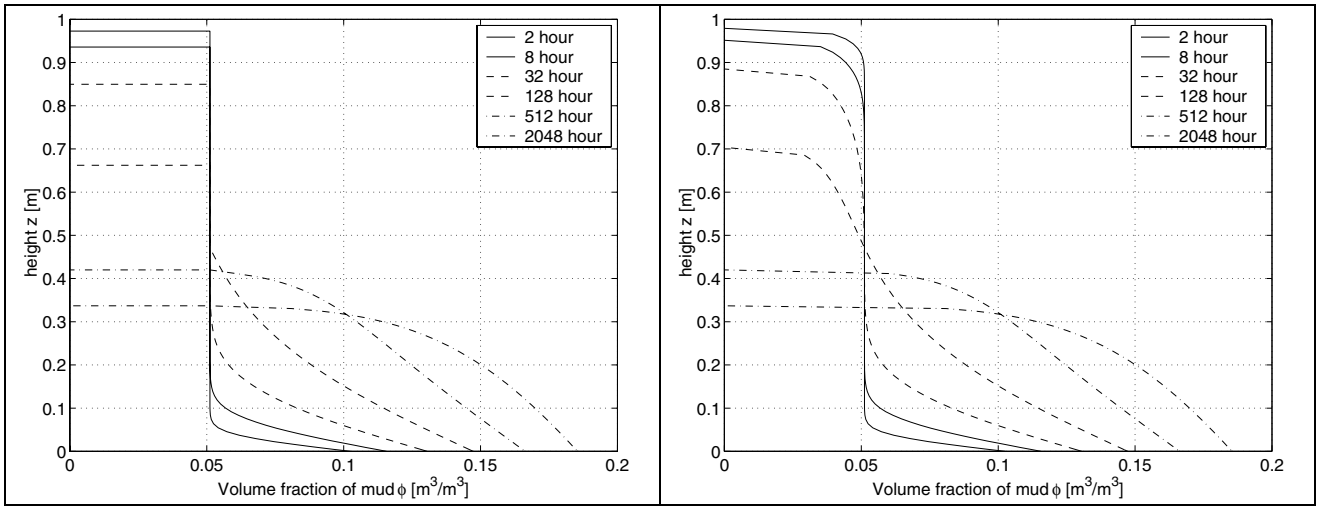

Figure 4.4 (L). The behaviour of the volume fraction of mud in a settling column with fully plastic material.

Figure 4.5 (R). The behaviour of the volume fraction of mud in a settling column with fully elastic material.

In reality the material will neither behave fully plastic, not fully elastic. Therefore, three models are discussed that allow the material to swell partially. For reasons of simplicity, these models will be straight lines on (semi) log scale. The models are: (iii) linear in the e-log(σ'_v) plane, (iv) linear in the log(ϕ)-log(σ'_v) plane or (v) linear in the ϕ-σ'_v plane.

iii) Linear in e-log(σ'_v) plane. The slope of the reloading relations can be assumed linear in the (e-log(σ'_v))-plane (lines AB, CD and EF in figure 4.1), as in equation 4.21. Lambe [1979] shows evidence that suggests that there is a linear relation between the void ration and the logarithm of the effective stress, both in the virgin loading regime and in the reloading regime. The ratio f between C_c and C_s is about 3 to 5 according to Van Kesteren [pers. com.]. The basic model concept is:

$$\frac{e_{\max}-e}{\log\sigma_v^{'}-\log\sigma_{v,\max}^{'}}=cons\tan t=\frac{1}{f}\frac{de}{d\log\sigma_v^{'}}\bigg|_{\phi=\phi_{\max}} \tag{4.25}$$

In figure 4.6 and 4.7, one of the lines AB, CD or EF from figure 4.1 is drawn in the ϕ-log(σ'_v) and the ϕ-(σ'_v) plane for different values of f. The fully plastic model (4.24) is a vertical line in these figures, whereas it would be a horizontal line in figure 4.1

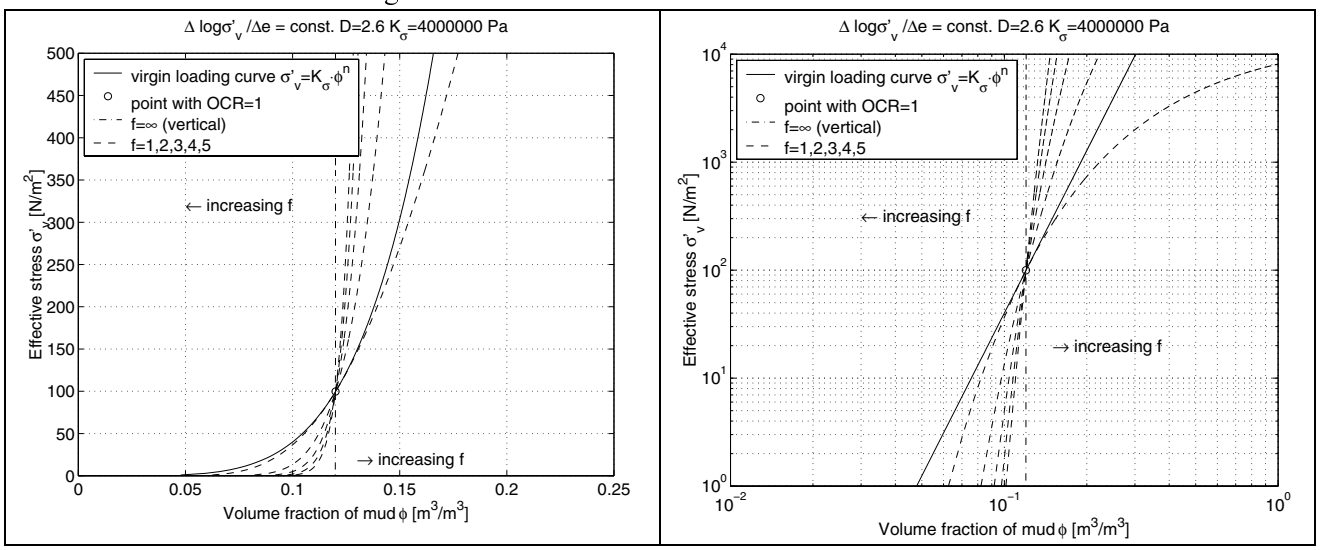

Figure 4.6 (L): Schematisation constitutive relation stress-volume fraction of mud (equation 4.30)

Figure 4.7 (R): Schematisation constitutive relation stress-volume fraction of mud at log scale (equation 4.30)

Combining

$$\frac{de}{d\log\sigma_v^{'}}=\frac{de}{d\sigma_v^{'}}\frac{d\sigma_v^{'}}{d\log\sigma_v^{'}}=\frac{de}{d\sigma_v^{'}}\sigma_v^{'} \tag{4.26}$$

and

$$e=\frac{1}{\phi}-1=\left[\frac{K_\sigma}{\sigma'_v}\right]^{\frac{1}{n}}-1 \text{ or } \sigma_v^{'}=K_\sigma\frac{1}{\left(1+e\right)^n} \tag{4.27}$$

and

$$\frac{de}{d\sigma'_v}=\frac{d}{d\sigma'_v}\left[\frac{K_\sigma}{\sigma'_v}\right]^{\frac{1}{n}}=-\tfrac{1}{n}K_\sigma^{\frac{1}{n}}\sigma'^{-(n+1)/n}_v \tag{4.28}$$

leads to

$$\frac{de}{d\log\sigma_v^{'}}\bigg|_{\phi=\phi_{\max}}=-\frac{1}{n\phi_{\max}} \tag{4.29}$$

When substituting 4.29 in 4.25, after some algebra, the result for the reloading branch of the constitutive relation reads

$$\phi\left(\phi_{\max},\sigma`_v\right)=-\frac{nf\phi_{\max}}{nf+\left(\log\sigma`_v-\log K_\sigma\phi^n_{\max}\right)} \tag{4.30}$$

We can see that if the effective stresses become very small, the volume fraction of mud does not reduce to zero. So when a deeper layer becomes the exposed interface (where the effective stress is zero), the density will not reduce to ϕ_{gel}. (If the effective stress becomes 1 Pa or smaller, log(σ'_v) becomes zero or even negative. And when σ'_v approaches zero, log(σ'_v) approaches -∞, leading to $\phi=0$. This reduction of ϕ was not

met in the simulations of chapter 7 however. A numerical example can illustrate this: when the effective stresses are only 0.1‰ of the maximum stresses $\sigma'_{v,max}$ and D=2.6, $\phi(\phi_{max}, \sigma'_v) = 0.2\phi_{max}$.)

In figure 4.6 and 4.7 we can see that the reloading branches lead to higher densities if the effective stresses are lower than $\sigma`_{v,\,max}$ and generally lead to lower densities if the effective stresses are higher than $\sigma`_{v,\,max}$. For one line, f=1, this does not hold: it leads to higher densities both in the reloading and in the virgin loading regime. This means that we cannot simply use the maximum of 4.30 and 4.21 to compute the volume fraction of mud.

iv) Linear in log(ϕ) -log(σ'_v) plane: The slope of the reloading relations can be assumed linear in the (log(ϕ)-log(σ'_v))-plane (figure 4.8 and 4.9), just like the material relations of Merckelbach [2000]. The fact that (4.21) is used for the virgin compression line, makes the choice of a Merckelbach-like relation for the reloading curve very logical. Lambe [1979] gives a similar function for both virgin loading and reloading as well. The basic model concept is

$$\frac{\log\phi - \log\phi_{max}}{\log\sigma_v^{'} - \log\sigma_{v,max}^{'}} = cons\tan t = \frac{1}{nf} \tag{4.31}$$

where f=1 is the virgin loading curve.
This can also be written as:

$$\log\phi = \log\phi_{max} + \tfrac{1}{nf}\left[\log\sigma_v^{'} - \log\sigma_{v,max}^{'}\right] \tag{4.32}$$

After some algebra it follows

$$\phi\left(\phi, \sigma`_v\right) = \phi_{max}^{1-\frac{1}{f}}\left[\frac{\sigma`_v}{K_\sigma}\right]^{\frac{1}{nf}} \tag{4.33}$$

Equation (4.33) can be written in the form of the virgin loading equation (4.21): $\sigma'_v = K^*_\sigma \phi^{n^*}$, where n^* gives the slope in the (log(ϕ)-log(σ'_v)) plane and K^*_σ is chosen to include the point (ϕ_{max},$\sigma'_{v,max}$). Since equation 4.33 always leads to larger values of ϕ in the reloading regime and always to smaller of ϕ values in the virgin loading regime (see figure 4.9), the following equation holds for all branches in the (σ'_v, ϕ)-plane.

$$\phi\left(\phi_{max}, \sigma`_v\right) = \max\left\{\phi_{max}^{1-\frac{1}{f}}\left[\frac{\sigma`_v}{K_\sigma}\right]^{\frac{1}{nf}}, \left[\frac{\sigma`_v}{K_\sigma}\right]^{\frac{1}{n}}\right\} \tag{4.34}$$

When the effective stresses reduce to zero, the volume fraction of mud becomes zero as well. That means that with this constitutive model the volume fraction of mud at the interface, where the effective stress is always zero, is always the same. Since the density at the interface determines the erosion rate, this reloading model will not lead to lower erosion rates of older material. This model is not very useful, although it would be logical to use it together with the virgin constitutive relationships that are also linear in the (log(ϕ)-log(σ'_v)) plane.

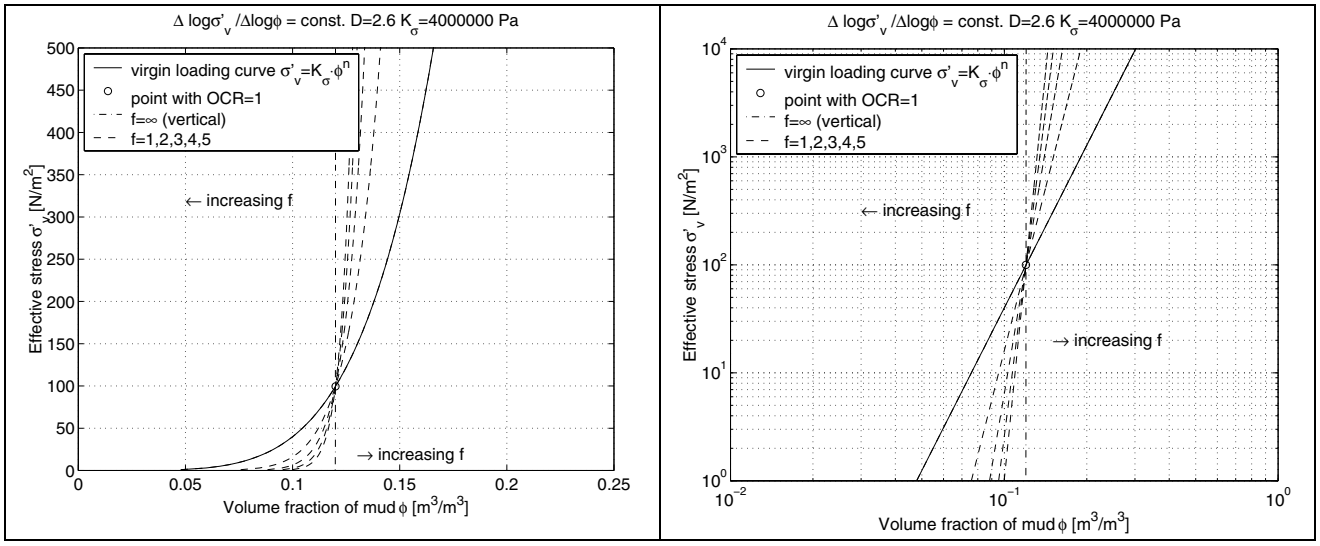

Figure 4.8 (L): Schematisation constitutive relation stress-volume fraction of mud (equation 4.34)

Figure 4.9 (R): Schematisation constitutive relation stress-volume fraction of mud at log scale (equation 4.34)

v) Linear in ϕ–(σ'_v) plane: The slope of the reloading relations can be assumed linear in the (σ'_v, ϕ)-plane (figure 4.10 and 4.11). The basic model concept is:

$$\frac{\phi-\phi_{\max}}{\sigma'_v-\sigma'_{v,\max}}=\text{constant}=\frac{1}{f}\frac{d\phi}{d\sigma'_v}\bigg|_{\phi=\phi_{\max}} \tag{4.35}$$

After some algebra this results in

$$\phi\left(\phi_{\max},\sigma'_v\right)=\phi_{\max}\left(1-\tfrac{1}{nf}\right)+K_\sigma^{-1}\,\tfrac{1}{nf}\,\phi_{\max}^{(1-n)}\sigma'_v \tag{4.36}$$

In this model the density does not reduce to zero if the effective stresses are used. Just like with model III, with this model it is not possible to use the maximum of 4.21 and 4.36 to compute the volume fraction of mud. All the reloading lines (with finite f) in figure 4.11 lead to higher densities in the virgin loading regime.

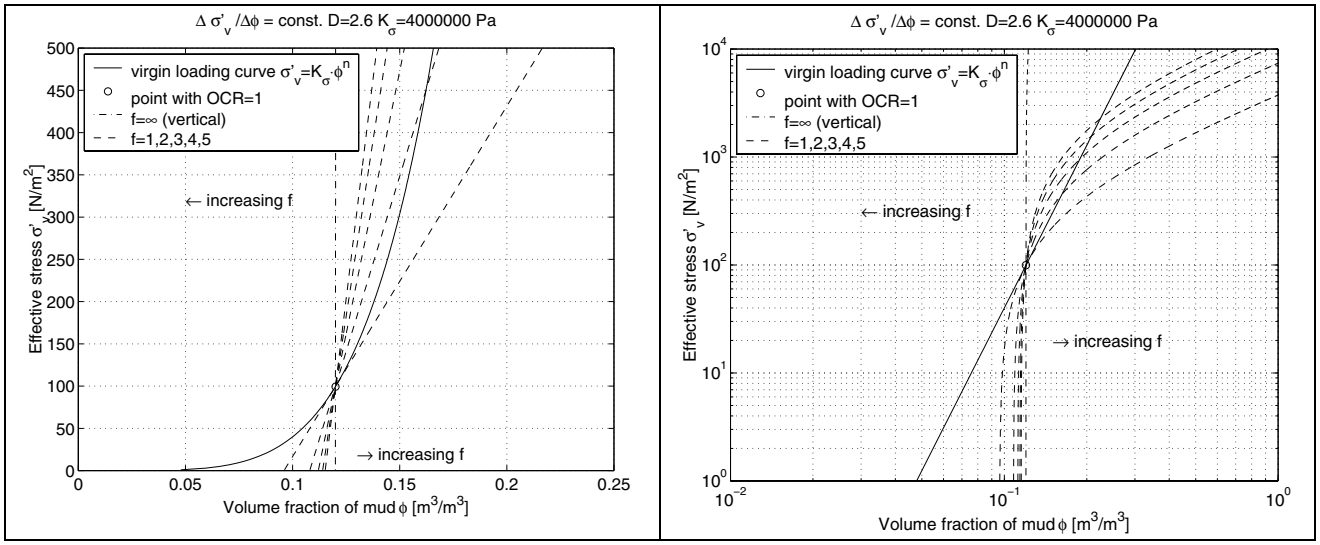

Figure 4.10 (L): Schematisation constitutive relation stress-volume fraction of mud (equation 4.36)

Figure 4.11 (R): Schematisation constitutive relation stress-volume fraction of mud at log scale (equation 4.36)

Conclusion: Two simple swell models and three linear swell models have been treated in this section. The simple swell models simplify the behaviour of swell too much to be useful. Swell model (iv) can not be used, since it always reduces the density to zero at the interface. Accordingly swell model (iii) and (v) remain. Model (v) could theoretically also reduce the density to zero at the interface all the time, but in normal situations it does not show such behaviour. Accordingly, swell model (ii) is theoretically the safest model to use. In practical situations both model (iii) and (v) can be used.

In chapter 7 the 1-DV waterbed model is be validated. The effect of the extreme swell models (i) and (ii) is shown there to explore the limits of the 1-DV water bed model. For validation and calibration the useful linear swell models (iii) and (v) are be applied.

4.3 Direct numerical integration

The 1-DV Gibson equation can be solved in a number of ways. The approach is dependent on the type of calculation one wants to make. The type of calculation depends on the application.

The Gibson equation has been solved numerically by Merckelbach [2000], both for the consolidating bed and the hindered settling regime. The results describe the measured profiles of a settling experiment very well at a vertical resolution of a few mm. To assure stability with the explicit method used, a time step of a few seconds was necessary. Accordingly, the calculation of a 30-cm settling column for a period of 100 days takes about an hour. It is very well suited for modelling the experimental results of a single settling column.

Another application of a full numerical solution to the Gibson equation could be to determine the consolidation in a mud depot. The mud properties are the same at every location in the depot, so a single 1DV calculation is sufficient to determine the behaviour of the whole depot. The use of a time consuming numerical method is not a disadvantage here. Van Kesteren en Kuijper of WL | Delft Hydraulics made the numerical model *DelCon* that can account for this in material coordinates. A new separate set of n material coordinates with constant permeability is introduced for every deposition that occurs on top of the depot. Each deposition event will therefore increase the number of grid points. The boundary conditions between all the layers are accounted for of course. In a mud-depot not often new material is added on top of the material already present in the depot, so the number of separate layers is limited.

The numerical methods above will not be very useful for the alternating erosion and deposition that the 1DV-waterbed model has to deal with. When considering a complex real estuary for instance, a numerical solution is far from practical: the different current conditions and the spatial segregation of the sediment make the use of multiple 1-DV calculations across the estuary necessary. Calculating the sediment exchange processes with the bed in each gridpoint of a large scale, long-term model numerically, requires lots of calculation time. Here the use of a fast parameterisation would be a better choice. In the next part of this chapter a fast parameterisation is derived. The results of the numerical model of Merckelbach are compared to the results of this parameterisation in order to judge if the parameterisation behaves realistically.

4.4 Discussion parameterisation methods

The full 1-DV Gibson equation can be parameterised in order to be able to describe quickly the changes in the waterbed between two deposition periods. These parameterisations will deal with the bed in material coordinates to prevent moving boundaries. But a parameterisation cannot account for (irregular patterns of) repeating periods of erosion and deposition, since the sediment fluxes affect the domain on which the parameterisation holds. (Only a constant deposition flux might be parameterised.) Therefore after each deposition and erosion period the analytical solutions have to be adjusted or redetermined. Erosion and deposition have short time scales with respect to erosion. Therefore the adjustment must happen at time scales that are short with respect with the time scale for consolidation.

Besides the irregular erosion and deposition pattern, the parameterisation has to be able to deal with any initial condition. The analytical solutions therefore consist of a series that have to be superposed to determine the solution. Many different series are possible, to name a few: perturbation method (polynomials), Bessel series, Fourier series and convolution series (Duhamel method).

One option is to regard the entire consolidating bed as one single layer. Every time sediment deposits, the initial conditions change as well as the domain. Consequently, the analytical solution has to be adapted to the new initial condition. Thus the model is divided into the time domain to cover each deposition period. Because the entire bed has to be incorporated in one solution, a large number of (Fourier) components might be necessary when the effective stress profile is not smooth, but contains sharp gradients.

A second option is to consider the bed as one layer and to deal with every sedimentation/erosion period in a separate solution by the method of convolution. In this method the initial condition of the first timestep has to be the equilibrium situation. The effect of the extra load of a single deposition or the effect of the reduction of load by a single erosion, can be accounted for by a single solution starting at the moment the load is applied. This solutions holds for the interface material height at the moment of erosion. The model is divided in the space domain and the time domain to cover each deposition. This single solution will have an everlasting effect on the bed and must be kept in the computer memory until the end of the simulation. Because it will last forever, and because the extra load it takes care of is very smooth (it is a block function), this solution can be represented by one term only. When time increases the number of depositions and erosion periods that have passed increases and therefore the number of solutions that have to be carried along increases. When for instance a period of 10 years is to be simulated with consolidation steps of 1 hour, at the end the number of solutions will be in the order of 100.000. Due to the large relaxation times of these solutions, they cannot be discarded at a specific moment in time. It takes for instance in the order of 100 years to reduce the effect of a single solution to 1%. Hence the model will run slower when time passes. This can perhaps be remedied by merging old solutions. Another problem is that the part of the domain on which a single solution holds, is in time affected by erosion. If first erosion occurs and then deposition, a certain solution will only be valid up to the level where the erosion progressed. In the upper part of the bed, that has been formed by depositions after the moment a particular solution started, the particular solution will not be valid at all. Therefore for every solution (i) the starting moment, (ii) the load it represents, (iii) its initial domain and (iv) its current domain have to be remembered. This leads to a large use of memory. This approach will be discarded as well.

A third way to deal with this analytical solution is to use a multilayer system. In this approach, for instance, every sedimentation period would result in a separate layer. The model is divided in the space domain to cover each deposition layer rather than to cover each deposition period. This results in complicated boundary conditions of the layers. An interface criterion has to be met between two successive layers: the bottom condition of a given layer should be equal to the upper boundary condition of the layer below. This results in a system of n -1 equations (where n = number of layers). For every layer, a separate set of coefficients has to be calculated to construct a separate solution. These coefficients cannot be determined by starting with the top (or bottom layer) layer and successively determining the solution of the layers below. The solution of a given layer is determined both by the solution in the layer above it and in the layer below it. Hence a large linear system has to be solved and linear systems are known to consume a lot of computational time. The number of terms can be very small however (1 to 3) when an appropriate series is chosen (not a Fourier series), because inside one layer the solution is very smooth. Despite this advantage, this approach is also expected to result in a larger number of calculations than the single layer system and is therefore discarded.

Both the multilayer system and the convolution approach are not appropriate. Therefore the single layer option will further be elaborated on.

4.5 Single layer parameterisation

4.5.1 Derivation of differential equation

The Gibson equation has been derived in section 4.1. This differential equation is valid both in the water column and in the consolidating bed. Different formulations for the 'permeability' have to be used in these two regimes in the vertical. In this section an analytical solution will be sought for the Gibson equation. This parameterisation will only be used in the consolidating bed, not in the water column. Therefore the constitutive material relations of section 4.2 can be used, that are valid for concentrations above the gelling point (structural density) only.

In the consolidating bed the Gibson equation is valid both in the virgin loading regime and in the reloading regime. When the constitutive relations of Merckelbach (4.20) and (4.21) are substituted however, the result is only applicable to the virgin loading regime. It can therefore only be used to describe the behaviour of consolidating material, not the behaviour of swelling material. When the Gibson equation should be applicable to both virgin and reloading, a constitutive relation that is valid in both these regimes should be substituted. In section 4.2 it was shown that the relations for reloading are different from those of virgin loading. Unfortunately such a complete relation does not exist at present. Therefore a mud bed alternately exposed to erosion and deposition cannot be described with one single differential equation with one state variable. It follows that a general parameterisation of the differential equation is not possible. In order to be able to make a parameterisation despite these problems, the model will be split in two parts. (i) The Gibson differential equation will be calculated with only the constitutive relations for virgin loading. The effective stresses are taken as the dependent state variable (the volume fraction of mud ϕ or the permeability k would also have been possible). This results in a non-linear partial differential equation with one dependent variable. The parameterised solution of this differential equation gives the effective stress profile. (ii) With this effective stress profile, the density will be calculated using the constitutive relations for reloading. To perform step (i), the constitutive equations 4.21 and 4.22 have to be rewritten. This gives

$$\phi = \left(\sigma_v^{'} / K_\sigma\right)^{\frac{3-D}{2}} \tag{4.37}$$

and

$$k = \frac{K_\sigma K_k}{\sigma_v^{'}} \tag{4.38}$$

Substituting 3.37 and 4.38 in 4.16 gives

$$\frac{\partial \sigma^{'}}{\partial t_m} + A_1 \cdot \sigma_v^{'\frac{2-n}{n}} \left(\frac{\partial \sigma_v^{'}}{\partial \zeta}\right)^2 + A_2 \cdot \sigma_v^{'\frac{2-n}{n}} \frac{\partial \sigma_v^{'}}{\partial \zeta} - A_3 \cdot \sigma_v^{'\frac{2}{n}} \frac{\partial^2 \sigma_v^{'}}{\partial \zeta^2} = 0 \tag{4.39}$$

where

$$A_1 = \tfrac{1}{\rho_w g} K_k \left(n-1\right) K_\sigma^{\frac{n-2}{n}} \tag{4.39a}$$

$$A_2 = \Delta K_k \left(n-1\right) K_\sigma^{\frac{n-2}{n}} \tag{4.39b}$$

$$A_3 = \tfrac{1}{\rho_w g} K_k n K_\sigma^{\frac{n-2}{n}} \tag{4.39c}$$

The initial condition can be any effective stress profile

$$\sigma_v^{'}\left(\zeta,0\right) = \sigma_{v,0}^{'} \quad 0 < \zeta < \zeta_i \tag{4.40}$$

where the subscript i stands for bed-water interface. In the case of a single layer, the boundary conditions for Gibson equation (4.39) are (4.18) and (4.19). The first boundary condition implies that the layer has a rigid and impermeable bottom, so the settling velocity is zero there:

$$\frac{\partial \sigma_v'(t_m,\zeta_i)}{\partial \zeta} = -(\rho_s - \rho_w)g \quad t_m > 0 \tag{4.41}$$

The second boundary condition (4.19) implies that the effective stresses at the interface are 0:

$$\sigma_v'(t_m,0) = 0 \quad t_m > 0 \tag{4.42}$$

The complexity of the problem is reduced if the deviation of the actual stress from the equilibrium stress is considered instead of the actual effective stress itself. In the stationary case $\partial \sigma_v' / \partial t_m \approx 0$, which implies

$$\sigma_{v,\infty}' = p_e + \sigma_v' = (\rho_s - \rho_w)g(\zeta_i - \zeta) \tag{4.43}$$

The deviation of the actual effective stress σ'_v from the equilibrium stress $\sigma'_{v,\infty}$ equals the excess water pressure p_e. A last step to simplify the differential equation is to rewrite the problem in a dimensionless depth coordinate ξ and a time coordinate τ:

$$\frac{\partial p_e}{\partial \tau} + \frac{n-1}{n}\frac{1}{\sigma_v'}\left(\frac{\partial p_e}{\partial \xi}\right)^2 + \frac{n-1}{n}(\rho_s - \rho_w)g\frac{\zeta_i}{\sigma_v'}\frac{\partial p_e}{\partial \xi} - \frac{\partial^2 p_e}{\partial \xi^2} = 0 \tag{4.44}$$

where

$$\xi = \frac{\zeta}{\zeta_i} \tag{4.45}$$

where ζ_i is the interface material height and

$$\tau = \frac{t}{T} \quad \text{with} \quad T = \frac{\rho_w g \zeta_i^2}{K_k K_\sigma^{\frac{n-2}{n}} n \sigma_v'^{2/n}} \tag{4.46}$$

Notice the presence of the (still) unknown stress σ_v' in the differential equation besides the coefficients A_1 and A_2 due to which the dimensionless time τ is not constant with depth.

4.5.2 Parameterisation

Up to this point no further simplifications or assumptions have been made. The resulting differential equation 4.44 in non-dimensional material coordinates is non-linear. The coefficients A_1 and A_2 to the advection terms in (4.39) are functions of the unknown and depth variable effective stress σ'_v. After a timestep *dt* the effective stresses have changed and therefore the coefficients will have changed. Accordingly the analytical solution will be different after a time step *dt*. That means that an explicit analytical solution cannot be constructed by using the initial conditions.[14] Consequently, we can conclude that finding an analytical solution is difficult and some simplifications have to be made. First of all, the non-linearity has to be overcome. Therefore the two non-linear advection terms will be ignored for reasons of simplicity. The remaining terms of 4.44 are

$$\frac{\partial p_e}{\partial \tau} - \frac{\partial^2 p_e}{\partial \xi^2} = 0 \tag{4.47}$$

This differential equation is the starting point for the parameterisation. The boundary conditions are given by:

$$p_e(1,\tau) = 0 \ (\tau > 0) \text{ (Neumann boundary condition)} \tag{4.48}$$

[14] An implicit solution could be possible, e.g. the curve $\sigma'_v(t_m)$ with the curve $\zeta(t_m)$.

$$\frac{\partial p_e(0,\tau)}{\partial \xi} = 0 \ \left(\tau > 0\right) \text{ (Dirichlet boundary condition)} \tag{4.49}$$

The initial condition is given by

$$p_e(\xi,0) = p_0(\xi) \ \left(0 < \xi < 1\right) \tag{4.50}$$

The problem resembles the classical consolidation equation. The solution to this problem is found in all kinds of literature, for instance Barends [1992]. It can be derived using the method of separation of variables. The solution reads:

$$p_e(\xi,\tau) = \sum_{k=1}^{\infty} f_k \exp\left(-\pi^2\left(k-\tfrac{1}{2}\right)^2\tau\right)\cos\left(\pi\left(k-\tfrac{1}{2}\right)\xi\right) \tag{4.51}$$

where the coefficients are

$$f_k = 2\int_0^1 p_0(\xi)\cos\left(\pi\left(k-\tfrac{1}{2}\right)\xi\right)d\xi \tag{4.52}$$

The number of Fourier components will be discussed in chapter 5. The effective stress in the non-dimensional time τ (equation 4.46) is assumed constant and equal to the highest possible equilibrium stress in the bed: $\sigma'_v = \sigma'_{v,rep} = (\rho_s - \rho_w)g\zeta_i$.

Analytical coefficients f_k are only available for analytical profiles. For the initial condition in a settling column for example, where initially the excess pore pressures carry the full load $\sigma'_{v,\infty}$ (equation 4.43), the coefficients can de determined analytically.

$$f_k = 2\int_0^1 (\rho_s - \rho_w)g\zeta_i(1-\xi)\cos\left(\pi\left(k-\tfrac{1}{2}\right)\xi\right)d\xi = \frac{8(\rho_s-\rho_w)g\zeta_i}{\pi^2(2k-1)^2} \tag{4.53}$$

In WAQ the profiles are subject to alternating erosion and deposition. The profiles can therefore have any shape. Consequently, the coefficients are calculated by numerical integration using the trapezoidal rule for integration.

The last steps to obtain the solution for the effective stress is to revert solution (4.51) to dimensional variables and subtract the (dimensional) solution from the steady state solution.

The effective stresses are a function of the dimensionless time parameter ι and the non-dimensional parameter ξ. The time parameter τ itself is a function of numeric coefficients and of the effective stress $\sigma'_v(\xi,\tau)$. Therefore the parameterisation is in fact non-linear as well. Near the interface, the effective stress $\sigma'_v(\xi,\tau)$ is smaller and accordingly the dimensionless decay time τ is larger (equation 4.46). A representative value of the effective stress in 4.46 has to be chosen to use the parameterisation. If the σ'_v-profile is already close to the steady state solution, the maximum equilibrium stress in the layer $\sigma'_v = (\rho_s - \rho_w)g\zeta_i$ can be used.

The evolution of the effective stress profiles can be calculated with the parameterisation in the virgin loading regime. In the reloading regime it is not valid, because the model is derived by substituting the constitutive relations of Merckelbach, which are only valid in the virgin loading regime. Since no better parameterisation has been derived, the current parameterisation is used to calculate the effective stress both in the virgin and in the reloading regime. In the virgin loading regime the density associated with the effective stress level is calculated by equation 4.21, in the reloading regime one of the linear or plastic constitutive relations for reloading from section 4.2.2 is used.

4.5.3 Comparison of parameterisation and numerical solution for settling column experiment

In this section the validity of the parameterisation is assessed. The behaviour in a settling column is simulated with the numerical model of Merckelbach [2000] and the parameterisation (with the assumption that $\sigma'_v = (\rho_s - \rho_w)g\zeta_i$ in equation 4.46). The results for the effective stress and the volume fraction of mud are

compared in figure 4.12 to 4.15. In figure 4.16 and 4.17 the difference between the numerical solution and the analytical solution is shown and in figures 4.18 and 4.19 the ratio between the numerical solution and the parameterisation.

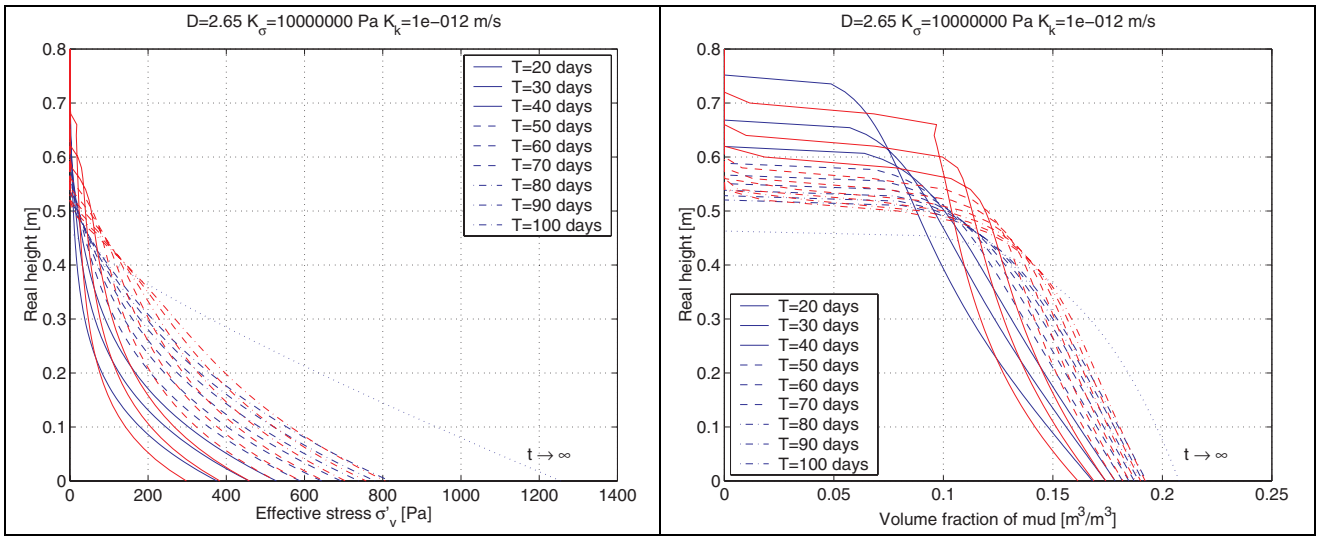

Figure 4.12 (L): The effective stress profiles in real coordinates at different moments in time by the numerical solution (red) and the parameterisation (blue).

Figure 4.13 (R): The profile of the volume fraction of mud in Gibson material coordinates at different moments in time by the numerical solution (red) and the parameterisation (blue).

From the results we conclude that the parameterisation gives reasonable results. The difference between the numerical solution and the parameterisation is largest near the interface. Here, the effective stresses and the density are underestimated by the parameterisation. This is in accordance with the numerical findings of Gibson [1981]. Accordingly, the density and the associated shear strength (equation 3.22) will be underestimated. That is inconvenient since the parameterisation should especially be valid near the interface, as it is used to calculate the resuspension from the bed by means of the density at the interface.

The difference between the numerical solution and the parameterisation is due to the deletion of the non-linear advection terms. Therefore an analysis of the different terms in the equation 4.39 will be carried out to find out how the various terms contribute to the differential equation. The full numerical solution is substituted in the differential equation (differentiated discretely). The parameterisation (with two Fourier components) is substituted in 4.39 as well (differentiated analytically). Even though the advection terms are not included in the parameterisation, it is still possible to calculate these terms with the solution of the parameterisation). The results are compared in figures 4.20 to 4.24.

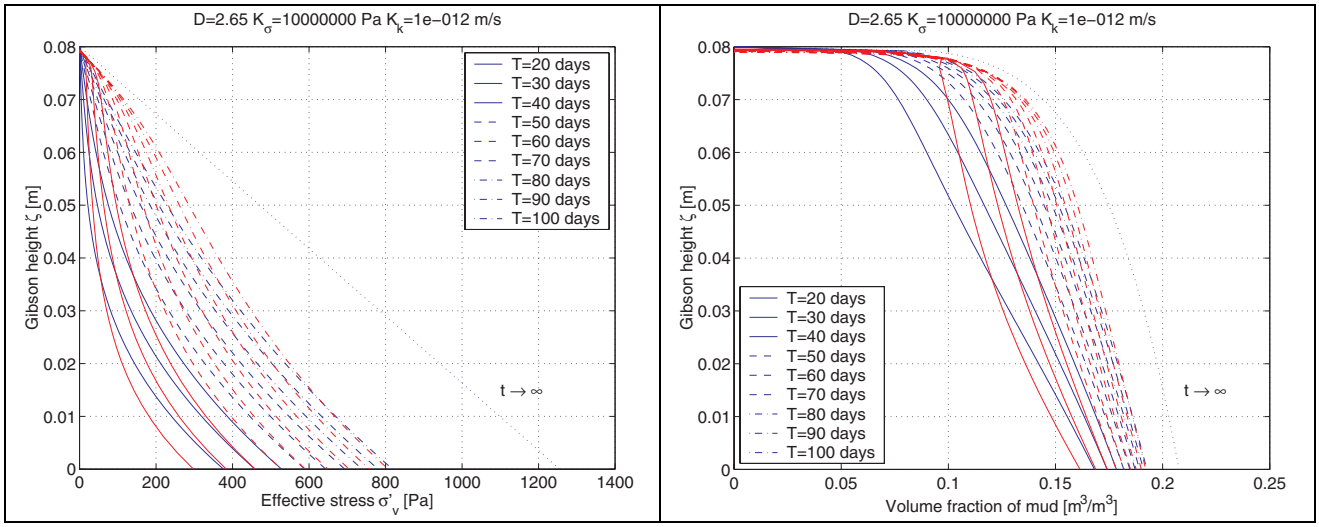

Figure 4.14 (L): The effective stress profile in Gibson material coordinates at different moments in time by the numerical solution (red) and the parameterisation (blue).

Figure 4.15 (R): The profile of the volume fraction of mud in Gibson material coordinates at different moments in time by the numerical solution (red) and the parameterisation (blue).

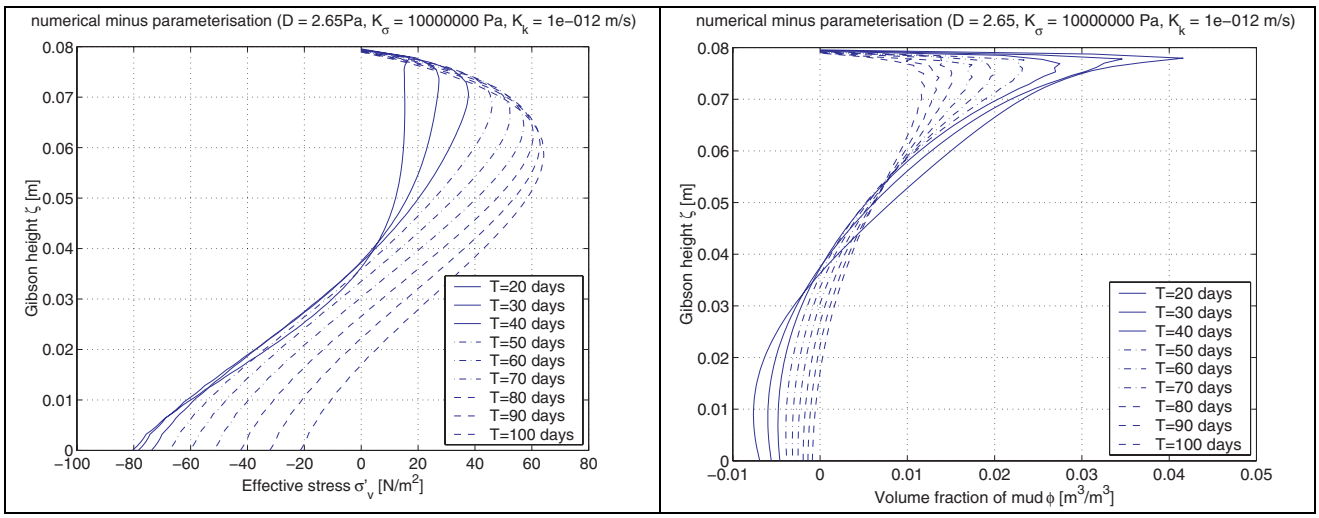

Figure 4.16 (L): The difference between the effective stress profiles in Gibson material coordinates at different moments in time as obtained by the numerical solution and the parameterisation.

Figure 4.17 (R): The difference between the profiles of the volume fraction of mud in Gibson material coordinates at different moments in time as obtained by the numerical solution and the parameterisation.

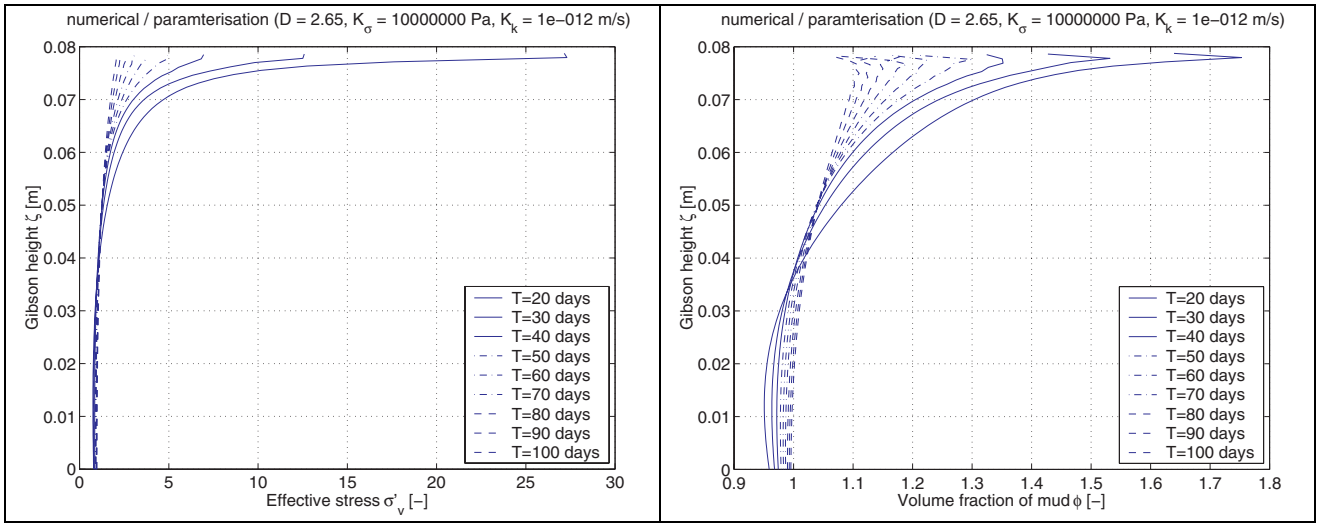

Figure 4.18 (L): The ratio between the effective stress profiles in Gibson material coordinates at different moments in time as obtained by the numerical solution and the parameterisation.

Figure 4.19 (R): The ratio between the profiles of the volume fraction of mud in Gibson material coordinates at different moments in time as obtained by the numerical solution and the parameterisation.

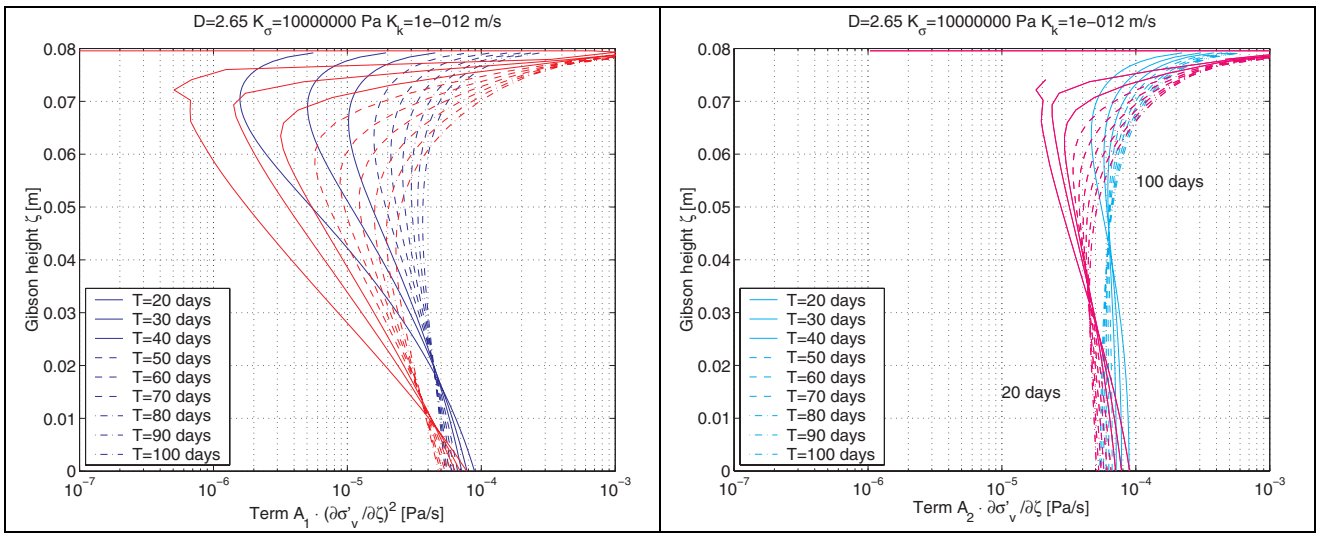

Figure 4.20 (L): The second (squared advection) term in equation 4.44 in Gibson material coordinates at different moments in time as obtained by the numerical solution (red = positive) and the parameterisation (blue = positive).

Figure 4.21 (R): The third (advection) term in equation 4.44 in Gibson material coordinates at different moments in time as obtained by the numerical solution (pink = negative) and the parameterisation (light blue = negative).

From figures 4.20 to 4.22 we can conclude that the two non-linear advection terms are equally important: they are of the same order of magnitude. Only at the start of the consolidation the squared advection term (no. 2) is one order of magnitude smaller than the linear advection term (no. 3). The ratio between these two non-linear advection terms can also be estimated be analytically:

$$\frac{term\ 2}{term\ 3} = \left(\frac{n-1}{n} \frac{1}{\sigma'_v} \left(\frac{\partial p_e}{\partial \xi} \right)^2 \right) \Bigg/ \left(\frac{n-1}{n} (\rho_s - \rho_w) g \frac{\zeta_i}{\sigma'_v} \frac{\partial p_e}{\partial \xi} \right) = \frac{1}{(\rho_s - \rho_w) g \zeta_i} \frac{\partial p_e}{\partial \xi} \tag{4.54}$$

In the initial stage of consolidation, the effective stresses are almost zero and the excess pore pressures carry all the weight $\sigma'_{v,\infty}$. Consequently the gradient $\partial p_e / \partial \xi$ can be estimated as

$$\partial p_e / \partial \xi = (\partial p_e / \partial \zeta)(\partial \zeta / \partial \xi) = (\rho_s - \rho_w) g \zeta_i \tag{4.55}$$

When this is substituted in 4.54, this leads to a ratio of unity between the two advection terms: they are equally important in the initial moments of consolidation. This means that both terms have to be dealt with when an attempt is made to improve the parameterisation.

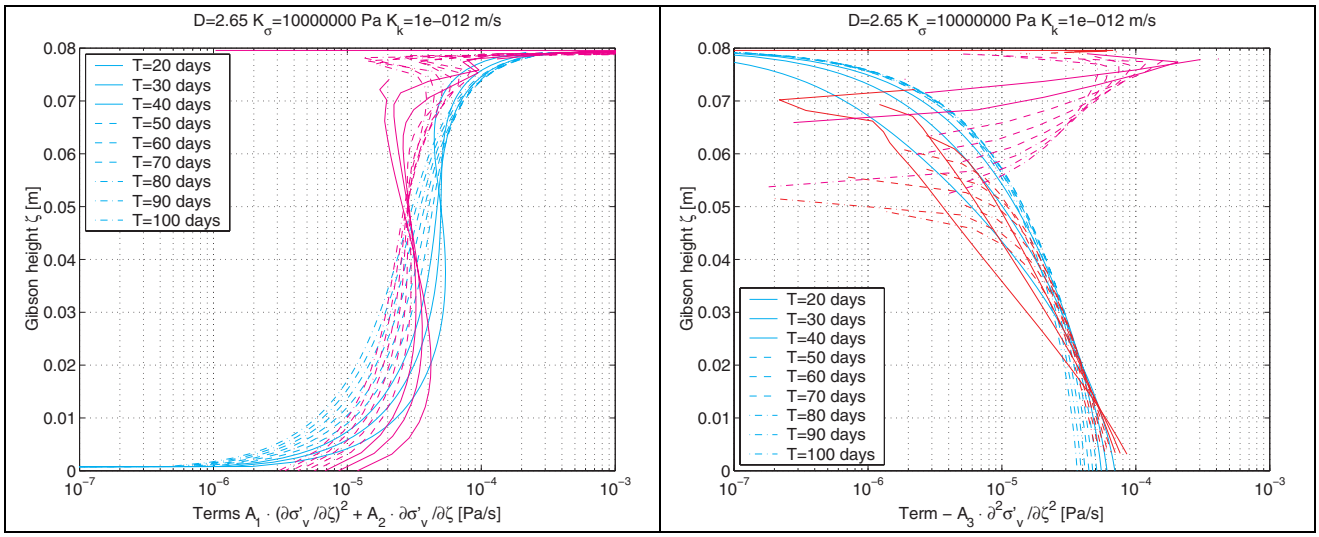

Figure 4.22 (L): The second + third (advection) terms in equation 4.44 in Gibson material coordinates at different moments in time as obtained by the numerical solution (pink = negative) and the parameterisation (light blue = negative).

Figure 4.23 (R): The fourth (diffusion) term in equation 4.44 in Gibson material coordinates at different moments in time as obtained by the numerical solution (red = positive, pink = negative) and the parameterisation (blue = positive).

From figure 4.22 and 4.23 we can conclude that the diffusion term is generally of the same order of magnitude as the two advection terms (averaged over the vertical). However, near the rigid bottom the diffusion term is more important than the advection term, but near the interface the advection terms are more important. We can explain this behaviour: the advection term scales with the layer height δ while the diffusion term scales with δ^2. This means that the advection term is important near the interface and on short time-scales. In the parameterisation, the diffusion term has the same sign over the entire bed domain. Near the interface the diffusion term becomes several orders of magnitude smaller than the advection terms. In the numerical solution however, the diffusion term gets the opposite sign near the interface and is of the same order as the advection terms over the entire vertical.

The fact that the parameterisation underestimates the density near the interface might cause a problem for the 1DV-waterbed model. Near the interface the density is very important for predicting the erosional behaviour. The advection terms, which account for the higher density near the interface, are more prominent in the initial moments of consolidation. Parameterisation 4.51 will always run for short periods t: a new Fourier series has to be constructed after every single deposition or erosion period that affects the domain of the parameterisation. Deposition and erosion occur very often with respect to the time scale of the consolidation. Therefore a new solution has to be constructed long before the consolidation process reaches its equilibrium situation. So the advection terms remain important in every timestep.

Near the interface the consolidation has two effects. First the Fourier series accounts for the strengthening of the freshly deposited layers. Second, it accounts for the swelling of the bed near the interface in the case of erosion, where the decrease of the effective stress is calculated with the virgin compression constitutive relation (because only this relation was substituted in the differential equation). The associated decrease in the density will be determined with a reloading model. Since the advection terms are important near the interface, the skipping of the advection terms will have a large influence both on the swelling of the bed and on the strengthening of freshly deposited layers. These effects of the skipping of the advection term will be present during the entire simulation.

4.6 Summary

- One can describe the time and depth dependence of the density, the permeability and the effective stress in a waterbed with the Gibson finite strain consolidation equation. When rewriting the model in Gibson material coordinates instead of Eulerian coordinates, the boundaries do not move when the sediment in the waterbed settles.
- Constitutive relations, which relate the permeability, the density and the effective stress to each other are necessary to solve the Gibson model. The constitutive relations of Merckelbach in terms of the volume fraction of mud and based on a fractal description of clay flocs, can be used in the virgin loading regime. Substituting these models in the Gibson equation results in a non-linear differential equation.
- The waterbed will not only consolidate, but will also swell due to erosion and subsequent reduction of the self-weight load in the deeper layers. For this reloading regime other constitutive models are necessary than the relations of Merckelbach. Generally, the stiffness in the reloading regime is a factor 3 to 5 higher than the stiffness in the virgin loading regime. When in the reloading regime the same constitutive relation is used as in the virgin regime (fully elastic material), the bed does not have a memory of historic loads. This can result in strange behaviour. Accounting for the history of loading is certainly necessary. A few models, which are linear on normal or log scale, are mentioned that do take into account the swell. They resemble the constitutive relations of Merckelbach and other common constitutive relations.
- The Gibson model with the constitutive relations can be solved by direct numerical integration with time steps of the order of seconds and a spatial resolution of a few mm. For the purpose of the 1DV waterbed this method is too time consuming. A fast parameterisation method is favourable. Such a method will consist of some kind of mathematical series that allows any initial condition of the bed profile.
- In an analytical solution it is not possible to use different constitutive relations for both virgin loading and reloading. Therefore only the Merckelbach equations for virgin loading will be substituted.
- The resulting differential equation can be simplified when rewriting it in terms of the excess pore water pressure and using non-dimensional material coordinates. It contains four terms: one time-dependent term, two non-linear advection terms and a diffusion term. This model is too complex to find a parameterisation. For reasons of simplicity the two non-linear advection terms are neglected. Without these advection terms the model is still a finite strain consolidation model, since the model is written in terms of material coordinates. The resulting model is a standard diffusion equation with two terms, for which readily a general solution is available: a Fourier series, in which each term decays.
- The parameterisation has been compared to the solution of the numerical model prepared by Merckelbach [2000] for the settling in a settling column. The results for the effective stress and the density are presented in real and in material coordinates. The difference and the ratio between the solutions are also presented. The results look reasonable, but the parameterised model underestimates the densities and effective stresses near the interface. Consequently, the 1-DV waterbed model will underpredict the strengthening of the bed and will overrate the resuspension.
- The different terms in the differential equation have also been compared. The two advection terms are equally important. The sum of the two advection terms and the diffusion term are equally important: they are of the same order of magnitude in the entire bed. When one would attempt to take them into account in a parameterisation, one would have to deal with both of the advection terms.
- It is concluded that the parameterisation developed shows reasonable agreement with the numerical results. Neglecting the advection terms results in a lower density near the interface than in reality however. Moreover, the behaviour during reloading in the case of erosion is not properly accounted for.

5 Implementation 1-DV water bed model

In chapter 2 the requirements of the 1-DV water bed model are formulated: the waterbed model consists of an erosion module and a consolidation module. The erosion module has been treated in chapter 3. The consolidation module has been derived in chapter 4 and is validated in chapter 6. In this chapter the relation between the two modules and their relation to the 1-DV water bed model is treated (figure 5.1).

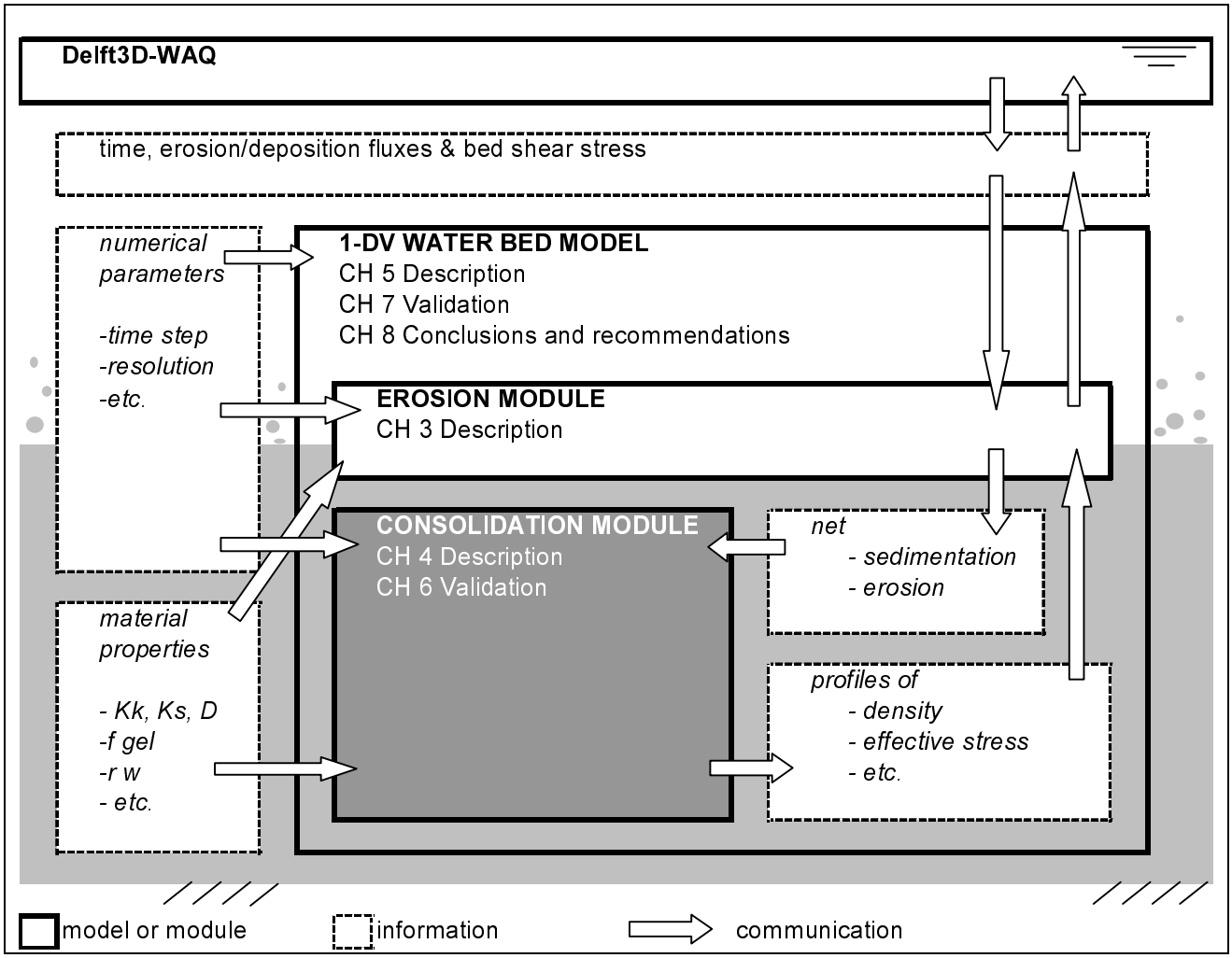

Figure 5.1: Relation of the different modules of the 1-DV water bed model

The erosion and the consolidation have different time scales. The time scale of the consolidation module is expected to be longer than the time scale of the erosion module. Using different time steps for these two modules might result in a minimisation of the calculation time, because the consolidation module consumes most of the computation time. Therefore a configuration is proposed in section 5.1 that allows the erosion and the consolidation module to have different time steps.

Section 5.2 deals with the set-up of the entire 1-DV waterbed model. The input parameters are listed in figure 5.6, sorted by the function they have in the exchange of information between the modules according to figure 5.1. A program structure diagram is presented as well (figure 5.7), showing the sequential (procedural) relation between the modules.

In section 5.3 the vertical spatial representation of the bed is discussed. A few numerical (discrete) coordinate systems are presented. A so-called *sigma*-coordinate system is chosen. This system deals with

erosion and deposition by means of redistribution. This redistribution and the associated complications, are dealt with in section 5.3.3 and 5.3.4.

In section 5.4 the temporal resolution of the consolidation module is discussed. The time step of the consolidation influences the required number of Fourier components in the parameterised consolidation model. A summary concludes this chapter

5.1 Relation erosion and consolidation module

5.1.1 Different time scales

The 1-DV water bed model consists of a separate erosion and deposition model. The time steps of these models may differ. The time scales of the processes determine the relation between the time steps.

- The 1-DV water bed model is incorporated in Delft3D-WAQ. The intervals for deposition and erosion sgenerally used in Delft3D-WAQ are 10 minutes to 1 hour.
- The time scale for deposition can be estimated by means of the settling velocity, that is in the order of 10^{-5} m/s (particles) to 10^{-3} m/s (large flocs). All the sediment in a 10-meter water column will therefore settle within 3 to 300 hours. When there is a large ratio between the concentrations near the bed and the depth mean concentration, the sediment can settle much faster. Hindered settling effects can increase the time scales however.
- The time scale for erosion is 15 minutes to one hour. When the bed shear stress is increased, the erosion rate is initially very high, after which it exponentially decreases to a constant erosion rate, which it reaches after about 1 hour.
- The time scale for consolidation is larger than the time scale for erosion and deposition. The parameterised consolidation model has been derived by discarding the non-linear advection terms from the full differential equation. The time scale of this model is then given by:

$$T = \frac{\rho_w g \zeta_i^2}{K_k K_\sigma^{\frac{n-2}{n}} n \sigma_v'^{2/n}} \tag{5.1}$$

Substitution of representative values gives a time scale T of one to several days. In the time scale the thickness of the bed is present to the power 2. That means that the bed will consolidate much faster if the bed is very thin. The time scale of the advection terms is much smaller than the time scale of the diffusion term. “We observe from the full differential equation that two time scales T_c for consolidation can be defined, determined by the permeability term (advection term) and by the consolidation (diffusion) term. The first time scale amounts to $T_{c,p}=\delta/\Delta\phi$ where δ is the thickness of the fluid mud layer, and the second time scale to $T_{c,d}=\delta^2/\Gamma_c$, in which $\Gamma_{c,d}=2K_kK_\sigma/(3-n)g\rho_w$ is the consolidation coefficient. In general the consolidation rate is governed by $T_{c,p}$ except possibly for very permeable or very thin layers of fluid mud, when $T_{c,d}$ may become smaller than $T_{c,p}$. This is illustrated with a numerical example for a 0.1 m thick layer of fluid mud with an initial concentration of 100 g/l. If we take $K_k=2\cdot10^{-14}$, $\Gamma_c=3\cdot10^{-9}$ m^2/s and n=2.71, we find that $T_{c,p}$ =34 hours and $T_{c,d}$ is 38 days. This means that during slack tide (a period of about 1 hour) already considerable consolidation can take place, possibly with some strength development, affecting the resuspension of the fluid mud layer and the turbulence production at the water- fluid mud interface.” [Winterwerp, 1999]. Moreover, the time scale T is not uniform over the vertical. Near the interface the consolidation will be much faster. This fast consolidation is not accounted for in the 1-DV water bed model due to the absence of the advection (permeability) terms and the assumption of a constant effective stress in 5.1. So in the 1-DV water bed model the consolidation time scale is much longer than the time scale of erosion and deposition.

5.1.2 Relation erosion and consolation modules

Consolidation (in the parameterisation model) is a much slower process than erosion and deposition. The parameterised consolidation model has a time scale of the order of days. Consequently consolidation of the bed is negligible on the time scale of hours typical for the erosion and deposition fluxes. Therefore it is expected that it is physically not necessary to deal with the consolidation model in the time step of WAQ (hereafter called *delt*), in which erosion and deposition are accounted for. A small consolidation time step leads to a considerable increase in calculations time. Therefore the consolidation time step (hereafter called *deltc*) should be chosen as large as possible in order to minimise calculation time. Chapter 7 investigates whether this leads to good results when dealing with erosion and sedimentation.

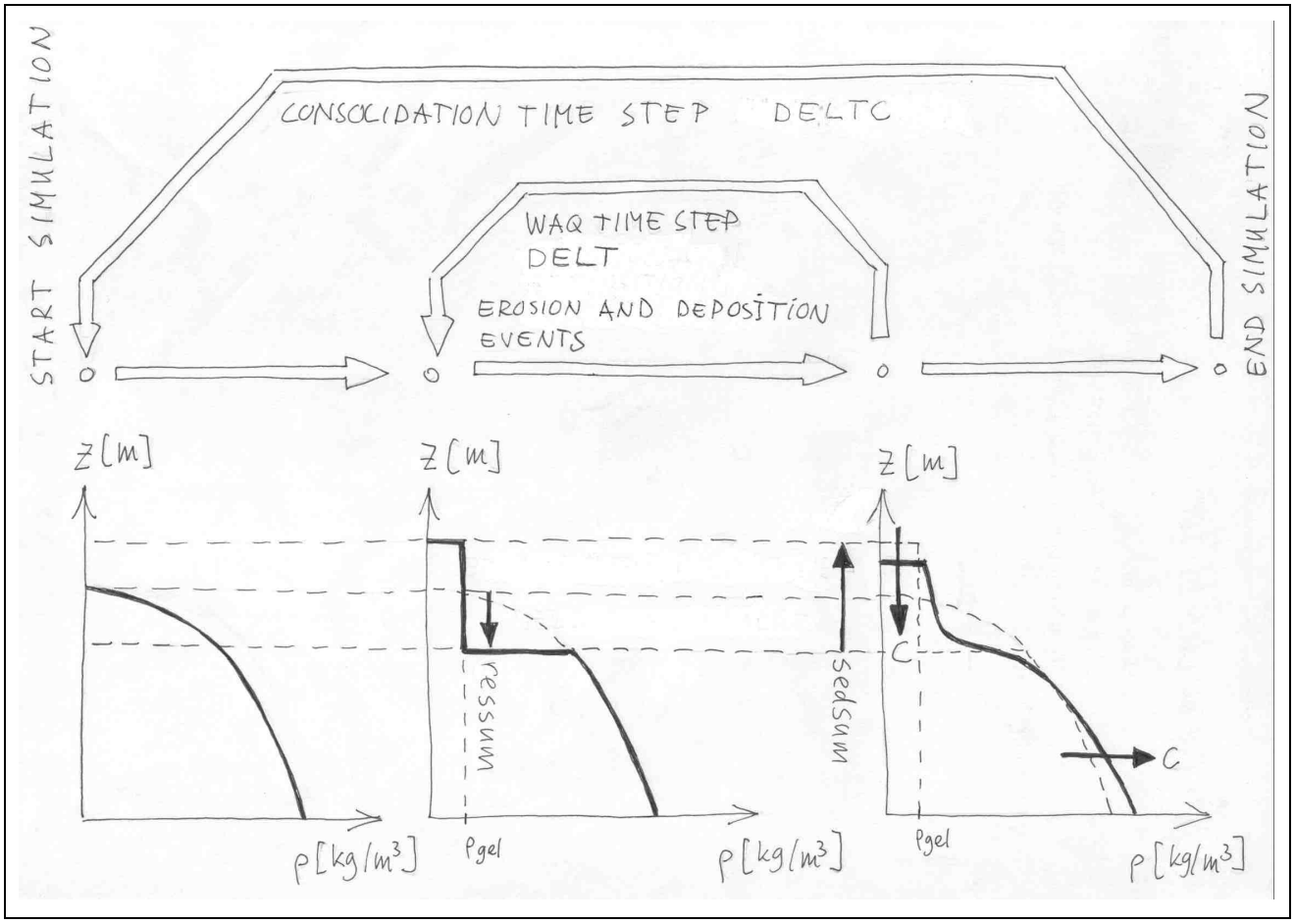

Figure 5.2: Different time scales for dealing with sedimentation, erosion and consolidation. For a detail of one consolidation time step see figure 5.3 (*ressum* is the erosion cache, *sedsum* is the deposition cache).

Figure 5.2 shows the newly proposed interaction between the erosion/deposition and the consolidation. The cumulative erosion and deposition during a consolidation time step will be stored in a cache variable in WAQ. Two different caches are necessary to deal with the cumulative changes: an erosion cache *ressum* and a deposition cache *sedsum*. If the erosion cache is as large as the deposition cache, the amount of material in the bed has not changed. The density profile has been changed in this case however. The density in the upper *ressum* part has vanished and has been replaced by a layer *sedsum* with the low density ϕ_{gel}. The quantity *sedsum* of the material in the deposition cache may be subject to entrainment if erosion occurs in the same consolidation time step in which deposition has occurred (see figure 5.2 and 5.3)

5.1.3 Consolidation time step

The consolidation period is not a fixed time interval. A fixed consolidation time step may lead to unnatural erosion behaviour. When the consolidation occurs in the middle of an erosion period for instance, the erodibility suddenly decreases. A few preliminary calculations with the 1-DV water bed model with a fixed consolidation period showed that the following happens. The (numerical) period for consolidation and the period of the transition from deposition to erosion (due to the semidiurnal tide) can interact and lead to artificial higher harmonics in the resuspension behaviour. Therefore it is proposed that the consolidation should only be applied at the transition from a period of deposition to a period of erosion. The 1-DV water bed module determines when such a consolidation 'event' takes place.

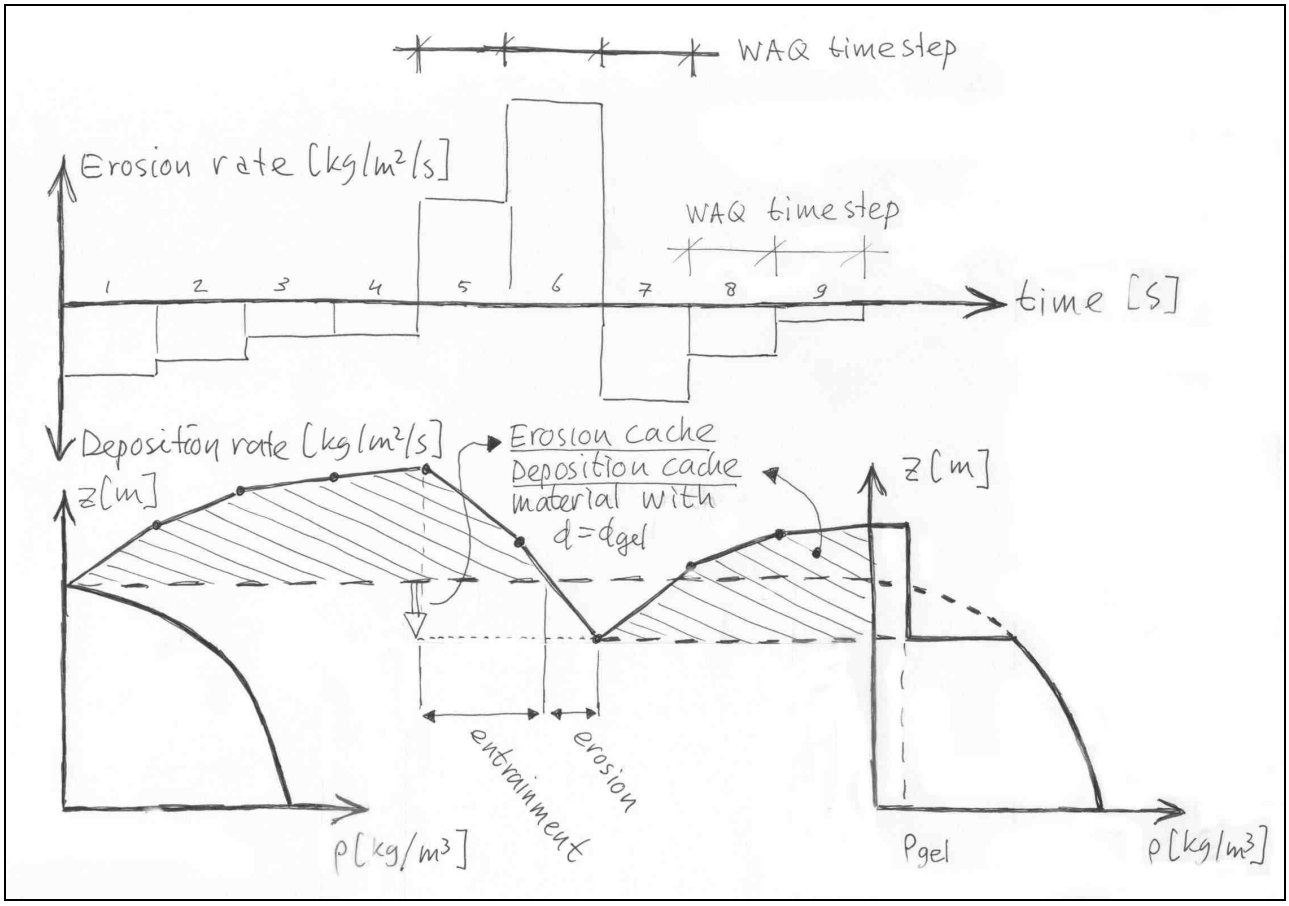

Figure 5.3: Entrainment, erosion and deposition during one consolidation time step. For a detail of one WAQ time step see figure 5.4.

A maximum time step *deltcmax* should be taken into account for the consolidation period *deltc*. In a lake for instance, erosion almost never happens. If the time step for consolidation in the 1-DV water bed module would be equal to the deposition – erosion interval, this would result in very large consolidation time steps. Consequently, a huge amount of material would accumulate in the deposition cache, and all this material would not age. Therefore the 1-DV water bed module will activate the consolidation module at least every period *deltcmax*.

A minimum time step *deltcmin* should be taken into account as well for the consolidation period *deltc*. The transition from erosion to deposition can also occur too often. While a very short consolidation time step does not lead to incorrect physical behaviour, it requires too much calculation time. It also requires the use of more Fourier components and sampling points (see section 5.4). Therefore the consolidation module will only be activated if at least a period *deltcmin* has passed since the last consolidation 'event'. In an

estuary for instance, the current speeds on tidal flats can be very low. When the associated bed shear stresses are almost equal to the critical shear stress and when the bed shear stresses fluctuate slowly in time, erosion and deposition periods can alternate very frequently (every other *delt* at most). Both the proposed limitations *deltcmin* and *deltcmax* have been implemented in the 1-DV water bed model.

The moments in time at which consolidation is accounted for, will be different for every segment. In the lake mentioned above, consolidation might be necessary more often near the entrance of a river than in the quiet middle part. In the estuary mentioned above, consolidation will be accounted for more often on the tidal flats than in the main channels. Moreover, the turn of the tide will not happen at the same moment in time in the entire estuary.

The actual consolidation time step is always a multiple of *delt*, while *deltcmin* and *deltcmax* are not necessarily a multiple of *delt*. Therefore consolidation is accounted for the first multiple of *delt* after *deltcmin* and *deltcmax* have passed.

All material in the deposition cache *sedsum* is assumed to be deposited at the moment of the previous consolidation event. The age for all the sediment in the cache is the same. Accordingly, sediment that was deposited at the very moment before the new consolidation 'event' started, will also be subject to this long consolidation period. In chapter 4 it was shown, however, that the parameterised consolidation module underestimates the density near the interface. The longer consolidation times for the cache *sedsum* increases the density near the interface and can perhaps compensate this shortcoming.

5.1.4 WAQ time step

Within one time step *delt* both erosion and deposition have to be dealt with by the 1-DV water bed module. In the physical world erosion and deposition generally do not occur simultaneously [Partheniades, 1965]. In the WAQ model erosion and deposition do not occur simultaneously either. But when a *delt* time step is relatively long, the physical transition from an erosion period to a deposition period can occur within one time step. Consequently the 1-DV water bed receives the sediment that has been deposited the previous time step, as well as the bed shear stress that leads to erosion in the coming timestep.

Within one timestep *delt*, sediment is deposited at the start of the time step. This flux is determined by the WAQ water/sediment flux equations of the previous time step. The erosion rate is then determined by the strength profile of the bed. This profile consists of the remaining part of the consolidating bed plus the freshly deposited material *sedsum* on top of it (see figure 5.3) When erosion occurs within *delt*, first the freshly deposited material *sedsum* is entrained. This material is a gel and only has (some) cohesion and no effective stresses yet. Accordingly it has a large, but finite erosion rate and hence a short, but non-negligible time interval is required. Only when all of this fresh material has been eroded, can the previously calculated consolidating bed start to erode. For this part of the profile the erosion formulation 3.17 is used. The cumulative erosion of the previously calculated consolidating bed is stored in the variable *ressum*. Concluding: two successive steps have to be made within one single WAQ timestep: These steps (i) account for the entrainment of the freshly deposited material and (ii) take care of the erosion of the consolidated bed in the remaining part of the WAQ-timestep.

Once the consolidated bed starts to erode, the rate of erosion depends on the progression of the erosion itself. With progressing erosion, the material becomes stronger and stronger. The total erosion has to be calculated by integrating the erosion-depth dependent erosion rate over the WAQ time step *delt*. The strength of the exposed top layer can be used to calculate the erosion rate of the exposed top layer. Using this erosion rate to calculate the total resuspension of the bed during *delt* may result in over rating of the resuspension, since the erosion rate decreases with progressing erosion (see figure 5.4). The associated decay in the erosion rate may be so fast, that it is not correct to assume that it is constant during one step *delt*. Accordingly it is necessary to calculate the erosion with smaller time steps than *delt*. Erosion has to be accounted for with a third time scale, besides *delt* and *timec*. The time step by which the erosion is

calculated is *deltE*. The number of time steps *notE* is determined by dividing the part of the timestep *delt* that remains after entrainment by *deltE* (*notE*=4 in figure 5.4).

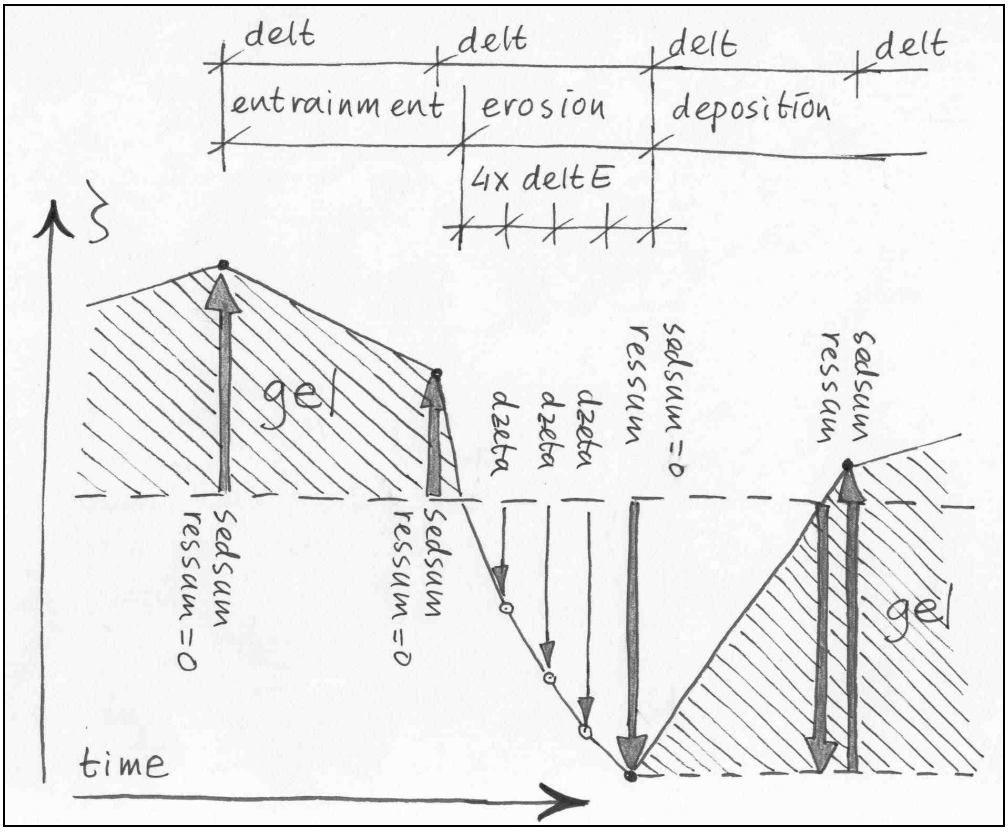

Figure 5.4: Entrainment, erosion and deposition during one WAQ time step. For a detail of one of the *notE* time steps see figure 5.5.

The erosion rate varies with depth. Two options are available to calculate the erosion: (1) an iterative method and (2) an analytical method. Both methods are written in the material coordinate system ζ. Accordingly, the erosion rate E in [kg/m2/s] has to be rewritten in a change in the material height $\Delta\zeta$ in [m/s] by

$\Delta\zeta = \int E(\zeta) dt/\rho_s$.

1. Within one of the small erosion time steps *deltE*, a few iterations are necessary to calculate the progression of the erosion (see figure 5.5). Preliminary tests with the 1-DV waterbed model showed that two iterations are sufficient. The reason for this is that the profile is linear between two sampling points (see section 4.3). A curved profile would have needed more iterations. The working of the iteration procedure is as follows.

   On the horizontal axis in figure 5.5 the erosion rate E is depicted as a function of depth. This erosion rate profile is calculated by means of the density profile, the cohesion profile and the bed shear stress profile (with equation 3.17 and 3.22). The erosion rate E_1 is the erosion rate at the uppermost exposed layer. The material co-ordinate ζ of this uppermost exposed layer at which $E(\zeta)=E_1$, is $\zeta=\zeta_{interface}$-*ressum-dzeta;* this equals the present interface height ($\zeta_{interface}$) minus the erosion that has already occurred in the previous WAQ time steps (*ressum*) and minus the erosion *dzeta* that has already occurred in earlier steps *deltE* of the current WAQ time step (see figure 5.4). The formulation $\int E(\zeta) dt$, that calculates the erosion depth, has to be integrated. This integral is evaluated simply by Eulers method. That is multiplying the erosion rate E with the time step *deltE*. Consequently, the erosion rate E_1 at the top gives the erosion depth $\Delta\zeta_1 = E_1 \cdot deltE/\rho_s$. This erosion depth $\Delta\zeta_1$, is used as an upper guess of the actual erosion depth $\Delta\zeta$. The new material height corresponding with this upper guess of the erosion depth reads: $\zeta = \zeta_{interface}$-*ressum-dzeta*-$\Delta\zeta_1$. Next, the erosion rate E_2 at the estimated upper new

material height can then be calculated. This erosion rate E_2 is lower than the erosion rate E_1 of course, since deeper material is stronger. The erosion rate E_2 can be used as a lower guess of the actual erosion depth: $\Delta\zeta_2 = E_2 \cdot deltE/\rho_s$. The average of the upper guess $\Delta\zeta_1$ and the lower $\Delta\zeta_2$ is considered to be the actual erosion depth $\Delta\zeta = (\Delta\zeta_1 + \Delta\zeta_2)/2$.

2. It is also possible to calculate the exact erosion depth without using the subdivision of *delt* into time steps *deltE*. The progression of the erosion can be calculated analytically for the whole WAQ time step *delt*. Since the the *E*-profile is linear between two successive sampling points: $E = a\zeta + b$. In this relation, *a* and *b* can be determined by substitution of the co-ordinates of the sampling points (E_i, ζ_i) and (E_{i+1}, ζ_{i+1}) at both ends of the line. This leads to:

$$E = \frac{E_{i+1} - E_i}{\zeta_{i+1} + \zeta_i}\left(\zeta - \zeta_i\right) + E_i \tag{5.2}$$

The erosion depth can be determined with

$$\frac{d\zeta_{interface}}{dt} = -\frac{E(\zeta)}{\rho_s} = -\frac{a\zeta + b}{\rho_s} \tag{5.3}$$

The solution to this equation, with the interface height $\zeta_{interface} = \zeta_0$ at the start of the time step reads

$$\zeta_{interface} = \left(\zeta_0 + \tfrac{b}{a}\right)\exp(-at) - \tfrac{b}{a} \tag{5.4}$$

This solution is only valid between two successive sampling points. When the erosion passes a sampling point, the coefficients *a* and *b* change, as well as the boundary condition ζ_0. In the first second of *delt* this boundary condition reads $\zeta_0 = \zeta_{interface}$-*ressum-res*. When the erosion passes a sampling point, the boundary condition becomes $\zeta_0 = \zeta_{i+1}$ ($< \zeta_{interface}$-*ressum-res*). So when using this exact method, one has to keep track of the progression of the erosion in relation to the sampling points. This is time consuming and needs much effort to implement. Because the 1-DV water bed is under development, this exact method has not yet been implemented. The simple iterative method mentioned above is used.

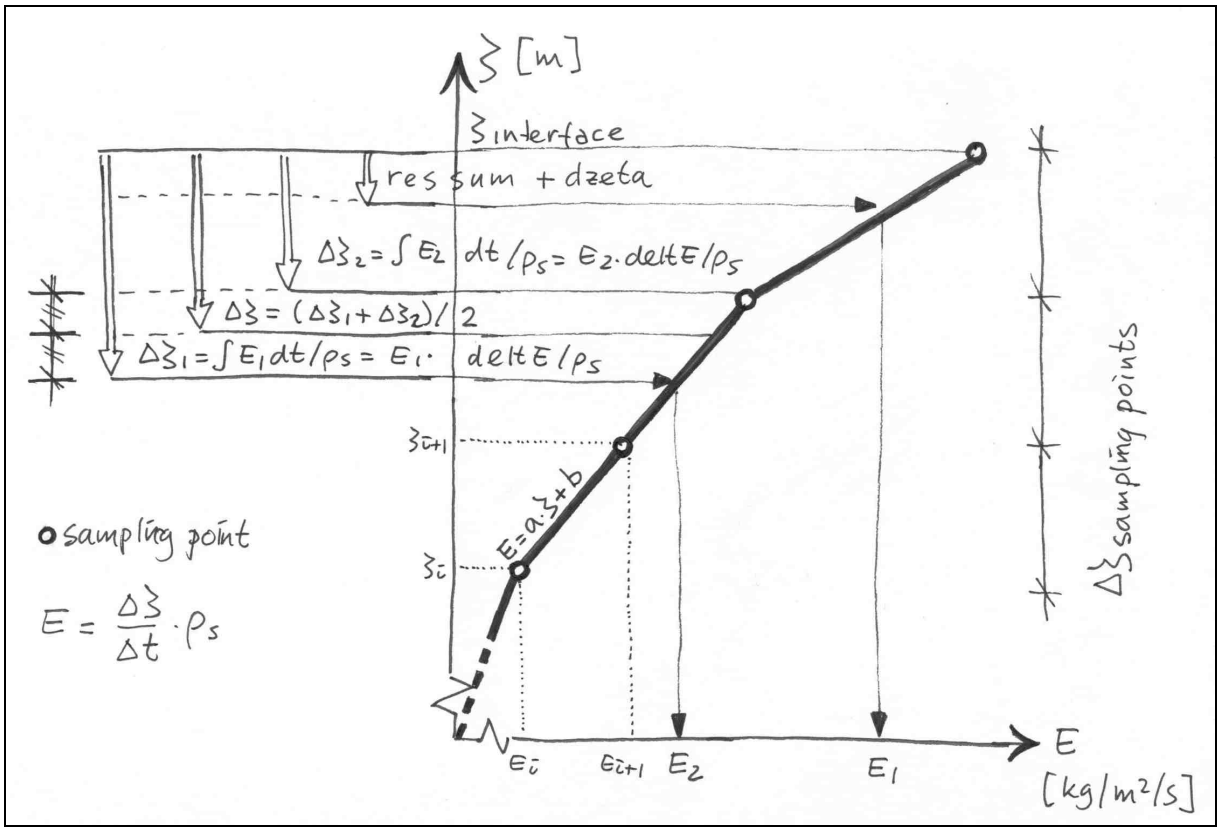

Figure 5.5: Erosion of the consolidated bed during a time step *deltE* (after entrainment of *sedsum*).

5.2 Set-up of 1-DV water bed model

The 1-DV water bed model consists of three modules: the erosion module, the consolidation module and the main 1-DV water bed module itself (figure 5.1). The enveloping Delft3D-WAQ software can be seen as a fourth module. These different modules have to communicate with each other (figure 5.1). The communication is performed by exchanging variables. These variables are listed in section 5.2.1. The sequential (procedural) set-up of the model is presented in section 5.2.2.

5.2.1 Variables [15,16]

All information present in the 1-DV water bed model has been clustered in four main groups. The parameters of each group are mainly related to each other by the way in which they are used: as input by the user, or as output to the user (global variables), or instrumental in calculating other parameters (local variables in the 1-DV water bed module) (see figure 5.1). The four groups have been divided into subgroups, that are grouped according to the parameters they represent. All the groups and their parameters are shown in figure 5.6.

1. The material properties are required as input by the user. The critical shear stress τ_{cr} for erosion is required as an input parameter, while the erosion formulation used in the 1-DV water bed model (equation 3.17) used does not contain such a critical shear stress. The critical shear stress for erosion is never the less applied. One reason is to make a clear distinction between erosion and deposition periods, necessary for determining when consolidation has to be applied. The second reason is to make the 1-DV water bed model compatible to the current erosion model in Delft3D-WAQ: the differences between the results can then only be attributed to different erosion rates and not to the duration of the erosion.

2. Numerical properties are required as input by the user. Monitoring segments are the segments in which the user can monitor all the fluxes and processes. In these segments the bed profiles are to be saved for every consolidation time step. A segment consists of all layers in one Delft3D-WAQ grid cell. The other parameters of group 2 have been explained in the previous section.

3. The bed parameters are instrumental in calculating other parameters. They can be given as output to the user in the monitoring segments. The user is strongly recommended to monitor at least one profile to ensure that no errors have been made in the input parameters (e.g. resolution and time step *deltE*). This profile should be chosen at the location where the erosion and deposition dynamics is most severe. The profiles are different for each segment. Even when the bed properties are the same for each segment, the sediment fluxes may differ in each segment and then separate profiles are necessary.[17]

---

[15] Some of the parameters in figure 5.6 can be different for each segment, others should be the same for all the segments in the entire Delft3D-WAQ model grid. The latter group includes *deltcmin, deltcmax, non, nok, time* and *delt*. In the code a check is performed for the parameters that need to be the same. (as well as for *nok <= non, see section 5.4*).

[16] The WAQ user interface offers the user the option to define the properties that are valid for the entire model. For all segments, default values are to be given. These values are determined in the coming chapters, that contain the validation of the consolidation module and the validation of the erosion module.

[17] For all the independent bed variables a profile is stored. These variables are ζ, $\sigma`_v$, $\zeta$, $\phi$, $\phi_{max}$ and $c`_a$ (the latter if time dependent). The yield stress τ_y is not an independent variable, since it can be calculated from the volume fraction of mud ϕ and the cohesion $c`_a$. It is not necessary to store the profile of this variable. The value of the yield stress can

At the start of the simulation initial profiles have to be given. The user has to provide the amount of material in the bed at the start of the simulation.[18] The amount of material present in the bed equals the highest material co-ordinate ζ. This parameter will only change when material is eroded or deposited. This leads to the conclusion that the model does not have circular assignments resulting in cumulative errors of the mass present in the bed. When all the material in the bed has been eroded, the computation stops. A 'clean bottom' is not yet possible in the 1-DV water bed model.[19]

The 1-DV water bed model works with SI-units, where erosion and deposition are applied in meters of material height per second [m/s], while Delft3D-WAQ uses fluxes in [kg/m^2/s]. This requires some extra variables in the code.[20] Extra variables are also needed in the code to account for the proper activation of the consolidation module.[21]

4. The time, the bed shear stress [22] and the sediment fluxes are output to the user. WAQ passes the global model time to the 1-DV water bed model as well as the magnitude of the present timestep.

   WAQ accounts for 9 different cohesive fractions, six organic and three inorganic. The organic material, i.e. algae, is modelled as a component of the sediment. Accordingly, they are subject to deposition and resuspension. The 1-DV water bed model however requires a uniform bed with uniform properties. Hence these 9 fractions have to be merged into a single flux (or one should only use one fraction). WAQ contains special functions for this merging. When material erodes, the eroded material has uniform properties. This material has to be distributed over the various fractions again. The distribution of sediment over the fractions is not constant in WAQ. The fractions are determined from the average properties of the eroding layer. The 1-DV water bed model does not account for the distribution over the fractions. The current layer model of WAQ should be used together with the 1DV-waterbed model to give this distribution.

---

also be evaluated in the erosion module at the moment it is needed. Since computation time is scarcer than memory in Delft3D-WAQ, a profile of τ_y will be calculated though. It is faster to calculate τ_y once and for the entire bed, than to evaluate it every time in the erosion module. Other parameters such as the density and the real coordinates z are not calculated at all, since these parameters are not necessary in the erosion module.

[18] This material is given by the mass in a segment (the mass in layer 1 *IMS1*(WAQ Fortran name) and the mass in layer 2 *IMS2* (id.)) and the surface surf (id.) of a segment. The material height is then calculated as (*IMS1* + *IMS2*) / *surf* /ρ_s. The model calculates the equilibrium profiles associated with this amount of material. It might be a wish of users to use initial profiles so that they are equal to the profiles at the end of a previous simulation. Or to use profiles measured in the field or laboratory. For this option the user will have to make changes in the 1-DV water bed code however.

[19] Make sure that enough sediment is available in the segment. But do not put too much sediment in the bed initially however, since that would reduce the resolution of the bed (see section 5.3)

[20] Deft3D-WAQ gives the erosion and deposition fluxes in [g/m2/d]. The 1-DV water bed model applies water-bed exchange rates in m/s (N.B. material height per second). Therefore the WAQ in/output parameters fsedDM (WAQ Fortran name) and fresDM (id.) in [kg/m2/s] are not used inside the 1-DV water bed model. The parameters res (WAQ Fortran name) and sed (id.) in [m/s] are used.

[21] The parameters *tauold* (Fortran name), the bed shear stress τ_b in the previous timestep, and *deltc* are used to account for the right consolidation time step. They will be compared with respectively τ_b (Fortran name: *tau*) & τ_{cr} (Fortran name: *tcrDM*) and *deltcmin* & *deltcmax*.

[22] The parameters *mindep* (WAQ Fortran name) and *depth* (id.) are included to account for the uncertainties in the formulations of the bed shear stress *tau*. In segments with a small water depth, the bed shear stress may not be calculated accurately. Moreover, in segments with a small water depth, erosion will immediately lead to high concentrations. For these two reasons, erosion is not allowed to occur in segments with a small water depth.

No.	Group:	Symbol or Fortran name	Units:	Description:
I	Material properties			
I a	General properties	ρs	kg/m3	density of bed material
		ρw	kg/m3	density of pore water
		ϕgel	m3/m3	structural volume fraction of mud
I b	Strengthening properties	*K*k	m/s	empirical permeability parameter
		Kσ	Pa	empirical effective stress parameter
		D	-	fractal dimension
		f	-	ratio of stiffness at reloading and VCL
		swelling	-	swelling model
		c`a	Pa	cohesion parameter (*c`a = c`a* (time)?)
		φ`	deg	angle of internal friction
		*K*0	-	coefficient of lateral friction
I c	Erosion properties	*M = we * ϕ*	kg/m2/s	erosion rate / entrainment rate
		τcr	Pa	critical shear stress for erosion
II	Numerical properties			
II a	Consolidation	*non*	#	number of sampling points
		nok	#	number of Fourier components
		deltcmin	d	minimum time step for consolidation
		deltcmax	d	maximum time step for consolidation
II b	Erosion	*deltE*	#	timestep for iterative calculation of erosion of consolidated profile
II c	Monotoring	*(no 1, no 2,…)*	#	monitoring segments
III	Bed representation			
III a	Profiles	$\zeta(\zeta)$	m	material height
		$\phi(\zeta)$	m3/m3	volume fraction of mud
		ϕmax(ζ)	m3/m3	maximum volume fraction of mud (OCR=1)
		τy(ζ)	Pa	bed yield strength
		σ`v(ζ)	Pa	effective stress
		c`a(ζ)	Pa	Cohesion
III b	Initial conditions	*IMS1+ IMS2*	g	amount of material in segment at start
		surf	m2	surface of segment
III c	Changes to domain of profiles	*sedsum*	m	sedimentation cache during *timec*
		ressum	m	erosion cache during *timec*
		sed	m/s	sedimentation flux during *delt ~ FsedDM*
		res	m/s	erosion flux during *delt ~ FresDM*
III d	Validity of changes to domain of profiles	*tauold*	Pa	bed shear stress in previous time step
		deltc	sec	time since last consolidation
IV	Time and fluxes			
IV a	Time	*time*	sec	time in simulation
		delt	day	current time step for deposition and erosion
VI b	Imposed (forcing of) sediment fluxes	τb	Pa	bed shear stress
		fsedDM	g/m2/d	sedimentation flux
		depth	m	water depth in segment
		mindep	m	minimum water depth for erosion to occur
IV c	Erosion	*fresDM*	g/m2/d	erosion flux

Figure 5.6: Input parameters

5.2.2 Structure

A sequential (procedural) Program Structure Diagram (PSD) of the 1-DV water bed model is presented in figure 5.7. The information that should be passed to each module is presented in the left column. The output from each module is also given in the list.

Input:	Process:	Output:
	Delft3D-WAQ	
I,II	For all timesteps do	(III a)
III b	-> *1-DV water bed module*	(III c)
IV a,b		IV c
	1-DV water bed module	
I	Read input parameters with use of the input pointers	(III a)
II	Check for errors in input	(III c)
IV a	Initialise parameters that are the same for every segment	IV c
IV b	Once: Initialise parameters that are the same for every timestep and every segment	
	Once: allocate the profiles and other local parameters	
	For all segments with a bed do	
	Initialise parameters that can be different for every segment	
	Once: Initialise parameters that are the same for every timestep and can be different for every segment,	
	Once: account for initial conditions in profile	
	if (i) the last consolidation was longer ago than *deltcmax* OR if (ii) during the previous timestep deposition occured AND this timestep erosion occurs AND and the last consolidation was not shorter ago than *deltcmin*	
	-> *Consolidation module*	
	(save the profiles for the monitoring segments)	
	-> *Erosion-deposition module*	
	Account for increment in the input pointers	
	Consolidation Module	
I a	Account for cached erosion *ressum* and sedimentation *sedsum* by redistribution	III a
I b	Set cached erosion *ressum* and sedimentation *sedsum* to zero	III c
II a	Determine final equilibrium profile and excess pore pressure profile *pe(zeta)*	
III b	Fourier transform the profile *pe(zeta)*	
III c	Construct new *pe(zeta)* profile after consoldiation during period *timec* with Fourier series	
III d	Determine new *s(zeta)* profile	
IV a	Determine new *phimax(zeta)* profile after that *phi(zeta)* profile with the swelling model	
IV b	Determine *ca(zeta)* profile	
	Determine *ty(zeta)* profile	
	Eosion-deposition Module	
	dzeta = 0, *res* = 0	
I a	Calculate entrainment *dzeta_entrain* [m] of cache sedsum	III c
I c	Calculate time *deltres* is left during this timestep *delt* after entrainment period	IV c
II b	if (*deltres* > 0)	
III a	For all time steps *deltE* do	
IV a	calculate erosion *dzeta1* [m] in first iteration	
IV b	if (*ressum* + *dzeta1* + *dzeta* > total bed height) -> *quit*	
	calculate erosion *dzeta2* [m] in second iteration	
	dzeta = *dzeta*+ (*dzeta1* + *dzeta2*) /2 [m]	
	if (*ressum* + *dzeta* > total bed height) -> *quit*	
	ressum = *ressum* + *dzeta* [m]	
	res= (*dzeta* + *dzeta_entrain*) /*delt* [m/s]	

Figure 5.7: Set-up of the 1-DV water bed model

5.3 Vertical resolution

The representation of the profiles of the bed properties in the computer cannot be continuous for obvious reasons. The continuous analytical functions are sampled at a finite number of intervals to gain these profiles. The method of sampling and the accompanying complications will be discussed in section 5.3.1.

5.3.1 Principle of sampling

The parameterisation gives a continuous description of the bed. This continuous representation must be transformed into a discrete profile for numerical computations. Sampling the continuous representation at an adequate resolution with n points accounts for this. In the discrete numerical model, the bed is presented by a set of n values containing all the information of the (profiles of the) different parameters in the bed:

$$\left\{\left(\zeta_1,\phi_1,\sigma_1^{'},\phi_{\max,1},\tau_{y,1},c_{a,1}\right),\left(\zeta_2,\phi_2,\sigma_2^{'},\phi_{\max,1},\tau_{y,2},,c_{a,2}\right),\ldots,\left(\zeta_n,\phi_n,\sigma_n^{'},\phi_{\max,1},\tau_{y,n},,c_{a,n}\right)\right\} \qquad (5.5)$$

This set holds for a finite number of sampling points in the vertical direction, referred to as layers in this section.[23] The properties are assigned to the sampling points themselves rather than to the intervals in between. The values between the sampling points are interpolated.

The lowest sampling point coincides with the rigid bottom, the highest with the interface between the water and the bed. In reality however the values apply to intervals. When transforming between the real and the material co-ordinate systems, this leads to a problem: the number of sampling points is one larger than the number of intervals in between. Transforming all but the upper sampling points solves this. This relation between the sampling coordinates in real and material coordinates in discrete form, derived from the continuous co-ordinate system transformation (equation 4.10), reads (see figure 5.8):

$$\zeta_j = \sum_{j=1..i}\left(z_i\phi_i\right) \Leftrightarrow \begin{cases} i=1 & z_1 = 0 \\ i=2..n & z_i = \sum_{j=1..i}\left(\dfrac{\zeta_j-\zeta_{j-1}}{\phi_{j-1}}\right) \end{cases} \qquad (5.6)$$

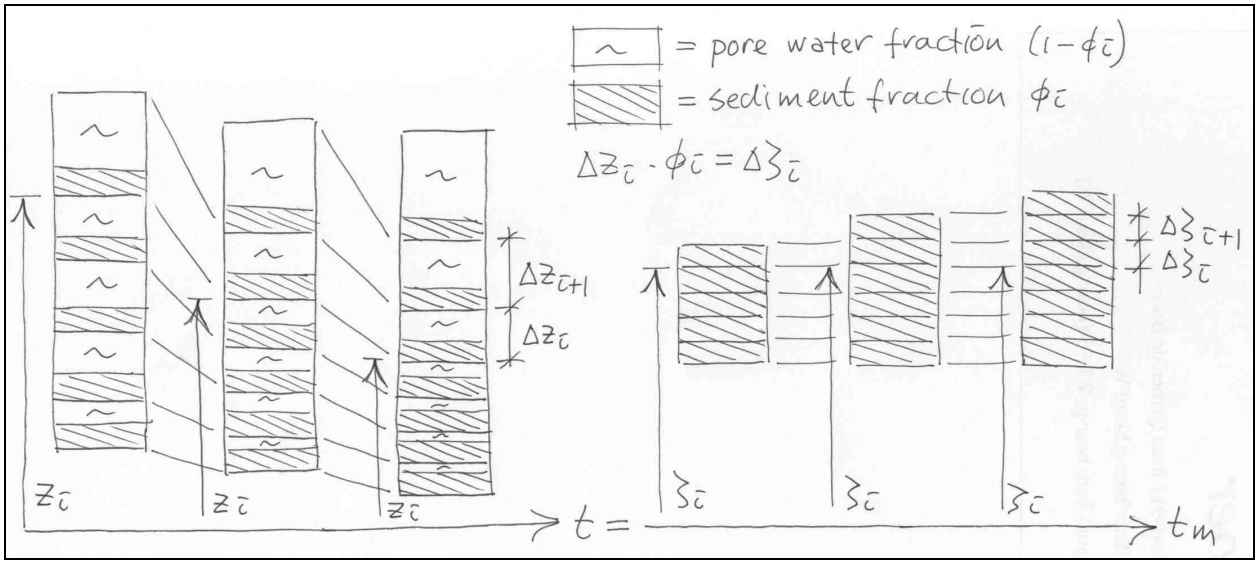

Figure 5.8: Relation real and material coordinate system, subject to deposition.

[23] Do not confuse these layers with the domains on which the parameterisations are valid as described in section 4.4 nor with the layer approach of dealing with the bed as described in chapter 3.

5.3.2 Sampling configuration

The bed is discretized into a finite number (order 100) of sampling points. When sedimentation and erosion occur, the height of the bed changes and thereby the number and/or configuration of the layers. Several options exist for dealing with the layers. A first choice has to be made as to whether a fixed number of layers will be used or a variable number. A second choice is whether or not equidistant layers are used. All possible options are visualised in figure 5.9. The pros and cons of these options will be listed in table 5.1.

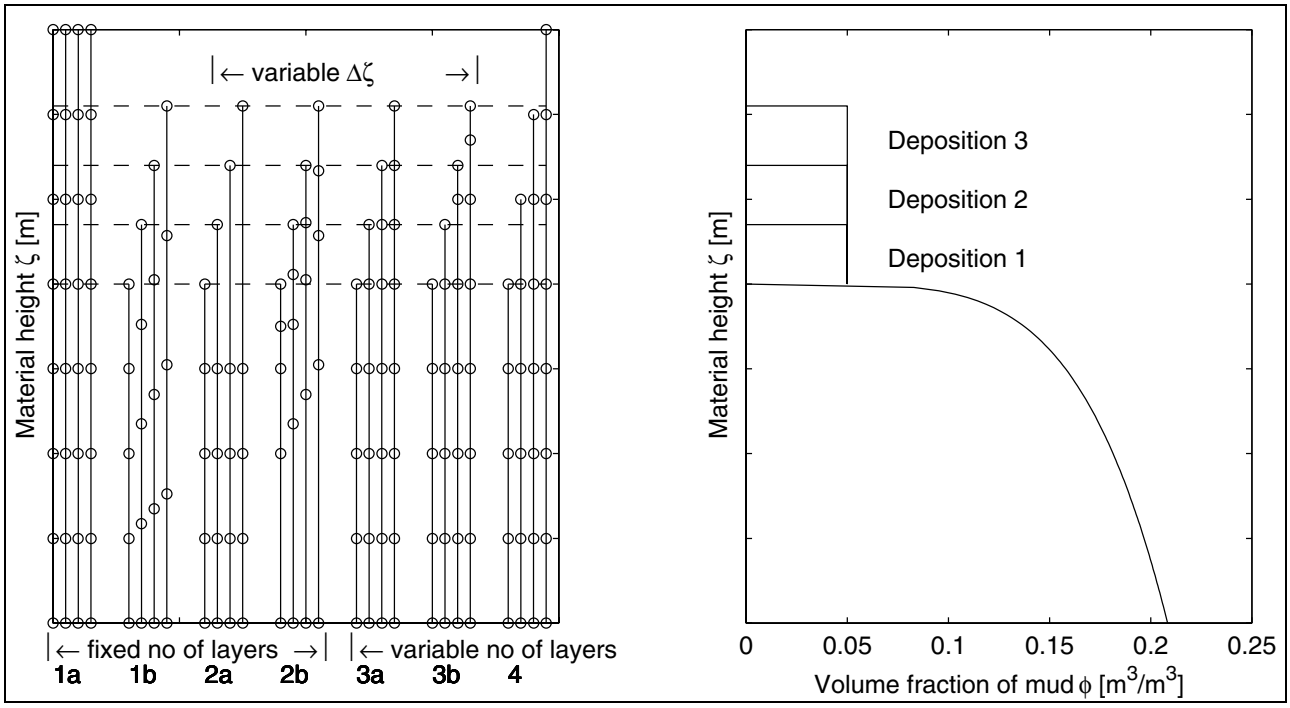

Figure 5.9: Possible sampling configuration types.

1. A uniform spatial step can be combined with a fixed number of layers.
   a The bed can be described in terms of a non-allocatable 'Eulerian system'. In this option all the layers have to be present at the start of the calculation. Hence, an estimation of the maximum occurring material height has to be made in advance of a simulation. When deposition on the bed would increase the amount of material on the bed more than expected, the upper part of the bed falls out of the co-ordinate system. And when the amount of material does not increase as much as expected, many sampling points are never used and yet still require computational storage space. The numerical model of Merckelbach is written in this type of co-ordinate system (in real coordinates however, not in material coordinates.) For the modelling of a settling column, this method can be very useful, since the amount of material in the column does not change. In the 1-DV water bed model alternating periods of erosion and deposition occur, leading to a fluctuating bed thickness. Accordingly this is not a useful option.
   b The bed can be represented by a so-called sigma co-ordinate system, as used for example in Delft3D flow to calculate the water motion. The co-ordinate system 'breathes' between the top of the material height, which changes in time, and its bottom. When material is removed or added to the bed (to the material height), all the sampling points have to be redistributed uniformly over the entire material height. This redistribution is performed by means of interpolation and that is *time consuming*.

2. A variable space step can be combined with a fixed number of layers. A few useful configurations are possible.
   a The upper layer 'breathes' with the erosion and deposition. When the upper layer becomes too thick, or when erosion depletes the upper layer, material has to be redistributed. A complication is that a decision criterion has to be formulated for the length of the time intervals after which redistribution has to be performed.
   b A sigma-co-ordinate system with a spatial step that is small near the interface and large near the rigid bed can be used. With a minimum amount of layers, a maximum accuracy of the profile can be obtained where it is most useful. Near the interface, the gradients in the density profile are the largest. Moreover, at the interface all the erosion and deposition fluxes have to be accounted for, possibly leading to stepwise gradients. Despite this advantage, this option may not have a positive influence on the accuracy of the Fourier components, due to the large steps near the rigid bottom.
3. When a variable space step is combined with variable number of layers, the changes in the density near the interface due to consolidation might be represented very accurately with an acceptable number of layers (see section 5.4.3).
   a A single layer for every deposition can be chosen, so the profile can be very accurate. The number of layers may become very large in this method leading to large memory usage.
   b All the layers have the same thickness, except for the uppermost layer. This layer adjusts its height to the available sediments: it shrinks when erosion occurs and it growths when deposition occurs. When the height of this layer becomes equal to the height of the others, a new uppermost layer will be added.
4. A uniform space step can be combined with the variable number of layers: an allocatable 'Eulerian system'. In this method no new layer will be added until the previous layer is filled with sediment. A discrete number of fixed intervals can never match the material height however, especially when the number of layers is not very large. Due to this, near the water-bed interface some small *rounding off* errors always occur. The top of the highest layer will always reach above than the actual bed. This leads to a reduced accuracy near the water-bed interface. Near the water-bed interface however, accuracy is most required, so this option is not very useful.

When the layers vary in thickness (1&4 against 2&3 in figure 5.9), the determination of the Fourier components becomes less *accurate*. One thick layer at the end of the domain can lead to a *relative* large error in the numerical evaluation of the integral (trapezoidal rule). The reconstruction of the profile is very sensitive to small changes in the main Fourier components. For instance even using the rectangular discrete integration rule, instead of the trapezoidal discrete integration rule at a resolution of 100 sampling points does not give reasonable answers. So using a variable spatial resolution can spoil the whole parameterisation. Moreover, the integrals that are used to calculate the Fourier components will contain more operations when a variable $\Delta\zeta$ step is used. Every multiplication reads $p_{o,i}\cdot\cos(\pi(k\text{-}0.5)\xi_i)\cdot\Delta\xi_i$ while with an equidistant spatial step, the answer f_k can simply be multiplied in one operation by $\Delta\xi$. So the model becomes *slower* than a model using equidistant layers. Third, the computational space required will increase, because a $\Delta\zeta$ profile has to be stored besides other profiles (ϕ, σ'_v etc.).

When a variable number of layers is chosen (1&2 against 3&4 in figure 5.9), the *calculation time* needed does not remain constant throughout a simulation. Since the number of Fourier components is directly coupled to the number of layers, as we will see in section 5.4, the number of Fourier components will fluctuate as well. As a result of this, one cannot properly estimate in advance the amount of computer time the model will need (especially when the model covers a longer period).

A very important criterion is the ability of the model to be mass conserving. The co-ordinate system is not only a reference system, it is also the storage place for material: the uppermost co-ordinate equals the material height (which is the available sediment). A few options cannot exactly fit the material height and have to be discarded: 1a and 4. The accuracy of the erosion will be determined by the accuracy of the

system used to represent the profile near the interface. Option 2a is therefore also discarded. Option 3b is just as good as 3a, but it has a smaller number of layers, so 3a can be discarded. The three remaining options are worth further consideration: 1b, 2b and 3b.

A fixed number of equidistant layers will be chosen (1b), since this option has a steady calculation time, an easy and fast Fourier transformation and is easy to implement. The most important disadvantage is the necessary redistribution of the sampling levels after each deposition event. The two other remaining options may be investigated as well from a computational point of view. From an engineering point of view however it is no use to spend a lot of time on optimising the discrete representation. The 1-DV water bed model is still research software, since it has not been fully tested yet. *Probably* the majority of the uncertainty is in the physics and not in the numerics.

Layer type	1a	1b	2a	2b	3a	3b	4
Layer thickness uniform?	y	y	n	n	n	n	y
Number of layers constant?	y	y	y	y	n	n	n
Criteria							
Accuracy Fourier transformation	-	+	-	-	o	o	-
Speed: Fourier transformation	+	+	-	-	-	-	+
Speed: Redistribution	+	-	o	-	+	+	+
Memory use	+	+	-	-	-	-	+
Predictability: Steady calculation time	+	+	+	+	-	-	-
Failure chance: Explosion calculation (time)	-	+	+	+	-	+	+
Accuracy profile near interface	-	o	-	+	+	+	-
Difficulty implementation	o	+	-	+	-	-	o

Table 5.1 Pros and cons of possible sampling configurations

5.3.3 Redistribution after sedimentation and erosion

When sedimentation and erosion occur, the domain of the parameterisation changes. One or more sampling points may disappear due to this erosion and when (subsequently) material is deposited, sampling points have to describe this extension of the domain as well. Normally erosion and deposition do not occur at the same time [Partheniades, 1965]. Because the consolidation time step *timec* can be much larger than the erosion time step *delt*, net erosion and deposition can happen during a consolidation timestep in the 1-DV water bed model. So both *sedsum* and *ressum* have to be accounted for.

The sampling configuration chosen in the previous section deals with changes in the domain by means of redistribution. The method of dealing with the redistribution due to erosion and deposition is described below and is illustrated in figure 5.10. Three successive steps have to be performed to construct the new profile from the old profile and the deposition and erosion cache.

1. When material is eroded, the remaining material height is redistributed over the same number of sampling points. The properties $F_i = \left(\zeta_i, \phi_i, \sigma_i', \phi_{\max,i}, \tau_{y,i}, c_{a,i}\right)$ (material height level, volume-fraction of mud, effective stress, volume fraction with OCR=1, undrained yield strength and cohesion) adhered to the material height are interpolated (linearly) to this new height $\zeta_{\text{interface}}$ - *ressum*.

$$\left\{(F_1),(F_2),\ldots,(F_n)\right\}_t \Rightarrow \left\{(F_1),(F_2),\ldots,(F_n),(F_{n+1})\right\}_{t^*} \tag{5.7}$$

2. Sedimentation leads to a new layer on top of the bed with entirely uniform properties (corresponding with the gelling material). One point is added to all the arrays that contain the bed properties. This set contains the gel properties. The resulting set is

$$\{(F_1),(F_2),\ldots,(F_n)\}_{t^*} \Rightarrow \{(F_1),(F_2),\ldots,(F_n),(F_{n+1})\}_{t^{**}} \tag{5.8}$$

Where $F_{i+1} = \left(\zeta_{\text{interface}} - ressum + sedsum, \phi_{gel}, \sigma_v^{'} = 0, \phi_{\max} = \phi_{gel}, \tau_{y,0}, c_{a,0}\right)$

3. This set is once again interpolated to a set containing n equidistant sampling points:

$$\{(F_1),(F_2),\ldots,(F_n),(F_{n+1})\}_{t^{**}} \Rightarrow \{(F_1),(F_2),\ldots,(F_n)\}_{t+\Delta t} \tag{5.9}$$

When only erosion occurs, only the steps 1 and 3 are the performed: the second step from t^* to t^{**} is not skipped. Likewise, when only deposition occurs, only the steps 2and 3 are performed: the first from t to t^* step is skipped. When both erosion and deposition occur in one consolidation time step, both steps are performed. This type of redistribution is not optimal for both erosion and deposition: two successive time-consuming redistributions have to be performed. This approach can certainly be improved, by constructing one intermediate profile at t* that accounts for both erosion and consolidation. This means introducing a new sampling point at the level where the erosion stops and a second new point at the level up to where the bed reaches after deposition. This profile can then be dealt with in one single redistribution. Since erosion and deposition do not occur very often within one consolidation time step, the simple method above is preferred.

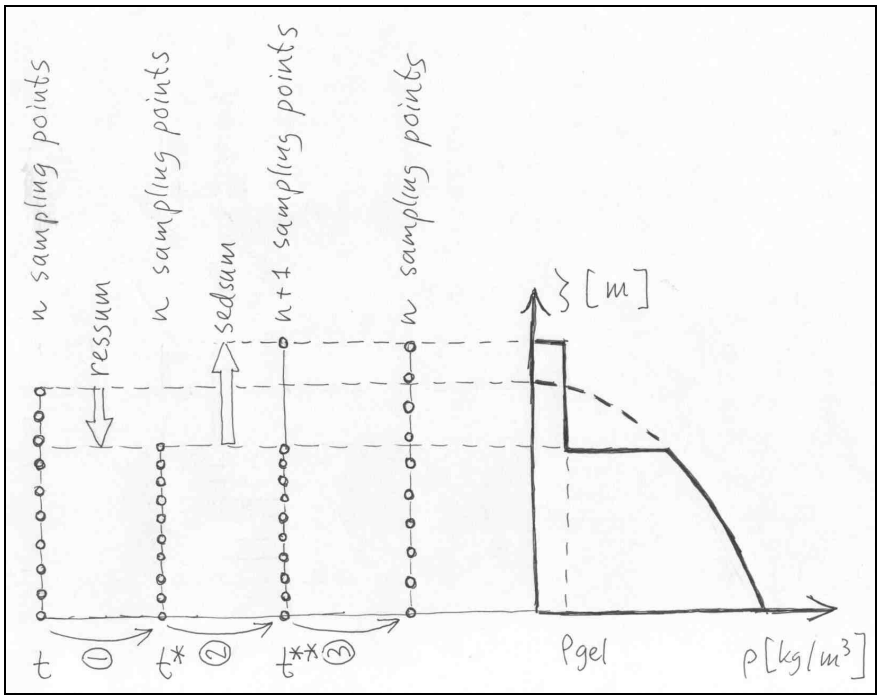

Figure 5.10: Redistribution of material to account for sedimentation and erosion

5.3.4 Linear interpolation

For reasons of simplicity, the redistribution is performed by means of linear interpolation. This can result in interpolation inaccuracies. When a deposition occurs on top of a bed with a high density near the interface, the density near the interface cannot always be represented properly (see figure 5.11 with the density profile as example). When a deposition event occurs that is much smaller than the spatial resolution, the average existing density can decrease after redistribution. This will result in an overestimation of the erosion rate. When a deposition occurs that is of the same order as the resolution, the density of the freshly deposited part will be overestimated, resulting in an underestimation of the erosion rate. Only when the spatial resolution is much finer than the deposition, can the density be represented accurately[24].

[24] Choosing cubic or spline interpolation can remedy the above phenomenon. An attempt has been made to use this kind

With some rough values of the deposition rate and the bed thickness, an estimate of the ratio between the resolution and the deposition rate can be given. We assume a 10 m water column. The concentrations in this column are, according to the requirements chapter 2: 10 mg/l to 100 mg/l. When all the sediment in this column settles, this leads to an amount of material $\Delta\zeta$ (in material coordinates with ρ_s = 2600 kg/m^3) on top of the bed of 40 to 400 μm. The time scale of this settling can also be estimated. The settling velocity is order 10^{-5} m/s (clay particles) to 10^{-3} m/s (large flocs). The sediment will therefore settle within 3 to 300 hours, while the time step of the consolidation is in the order of one day. Therefore almost all the sediment will settle within one timestep of the consolidation and the $\Delta\zeta$ above is the quantity we have to deal with in the redistribution. When we assume a bed of 50 cm with a concentration of 200 kg/m^3, the bed has a material height of about 4 cm. The resolution and the deposition are of the same order if *non* = 40 mm / 0.4 to 0.04 mm = 100 to 1000. The resolution in the bed in the 1-DV waterbed model is generally in the order of 50 to 200, so both mentioned inaccuracies in the density can occur. Using a resolution of 1000 sampling points or over is very time consuming and is not recommended.
The user should always be aware of the consequences of the spatial resolution. Choosing a small number of sampling points will make the model very fast, but it can result in severe errors. Some errors are due to the redistrubution described above. Other problems are due to the number of Fourier components. This will be described in the next section.

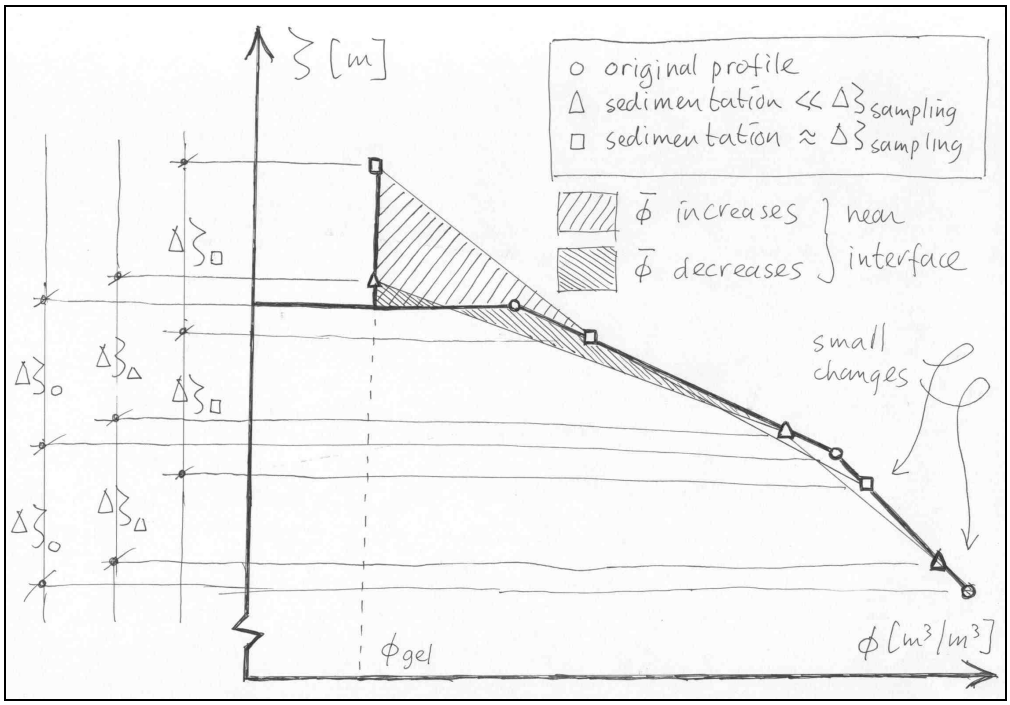

Figure 5.11: Effects of linear redistribution of material on profiles

---

of interpolation using an interpolation function from the Visual Fortan IMSL Windows library (that cannot be used in WAQ, since WAQ has to be compilable on Unix platforms as well). The result was a very 'grassy' profile, sometimes even with infinite values. Better results might be possible when implementing another spline interpolation method. Yet this method is not explored further, since it is a very time consuming problem. Within the scope of this study it not considered a worthwhile improvement of the 1-DV water bed model. The model is based on a lot of assumptions and simplifications and, more importantly, it is only a research version.

A stepwise interpolation method might also be used to prevent the average density either from increasing or from decreasing. The errors in the densities will be larger than the errors in the linear interpolation. But at least one knows that the results are either too high or too low. The method with the linear interpolation is preferred, for it gives smaller errors.

5.4 Consolidation time scale and Fourier components

In the parameterisation solution to the consolidation the solution is formed by a series (equation 4.51):

$$p_e(\xi,\tau) = \sum_{k=1}^{\infty} f_k \exp\left(-\pi^2 \left(k - \tfrac{1}{2}\right)^2 \tau\right) \cos\left(\pi\left(k - \tfrac{1}{2}\right)\xi\right) \tag{5.10}$$

with the dimensionless time parameter

$$\tau = \frac{K_k K_\sigma^{\frac{n-2}{n}} n \hat{\sigma}'^{2/n}}{\rho_w g} \frac{t}{\zeta_i^2} \tag{5.11}$$

This parameterisation can become inaccurate or unstable due to the presence of oscillations. The oscillations distort the profiles. When a profile with oscillations is present in the model, the oscillations will grow exponentially after every new calculation of the consolidation by means of eq. (5.10). The amplitude of the harmonic component in (5.10) with the same 'wave number' as the oscillations, will grow every time the profile is Fourier transformed. This leads to larger amplitude of the oscillation with that specific 'wave number', which in turn leads to a larger amplitude of the Fourier component. This is a positive feed-back loop, leading to instability. This problem and the way to prevent it are treated in this section.

First, in the analytical parameterisation approach, very small time steps t for consolidation are not possible. The solution of the Gibson consolidation equation is a superposition of an infinite number of decaying harmonic solutions. In mathematical terms, the complete series forms an exact solution of the problem. In reality however, one can only deal with a finite number of components. When one takes too few terms into account, inaccurate and oscillating solutions can occur, especially near spots with sharp gradients. (see annex 5.1 for an example). This effect plays a role near the edges of the bed (e.g. the underlying rigid/impermeable bottom and near the water-interface) or when material at the gelling point is deposited on a consolidated bed, leading to a step in the density profile. The oscillations in the stress and density profiles lead to erosion rates fluctuating over the vertical near the surface. This should be prevented.

The oscillations arise only when dealing with too few terms in (5.10). The number of terms that is sufficient, depends on the decay of the exponential time factor $\exp(-\pi^2(k\text{-}0.5)^2\tau)$ in equation (5.10).

- In the case that the time factor $\exp(-\pi^2(k\text{-}0.5)^2\tau)$ in equation (5.10) is one (τ=0), the oscillations will occur with any number of terms. When introducing more terms, the area over which the oscillations are present becomes smaller (concentrated near the sharp gradients), but the oscillation peaks themselves become larger. When a large number of terms are used, the profile will look somewhat like an 'American football goal' (H). This is known as the Gibbs effect.
- When we want to calculate the bed after a very long time, the time factor becomes zero and no term is necessary at all.
- Equation (5.10) will be used to calculate the excess pore pressure profile after some time t. In this case the use of a sufficiently large, but finite number of terms can prevent the occurrence of oscillation completely. For the time steps in the 1-DV water bed model the time term will have to be set between 1 and 0 and accordingly the required number of terms will be between infinite and zero. When the decay of the terms increases, the required number of terms drops.

The decay of the terms depends on the time factor τ. In equation (5.11) we can see that the time step t governs this decay. Smaller time steps lead to a smaller decay. But in equation (5.11) we can also see that the decay is affected by the thickness squared of the consolidating bed ($\tau :: \zeta_i^{-2}$), the effective stress, and by the combination of the material coefficients as well. In the model the relation $\sigma'_{v,max} = (\rho_s\text{-}\rho_w) g \zeta_i$ is used. So the parameter τ is dependent on ζ_i as $\tau : : \zeta_i\, 2^{((1\text{-}n)/n)}$.

How many terms do we need? What we do know about the oscillation is that each term k decays with a its own factor in (5.10), and that the smaller terms decay most quickly. The oscillation is the result of a sum all the terms, in which not only the highest order terms (k=1,2) matter. The relation between the number of Fourier components *nok* and the τ-steps on the verge of oscillation has been investigated. A severe test is

used: a profile with one uniform density in the upper half and second higher uniform density in the lower half. The transition between these densities is a jump. The results of the profiles can be seen in annex 5.2 to 5.4. In the table 5.2, the combination of factors for which the oscillation effect could just visually be discerned has been gathered. (The criterion that the oscillation had to be visible is a qualitative and subjective criterion, but it is useful.)

$-\pi^2 \cdot nok^2 \cdot \tau$	τ [-]	Time [sec]	Time [hours]	Number of Fourier components *nok*	nok^2 [#]
2.5 to 5	2.50E-02	360000	100	5 to 7	25 to 50
2.5 to 5	2.50E-03	36000	10	17 to 22	250 to 500
2.5 to 5	2.50E-04	3600	1	50 to 70	2500 to 5000
2.5 to 5	2.50E-05	360	0.1	170 to 220	250000 to 50000

Table 5.2: combination of factors at verge of presence of oscillation.

The conclusion one can draw from table 5.2 is that in order to prevent oscillations, the argument of the exponential decay function in (5.10) should be 2.5 to 5 for the term with the highest number *k*. The associated decay for the smallest component during one time step is in the order of 1% (exp(-2.5)=0.08 and exp(-5)=0.007). Since for large *k* $(k-0.5) \approx k$, we can also say that τ times the number of Fourier components *nok* should be 2.5 to 5. This leads to the following conservative rule of thumb stability criterion:

$$nok \cdot \tau > 0.5 \tag{5.12}$$

For problems without steep gradients, the number of Fourier components could be smaller without worrying about oscillations.

The number of Fourier components *nok* depends on the dimensionless time τ. The number of Fourier components should be chosen to meet (5.12) based on the value of this parameter τ. This parameter is governed by (i) the minimum time step of the consolidation *deltcmin*, (ii) the maximum expected material layer height ζ_i and (iii) the coefficients K_k, K_σ and D. The values of these parameters have to be known to determine τ and, subsequently, *nok*. The parameters *deltcmin,* K_k, K_σ and D are fixed. The material height ζ_i however, changes during the simulation. Therefore, a maximum value of this parameter has to be estimated to determine *nok*. If the estimate of the material height is too low, the computation can become unstable. A nice example of this is, when sedimentation occurs at a large and constant rate for a long period. In this case the parameter τ decrease in time according to

$$\tau \sim \frac{t}{\zeta_i^2} = \frac{t}{\left(\zeta_0 + v_s \phi \cdot t\right)^2}\bigg|_{t \to \infty} \approx \frac{t}{\left(v_s \phi \cdot t\right)^2} \sim \frac{1}{t} \tag{5.13}$$

Likewise, the required number of Fourier components increases in time.

The number of Fourier components *nok* cannot be chosen freely to meet 5.12. The number of components *nok* should always be equal to or less than twice the number of discrete points *non* in order to get meaningful Fourier components. The reason for this is that evaluating the Fourier coefficient f_k for a specific component, the integral (4.52) should provide at least two sampling points for each whole (co)sinus $\cos(\pi(k-0.5)\xi)$. The highest 'frequency' for which this occurs is the Nyquist frequency.

The solutions of the consolidation equation are symmetrical with respect to the rigid bottom. Hence the coefficients are determined with an imaginary continuation of the profile below the rigid bottom. Accordingly the number of discrete points is thus twice the number of sampling points *non*. Consequently the number of Fourier components *nok* should always be less than or equal to the number of sampling points *non*.

$$nok \leq non \tag{5.14}$$

The above means that in order to determine the consolidation solution, any small time step is possible and any combination of parameters is possible, provided a sufficient number of Fourier components is used, and accordingly a sufficient number of sampling points. This leads to an increased amount of calculation time, possibly conflicting with the first purpose of making a model fast with respect to numerical solutions.

The calculation time increases more than linearly with the number of sampling points. A more exact relation will be given in chapter 7, where the 1-DV water bed model will be validated.

5.5 Summary

- The 1-DV waterbed model consists of three modules: a deposition and erosion module, a consolidation module and the enveloping 1-DV water bed module. The erosion, deposition and consolidation processes have different time scales. The time scale of the diffusion term in the Gibson equation is in the order of a few days, which is much longer than the time scale of the erosion and deposition, which are in the order of hours. The time scale of the advection term in the consolidation equation is a few hours as well. Accordingly already considerable strengthening can occur during slack tide (a period of about 1 hour). The advection term is not present in the parameterisation however. Therefore, in order to minimise calculation time, the consolidation can be solved in a physically correct manner at a longer time step than the time step used to account for erosion and deposition. Since the consolidation is numerically an expensive process, this is very useful.
- An implementation (configuration) of the different modules is proposed that allows erosion and consolidation computations to have different time steps. This leads to some complications however. The erosion and deposition in the 1-DV water bed model have to be computed more often than the consolidation module. The cumulative erosion from the density and effective stress profiles and the cumulative deposition, have to be stored in a cache before the consolidation module can account for them. The cached deposition is subject to entrainment when it has not yet been exposed to consolidation.
- The consolidation time step is not fixed. Consolidation is only activated when a transition from deposition to erosion occurs. In a lake for instance, erosion almost never occurs, so a maximum consolidation time step has to be accounted for. To optimise the calculation procedure, a minimum time step for the consolidation has to be taken into account.
- The erosion rate during a WAQ time step and the progression of the erosion is determined by means of an iteration process using smaller time steps than the WAQ timestep.
- The profiles of the bed properties have to be sampled to store them in the computer. A sampling system with a fixed number of sampling points and equidistant spatial steps in material coordinates is chosen. It resembles the sigma-coordinate system of Delft3D-flow. This system is easy to implement and keeps the same calculation time during an entire simulation. A disadvantage is that every time erosion or deposition takes place, all the sampling points have to be redistributed over the new material height. At the same time the profiles of the density, the effective stress and the other parameters have to be interpolated linearly. This is time consuming. Moreover, the linear interpolation can affect the average properties near the interface if the sampling resolution is too coarse. The influence of this effect is not known yet. The constant number of sampling points demands that when assessing the spatial resolution, the amount of material in the system has to be estimated. The user should always be aware of this.
- The solution of the consolidation equation is written as a Fourier series. When too little components are used, the profiles show oscillations and become unstable. On the basis of a numerical experiment for a steep initial density gradient, a stability criterion is formulated: when the number of Fourier components times the non-dimensional time parameter τ is more than 0.5, oscillations will not occur. The parameter τ increases when (i) the time steps of the consolidation increase, (ii) when the amount of material ζ_i in the bed decreases and (iii) when another combination of the parameters K_k, K_σ, and D is chosen. The number of Fourier components should not exceed the number of sampling points.

6 Validation consolidation model

This chapter has two aims. The first is to validate the consolidation model that has been derived in the previous chapter. The second is to perform a sensitivity analysis of this model. The model is validated using data from a consolidation experiment that was performed on the same mud on which an erosion experiment has been performed. The results and conclusions from the consolidation experiment are used when testing the erosion model in the next chapter.

In this chapter much attention is paid to the determination of the input parameters of the 1DV-waterbed model. The input parameters are the empirical coefficients in the constitutive relations of Merckelbach based on a fractal description of mud. He also gave a method to determine these parameters. From his study it is known that the proposed method to determine the parameters works: representative values of the parameters can be obtained and it is possible to describe the development of the density profiles in time with these parameters. Through this, the validity of the theory of the fractal description of the material has been corroborated. The aim of this study however, is to create a generic model for engineering purposes with a wide field of application. For these kinds of applications, knowledge about the variation in parameters is indispensable as well. Therefore an extensive analysis of the data was considered useful. The purpose of this extensive analysis is to judge whether the parameters can be obtained easily. The measurements of Merckelbach [2000] are very accurate and precise, whereas the measurements of Kuijper [1990], which are used in this study, are less accurate and less precise. In engineering practices measurements are often performed with a limited accuracy, while the model will be used in this very engineering practise. Another purpose of the extensive data analysis is to assess whether the parameters obtained this way are accurate and reliable.

The model parameters may vary in a number of ways: variation because of different kinds of mud, variation due to errors in the method of determination, and intrinsic maximum accuracy. The variation between different kinds of mud cannot be determined accurately at present, since only a few kinds of mud have yet been analysed with the fractal description. A first comparison can be made with the results from Merckelbach [2000] however. The variation in the parameters due to the method of determination is the main issue in this chapter. The intrinsic inaccuracy is due to some simplifications of reality in the fractal model (no gas, no biological activity, no thixotropy, not too much sand/silt). Hence the parameters can never be determined with 100% accuracy. This intrinsic variation can be judged by modelling the experimental results with the fitted parameters.

The structure of this chapter is as follows. First the experiments that have been performed are described. Then, successively, the permeability parameters, the effective stress parameters and the yield stress parameters are determined. With these parameters, the results of the parameterisation and the numerical consolidation model can be compared with the results of the consolidation tests. Once the parameters as well as their variation are known, the erosion tests can be modelled as described in the next chapter. With the knowledge of the variation of the parameters, a well founded sensitivity analysis can be performed. A summary concludes this chapter.

6.1 Measurements of mud properties

Various chemical and physical properties of the sediment have been measured before the erosion tests in the rotating annular flume at WL | Delft Hydraulics. The sediment properties are enclosed in annex 6.1. Two tests have been performed that can be used to determine the parameters of the fractal description of mud.

First, the remolded shear strength has been measured with a roto-viscometer. With a relation derived by Kranenburg [1994], these data can be used to determine the fractal dimension D. Second, the consolidation

behaviour of the sediment has been studied. Because of practical considerations, the consolidation of the sediment layer was studied in a separate column, and not in the flume where it has been exposed to erosion. After thorough mixing, the settling column is filled to a height of 0.3 m (with an initial concentration of c = 54 kg/m^3 for the first and 56 kg/m^3 for the second experiment, this equals a material height of $\zeta = h \cdot c / \rho_s$ = (0.3 m) * (54 a 55 kg/m^3) / (2600 kg/m^3) = 6.2 a 6.5 10^{-3} m material). Two types of measurements have been performed in this experiment.

In this consolidation experiment, the height of the interface between the suspension and the clear water above has been measured as a function of time. The height of the sediment-water interface is determined by visual observation. This interface is sharp and can be measured accurately by visual observation (error in the order of the meniscus height < 0.5 mm). From this data, the permeability parameter K_k and the fractal dimension D are obtained in section 6.2. The dry density profile within the bed has been measured as well.[25] From this data the effective stress parameter K_σ and the fractal dimension D will be obtained in section 6.3.

6.2 Permeability

6.2.1 Methodology for determination of parameters

The fractal dimension and the permeability parameter K_k can be obtained from the settling data by plotting the interface height versus the time on double logarithmic paper [Merckelbach, 2000]. The slope of the line can be related to the fractal dimension and the position of the line to the permeability parameter. The relation by which these parameters can be determined is a simplification of the Gibson equation. The assumption for this simplification is that during the initial consolidation process, the effects of effective stress are negligible. The Gibson equation can then be simplified by discarding the diffusion term (the only term containing the effective stress). Substitution of the permeability relation $k=K_k\phi^n$ yields:

$$\frac{\partial \phi}{\partial t} - K_k \Delta(2-n)\phi^{1-n}\frac{\partial \phi}{\partial \zeta} = 0 \qquad (6.1)$$

This result is a non-linear convection equation, similar to Kynch's [1951] sedimentation equation. This equation can be solved using the method of characteristics. The solution can be depicted in a Kynch-plot, that looks similar to figure 6.1 (but then with the characteristics included). In order to judge when the simplification 6.1 is valid, the settling behaviour will be described shortly by means of this figure.

Initially two discontinuities are often [26] observed: the interface between the overlying water and the suspension and the interface between the suspension and the bed. To the left of figure 6.1 the whole sediment-water mixture is still in the suspension phase. The suspension settles initially with the same velocity over the vertical. As a result a bed starts to form near the rigid bottom of the column: in the lower parts the density already exceeds the gelling point, while the rest of the column is still in suspension phase. This is the first interface. At the same time, all the sediment disappears from the upper part of the column by the settling of the sediment. The water becomes clear there. This is the second interface.

[25] "The dry density is measured with a probe that detects the attenuation of an acoustic signal due to the presence of the sediment (mass). The transducers are shaped as small cylinders with a diameter of 10 mm and a thickness of 8.5 mm. The vertical resolution is about 3 mm. The profile is measured by lowering the transmitter and receiver into the sediment layer. During the successive measurements a lowering of the sediment-water interface is observed at the location of the measurements. This affects mainly the concentration in the top layer. The measurements are performed during the consolidation period of 7 days. (..) Because of the size of the transducers the measurements in the upper few millimetres of the layer are unreliable." Kuijper [1990].

[26] If the initial density is higher than a certain density, only one interface is present from the beginning of the experiments according to Kranenburg [1992].

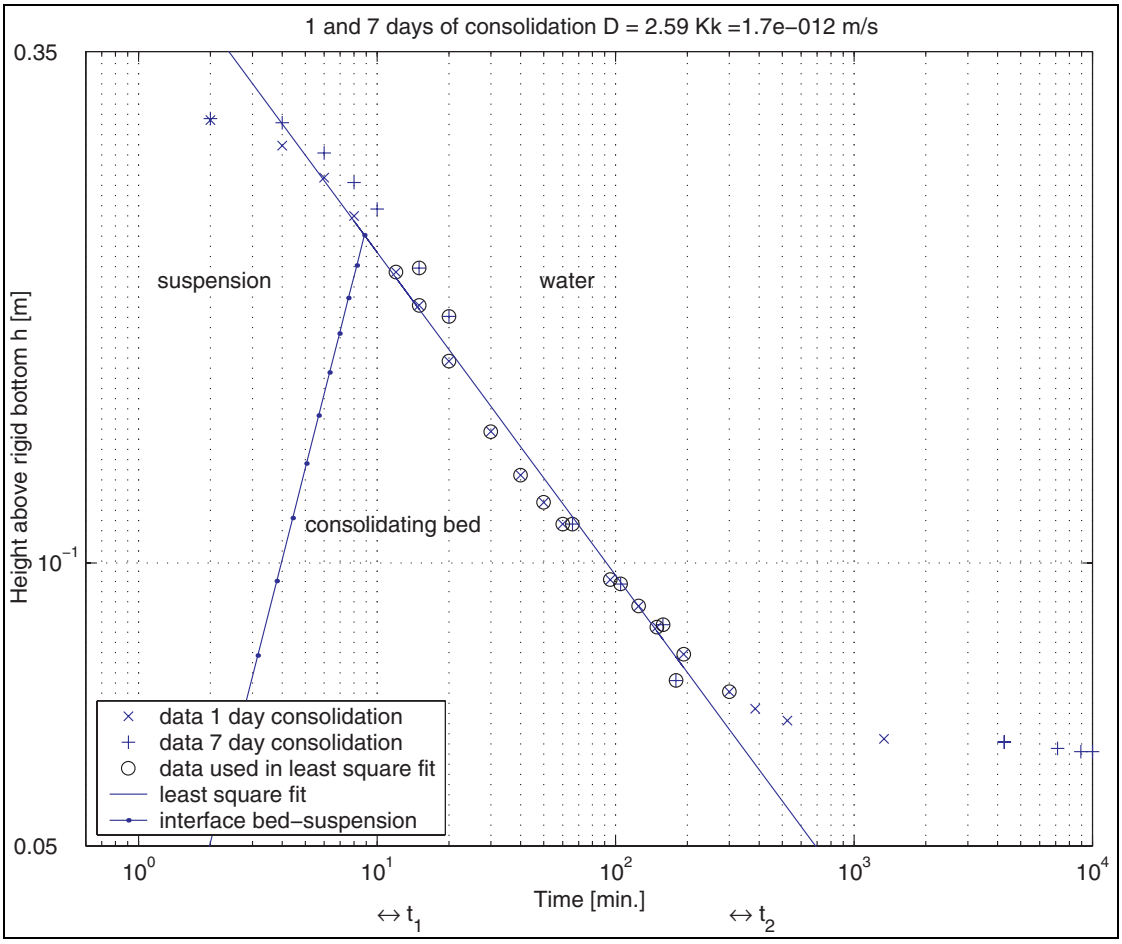

Figure 6.1 : Average example of a least square fit of the interface vs. time to determine the K_k and D.

During the period $t = 0$ to $t = t_1$ the solution of the upper (suspension) part of the density profile is still determined by the hindered settling formulation, which is not incorporated in the permeability function used to derive 6.1. Consequently equation 6.1 is not valid for $t < t_1$. The two interfaces meet at time $t = t_1$, after which one single discontinuity remains, between the water and the bed. At $t = t_1$ the entire suspension has reached its gelling point (structural density). From that moment on, all the sediment in the settling column is present in the consolidating bed, but the effective stresses in the bed are still small ($t < t_2$). From $t = t_1$ to $t = t_2$ the solution of the density profile is determined by 6.1. The solution for $t > t_1$ on is independent of the initial conditions. The effective stresses start to become dominant at $t > t_2$. Equation 6.1 has been derived by neglecting the effective stress terms, so equation 6.1 is not valid for $t > t_2$. Accordingly, the period $t_1 < t < t_2$ is considered the initial phase of consolidation when the approximation of the Gibson equation to determine the parameters D and K_k is valid. For the interface height as a function of time for the period $t_1 < t < t_2$, an analytical solution has been derived by Merckelbach [2000]. It reads:

$$h(t) = \left(\zeta \frac{2-n}{1-n}\right)^{\frac{1-n}{2-n}} \left(K_k \Delta (n-2)\right) t^{\frac{1}{2-n}} \tag{6.2}$$

According to this equation, plotting the interface height vs. time on a double log paper results in a straight line:

$$\log h = \log\left[K_k \Delta (n-2) \left(\zeta \frac{2-n}{1-n}\right)^{\frac{1-n}{2-n}} \right] + \frac{1}{2-n} \log t \tag{6.3}$$

When plotting the data on double log paper, the slope of the straight line through the data, R, equals $(2\text{-}n)^{-1}$. This means that D can be determined according to

$$D = \frac{4R+3}{2R+1} \tag{6.4}$$

Furthermore, the permeability parameter K_k can be determined by substitution of a single measurement (h,t) in 6.2. Two complications are met in this approach however: when does the transition from the (hindered) settling regime to the actual consolidation regime (t_1) occur, and when are the effective stresses no longer negligible (t_2)?

At the time of observation of the first data points, the settling column is still in the suspension phase and the method to determine the parameters is not valid. The approach is valid a short period after the moment when the interface between the water and the suspension and the interface between the suspension and the consolidating bed reach each other (t_1). The interface between the suspension and the consolidating bed however, has not been measured. Often this interface cannot be measured by visual observation, since the deeper parts of the settling column are very turbid. Moreover, this interface is not sharp at all.[27] So even when we can measure this interface by means of visual observation, the error is quite large. An echo sounder, leadline [Mehta, 1990] or a radioactive device should be used to measure this accurately. These kinds of measurements are very expensive though. This means that generally we do not accurately know t_1.

The method to determine the permeability parameters is valid until the effective stresses are no longer negligible. The effective stresses start to become significant at $t \approx t_2$. At the time of the observation of the last data points, the interface location hardly changes any more. The sediment water interface changes only 0.002 m in the period between 1 day and 7 days after the start of the consolidation, which is less than 1% of the total variation (≈ water depth). By then the sediment has formed an almost fully consolidated bed where the effective stresses are no longer negligible. Hence the development of the effective stresses are not reflected in the interface height. This means that we generally do not know t_2 accurately either.

Summarised: The data cover a longer period than the period that is needed (or rather allowed) for the determination of the parameters. Thus the approximation of the Gibson equation is valid for some of the data points in the middle of the measurement series. It is not directly clear which data points should be incorporated in the analysis. When fitting the data points on double logarithmic paper by a straight line, this line should be based on some of the middle data points. But the choice of leaving out another data point at either end of the data series or not, influences the slope and the offset of the line: different lines are possible. This implies that if different people determine the permeability parameters on the same

[27] I performed some experiments in a settling column as well. The goal of this was to get a feeling for the real behaviour of mud. I observed a few things. First the interface between the suspension and the settled bed cannot be observed by means of colour. Second, the suspension part and the consolidated bed can be discerned by means of fine 'pattern' at the glass outer wall of the column. In the suspension many fine channels and irregularities can be seen, whereas the consolidated bed looks homogeneous. The accuracy of this distinction is in the order of a few cm. However, this is only observed when the column is not exposed to small vibrations. Third, at the transition between these two observed regimes, larger canals (diameter order 1 mm) develop, steadily growing upwards. The upward velocities in these channels is at least equal to the upward velocities of the moving sediment particles in the channels, that have been estimated to travel in the order of a few mm per second. The largest channels sometimes even reached the interface between the suspension and the clear water. As the channels develop upwards, the speed in these channels drops. Successively new channels are initiated at a higher levels, often using (parts of) the route of the earlier channels that have gone out of use. Channels stay present in the consolidating bed after they have stopped to transport water. This obviously leads to a larger permeability of the bed than predicted by the fractal theory. But when exposed to small vibrations (as on a desk), the channels cannot be seen. So in estuarine beds the fractal approach will be more valid than in the laboratory. Moreover, when the water above the bed has become perfectly clear (after 1 day), at the interface between the bed and the water lots of small craters can be observed. The channels therefore not only develop next to the outer wall of the column, where they can actually be seen, but probably also over the entire cross-section of the column. My hypothesis is that channels start to develop at the interface between the suspension and the bed. The forming of a volume-filling network leads to sharp gradients in the permeability resulting in sharp gradients in the pore pressure. This can lead to local failure of the structure.

measurements, the results will be different. A formal procedure is needed that will guarantee the reproducibility of the results. Such a method will be proposed in section 6.2.3. First one fitting case will be given as illustration.

A representative fit of the data can be seen in figure 6.1. The moment of gelling t_1 of the bed-suspension and the suspension-water interface at that time can be calculated once the permeability parameter and the fractal dimension are determined by a least square fit (see Merckelbach [2000]). This intersection should be on the left part of the least square fit. As one can see this holds for this fit. On the right side of the graph one can see that the data points tend to a horizontal line: the bed is in its final stage of consolidation ($t > t_2$) The derivative with respect to time in the Gibson equation is zero. The approximation of the Gibson equation to determine the parameters D and K_k is not valid any more in this part of the graph. One can see that all the data points that are included in the least square fit, are indeed on the straight line. Moreover, one can see that the data points where the bed is in its final phase are not on the line any more.

The parameters as determined by this fit are D=2.59 and K_k= $1.7 \cdot 10^{-12}$ m/s. They are in the same order of magnitude as the parameters found by Merckelbach [2000], who found D=2.60 to 2.75 and values of K_σ in the order of $8 \cdot 10^{-13}$ to $1 \cdot 10^{-15}$ m/s (see table 6.2). With this single fit, one can conclude that it is possible to determine the parameters D and K_k on the basis of one simple observation of the settling of the interface in a settling column. But other fits might also lead to good results. Hence the next question is whether these values are accurate and reliable.

6.2.2 Variation of parameters: multiple least square fits

By fitting a single line, representative values for D and K_k can be obtained. But as argued in the introduction of this chapter, this is a new technique and it is very useful to have information of the variation of this parameters as well. A method to account for this is to generate a large number of valid least square lines automatically. [28] Each of these lines results in a different combination of D and K_k. This set ($\underline{D}$,$\underline{K_k}$) can be used as an estimate of the distribution of D and K_k. It gives an indication of the possible range of the parameters. A method has to be found to generate sets on which least square fits can be based.

An option is to generate all possible combinations of leaving out an arbitrary number of the first and/or last data points of the measurement series. This method is based on the knowledge that the approach is only valid for a set of data points in the middle of the range. (To account for the errors in the data set, one could also fit lines for all combinations of leaving out 1,2,..,n random chosen data points. This method from statistics is known as the Bootstrap method.) However, at least two points are needed to determine a line in a plane. Lines fitted on only two data points, however, can lead to unrealistic results that are immediately seen to be invalid. Therefore the requirement is used that at least three data points should be used for a

---

[28] A data set $\left(\underline{x},\underline{y}\right) = \left(\left[x_1 \quad x_2 \quad \ldots \quad x_n\right]^T, \left[y_1 \quad y_2 \quad \ldots \quad y_n\right]^T\right)$ can be described by a relation $\underline{y} = C \cdot \underline{x}^p$. This relation can be written as a linear relation when taking the natural logarithm of both sides:

$$\log \underline{y} = \log\left(C \cdot \underline{x}^p\right) = p \log \underline{x} + \log C \Leftrightarrow \underline{Y} = a\underline{X} + b .$$

Herein the data set $\left(\underline{X},\underline{Y}\right)$ is known and the set $\left[a,b\right] = \left[p, \log C\right]$ has to be determined. This relation can be written in matrix form:

$$\underline{Y} = a\underline{X} + b \Leftrightarrow \underline{Y} = \left[1 \quad \underline{X}\right]\begin{bmatrix} b \\ a \end{bmatrix} \Leftrightarrow \underline{Y} = M\underline{A}$$

The least square solution of this problem is [Lay, 1993]:

$$M^T \underline{Y} = M^T M \underline{A} \Leftrightarrow \underline{A} = \left(M^T M\right)^{-1} M^T \underline{Y}$$

The inverse calculation can be carried out by Matlab very fast.

single line. Even this requirement, though, can lead to very unrealistic fits. These fits will be omitted on the basis of visual inspection. Some examples of these unrealistic fits can be seen in annex 6.2.

The settling of the interface has been measured for a one day period and a seven day period separately (although a one day experiment is also a part of a seven day experiment). The first experiment covers 19 observations and the second 16. The data covering the first day of these two separate measurements should coincide, but they show a relatively large variation. This difference between these two measurements can be used as an estimate of the experimental errors. To account for this, a third set is assembled by joining the results of the two experiments (with 19 + 16 = 35 observations). The distribution of D and K_k will be obtained for the 1 and 7 day experiment together and separately. This results in three pairs of parameters (see Table 6.1).

Experiment	Number of observations	Number of possible least square fits
1 day consolidation	19	153
7 day consolidation	16	105
1 and 7 day consolidation	35	561

Table 6.1

In figure 6.1 one can see one of these generated fits. (Note that both axes are on log scale.) The data of the 1 and 7 day experiment have been used both in this fit, nine data points have been discarded on the left side and seven on the right side. The results of all the fits are depicted in figure 6.2 and 6.3.

The parameters have been determined for all 561 possible ways of leaving out of data points at the start and end of the series. The average values of K_k =$5\cdot10^{-14}$ m/s and D=2.65 show good agreement with the parameter values that are determined by Merckelbach, who found D=2.60 to 2.75 and values of K_σ in the order of $8\cdot10^{-13}$ to $1\cdot10^{-15}$ m/s (table 6.2). Moreover, the modal values (the values near the peak of the distributions or the most frequent values) are in the same order (figure 6.2). The values of the parameters however show a large variation. Especially the variation in the permeability parameter is large. The sensitivity of the permeability parameter to the fractal dimension is high. This was already recognised by Merckelbach and can be observed from his results of his CT series as well (table 6.2). Moreover, the fractal dimension does lie in the theoretical expected range in the bed of about 2.6 to 2.8 according to Winterwerp [1999].

Experiment	μ (D)	σ (D)	μ (K_k)	σ (log(K_k)) [29]
			m/s	m/s
Kuijper [1990] – current analysis	2.65	0.08	2 to $5\cdot10^{-14}$	$10^{3.3}$
Merckelbach [2000] CS series	2.75		$1.2\cdot10^{-15}$	
Merckelbach [2000] CT series by permeability data	2.67		$4.5\cdot10^{-13}$	
Merckelbach [2000] CT series from settling interface	2.75		$2.2\cdot10^{-15}$	
Merckelbach [2000] DT series	2.72		$1.4\cdot10^{-14}$	
Merckelbach [2000] Townsend & Mc Vay	2.60		$7.64\cdot10^{-13}$	

Table 6.2 Statistical properties (average μ and standard deviation σ) of the results of the all the least square fits of the interface vs. time to determine the K_k and D

The range of the parameters obtained is large. What value can we consider to be representative? The modal values in figure 6.2 give the fit with the highest probability of being fitted in a single least square fit procedure. Therefore the recommendation is to use the modal value of the distribution of D and the

[29] The standard deviation σ of log(K_k) is σ=3.3. And $10^{3.3}\approx2000$. This means that the standard deviation is 3.3 orders of magnitude and that 65 % of the data lie within a *factor* 2000 of the average value: 10^{-17}-10^{-10}. Note that the constitutive relation can also be written in a way that leads to a much smaller variation in the parameters. The parameter $K_k^{-1/n}$ shows a much smaller variation than K_k: $k = K_k\,\phi^{-n}=(K_k^{1/n}\phi)^{-n}$.

corresponding K_k (see figure 6.3) as the material parameters and not the average values: D=2.59 is recommended. This peak value is independent of the person who performs the analysis, and independent of the number of data points used (discarded) in the analysis. Therefore it complies with the criterion of reproducibility of the analysis. It should be checked though that the line corresponding to the peak value looks satisfactory on log-log scale. The least square example in figure 6.1 has a fractal dimension equal to the peak value (D=2.59) and does indeed look satisfactory.

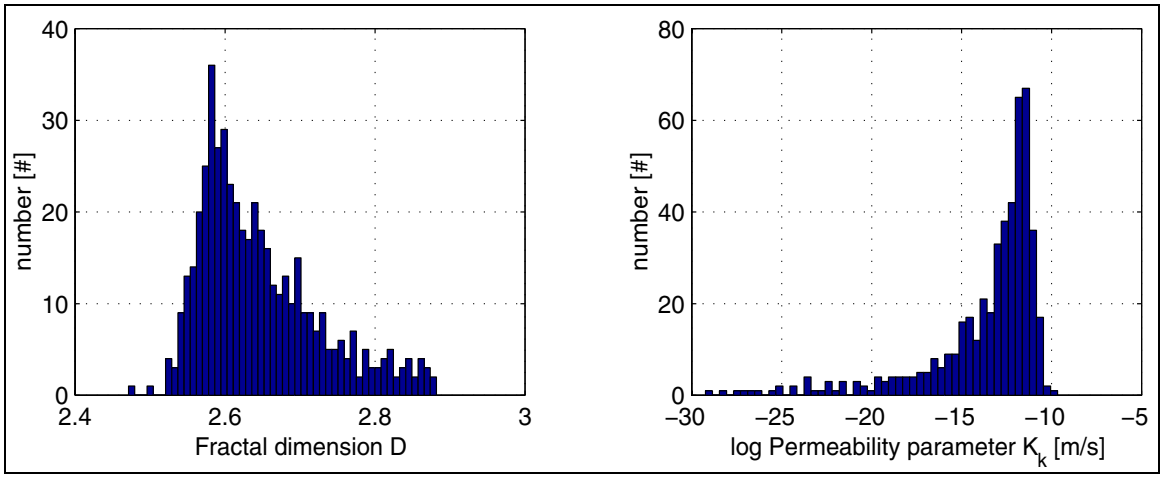

Figure 6.2 : Histogram of the results of the all the least square fits of the interface vs. time by Kuijper et al. [1990] to determine the K_k and D (1 and 7 day experiment together). Modal value of fractal dimension is D=2.59.

The graphs with all the least square fits have been inspected individually. For most of these graphs, the point where the suspension phase disappears between the fresh water and the consolidating bed (t_1), is on the least square line. The very low values of the permeability parameters correspond with the case where only the points on the very right side or the points on the very left side are fitted. These lines are very flat: they lead to a low permeability parameter and a high fractal dimension. (For extreme examples see annex 6.2.) The few very high values of the permeability parameter correspond with cases where only 3 to 5 points of the middle part of the graph have been fitted. The small errors in these observations can lead to very steep, odd lines (see annex 6.2).

The graphs of the distributions suggest that one can use the statistically derived average or the modal value (most frequent value) of each parameter. This is not true, because the values of permeability parameter and the fractal dimension from a single fit are coupled to each other. This can be seen in figure 6.3. In this figure every point represents the values (K_k ,D) obtained from one single fit. Small values of the fractal dimension are accompanied by large values of the permeability parameter and vice versa. The combination (K_k ,D) to represent the data, should fit this relationship. This relationship is not one with a physical basis however. All possible lines through the mass centre point of the data $(\bar{h},\bar{t})$ obey this relationship: a steeper line (larger D) will have a higher intersection with the log(h) axis, leading to a smaller K_k. Because of the log scales, a small change in the slope of the lines is accompanied by a large change in K_k. Moreover, the parameter n=2/(3-D) governs the slope. Since D is close to 3, a small change in D is accompanied by a large change in n. These effects account for large variation in K_k. However, not all the fitted lines go through the point $(\bar{h},\bar{t})$. Some lines fit mainly the data points with the low interface height at 100 minutes or more. Other lines mainly fit the data points with the interface height of almost 30 cm in the first hour. The upward or downward shift of these fitted lines is much smaller than one order of magnitude (less than 30 cm) and hence this will not significantly affect the position of the pairs K_k and D to the solid line in figure 6.3. Note that the parameters obtained by Merckelbach [2000] are also close to this line.

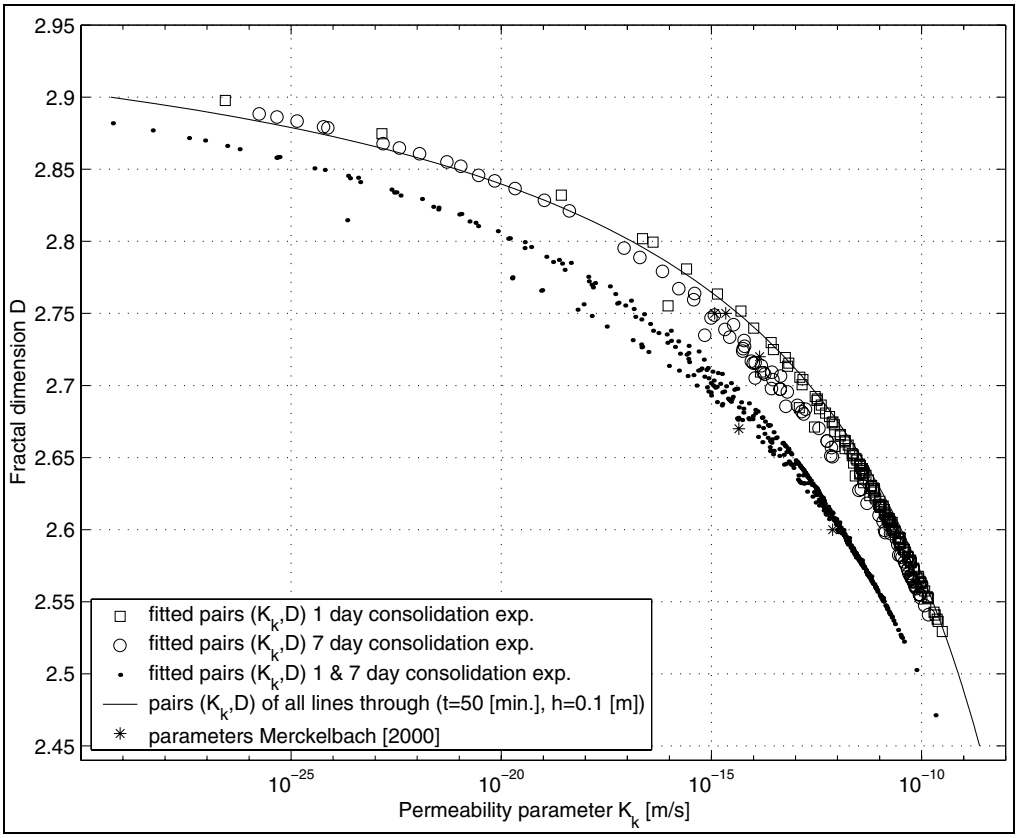

Figure 6.3 : Relation between D and K_k of each fit

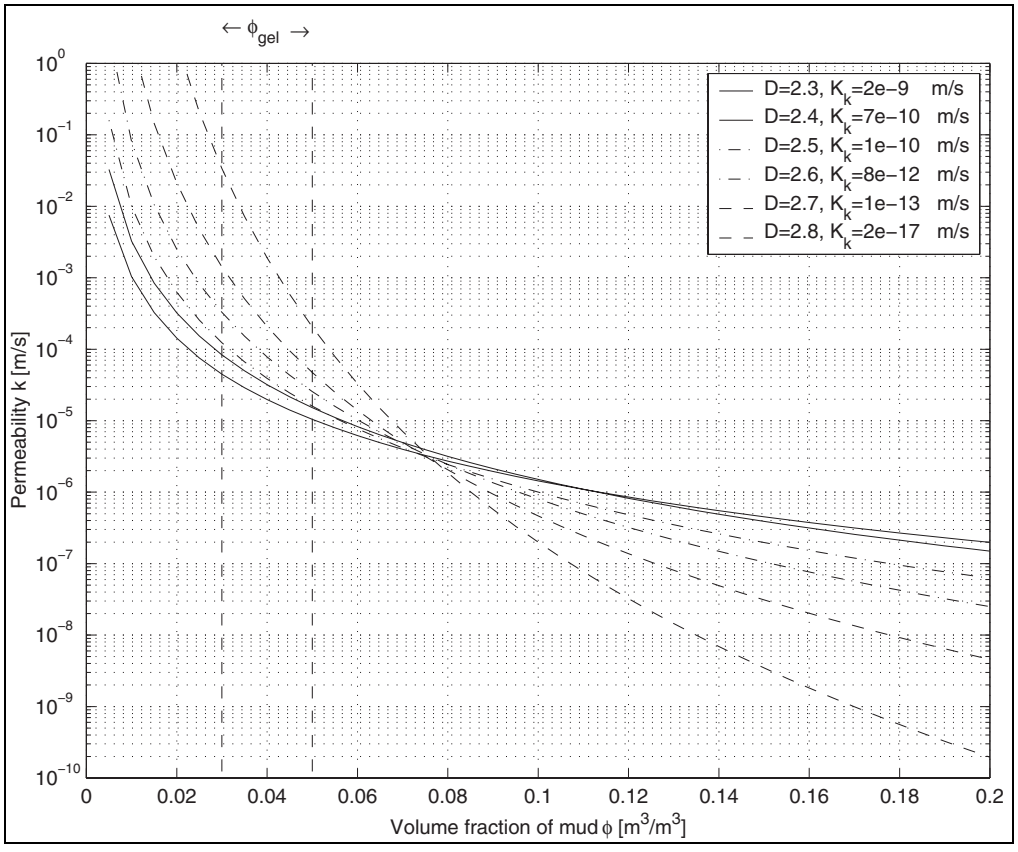

Figure 6.4 : Relation permeability k and ϕ for various sets D and K_k

The relation between the permeability k and ϕ has been plotted in figure 6.4 for different combinations of D and K_k from figure 6.3. The lower the fractal dimension, the more gradual the increase of the permeability with ϕ. The higher the fractal dimension the higher the permeability at the gelling point. All the lines intersect at densities just above the gelling point ϕ_{gel}, which is 0.03 to 0.05. That means that the choice of a set D and K_k does not matter much in this regime. That is convenient since the 1DV-waterbed model uses the density near the interface to calculate the erosion rate. At the gelling points and at higher volume fractions of mud (0.2) however, the permeability can change by one or more orders of magnitude.

6.3 Effective stress

6.3.1 Methodology for determination of effective stress parameter

The effective stress parameters can be obtained by considering the equilibrium solution of the Gibson equation: $\partial\phi/\partial t = 0$. This simplification is valid at the final stage of consolidation only, that is well past $t = t_2$. Merckelbach [2000] has derived an analytical solution of the relationship between the height below the final interface and the density in steady state:

$$h - z = 2\frac{K_\sigma}{(D-1)(\rho_s - \rho_w)g}\phi^{\frac{D-1}{3-D}} \tag{6.5}$$

According to this equation, plotting the distance below the interface vs. the density on a double log paper results in a straight line:

$$\log(h-z) = \log\left[\frac{2K_\sigma}{(D-1)(\rho_s-\rho_w)g}\right] + \frac{D-1}{3-D}\log\phi \tag{6.6}$$

When plotting (h-z) vs. ϕ on double log paper, the slope of the straight line through the data, R, equals $(D-1)/(3-D)$. K_σ can be determined by substituting one pair (h-z,ϕ). Three difficulties arise when applying this method.

First, the measurements of 24 hours and later cannot be discriminated clearly in figure 6.5. The measurement at 168 hours does not depict the profile with the highest densities, as one would expect. This suggests that the accuracy of the measurements is not very good. The accuracy is in the order of $\Delta\rho_d/\rho_d \approx 50/250 \approx 20\%$. One explanation for the differences between the profiles is that all profiles of 24 hours and later are in the equilibrium situation and that the differences are only due to measurement errors. Another explanation is that some of the profiles are not yet at equilibrium and that the difference is (partly) due to the excess pore pressures. The densities of the profiles of 24 and 50 hours are indeed lower than the densities of the other profiles, so they can still have larger excess pore pressures than the others. The question that needs to be answered is: What moment in time can be considered as the final stage of the consolidation? The time scale of the consolidation is (see equation 4.46)

$$T = \frac{\rho_w g \zeta_i^2}{K_k K_\sigma^{D-2} n \sigma_{rep}^{3-D}} \tag{6.7}$$

With an estimate for the parameters (D=2.65, K_σ=1·10^{-12} Pa, K_k=1·10^7 m/s, ζ_i= 0.3 m · 55 kg /m^3 / 2600 kg /m^3 = 6.4 mm and σ'_{rep}= ($\rho_s - \rho_w$) · g · ζ_i) the time scale of the consolidation amounts to $T \approx 3\cdot10^5$ sec. ≈ 84 hr. The first term in the solution series of the parameterisation (equation 4.51) decays with $\exp[-(\pi/2)^2 t/T] \approx \exp[-2.5\cdot t/T]$ The others terms decay faster. That means that after 24 hours about 50 % of the consolidation has been achieved, after 50 hours ca. 80%, and after 72 hours 90%. At 50 hours, the excess pore pressures are about equal to the error in the measurements. Therefore, the profile can be

considered to be in the final stage of consolidation after about 50 hours. Thus all the data points except the ones at 4 and 24 hours can be used to determine the effective stress parameter and the fractal dimension.

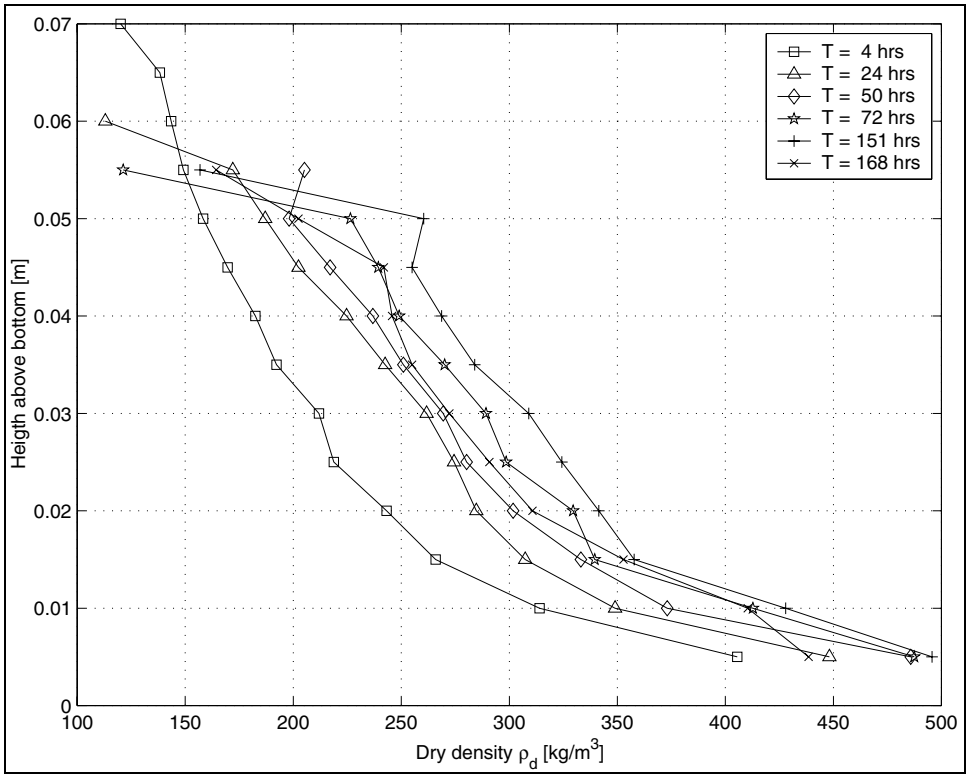

Figure 6.5 : Measurements by Kuijper et al. [1990] of density profiles at regular intervals of 5 mm.

A second complication is that the equilibrium profile as described by the Gibson equation and the constitutive relations of Merckelbach [2000] shows a linear increase of the effective stress with depth and a smooth curved density profile without inflection points. Moreover, the density gradient near the rigid bottom is almost zero. The measured profiles however show a density profile with a tail with a very high density near the rigid bottom (and thus an inflection point). Moreover the gradient near the rigid bottom is very large. Such behaviour can be explained by the presence of sand, according to Merckelbach [2000]. The composition of the sediment has been determined in Kuijper [1990]. Indeed, the composition shows a quartz percentage of 30 %. Sand is known to have a much higher settling speed than mud (aggregates). During the consolidation the sand segregates from the mud and forms a sand layer near the rigid bottom (segregation is dependent on the initial condition though). On top of this sand layer the consolidating mud profile starts to form. Therefore the lower parts of the density profiles should be neglected when determining the effective stress parameters. However, the sand particles have a size distribution (quartz can even be present in the silt range). Therefore, not all the sand will settle so fast to form a sand layer below the clay layer. Some sand particles are small and will become part of the consolidating mud bed. Therefore the height of the sand layer is not immediately clear. Accordingly, it is not clear how many data points have to be discarded on this side of the measurement series. Most natural sediments contain some sand, and this problem is met in most engineering cases [Van Ledden, 2002].

The third complication is that the equilibrium profile as described by the Gibson equation and the constitutive relations of Merckelbach [2000] shows a steep gradient in the density profile near the interface. The measurements of the density in Kuijper [1990] have been performed at fixed levels. That means that some of the measurements were performed just below, others just above the interface. The level of the interface is not immediately clear in these experiments: it is only known in between two successive levels. Therefore the interface height is retrieved from the measurements of the settling of the interface. Due to the large gradient in the density near the interface, a small change in the measurement level will always be accompanied by a large change in the density. Additionally, the measurements near the interface are

unreliable due to the measuring device. The expected large errors near the interface are indeed reflected in the data. The interface height at the final stage of consolidation is 6.3 cm, while the highest measurement has been done at 5.5 cm. Moreover, the density measurements of the equilibrium profile at the top range from 120 to 210 [kg/m^3] (see table 6.3). Measuring the very small densities near the interface is difficult, as can also be seen in Merckelbach [2000]. This problem will be met in most engineering cases.

Consolidation time [hours]	50	72	151	168
Dry density at top [kg/m^3]	210	120	155	165

Table 6.3

Figure 6.6 shows a representative fit. (Note that both axes are on log scale). The fixed levels at which the measurements have been performed (see figure 6.5), are not present in this figure, since the actual interface height is used for each series. This interface height has been retrieved from the interface settling measurements. In this fit eight data points near the interface have been neglected as well as the twelve data points of the four lowest levels.

The parameters obtained this way are K_k= 4.0·10^4 m/s and D=2.36. They are not in the same order of magnitude as the ones mentioned in Merckelbach [2000] (table 6.5). The fractal dimension is not very close either to the fractal dimension as determined by the settling of the interface height in section 6.3. The envelope of the middle part of the data, the most representative part, looks like a trapezoid, with sides corresponding to a fractal dimension of about 2.5. That value is more in agreement with the fractal dimension for the permeability. A trapezoid corresponding with a fractal dimension of D=2.59, the value determined from the permeability experiment, is also depicted.

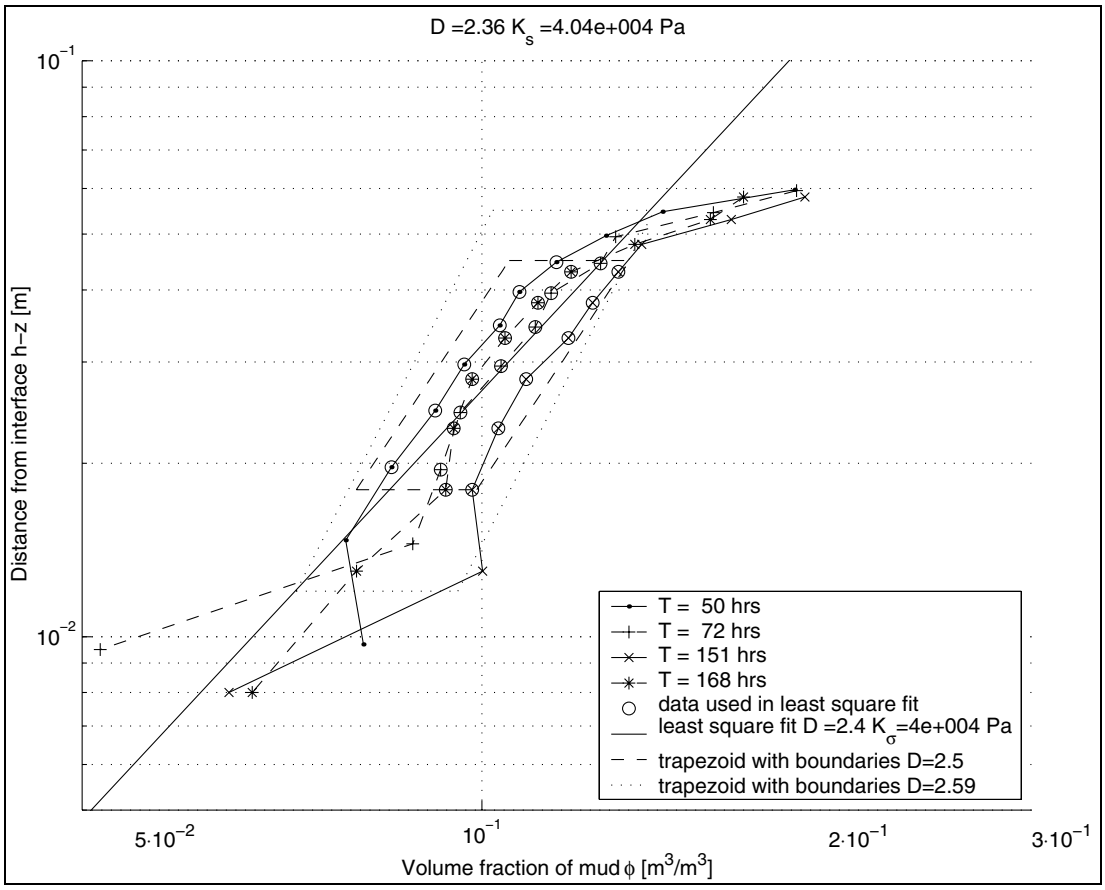

Figure 6.6: Average example of a least square fit of the density vs. height to determine K_σ and D.

6.3.2 Variation of parameters: multiple least square fits

We now know that the data set should be cut off at one side because of the presence of sand and on the other side because of large uncertainties in the measurements near the interface. However, it is not directly clear which data points should be incorporated in the analysis and which should not. Thus, when fitting the data points on double logarithmic paper by a straight line, this line should be based on some of the central data points. But the choice of leaving out other data points at either end or not, influences the slope and the offset of the line: different lines are possible. (When considering that the data points have an error as well, indicated by the difference between the different measured profiles, replacing all the data points by one single line is even less valid.) This is the same case as with the permeability parameter. Accordingly, also for the effective stress parameter many least square fits are generated automatically by leaving out data points at either side of the data set. For every fit another combination of data points is left out. This method gives a reproducible result: a kind of fingerprint or spectrum. Four profiles are considered. Therefore the choice is that at least 6 data point should be incorporated in the automatic analysis: 4 measurements at one level and 2 at a second level.[30] This results in 708 pairs (K_σ ,D) (Table 6.4). The results of all the fits are depicted in figure 6.7 and 6.8.

Experiment [Kuijper et al., 1990]	Number of observations	Number of least square fits
7 day consolidation with T = [50, 72, 151, 168] [hour]	4 moments in time x 11 levels = 44 observations	708

Table 6.4

The parameters have been determined for all 708 possible fits of leaving out of data points at the beginning and end of the series. The average values of K_σ and D (table 6.5) do not show good agreement with the parameters that were determined by Merckelbach: the effective stress parameters and D are much too low. The values near the peak of the distributions are higher than the averages (figure 6.7). The modal value of D in figure 6.7 (the value at the peak of the distribution or the most probable value) can be regarded as the fit with the highest probability of being fitted in a single least square fit procedure and can therefore be considered more representative than the average.

Experiment	μ (D)	σ (D)	μ (K_σ)	σ (log(K_σ)) [31]
			Pa	Pa
Kuijper [1990]	2.10	0.24	$5.4 \cdot 10^3$	$10^{0.61}$
Merckelbach [2000] CS series	2.75		$4.1 \cdot 10^9$	
Merckelbach [2000] CT series I	2.67		$2.9 \cdot 10^9$	
Merckelbach [2000] CT series II	2.75		$3.2 \cdot 10^9$	
Merckelbach [2000] DT series	2.72		$3.9 \cdot 10^8$	
Merckelbach [2000] Townsend & Mc Vay	2.60		$7.1 \cdot 10^7$	

Table 6.5 Statistical properties (average μ and standard deviation σ) of the results of the all the least square fits of the density vs. height to determine K_σ and D

[30] Due to Matlab constraints the data set is ordered at increasing densities, rather than at increasing distance from the interface. Since the density at one level can be higher then at the previous, the minimal number of 6 data points does not necessarily result in a configuration where 4 data points at one level and 2 at an adjoining level are used. A 3-3 or even a 1-1-4 configuration is also possible.

[31] The standard deviation σ of log(K_σ) is σ=0.61. And $10^{0.61} \approx 4$. This means that the standard deviation is 0.61 orders of magnitude and that 65 % of the data lie within a *factor 4* of the average value: $1.35 \cdot 10^3$-$2 \cdot 10^4$. Note that the constitutive relation can also be written in a way that leads to a much smaller variation in the parameters. The parameter $K_\sigma^{-1/n}$ shows a much smaller variation than K_σ: $\sigma`_v = K_\sigma \phi^n = (K_\sigma^{1/n} \phi)^n$

Theoretically the fractal dimension should be the same for the permeability and the effective stress. This is obviously not the case here. A trapezoid with slopes with a fractal dimension of 2.5 has been plotted in figure 6.6. These lines have the same slope as the sides of the middle part of the data block, which resembles a trapezoid. The middle part of the data is the most representative. These lines look satisfactory as well, and have a fractal dimension that is closer to the fractal dimension for the permeability (D=2.59). Hence the fractal dimensions can certainly be equal. However, the value of 2.5 does not appear in the statistical analysis of the effective stress though. The conclusion one can draw from this is that the density data are too bad to determine the effective stress parameters accurately (or that the proposed procedure is not very appropriate).

When a model is used that allows D to be different for the permeability and the effective stress, the recommendation is to use the modal value of D and the associated value of K_σ, as was the recommendation with the permeability. When a model is used that requires a single fractal dimension, simulations with different fractal dimensions have to be performed to know what D fits the experiment best. These simulations will be performed in sections 6.5 and 6.6 of this chapter.

The graphs corresponding with all the least square fits have been inspected individually. The (very) low values of the effective stress parameter (order of 100 Pa) correspond with the case where only the points near the bottom of the settling column have been fitted. These fits are the least representative: they fit only the data points containing sand. These lines are too flat: they lead to a low effective stress parameter and a low fractal dimension (for examples see annex 6.3). Some other extremely low values of the effective stress parameter correspond with cases where only 6 to 8 data points of the middle part of the graph have been fitted. Errors in these observations can lead to very unrealistic lines (see annex 6.3).

As with K_k, the graphs of the distributions suggest that one can use the individual statistically derived average values of the parameters. This is not true, because the values of K_σ and D from a single fit are coupled to each other (figure 6.8). The combination (K_σ, D) that will represent the data, should be chosen to fit this relationship. This relation describes merely all possible lines through the mass centre of the data $(h-\bar{z}, \bar{\phi})$ and does not have a physical basis. Note that the parameters obtained by Merckelbach [2000] are also close to this line.

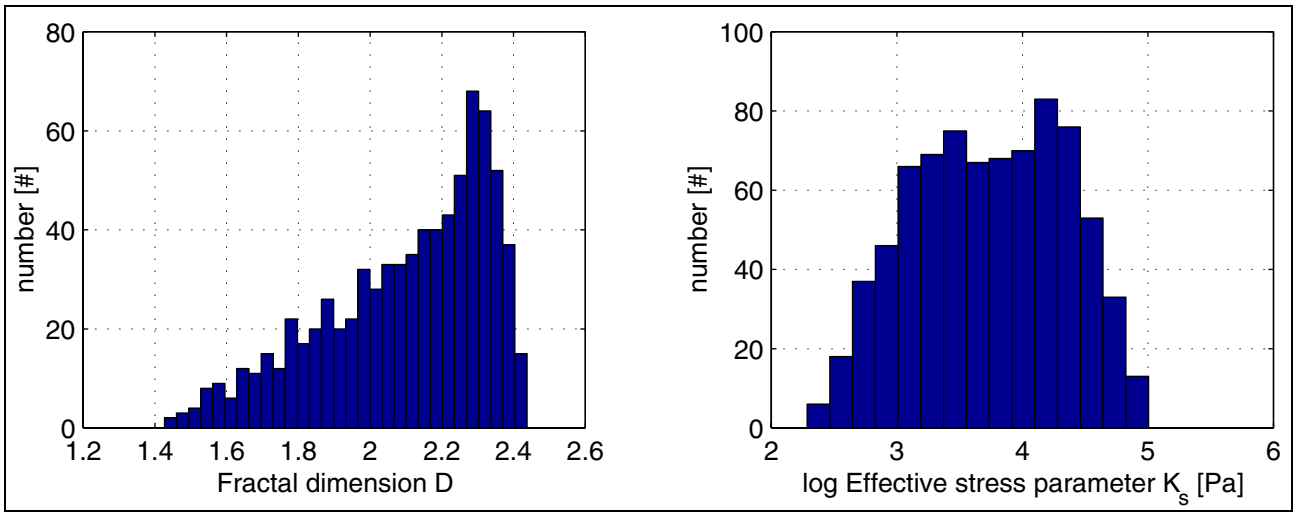

Figure 6.7: Histogram of results of the all the least square fits of the density vs. height by Kuijper et al. [1990] to determine the K_σ and D

The relation between the effective stress σ'_v and ϕ has been plotted in figure 6.9 for different combinations of D and K_σ from figure 5.8 The lower the fractal dimension, the more gradual the increase of the effective stress with ϕ. The lower the fractal dimension the higher the effective stress at the gelling point. All the lines intersect at about ϕ=0.1. That means that the choice of a set D and K_σ does not matter much in this regime.

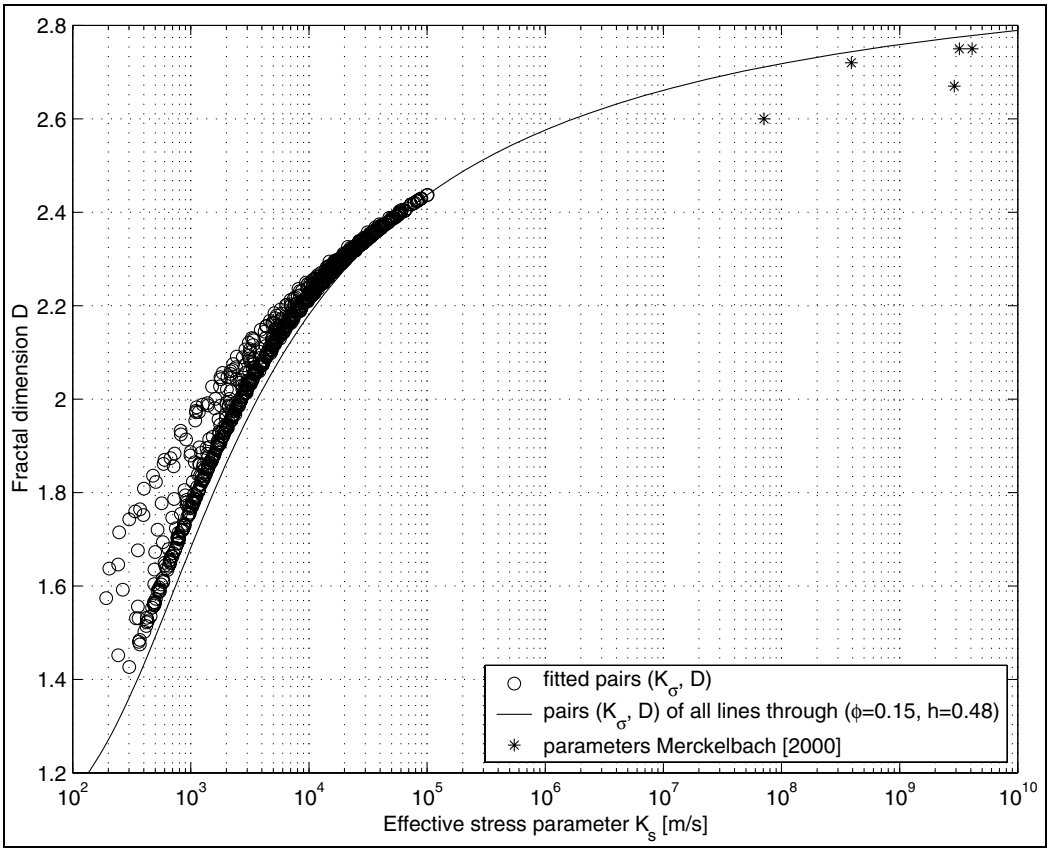

Figure 6.8: Relation between K_σ and D of each fit

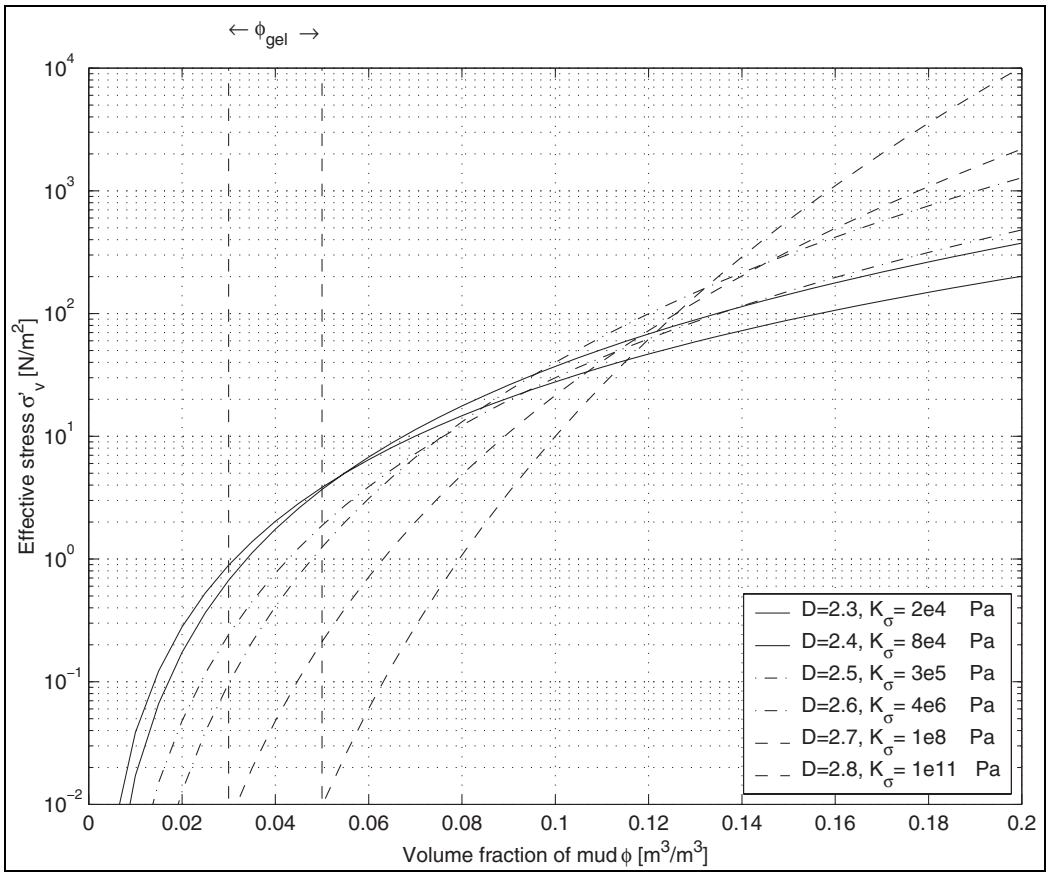

Figure 6.9 : Relation effective stress σ'_v and ϕ for various sets D and K_σ

6.4 Yield stress

The roto-viscometer tests can also be used to determine the fractal dimension. Kranenburg [1994] proposes the following relation

$$\tau_y = K_y \phi^n \tag{6.8}$$

Moreover, Merckelbach [2000] showed that the yield stress is, for a large part, determined by the effective stress. The fractal dimension (in n) in the above equation might result from this dependence.

Experiments with the roto-viscometer have been performed at various concentrations by Kuijper et al. [1990], some of which are below the gelling point. The above relation however, is only valid above the gelling point. Since the gelling point is not exactly known, it is not possible to judge beforehand which data points to use in the least square fit and which not. Therefore, the same procedure has been used as with the permeability and the effective stress parameter. For all possible combinations of leaving out data points with the lowest concentrations, least square fits are generated automatically (with a minimum of 3 point per fit). A characteristic fit is shown in figure 6.10.

All the sets of the remolded yield stress parameter K_y and the fractal dimension D are shown in figure 6.11. These parameter are coupled, as with the permeability and the effective stress parameter. One cannot arbitrarily select average values. The fractal dimension as obtained by the roto-viscometer tests are in the same order as the parameters derived by the other methods.

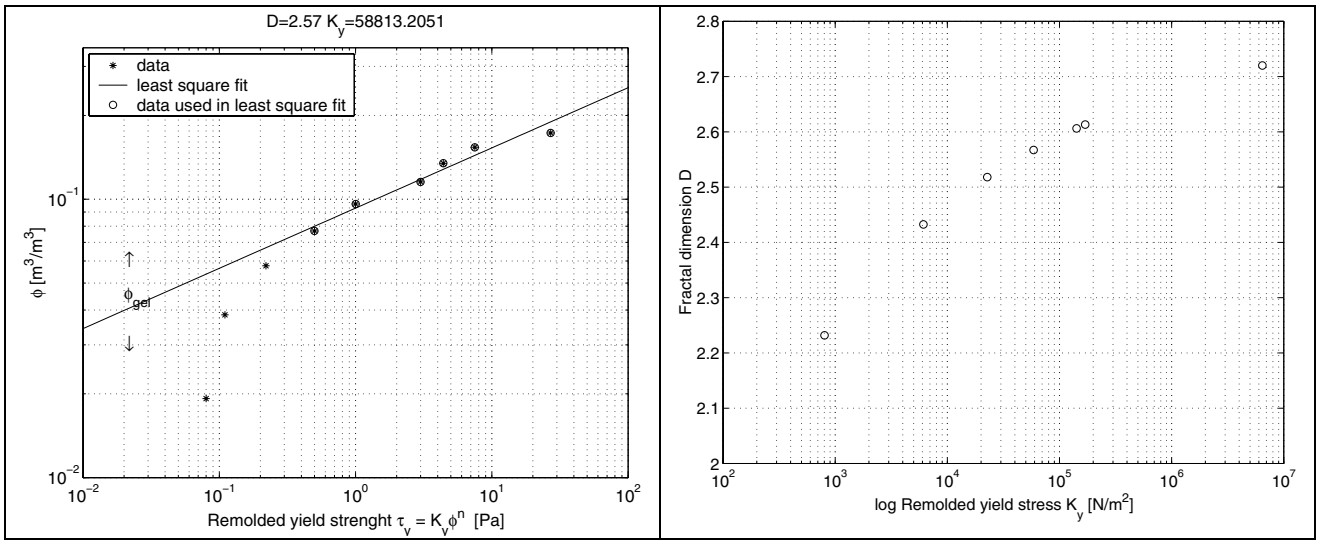

Figure 6.10 (L): Example of a least square fit of the remolded yield strength vs. volume fraction of mud to determine D and K_y [Pa]

Figure 6.11 (R): Relation between D and K_y of each fit

6.5 Simulation of consolidation with parameterisation

The effective stress parameter K_σ, the permeability parameter K_k and the fractal dimension D as determined in the previous sections, show a large variation. The best combination of these parameters is determined by investigating what combination of parameters can describe the development of the density profile and the interface height best. These experiments are done with the parameterisation model in this section and with the numerical model of Merckelbach in the next section. For reasons of convenience fractal dimensions rounded to one decimal (2.3, 2.4,…, 2,8) are used. In figures 6.12 and 6.13 one can see the results obtained with (about) the modal value of D obtained from the permeability: $D = 2.6$.

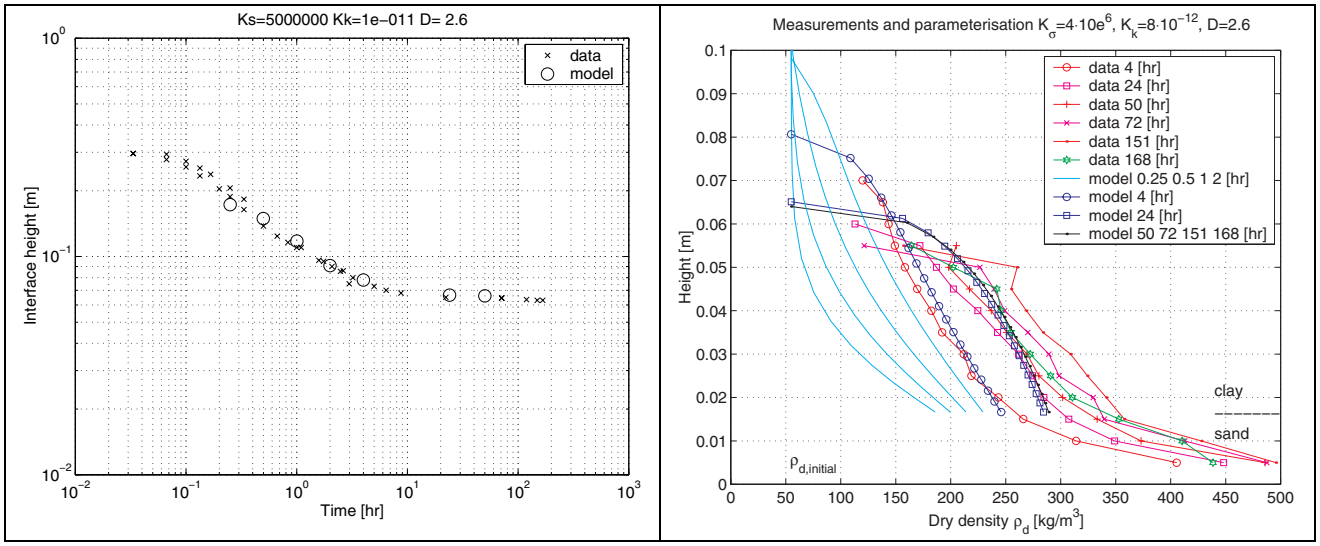

Figure 6.12 (L): Comparison data of interface height [Kuijper, 1990] with parameterisation model to find the parameters of the sediment (K_k [m/s] and K_σ [Pa]).

Figure 6.13 (R): Comparison data of density profiles [Kuijper, 1990] with parameterisation model to find the parameters of the sediment (K_k [m/s] and K_σ [Pa]).

The above results look reasonable. However, some more combinations (K_σ, K_k, D) are selected and applied. For a number of combinations of the fractal dimension D, the best values of K_σ and K_k are be determined by means of trial and error. The best combinations are selected by visual inspection and no quantitative criterion is used. Not all these figures are enclosed however, only the best fits are presented. The best results for the density profiles (table 6.6) are shown in annex 6.4 and the best results for the interface heights (table 6.7) are shown in annex 6.5. It turns out that with a single fractal dimension D, both K_k and K_σ are slightly lower for a best fit of the interface height than for a best fit of the density profiles. For all combinations of table 6.6 the relations between the fractal dimension and the effective stress and the permeability parameter are shown in figures 6.4 and 6.9.

Simulation		1	2	3	4	5	6
K_k	m/s	$2.0\cdot10^{-17}$	$1.0\cdot10^{-13}$	$8.0\cdot10^{-12}$	$1.0\cdot10^{-10}$	$7.0\cdot10^{-10}$	$2.0\cdot10^{-9}$
K_σ	Pa	$1.0\cdot10^{11}$	$1.0\cdot10^{8}$	$4.0\cdot10^{6}$	$3.0\cdot10^{5}$	$8.0\cdot10^{4}$	$2.0\cdot10^{4}$
D		2.8	2.7	2.6	2.5	2.4	2.3

Table 6.6 Best combinations of parameter for the optimal modelling of the density profiles [Kuijper et al., 1990]

Simulation		7	8	9	10	11	12
K_k	m/s	$3.0\cdot10^{-17}$	$1.5\cdot10^{-13}$	$1.0\cdot10^{-11}$	$2.0\cdot10^{-10}$	$1.0\cdot10^{-9}$	$5.0\cdot10^{-9}$
K_σ	Pa	$1.5\cdot10^{11}$	$2.0\cdot10^{8}$	$5.0\cdot10^{6}$	$4.0\cdot10^{5}$	$1.0\cdot10^{5}$	$2.0\cdot10^{4}$
D		2.8	2.7	2.6	2.5	2.4	2.3

Table 6.7 Best combinations of parameter for the optimal modelling of the interface height [Kuijper et al., 1990]

When inspecting all the results mentioned above, it turns out that the density profiles and the interface height can be modelled with reasonable accuracy with a fractal dimension ranging from 2.3 to 2.7, provided the appropriate values of K_σ and K_k are used.[32] The first thought might be that this is not reassuring for the validity of the Gibson model with the Merckelbach constitutive relations. However, all these combinations of (D, K_σ) and (D,K_k) are close to the (extrapolated) lines of figure 6.3 and 6.8. This means that all the combinations that can describe the development of the bed, are combinations that could be obtained with the 'log-log' fitting procedure. Thus the Gibson/Merckelbach model is corroborated, but the consolidation is not very sensitive with respect to the fractal dimension. The question is whether this lack of sensitivity is inherent to the Gibson/Merckelbach model or due to the simplifications made in the parameterisation. This question will be answered in the next section.

6.6 Simulation of consolidation with numerical model

Numerical simulations are carried out with the combinations of parameters obtained in section 6.6. Trying to find the right combinations of parameters by means of trial and error is too time consuming for the numerical simulations. The numerical model will be used both with one fraction (only cohesive sediments) as well as with two fractions (both sand and mud). The numerical model can deal with different fractal dimensions for the permeability and the effective stress. They will be chosen equal however, to be able to compare the results to the results of the parameterisation. In figures 6.14 and 6.15 one can see the results obtained with the modal values in the distribution the material parameters: D = 2.6. The results for all the combinations from table 6.6 can be seen in figure annex 6.6 and 6.6. The process parameters for the simulations are listed in table 6.9.

Parameter	Symbol	Values	units
Fractal dimension	D	**Combination**	-
Permeability parameter	K_k	**From**	m/s
Effective stress parameter	K_σ	**table 6.7**	N/m^2
Vertical resolution	Δx	2.5	mm
Time step	Δt	1	s
Density of sediment material	ρ_s	2600	kg/m^3
Density of pore water	ρ_w	1000	kg/m^3
Volume fraction of mud at gelling point	ϕ_{gel}	0.04	m^3/m^3
Fine sediment fraction	fsf	Both 0.8 and 1	m^3/m^3
Settling velocity cohesive fraction	w_s	$1 \cdot 10^{-4}$	m/s
Settling velocity non-cohesive fraction	w_s	$5 \cdot 10^{-4}$	m/s
Hindered settling formulation		None	
(Computation time on WL UNIX server		6	min.)

Table 6.9 Parameters used in the runs with the numerical consolidation model

The settling of the interface cannot be modelled easily with the numerical model. The height of the interface is severely affected by the formulation in the hindered settling regime. The hindered settling regime is not investigated in this thesis. Therefore the results of the interface height as a function of time are not included (although they were presented with the parameterisation model).

[32] The fact that the profiles and interface heights can be described with parameters with a wide range, suggests that there may be a combination of these parameters that is constant. A first hypothesis would be that the time scale T (equation 4.46) is constant. This is not the case however. This time scale slightly decreases with increasing fractal dimension. In the density profile results in annex 6.4 one can see the presence of oscillations. This is due to the decrease in the parameter T (equation 4.46)

For the two fraction model, a percentage of sand of 20% has been used. This is lower than the 30 % quartz the sediment contains. The quartz has a size distribution though. With a larger percentage of sand it turned out not to be possible to obtain reasonable results. Two phenomena can account for this. First, the smaller quartz particles will not separate from the cohesive sediments in the water column. They are in the silt range and are enclosed in the clay flocs. Second, Merckelbach has observed that when filling the settling column with sediment, the larger quartz particles will remain in the bucket from which the column is filled.

Both the numerical model with one fraction, as the one with two fractions can describe the profiles well with D ranging from 2.3 to 2.7. Hence this lack of sensitivity, also found in the parameterisation, is inherent to the Gibson/Merckelbach model. The conclusion one can draw from this is that the fractal dimension and the empirical parameters cannot be determined very accurately. It is no use to spend much time determining the parameters by fitting data points very accurately. Fitting one line is sufficient. Moreover, one should always be aware of the fact that precise representative values of D, K_k and K_σ do not exist. A value for D with three significant digits will be sufficient, and a value of two digits will be sufficient for the empirical parameters. Finally, the parameters should always be addressed as a set, not as separate values. Correspondingly a chosen set of the parameters should always be checked by means of simulations with the parameterisation or the numerical model. What happens if one chooses a set of parameters that deviates a little from a combination that gives good results? That question will be elaborated on in the next section.

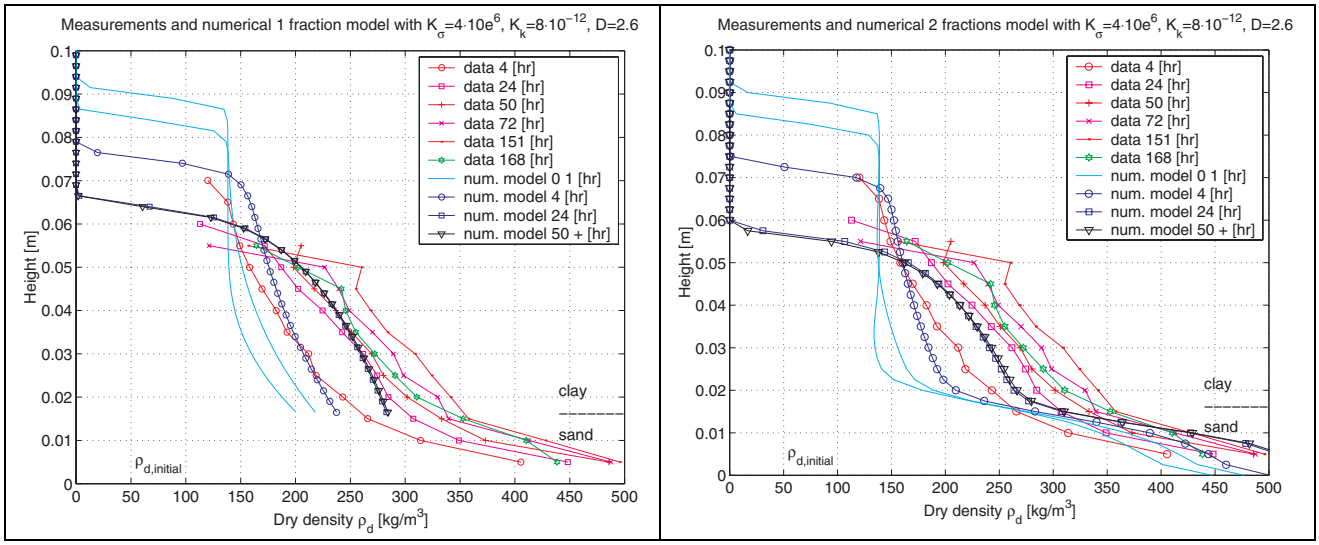

Figure 6.14 (L): Comparison data of density profiles [Kuijper et al., 1990] with numerical model with one fraction. (K_k [m/s] and K_σ [Pa])

Figure 6.15 (R): Comparison data of density profiles [Kuijper et al., 1990] with numerical model with two fractions. (K_k [m/s] and K_σ [Pa])

6.7 Sensitivity

In the above sections it turned out that the empirical parameters cannot be determined very accurately. Moreover, it was shown that the model could produce reasonable results with a wide range of values of the parameters. Despite the wide range, the parameters cannot be chosen freely. The parameters are coupled to each other. Only if a set (D, K_k K_σ) roughly agrees with a specific relation it can be used to simulate the measured results. How will the results be affected if this relation is not fulfilled? This will be investigated by changing the parameters one at a time from a proper set. The results for the fractal dimension, the parameter to which the model is most sensitive, can be seen in figure 6.16 and 6.17. The results for the empirical parameters can be seen in annex 6.8 and 6.9.

From all the sensitivity analyses one can conclude the following. When the fractal dimension is increased or decreased with by 0.05 (keeping K_σ and K_k constant), the model results are not acceptable any more. The standard deviation from the parameters that were determined from the experimental results were 0.08 for the permeability and 0.24 for the effective stress. The applied variation of 0.05 in the fractal dimension is smaller than the standard deviation of the experimental results. Consequently one can conclude that the model is very sensitive with respect to the fractal dimension, both with respect to the shape of the profile and the time scale.

The model is less sensitive to the other empirical parameters. When K_σ or K_k are doubled or halved, the results are still reasonable and sometimes even good. But the results become unacceptable if the parameters are changed by a factor 5. K_σ has the main influence on the (final equilibrium) profile shape, while K_k has the main influence on the rate of the consolidation process. This behaviour can be explained. (i) The shape of the final profile is actually only a function of effective stress parameter. The final effective stress profile increases linearly from 0 at the top to $(\rho_s-\rho_w)g\zeta_i$ at the bottom. The density profile is related to this effective stress profile by $\phi=(\sigma`/K_\sigma)^{1/n}$. This relation contains only the effective stress parameter. (ii) The rate of consolidation is more sensitive to the permeability parameter than to the effective stress parameter. This can be explained as well, because the time scale of the consolidation $T = \rho_w g \zeta_i^2 \cdot (K_k K_\sigma^{D-2} n \sigma_{rep}^{3-D})^{-1}$ contains the effective stress parameter to the power $(2\text{-}D) \approx 0.5$ and the permeability parameter to the power 1.

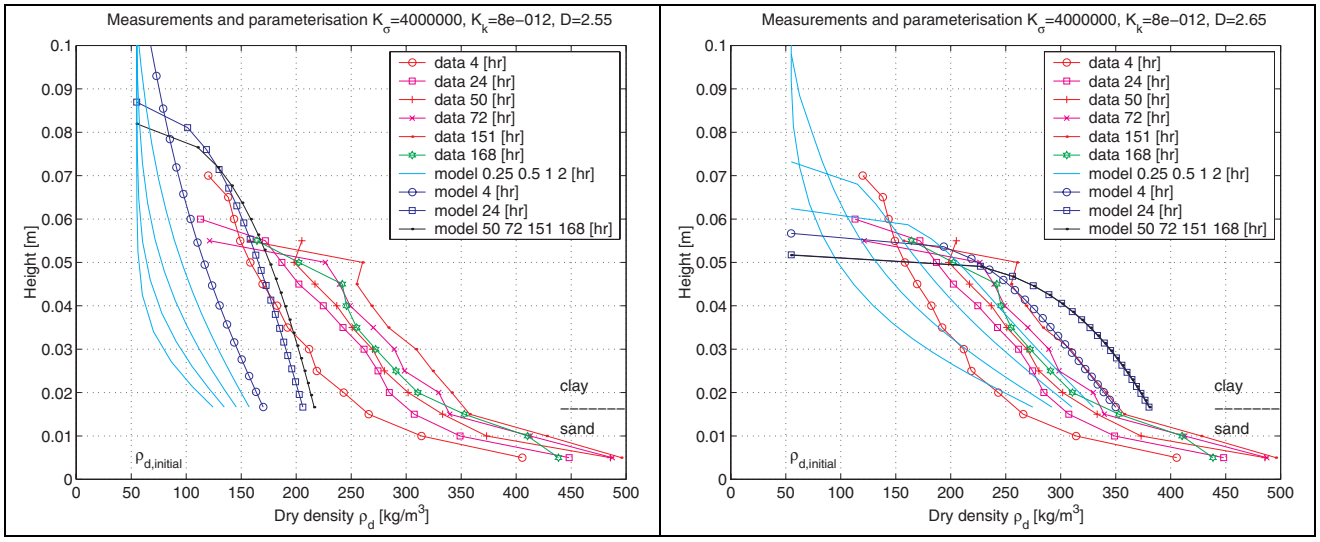

Figure 6.16 (L): Results for a slight lower fractal dimension, 2.55, then the results in figure 6.13 with D=2.6 (K_k [m/s] and K_σ [Pa])

Figure 6.17 (R): Results for a slight higher fractal dimension, 2.65, then the results in figure 6.13 with D=2.6 (K_k [m/s] and K_σ [Pa])

6.8 Summary

- The parameterisation consolidation model as derived in chapter 4 is able to give a proper description of the consolidation experiments.
- Merckelbach [2000] presented a method to obtain the parameters needed for this model by fitting the measurements of a settling experiment in a settling column to a double logarithmic scale. A representative set of the parameters can be obtained by performing a fitting procedure.
- The fitting procedure however, cannot simply be performed on all the measured data points. The physical limitations for which the fitting procedure holds, put a constraint on the number of data points that should be used in a single fit. Moreover, the set of data points that should be used is not accurately known in advance. That means that multiple fits are possible, each resulting in a different

set of parameters. Consequently, if different engineers perform the fitting procedure, the results for the values of the parameters will be different. A method is needed that produces an objective and reproducible output. Performing multiple independent fitting procedures on double log scale on these measurements can be such an objective method.

- The first result from this procedure is that it turns out that a value of D is always accompanied by a specific value of K_σ. The same holds for D and K_k
- The second result from this procedure is that the distribution of all the values of D obtained by the multiple independent fitting procedures yields a unique spectrum of the distribution of D, a kind of fingerprint. If the fractal dimension for the permeability and the effective stress are allowed be different in a consolidation model, the recommendation is to use the modal values of D in these spectra as the representative values of D, and the corresponding values of K_k and K_σ. The modal value of D gives the line with the highest probability of being fitted.
- Third, the parameters obtained from these multiple fitting procedures show a wide variation. There is not very good agreement between (i) the fractal dimension of the permeability and the fractal dimension of the effective stress, (ii) the lowest and highest value of the fractal dimension for either the permeability and the effective stress (large standard deviation) and (iii) the fractal dimension from this experiment and the values obtained by Merckelbach [2000].
- To investigate points (i) and (ii) simulations have been performed with the parameterisation model of chapter 4 and with the numerical model of Merckelbach. It turns out that the parameterisation gives results that are just as good as the results of the more complete numerical approach.
- It also shows that the model is very sensitive to the fractal dimension, and less sensitive to the other empirical parameters.
- This sensitivity does not imply that the parameters have a specific value. Further simulations (with both the parameterisation and the numerical model) have shown that the model can provide reasonable results with the fractal dimensions ranging from 2.3 to 2.7. In order to achieve this apparent insensitivity, the empirical parameters had to be changed by several orders of magnitude: when D is increased from 2.3 to 2.7, K_k has to range from 10^{-9} to 10^{-13} m/s and K_σ from 10^5 to 10^{11} pa to get reasonable results. Therefore the three consolidation parameters should always be addressed as a set (D, K_k K_σ), and never as individual values.
- The sets of parameters (D, K_k K_σ) that gave a good description of the results in the simulations obey the same relation (D, K_k) and (D, K_k) as found in the multiple fitting procedure.
- For use of the consolidation model in the 1DV-waterbed model a single set (D, K_k K_σ) has to be chosen to represent the bed. A set (D, K_k K_σ) that will be chosen to represent the waterbed should always be verified by means of the parameterisation model or the numerical model.

7 Validation erosion model

This chapter has two aims. The first is to validate the 1DV-waterbed erosion-consolidation model that has been derived in the previous chapters together with as the ECOM-SED 7-layer model. The second aim is to perform a sensitivity analysis of the 1-DV water bed model. The erosion model is validated using data of an erosion experiment. In this experiment the erosive behaviour of natural mud from lake *Ketelmeer* in the Netherlands has been investigated under various steady flow conditions. A rotating annular flume is used to quantify the parameters governing these processes. Various physico-chemical properties of the sediment from lake *Ketelmeer* have been measured (see annex 6.1). Consolidation experiments have been performed on this mud as well (chapter 6).

The erosion experiment are described in section 7.1. In section 7.2 the behaviour of the simple general erosion equation of Partheniades is given as illustration. The results of the 7-layer model of ECOMSED are discussed in section 7.3. After that the models that use the consolidation as strengthening mechanism are treated, starting with a simple model in section 7.4. In section 7.5 the 1DV-waterbed model is validated and a sensitivity analysis is performed. A summary concludes this chapter.

7.1 Annular flume experiment

7.1.1 Description of the erosion experiment [Kuijper et al., 1990]

An erosion experiment was carried out in a rotating annular flume with a water depth of 30 cm, a width of 20 cm and a mean diameter of 2.1 m. A circular lid at the surface drives the water. In order tot minimise the effect of secondary currents near the bottom, the channel itself is rotated in the opposite direction. The bed shear stresses in the annular flume are calculated with an expression as derived by Mehta and Partheniades (1973), where ω_1 and ω_2 are the angular velocities of the lid and the channel, r is the mean radius and a, b are coefficients (a=0.275 and b=1.37):

$$\tau_b = a\left(|\omega_1 - \omega_2| r\right)^b \tag{7.1}$$

The erosional behaviour of a sediment layer on the bottom of the annular flume is determined by increasing the bed shear stress in successive steps of 1 or 2 hours. The successive values of the bed shear stress which were imposed on the bed are: 0.05, 0.1, 0.15, 0.20, 0.25, 0.35, 0.45 and 0.55 Pa. These values are representative for the values of the bed shear stress in real water systems in average conditions.

The erosion is measured by determining the concentration of cohesive sediment in the flume every 30 seconds. The sediment is pumped from the flume at mid depth (0.14 m above the bottom of the channel) and led through a small cell with a diameter of 5 mm in which the light adsorption is measured. The suspension is returned to the flume at an elevation of 0.24 m. At regular time intervals, samples are taken from the flume to calibrate the optical probe.

Two tests were carried out to determine the erosional characteristics of the sediment. The first experiment is performed on a sediment layer with a consolidation period of one day resulting in a layer thickness of 0.065 m. One day after the start of the consolidation the dry density near the interface near the surface amounts to 100 kg/m^3 (see chapter 6). In the second case the consolidation period amounts to seven days resulting in a sediment layer of 0.063 m. After these 7 days the dry density near the interface is increased to 160 kg/m^3. The sediment beds are formed by deposition in still water (in the experimental flume) after a mixing period of approximately 12 hours. The concentration of the initial suspension is 56 kg/m^3 for the first and 54 kg/m^3 for the second erosion experiment.

7.1.2 Results

The results of the rotating annular flume experiment can be seen in figure 7.1. The bed has been exposed to a stepwise increasing series of bed shear stresses. The behaviour of the erosion rate at each value of the bed shear stress shows the same pattern. Directly after each stepwise increase in the shear stress, the rate of erosion is large. Next, the erosion rate gradually decreases to a low and almost constant value (the slope of for instance the line A-B in the left top frame of figure 7.1). When this almost constant rate would be become zero (i.e. if the line A-B were a horizontal line), the final eroded material height ζ would be referred to as the erosion potential ε (see section 3.6). In figure 7.1 line A-B clearly does not become horizontal, so no erosion potential can be discerned.

The almost constant erosion rate indicates that some kind of stationary situation has been reached. This dynamic equilibrium erosion is not due to a dynamic equilibrium between erosion and deposition, but is only determined by the swelling of the bed and the bed shear stress. Van Kesteren [1997] derived an equation that describes the rate of this equilibrium erosion (see section 3.3). In the 1-day experiment the last applied bed shear stress (0.55 Pa) has been applied to the bed for a longer period of time than for the other bed shear stresses. Here we can most clearly see that the erosion rate slowly decreases as the erosion progresses and becomes almost constant at the end of the experiment (A-B).

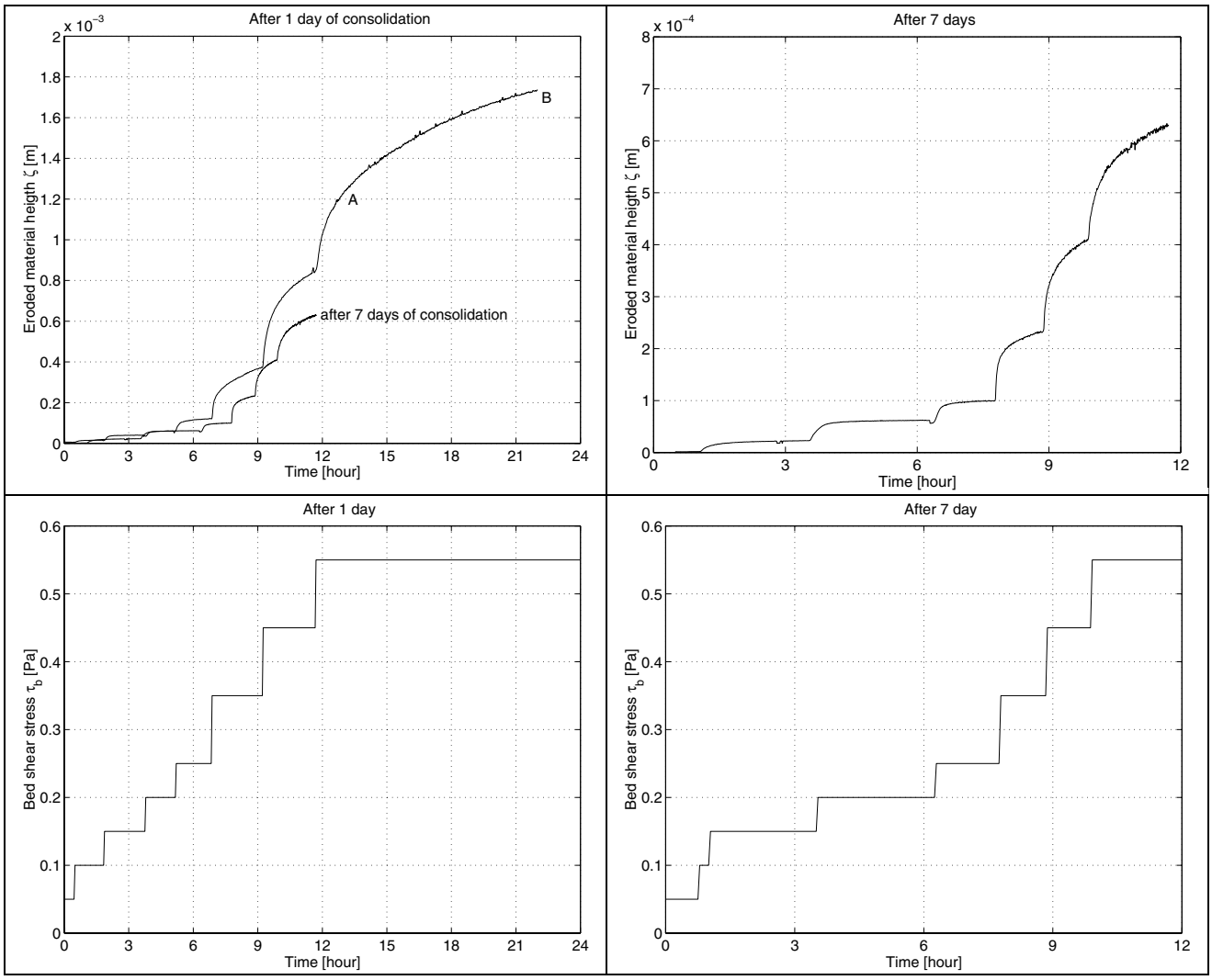

Figure 7.1: Results from erosion experiment [Kuijper et al., 1990] in rotating annular flume.

When an almost constant erosion rate has been reached at a certain level of the bed shear stress, the shear stress is stepwise increased again. The higher stress level forces the erosion to start again with the same pattern. The behaviour during each step of the bed shear stress can at first sight be described by an exponential decay function of the erosion rate at each level of the bed shear stress [Sanford et al. 2001]. The time scale of this exponential function is in the order of one hour.

To determine the time dependent erosion behaviour of the sediment, two erosion experiments have been carried out. The first erosion experiment has been performed after 1 day of consolidation and the second experiment after 7 days of consolidation. The final erosion in the experiment after 7 days of consolidation is more than 2 times smaller than the final erosion after 1 day of consolidation. The 1-day experiment lasted longer however. This can be attributed to the method used in the experiments. When the erosion rate reached an almost constant and low value, a new shear stress was applied. After 7 days of consolidation, this almost constant rate is reached earlier than after 1 day of consolidation. This accounts for the shorter duration of the erosion experiment. When (linearly) extrapolating the results after 7 days of consolidation to the experiment after 1 day of consolidation, the final erosion is also about two times smaller.

The differences in the final erosion after 1 and 7 days of consolidation as mentioned above can be attributed to two strengthening mechanisms: consolidation and thixotropy. The differences in input parameters of the model should reflect these differences in the erosion.

7.2 Partheniades formulation

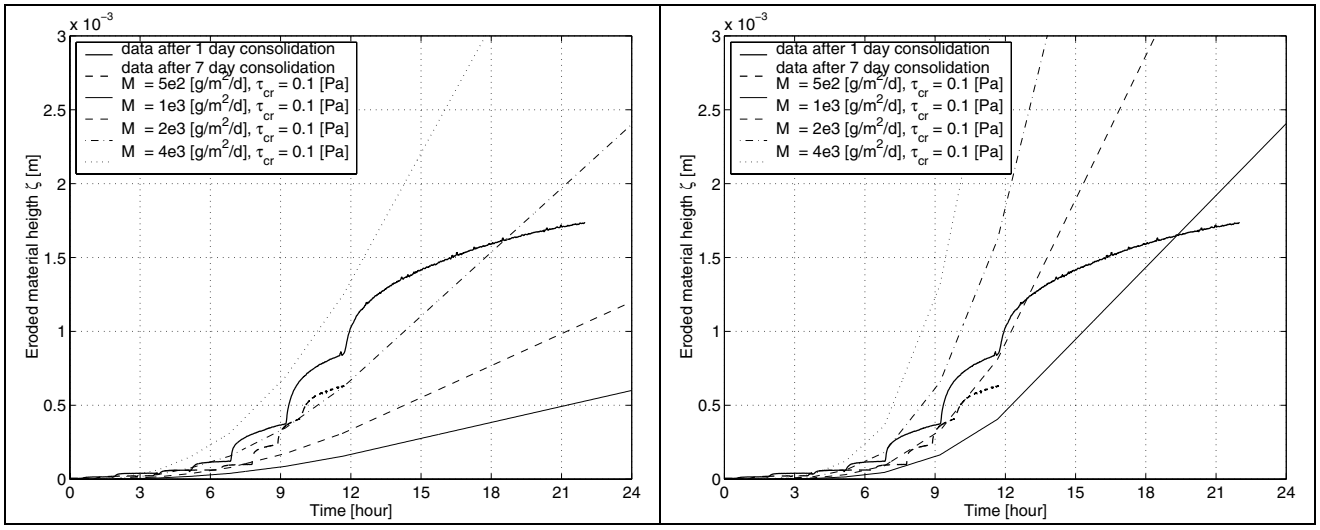

Figure 7.2 (L): Results from Partheniades erosion equation 3.1 with n=1, constant M and constant τ_c.

Figure 7.3 (R): Results from Partheniades erosion equation 3.1 with n=2, constant M and constant τ_c.

The results with the formula of Partheniades (equation 3.1) are shown in figure 7.2. They are mainly enclosed in this report to illustrate the increase in capabilities of the more sophisticated models in the remaining part of this chapter. Only the calculations with the Partheniades equation after 1 day of consolidation are shown. The calculations after 7 days of consolidation are exactly the same, since this model does not have any time dependency included. (The experimental results are included for both 1 and 7 days of consolidation.) The most striking feature of the classical erosion formulation is that the erosion rate does not decrease when the eroded mass increases. The data tend towards a stationary equilibrium situation with a low erosion rate, while the Partheniades equation does not tend towards any kind of equilibrium situation at all. By applying the so-called erosion potential or 'clean bed assumption' to the Partheniades approach, the erosion rate can be set to zero at a certain stage of the erosion. Then the steep lines suddenly

turn horizontal. This will underestimate the eroded mass after a long period of time, since in the experiment the erosion rate does not become zero on the long term.

Another important feature is that the model is sensitive to the erosion rate parameter M. Every change in M is reflected 100% in the results: multiplying M by 2 leads to twice the eroded mass. Not much is known about the value of M: in the literature it is found that its value ranges from 10^{-2} to 10^{-5} kg/m^2/s [Winterwerp, 1989]. Since this factor 1000 will be reflected 100 % in the results, one can immediately conclude that the Partheniades formula is not very useful for long term water quality engineering. In sections 7.3 to 7.5 better erosion models are presented.

7.3 ECOMSED [33]

7.3.1 Determination ECOMSED parameters

To reproduce the time series of the annular flume experiments with ECOM-SED, the parameters of the erosion potential equation 3.5 have to be determined. The erosion potential ε is the maximum amount of material that can erode at a certain bed shear stress. For the sake of convenience the equation is repeated here:

$$\varepsilon = \frac{a_0}{Z}\left(\frac{\tau_b - \tau_{cr}}{\tau_{cr}}\right)^n \quad for \quad \int_{t^*=0}^{t} Edt^* < \varepsilon \quad [\text{kg/m}^2/\text{s}] \tag{7.2}$$

where a_0 is an empirical sediment yield coefficient, Z is an empirical sediment age coefficient, τ_b is the bed shear stress, and τ_{cr} is the critical bed shear stress for erosion. In the data the presence of an erosion potential ε cannot be observed. How can we fit the parameter of the erosion potential if it is not present? To be able to determine the parameters the assumption is made that the erosion potential equals the highest measured eroded mass at a certain bed shear stress (independent of the duration of the experiment, which is discussed later on).

For the time dependent sediment age coefficient Z the equation $Z=T_d^m$ is used, in which T_d is either 1 day or 7 days. The critical shear stress for erosion τ_{cr} is (quite arbitrarily) fixed at 0.1 Pa. The three parameters a_0, m and n remain to be determined by fitting to the erosion experiment measurements. These parameters are fitted to the 16 data points that are available: 2 days times 8 different bed shear stresses.[34]

	τ_{cr}	a_0	T_d	m	n	RMS error
fit individually	[N/m^2]	[~mg/cm^2]	[day]	[-]	[-]	[kg/m2]
1 day consolidation	0.1	0.008	1	0.46	2.5	0.0171
7 days consolidation	0.1	0.025	7	0.46	1.7	0.0042
fit together						
1 day consolidation	0.1	0.016	1	0.46	2	0.0587
7 days consolidation	0.1	0.016	7	0.46	2	0.0162
Both	0.1	0.016	-	0.46	2	0.0315

Table 7.1 Parameters ECOMSED approach

[33] The ECOMSED model has not been validated with the actual ECOMSED FORTRAN code. This will be explained in in annex 7.1.

[34] At HydroQual, the custom is to choose 3 nice representative (interpolated) data points and calculate the coefficients analytically. I prefer to incorporate all the data points by means of a least square fit to determine the parameters. The 1 and 7 day experiments are fitted both individually and together. m has to be the same for the 1 and 7 day experiment. The other two parameters, a_0 and n, may turn out to be different when the 1-day data and the 7-day data are fitted separately, but they have to be the same for the 1 and 7 day experiment when they are used in the model.

The results of the fitting of the parameters are shown in figures 7.4 and 7.5 and in table 7.1. It turns out that despite the fact that in both experiments the same mud was involved (at different moments in time), the parameters a_0 and n are different for the two experiments. The exponent n decreases with time and the erosion coefficient a_0 increases with time. That means that even on a single site the erosion potential formula 7.1 (with constant n) is not capable of describing the resuspension rate precisely. The data of the individual experiments however, can be fitted to a high accuracy with this formula.

The value of the parameter n has been determined at about 2 from the fits, and m is about 0.5. The rule of thumb of HydroQual is that $m = 0.5$ for mud deposited in quiet conditions, $m = 2$ for mud deposited in dynamic conditions and $n = 2$ to 3. That means that the parameters in table 7.1 are in accordance with the values generally used when the fitted value of m corresponds to the dynamic conditions case. This may be explained by the fact that the bed has been formed inside the annular flume after severe mixing, apparently resulting in the type of flocs that are generally present in dynamic conditions.

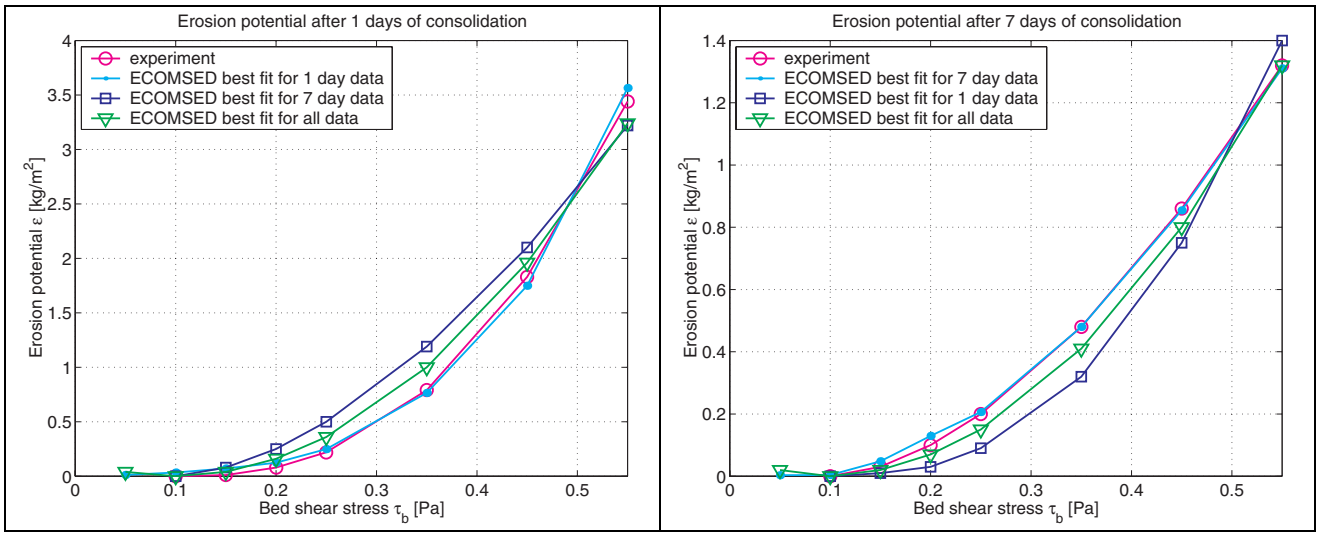

Figure 7.4 (L): Fitting resuspension potential ε after 1 day of consolidation

Figure 7.5 (R): Fitting resuspension potential ε after 7 days of consolidation

7.3.2 Results ECOMSED testing

The results of the time series produced by ECOMSED can be seen in figure 7.6. The results fit the experimental data quite well in an overall sense, but they reproduce the details only to a small degree. Three major types of differences can be observed between the results and the data.

1. First, the behaviour of the data of the experimental flume does not suggest that each shear stress allows only a certain maximum erosion to occur . The erosion rate tends towards a constant but low value so no resuspension potential can be discerned. This has two implications for the results of ECOMSED [35]. The resuspension potential coefficients have been determined by assuming that the highest measured volume of eroded mass at a certain bed shear stress is equal to the resuspension potential. In reality the erosion continues all the time. Accordingly the values of the parameters are affected by the duration of the experiment. When the parameters are fitted to the data with the assumption that the highest occurring erosion at a certain bed shear stress equals the erosion potential, a longer duration of the

[35] This has also implications for an exponential decay description of the erosion rate. An exponential decay rate formulation has leads to a finite amount of erosion as well, so it will not be valid in the long run.

application of a certain bed shear stress on the bed will result in an increase of the associated erosion potential.

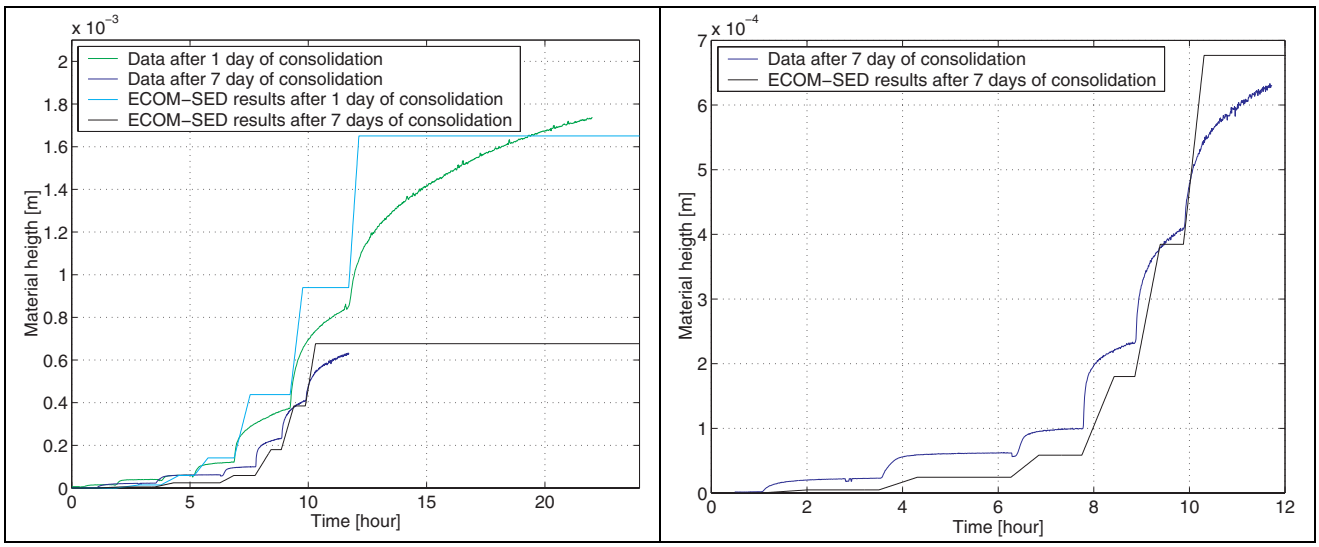

Figure 7.6: Results from ECOM-SED model (with detail of results after 7 days of consolidation in right frame)

In the experiments, the erosion rates show a low and almost constant value at the end of the application of a certain bed shear stress. This implies that the erosion would progress even further if the experiment would be continued for a longer period. In ECOMSED this secondary erosion, the erosion after the erosion potential has been depleted, is neglected. Consequently the model will underestimate the eroded mass if the bed shear stress acts on the bed for a period longer than the duration of the experiment.

2. A second shortcoming is that ECOMSED does not reproduce the eroded mass as a function of time accurately at a certain level of the bed shear stress: ECOMSED will allow the erosion rate to resuspend too quickly. Two phenomena account for this.

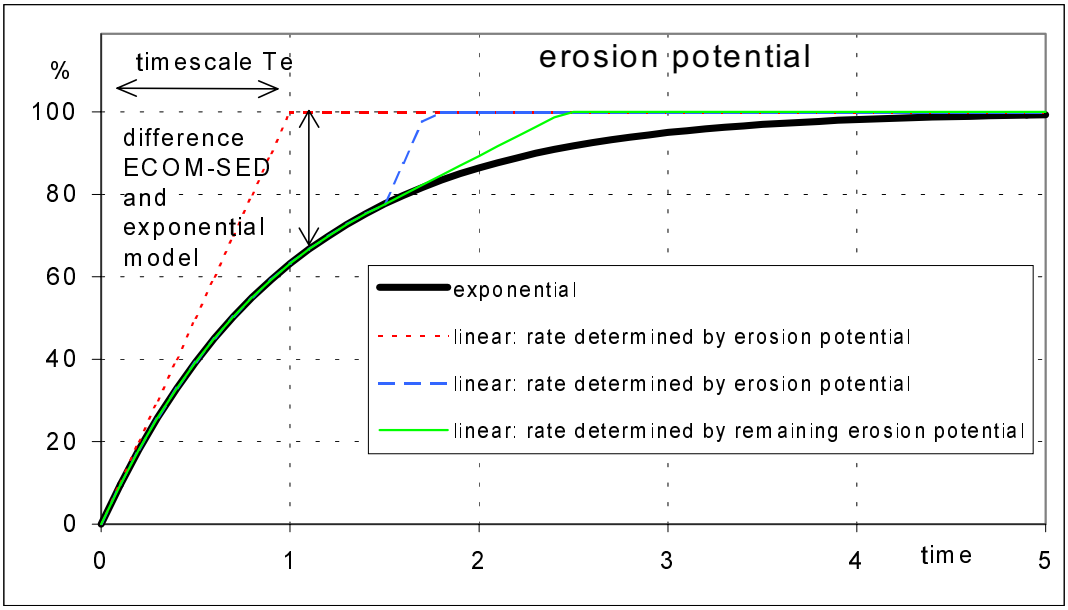

Figure 7.7: Behaviour exponential decay of erosion rate *E*.

First, ECOMSED assumes a linear erosion rate $E=\varepsilon/T_\varepsilon$ until the erosion potential has been reached. For T_ε a value in the order of one hour is chosen. In the experiments the erosion of the remaining part of the erosion potential ε can initially be described with a negative exponential function with a time scale of about one hour. The value of T_ε = 1 hour in ECOMSED is in accordance with the time scale of the experiments if T_ε is meant to represent the tangent of the exponential decay of the erosion rate. The assumption of an exponential decay function implies that in reality after a period of $3T_\varepsilon$ the erosion potential ε has been reached: about 5 % of the erosion potential is left after $3T_\varepsilon$. Moreover, after one period T_ε only 63 % of the erosion potential ε is eroded (figure 7.7), while ECOMSED will already have eroded the full erosion potential ε after this period. After a period T_ε therefore, ECOM-SED has already eroded the full erosion potential ε and gives an erosion rate E of zero. In the exponential model, the erosion potential ε is not yet depleted and the erosion rate E is not yet zero. The difference between eroded mass given by ECOMSED and the eroded mass in the exponential model will therefore be equal to the actual remaining erosion potential in the exponential decay function (see figure 7.7).

Second, when a major portion of the erosion potential ε has already been eroded at previous, lower shear stresses (which is often the case), the linearisation of the exponential decay function shows even more shortcomings. ECOMSED erodes the remaining part of the erosion potential at a rate based on the total resuspension potential. When a part of the resuspension potential has already been eroded at previous, lower shear stresses, the erosion rate should be determined from the *remaining* erosion potential as can be seen in figure 7.7. This remaining erosion potential leads to a lower erosion rate $E=\varepsilon/T_\varepsilon$ than the initial erosion rate.[36] When the bed shear stresses are high, the absolute error of using an erosion rate based on the total resuspension potential rather than the remaining, will be larger. After one period T_ε the relative error between ECOMSED and the exponential decay function is initially 37 %, after which is gradually drops. The absolute error is this the relative error times the erosion potential, which increases with the bed shear stress squared.

3. The third shortcoming of ECOMSED is that the erosion potential of the one day experiment and the erosion potential of the seven days experiment cannot both be fitted accurately by one set of parameters of the erosion potential equation. The erosion potential of the 7-day-old material is underestimated and the erosion potential of the one-day-old material is overestimated. That means that the model will overestimate concentrations when erosion and deposition alternate very frequently: less material will be allowed to consolidate than in reality and once material has been allowed to consolidate for seven days, the model will be too reluctant to give it back to the water column.

[36] This lower erosion rate cannot be attributed to a time scale increasing in time. The time scale T of any exponential decay does not change in time: an exponential decay function is a system without a memory.

7.4 Depth varying critical shear stress

The annular flume experiment can also be modelled with model 3.10 that gives a relation between the density and the erodibility by using a variable critical bed shear stress

$$\tau_{cr} = K_{cr}\phi^{n} \tag{7.5}$$

where ϕ is the volume fraction of mud, calculated by the consolidation model (with swelling parameter f).

The most logical approach would be to use the same power n as the power used for (i) the constitutive relation between the volume fraction of mud, the permeability and the effective stress or (ii) the fractal dimension found for the yield stress in section 6.4. With a fractal dimension of D_{cr}=2.3 it is possible to give reasonable results that do show the characteristic exponential behaviour at each bed shear stress. The resuspension at lower bed shear stresses is overrated though. The results are sensitive to the parameter K_{cr}. With a fractal dimension of 2.0 and 2.6 it is also possible to give reasonable results, provided an appropriate value of K_{cr} is chosen. (This resembles the relation between K_k, K_σ and D found in chapter 6, where the measurements could be reproduced at all fractal dimensions ranging from 2.3 to 2.8, provided appropriate values of K_k and K_σ were chosen.)

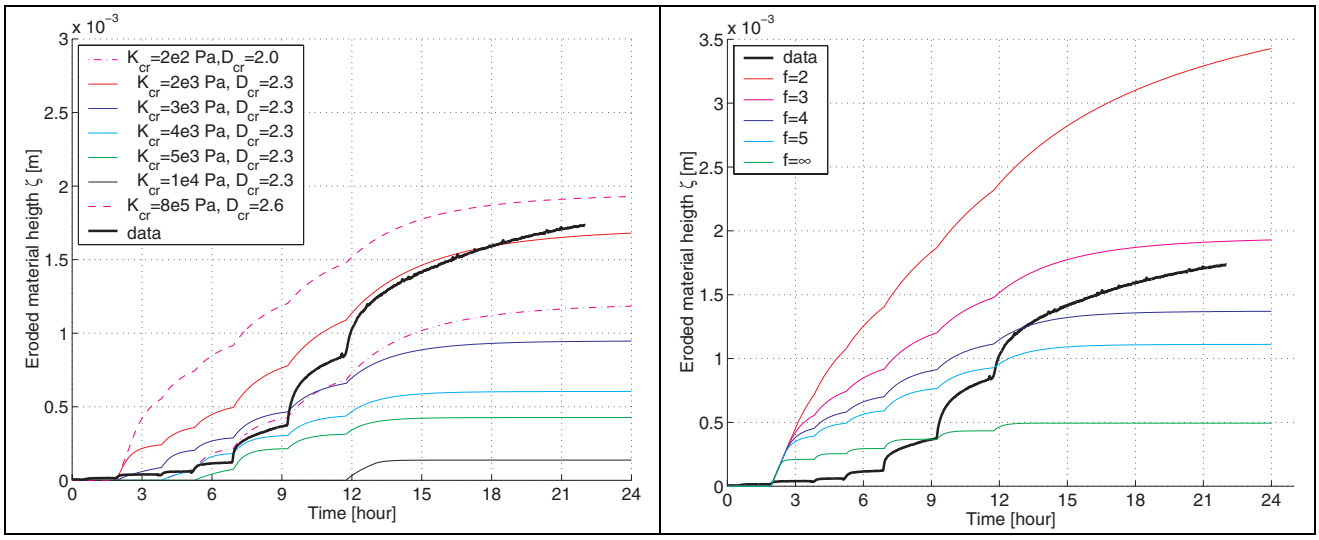

Figure 7.8: Results from erosion model with critical shear stress as function of density after 1 day of consolidation. Influence of K_y and D_y.

Figure 7.9: Results from erosion model with critical shear stress as function of density after 1 day of consolidation. Influence of swelling parameter f.

The results for the 7-day experiment are not included. The only ageing process that accounts for the difference between the 1-day experiment and the 7-day experiment is the consolidation, by means of changes in the density profile. The influence of the consolidation model on the erosion results is not investigated until the next section, where a more physically based model, also using the consolidation of the bed, is investigated. The influence of the swelling of the bed is investigated though. In figure 7.9 the results for different values of the swelling parameter f are shown (see section 4.2.2).

7.5 Erosion model with probability distribution of the bed shear stress

7.5.1 Input

In chapter 3 an erosion model was proposed using a Rayleigh probability distribution of the bed shear stress. For the sake of convenience it is repeated here.

$$E = M \cdot p\left(\tau_0 > \tau_y\right) = M \cdot \exp\left(-\alpha\left(\frac{\tau_y}{\tau_b}\right)^2\right) \tag{7.3}$$

where α and M are unknown coefficients, τ_b is the bed shear stress, E is the erosion rate in kg/m^2/s, and p is the probability that the actual bed shear stress τ_0 is larger than the actual bed shear strength of the bed τ_y, which is given by

$$\tau_y = c'_a \phi + \tan\varphi' \tfrac{1}{3}(1+2K_0)K_\sigma \phi^n \tag{7.4}$$

All the parameters that are used as input to the 1DV-waterbed model (section 5.2) are listed in table 7.2. The consolidation parameters have been determined from the consolidation experiments in the previous chapter. Some other physical parameters in the erosion model cannot be determined experimentally. These parameters are the cohesion $c`_a(z,t)$, the ratio f between the stiffness at virgin and reloading and the erosion rate coefficient $M = w_e \cdot \phi \cdot \rho_s$. Since these parameters are not known, the sensitivity of the erosion-consolidation model is investigated with respect to these parameters. These parameters can be used to calibrate the model. The choice of appropriate values of these parameters is discussed in this section before simulations are performed.

No theoretical relationship is available for the erosion rate coefficient M. This parameter is for sure not larger than the product of the entrainment rate w_e, if the bed were fluid mud, and the concentration of the entrained fluid $\rho_s \cdot \phi_{gel}$. Winterwerp and Kranenburg [1997] have investigated the initial entrainment rate w_e of a fluid mud layer, both numerically and by means of experiments. They found for w_e values ranging from $7 \cdot 10^{-3}$ to $7 \cdot 10^{-5}$ m/s just after the start of an experiment. With a volume fraction of mud of ϕ_{gel}=0.03 this results roughly in an erosion coefficient M of 0.5 to 0.05 kg/m^2/s. This is higher than the values of 10^{-2} to 10^{-5} kg/m^2/s found generally [Winterwerp, 1989]. The M in the Partheniades equation is the net erosion rate (including the effects of the probability distribution of the bed shear stress), while the M used in erosion model 7.3 describes the resuspension rate provided the bed shear stress exceeds the bed yield stress. Therefore the M used in this model is expected to be higher than the traditional M. The calibration runs are performed (arbitrarily) with a value of $w_e = 1 \cdot 10^{-3}$ m/s ($M \approx 0.1$ kg/m^2/s). To get a notion of the sensitivity of the results to M, computations with other values of M, ranging by a few orders magnitude, are also performed. Erosion formulation 7.3 contains another parameter besides M. For the scale parameter α of the Rayleigh probability distribution, arbitrarily, a value of 0.5 is chosen. With this value the regularly used bed shear stress τ_b equals the modal value (most probable value) of the actual bed shear stress τ_0.

The ratio f between the stiffness at virgin and at reloading compression is in the range of 3 to 5 (Van Kesteren, pers. com.). The sensitivity of the model with respect to f is investigated: values of f ranging from 1 to 5 are used. The influence of the type of swelling model is also examined. The two linear swelling models proposed in chapter 4 are tested. The swelling behaviour according to these models will always give results that are between the results for fully elastic behaviour (reloading according to the virgin loading curve) and fully plastic behaviour (f=∞). These enveloping models are also tested.

Two processes are responsible for the strengthening of the sediment in time according to equation 3.22: (i) the increase in physical strength by consolidation (density) and (ii) the increase in chemical strength (cohesion/thixotropy). The time dependent behaviour of the cohesion is not known. The cohesion term of

3.22 reads $c`_a\phi$. Both the increase in $\phi$ due to the consolidation and the increase in the cohesion parameter $c`_a$ lead to an increase of the cohesion. Merckelbach [2000] mentions a daily increase of the cohesion $c`_a\phi$ of about of 1 Pa/day for periods up to 95 days. In the time scales of this experiment, 1 to 7 days, this leads to cohesion of only 1 to 7 Pa. The volume fraction of mud $\phi$ is in the order of 0.1, so $c`_a$ is in the order of several times 10 Pa. Since Merckelbach uses an average ϕ for the entire bed, he does not indicate which part of this daily increase is due to the consolidation, and which part is due to the increase of $c`_a$ Therefore the assumption is made here that the entire increase in $c`_a\phi$ is due to consolidation.

The erosion is modelled with different constant values for the cohesion parameter $c`_a$ (several times 10 Pa) to see what the influence of the consolidation is on the erodibility, including the scenario $c`_a$=0. The decrease in erodibility that cannot be attributed to the consolidation effect, could be found (calibrated) by making $c`_a$ an appropriate function of time.

The only strengthening mechanism in the 1DV-waterbed model is now the increase in the density due to the consolidation: it is the only process that can account for the decrease in erodibility between the one-day and the seven-day experiment. The values of the consolidation parameters K_k, K_σ and D are known from the validation of the consolidation model in the previous section. They should not be used to calibrate the model. The sensitivity of the consolidation model to the consolidation parameters has been investigated in chapter 6 as well. These results are used to perform a founded sensitivity analysis of the 1DV-waterbed model.

Parameter	Symbol	Values	Units
Density of sediment material	ρ_s	2600	kg/m^3
Density of pore water	ρ_w	1000	kg/m^3
Volume fraction of mud at gelling point	ϕ_{gel}	0.03	m^3/m^3
Effective stress parameter	K_σ	$4\cdot10^6$	N/m^2
Permeability parameter	K_k	$8\cdot10^{-12}$	m/s
Fractal dimension	D	2.6	-
Ratio of swelling stiffness to virgin compression stiffness	F	3	-
Swelling model	$\Delta log(\sigma`_v)/\Delta e$=const.		
Cohesion	$c`_a$	20	N/m^2
Angle of internal friction	$\varphi`$	23.5	degr
Coefficient of lateral stress	K_0	0.75	-
Entrainment rate (Erosion rate $M = w_e\cdot\phi\rho_s$)	w_e	$1\cdot10^{-3}$	m/s
Scale parameter for Rayleigh distribution (with average $\mu = ½\cdot\tau_b\cdot\sqrt{(\pi/\alpha)}$	α	0.5	-
Critical shear stress for erosion	τ_{cr}	0.1	N/m^2
Number of sampling points	*non*	50	#
Number of Fourier components	*nok*	50	#
Time step consolidation (=maximum timestep for consolidation *deltcmax*)	*deltc*	5	min.
Time step for erosion and deposition (Delft3D-WAQ timestep)	*delt*	5	min.
Time step erosion calculation	*deltE*	6	sec.

Table 7.2 Parameters used in the runs with the consolidation- erosion model

The permeability parameter K_k has the main influence on the speed of the consolidation. The effective stress parameter K_s has the main influence on the shape of the profile. The expectation is that the shape of the profile will have the main influence on the erosional behaviour. Hence the consolidation parameters are chosen to give the best description of the density profiles: one of the combinations from table 6.6 is used (and not table 6.7). The influence of the consolidation parameters is investigated by using the same set of

parameters that was used to perform the sensitivity analysis of the consolidation with D=2.6 (annex 6.8 and 6.9). To compare these results with the other validation runs, a fractal dimension of 2.6 is chosen.

A simple calculation in chapter 6 indicated that only 20 % of the excess pore pressures are left after 24 hours of consolidation. This amount is in the same range as the error (or difference) between the measured density profiles in figure 6.5. To calculate these density differences, the consolidation parameters have to be given a value. These values are chosen according to the findings in the previous chapter. It was shown that the consolidation model can give reasonable results with a wide rang of values of the parameters D, K_s and K_k , provided the parameters are arranged into specific sets (Annex 6.4). All these computations give smaller differences between the profiles at 24 hour and later, than the measurements (annex 6.4). So the influence of the consolidation will be smaller than expected from the density measurements. The small differences between the profiles at 24 hour and 7 days, means that even before we have performed any simulation of the erosion, we can already conclude that consolidation will not have much effect on the erodibility. The simulations in this chapter show how small the influence of the density differences is.

7.5.2 Validation and sensitivity analysis estimated parameters

First the influence of the estimated parameters f, $K_{0,}$, ϕ', c'_a, α and $M= w_e \cdot \phi \cdot \rho_s$ in table 7.2 is investigated, in the next section the influence of the consolidation parameters is investigated. The validation runs have been performed for the 1-day experiment only. The only ageing mechanism that can account for the different decrease in erodibility between 1 and 7 day is the consolidation. The consolidation affects the validation runs for all the parameters the same way. Accordingly it is no use to perform the simulations twice. The erosion experiment after one day of consolidation was applied for 24 hours, the erosion experiment after seven days of consolidation for only 12 hours. The one-day experiment is therefore considered more useful for validation. The effect of the consolidation is investigated separately.

The results for different values of the parameters f, M, α , $K_{0,}$, φ' and c'_a can be seen figures 7.10 to 7.13. From these we can conclude that the 1-DV water bed model can give reasonable answers for a well chosen set of parameters. And, very important, the characteristic exponential behaviour is present in the results. From the figure we can conclude that erodibility increases if the cohesion parameter $c`_a$ decreases, if the entrainment rate $w_e$ (~ $M$) increases, if the swelling of the bed increases (parameter $f$ decreases), if the angle of internal friction $\varphi`$ decreases, or if the average bed shear stress increases. Good results can be obtained with many combinations of the parameters. Two one these good results are shown in this section (one with $c`_a$=20 in figure 7.10 and the other in figure 7.35).

A good result is obtained with a low value of f (f=3) and with a high value of w_e (w_e=1·10^{-3} m/s). These values are close to the limits of the range of values that are physically justifiable for these parameters. The use of values that are more in the centre of their respective ranges (a lower value of w_e and a higher value of f) gives a too low eroded mass according to the figures. $c`_a$ and $\varphi`$can be used to compensate for this lower erodibility. Using a lower value of $c`_a$ or $\varphi`$ it might be possible to give a reasonable answer for other combinations of the three mentioned parameters. In figure 7.37 for instance, the parameter $\varphi`$ is used to tune the data with f=∞.

Cohesion $c`_a$

Figure 7.10 shows that the 1DV-waterbed model is quite sensitive to the cohesion $c`_a$. An increment of 5 Pa in $c`_a$ leads to a decrease of the eroded mass of about 0.7 mm of material. If $c`_a$ =0 the erosion progresses almost linearly with a rate of (3·10$^{-3}$ m)·(2600 kg/m$^3$) / (16.5·3600 s) = 1·10$^{-4}$ kg/m$^2$/s. This line limits the results for the cohesion parameter on the left side, since $c`_a$=0 is the smallest value of the cohesion. This option resembles negation of the first term in equation 7.4. Also note that $c`_a$ hardly influences the slope at the end of the simulation.

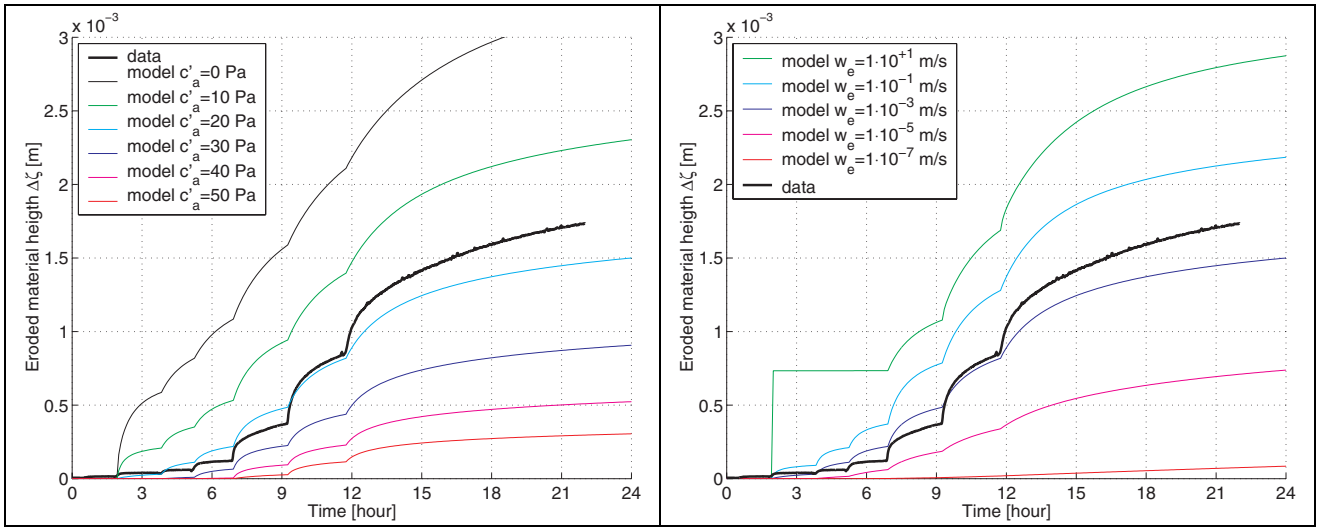

Figure 7.10 (L): Results 1-DV water bed model after 1 day of consolidation. Influence of cohesion parameter $c`_a$.

Figure 7.11 (R): Results 1-DV water bed model after 1 day of consolidation. Influence of entrainment rate w_e. (with $M = w_e \cdot \phi \cdot \rho_s$)

Erosion rate M

In figure 7.11 one can see the results of calculations performed with different values of the erosion parameter $M = w_e \cdot \phi \cdot \rho_s$. We can conclude that the total eroded mass is not sensitive to the entrainment rate coefficient w_e. Multiplying M by a factor 10 makes the final erosion only vary by a constant amount of about 0.7 mm of material height: the erosion rate is only affected by the natural logarithm of this parameter. Since no theoretical relationship is available for this parameter, it is very convenient that the model results are not severely affected by another choice of this parameter. The artificial stepwise increase visible at t=3 hours at $w_e = 1 \cdot 10^1$ m/s is due to a too small value for *deltE* (see section 7.5.4) and is not due to the very high value of the erosion rate parameter.

Scale parameter α of the Rayleigh probability distribution

Figure 7.12 shows the effect of the average value of the bed shear stress on the erosion. If α is lower, that is if the average bed shear stress $\mu = \frac{1}{2} \cdot \tau_b \cdot \sqrt{(\pi / \alpha)}$ is higher, the erosion rate is higher. Doubling of α almost halves the erosion.

General geotechnical parameters K_o and $\varphi`$

The model results for different values of the angle of internal friction and the coefficient of lateral stress are shown in figure 7.14. Since equation 7.4 contains these parameters in one factor $(1+2K_0)\sin\varphi`$, different values for this factor rather than for the individual parameters are used in the validation runs. The maximum of the product $(1+2K_0)\sin\varphi`$ is obtained at $\varphi`$=40 and $K_0$=3 and the minimum at $\varphi`$=0 (when the second term is totally skipped in equation 7.4). The runs for these two combinations will envelop the results for all other combinations. Within these envelopes, the model is quite sensitive to the geotechnical parameters.

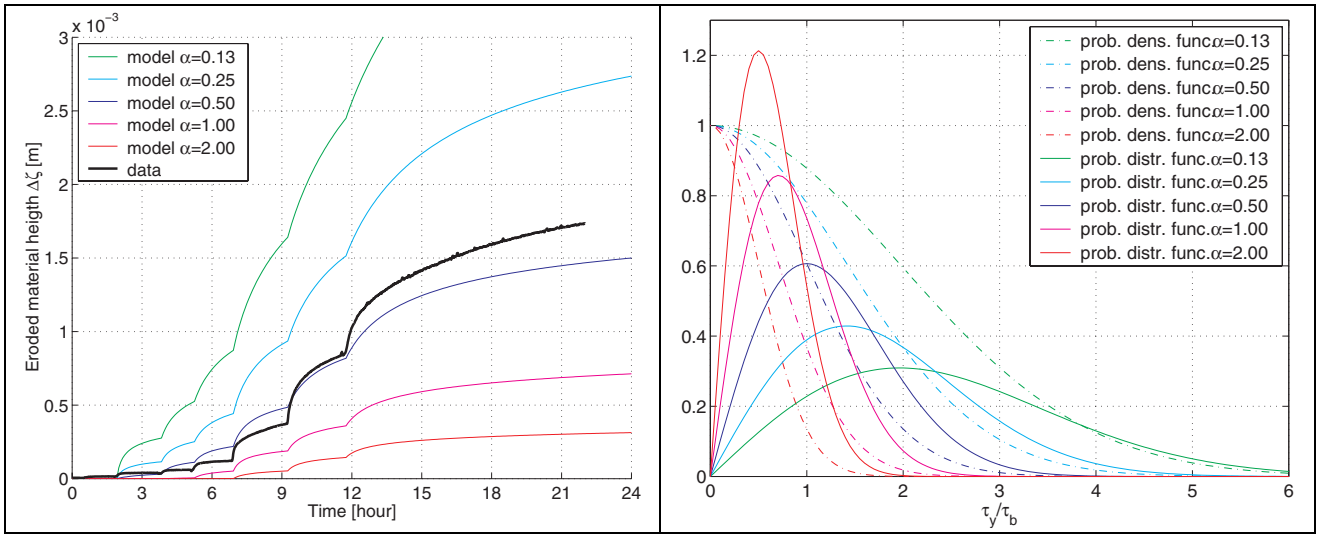

Figure 7.12 (L): Results 1-DV water bed model after 1 day of consolidation. Influence of the scale parameter α of the Rayleigh probability distribution.

Figure 7.13 (R): Rayleigh probability distribution for different values of its scale parameter α.

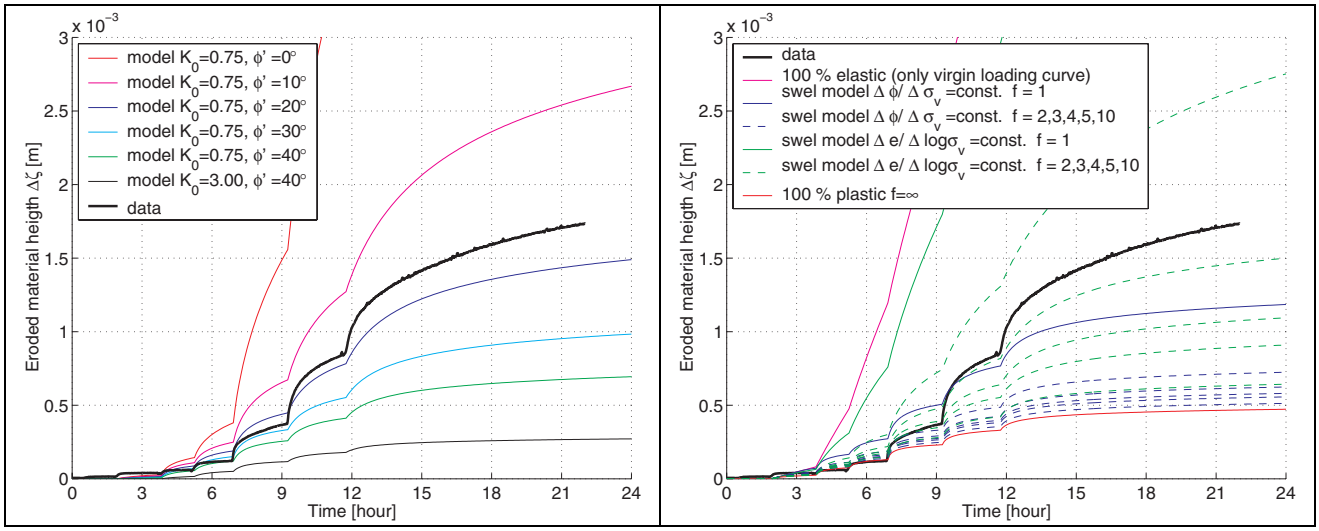

Figure 7.14 (L): Results 1-DV water bed model after 1 day of consolidation. Influence of K_0 and φ.

Figure 7.15 (L): Results 1-DV water bed model after 1 day of consolidation. Influence of swelling parameter f and swelling model.

Swelling behaviour

In figure 7.15 one can see that the swelling parameter f has a large influence on the erosion. The curves for the different values of f lie between the curves for f=∞ and the curve using the virgin loading relation in the reloading regime. We also see that the same value of f has different implications for each swelling model. The swelling model that is linear in the ϕ-σ'_v plane, needs a lower f to give the same swelling near the interface.

If the reloading curve is the same as the unloading curve (pink line), the results hardly show the characteristic exponential behaviour after each step in the bed shear stress. The erosion progresses almost linearly with an erosion rate of $(6{\cdot}10^{-3}$ m)*(2600 kg/m^3)*(6·3600 seconds) = $7{\cdot}10^{-4}$ kg/m^2/s. When we compare this to the erosion rate coefficient $M = \rho_s{\cdot}\phi{\cdot}w_e$ = (2600 kg/m^2/s)*0.03*$(1{\cdot}10^{-3}$ m/s) = $8{\cdot}10^{-2}$ kg/m^2/s, we see that the probability $\tau_b > \tau_y$ in equation 7.3 (Rayleigh distribution) is obviously very small, in the order of 1/100. The bed strength at the interface is indeed almost 3 Pa when the bed behaves fully plastic.

So erosion still occurs when the actual bed yield strength is at least about 5 times the average bed shear stress (τ_b=0.55 maximally). When the bed is 100 % elastic, the yield strength at the surface is about 0.58 Pa during the entire simulation, so the bed strength is 1 to 4 times the average bed shear stress. That means that the erosion is actually solely governed by the (very) tail of the Rayleigh distribution. The turbulent burst in the water are of paramount importance to the erosion. Accordingly it is very fortunate that even the simple Rayleigh distribution assumed gives good results.

The influence of the swelling on the bed profiles can be studied in figures 7.16 to 7.23. The results for the fully plastic model, the fully elastic model and the two swell models are enclosed. For the linear swell models, the results corresponding with the lines closest to the data in figure 7.15 are chosen. In the left pane of each set of two figures, the density profiles are displayed at regular intervals of one hour. In the right pane the density (colour shading) is depicted as an almost continuous function of time (horizontal axis) and depth (vertical axis). Each line in the left pane corresponds with one vertical line at exactly a whole hour in the right pane. The figure use material coordinates, in which the swelling does not lead to a rise of the interface. The swelling is visible as a decrease in the density-shading.

With a fully plastic model (fig. 7.16 and 7.17), all the lines in the left panes are almost on top of each other. Near the rigid bottom they are not, since the consolidation still progresses in the first moments of the experiment.

When a fully elastic model is used (fig. 7.22 and 7.23), the density near the interface is almost equal to the gelling density all the time. This leads to high erosion rates. Consequently the entire bed is totally eroded before the end of the simulations: after 13 hours.

With the linear swelling models, the behaviour is between the behaviour of the fully plastic and the fully elastic model. Two scenarios are depicted where the amount of erosion is almost the same. The shape of the density profiles is different for each swelling model. The model "linear in the log($\sigma`_v$)-*e* plane" (figure 7.20 and 7.21) leads to a larger decrease in the density in the deeper parts of the bed. The model "linear in the log($\sigma`_v$)-*e* plane" does not lead to $\phi=\phi_{gel}$ at the top all the time, as was mentioned in section 4.2.2. So it can be used.

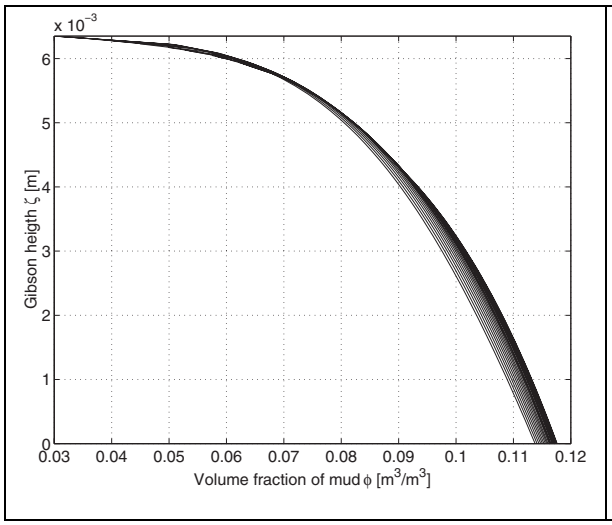

Figure 7.16 (L): Density profiles at intervals of one hour after 1 day of consolidation. Use of fully plastic model.

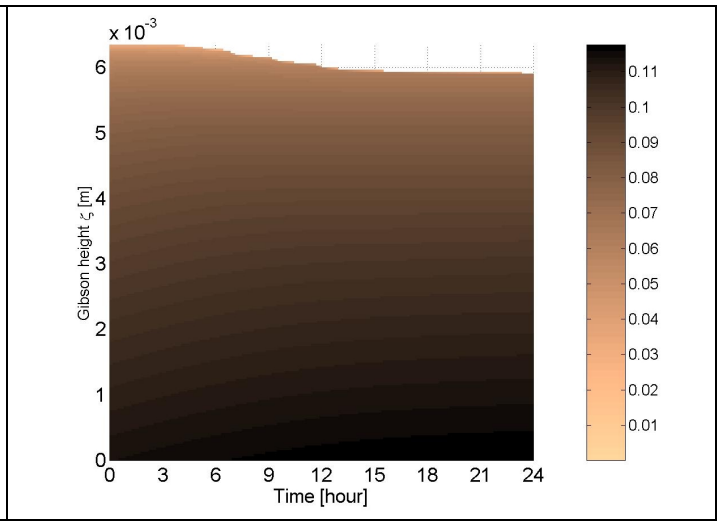

Figure 7.17 (R): Water bed after 1 day of consolidation. Use of fully plastic model.

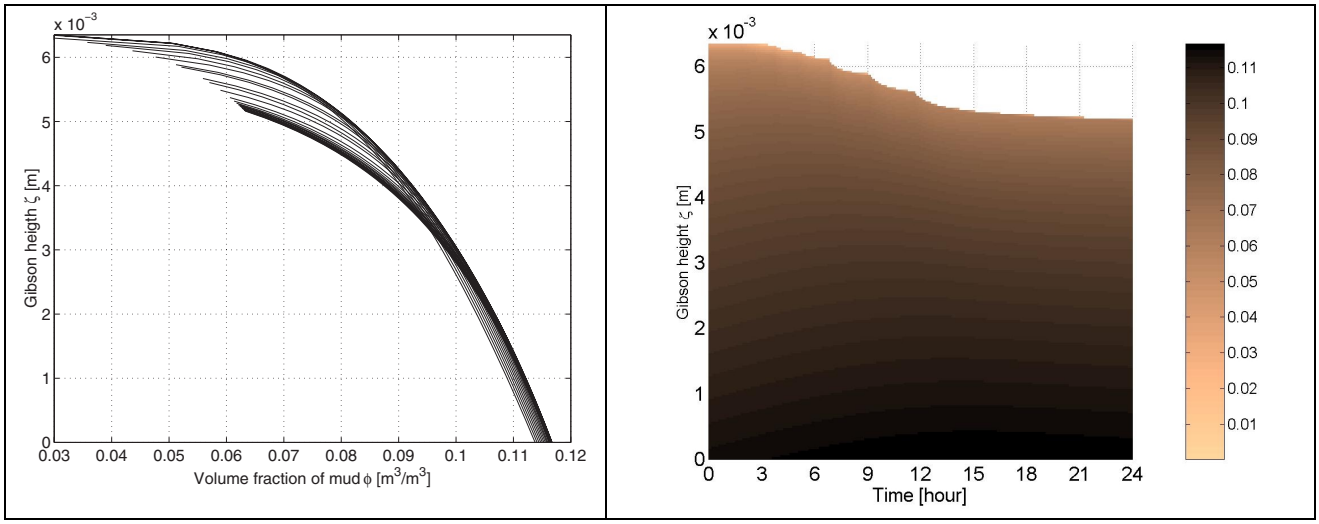

Figure 7.18 (L): Density profiles at intervals of one hour after 1 day of consolidation. Use of swelling model where $\Delta\sigma'_v / \Delta\phi$=constant in the reloading regime and f=1.

Figure 7.19 (R): Water bed after 1 day of consolidation. Use of swelling model where $\Delta\sigma'_v / \Delta\phi$=constant in the reloading regime and f=1.

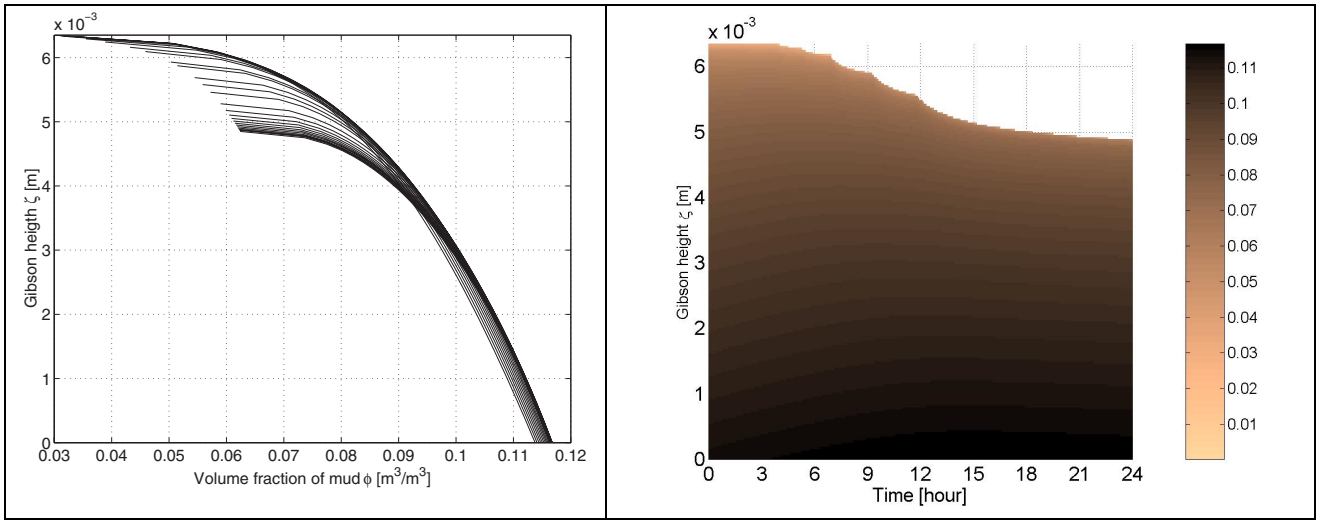

Figure 7.20 (L): Density profiles at intervals of one hour after 1 day of consolidation. Use of swelling model where $\Delta\log(\sigma'_v) / \Delta e$=constant in the reloading regime and f=3.

Figure 7.21 (R): Water bed after 1 day of consolidation. Use of swelling model where $\Delta\log(\sigma'_v) / \Delta e$=constant in the reloading regime and f=3.

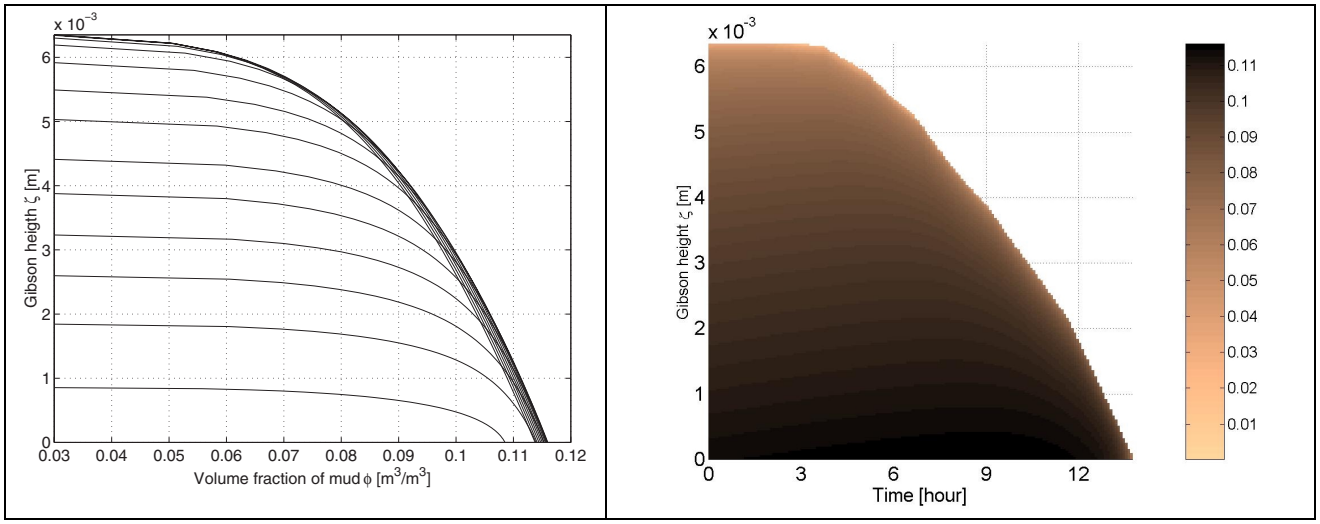

Figure 7.22 (L): Density profiles at intervals of one hour after 1 day of consolidation. Use of fully elastic model.

Figure 7.23 (R): Water bed after 1 day of consolidation. Use of fully elastic model.

7.5.3 Validation and sensitivity analysis consolidation parameters

The effect of the consolidation on the time dependent decrease in the erodibility has been established. Both the 1-day experiment and the 7-day experiment are modelled. In figure 7.25 we can see that the erosion is very sensitive to the fractal dimension, as discussed in chapter 6. In figure 7.24 the results can be seen for the permeability parameter and in figure 7.25 the results for the effective stress parameter. The reference case (D=2.6, K_k=8.0·10^{-12} m/s, K_σ=4.0·10^6 Pa) does not show the same decrease in the erodibility as the experiment. This can be attributed to the small difference between the profiles after 1 and 7 days of consolidation. The differences between the profiles after 1 and 7 days of consolidation can be seen in annex 6.8 and 6.9. (The values of five times K_k and K_σ from table 6.6 are not used, since these lead to the same results as twice the reference values.)

In figure 7.24 we see that a smaller value of K_k leads to larger difference between the 1 and 7 day results. Both the 1 day and 7 day erosion increases, only the 1 day erosion increases faster. For half K_k, the results after 7 days do not change any more when K_k is increased. This is due to the fact that the profile is already in equilibrium situation at half the reference value of K_k after 7 days. The fact that the speed of the consolidation is mainly a function of the permeability parameter accounts for this.

In figure 7.25 we can see that when increasing the K_σ to 8.0·10^6 Pa, which is twice reference value of K_σ, the 1-day and 7 day results are almost on top of each other. When a smaller value of K_σ is used than the reference value, the model gives a larger difference between the results after 1 day and after 7 days. A value of one fifth of the reference value of K_σ does show the measured decrease in the erodibility.

The reference case (D=2.6, K_k=8.0·10^{-12} m/s, K_σ=4.0·10^6 Pa) is the set that was best able to predict the measured density profiles in chapter 6. This set is not the best set for the erosion however. With one fifth of the effective stress parameter, K_σ=8.0·10^5 Pa, the results for the erosion are better: the decrease in erodibility between one and seven days of consolidation can be described with the 1-DV water bed model. The density and effective stress profiles with this value of K_σ Pa can be seen in figures 7.26 to 7.29.

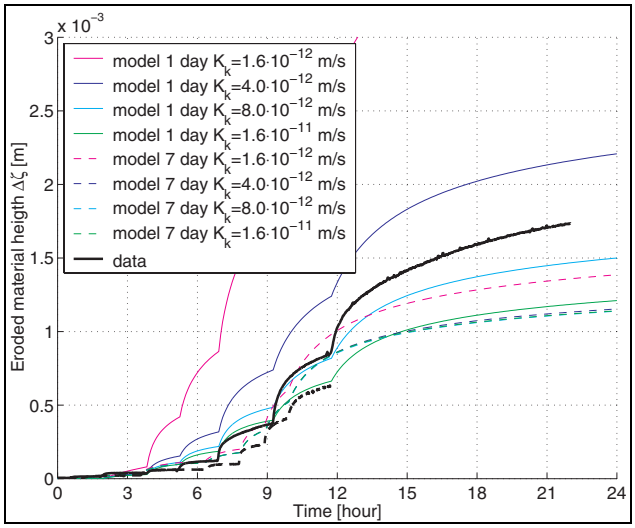

Figure 7.24 : Results 1-DV water bed model after 1 and 7 days of consolidation. Influence of K_k. (Reference case $K_k=8\cdot10^{-12}$ m/s)

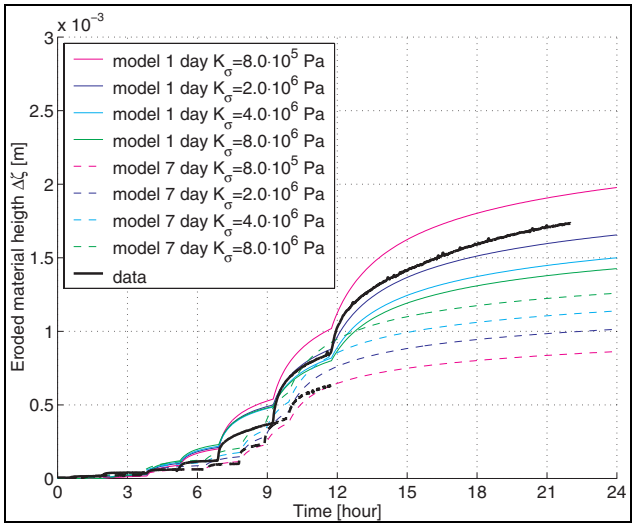

Figure 7.25 : Results 1-DV water bed model after 1 and 7 days of consolidation. Influence of K_σ.(Reference case $K_\sigma=4\cdot10^6$ Pa)

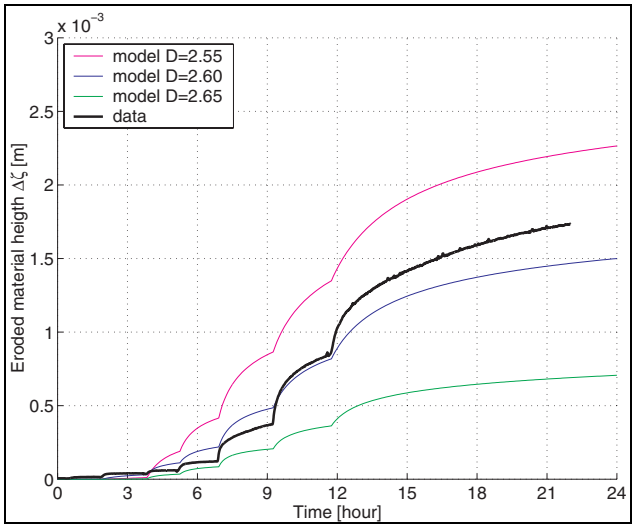

Figure 7.26 : Results 1-DV water bed model after 1 and 7 days of consolidation. Influence of D. (Reference case D=2.6)

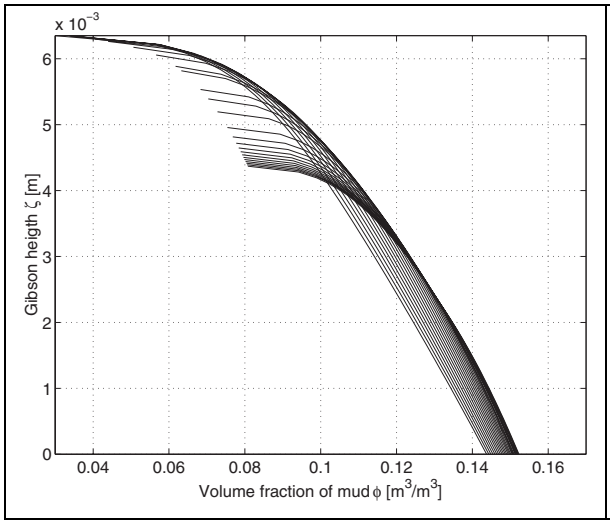

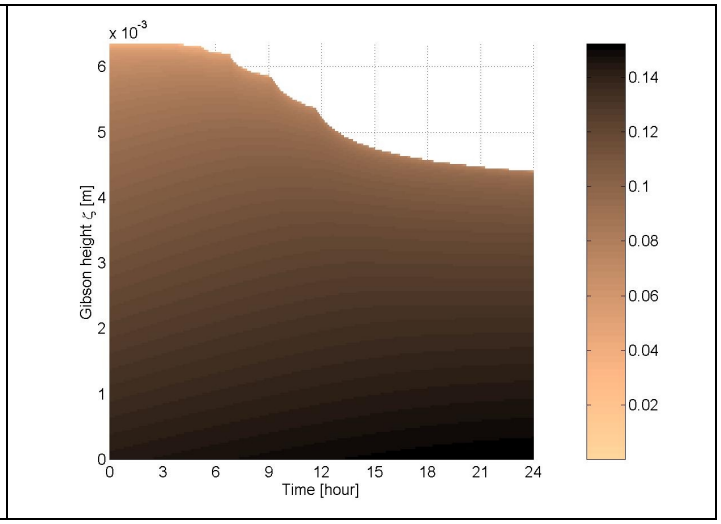

Figure 7.27 (L): Density profiles at intervals of one hour after 1 day of consolidation. D=2.6, K_k=8.0·10^{-12}, K_σ=8.0·10^5

Figure 7.28 (R): Density profiles after 1 day of consolidation. D=2.6, K_k=8.0·10^{-12}, K_σ=8.0·10^5

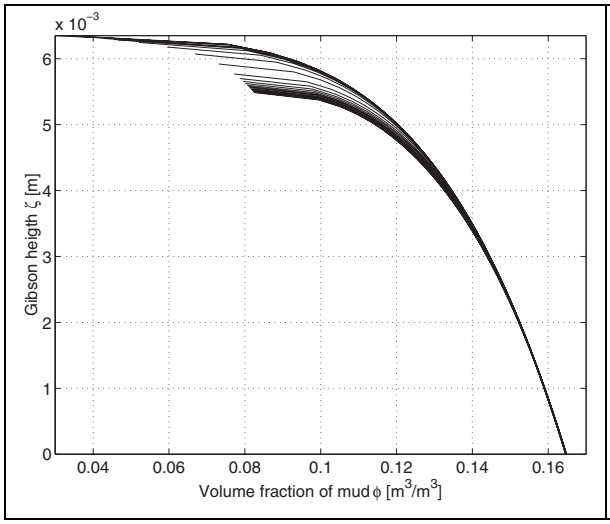

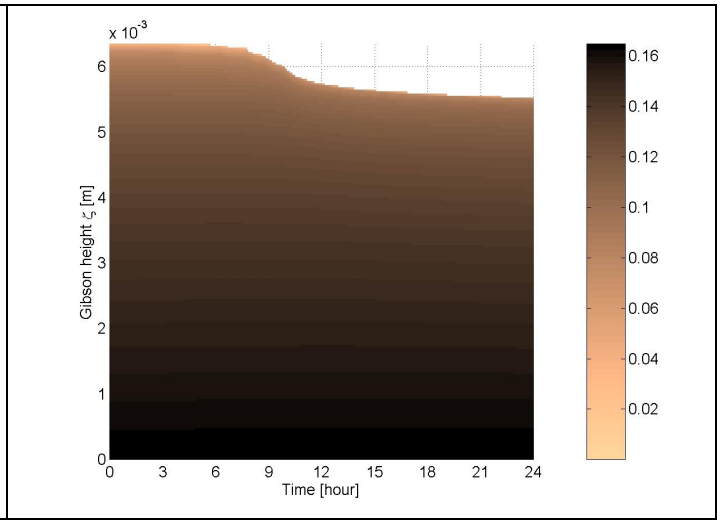

Figure 7.29 (L): Density profiles at intervals of one hour after 7 days of consolidation. D=2.6, K_k=8.0·10^{-12}, K_σ=8.0·10^5

Figure 7.30 (R): Density profiles after 7 days of consolidation. D=2.6, K_k=8.0·10^{-12}, K_σ=8.0·10^5

7.5.4 Numerical aspects

Influence spatial resolution (non)

In chapter 5 the influence of the deposition on the spatial resolution has been mentioned already. If a thin layer with a low density (ϕ_{gel}) deposits on top of a profile with a high density, the average density near the interface can be affected. To check this behaviour, small periods of deposition (5 minutes) are incorporated between two successive values of the bed shear stress. The depositions during these short periods are in the order of 10^{-7} m of material height. During the first deposition periods this amount of material is smaller, for the concentrations in the annular flume are still low. The resolution is about $\Delta\zeta=\zeta_i$ /non = 6 mm /50 $\approx 10^{-4}$ m and increases slightly when more material is eroded. The resolution is very coarse with respect to the depositions. The amount of deposition in these tests is very small. So if the model can stand this deposition test, it can very likely stand any alternation of erosion and deposition.

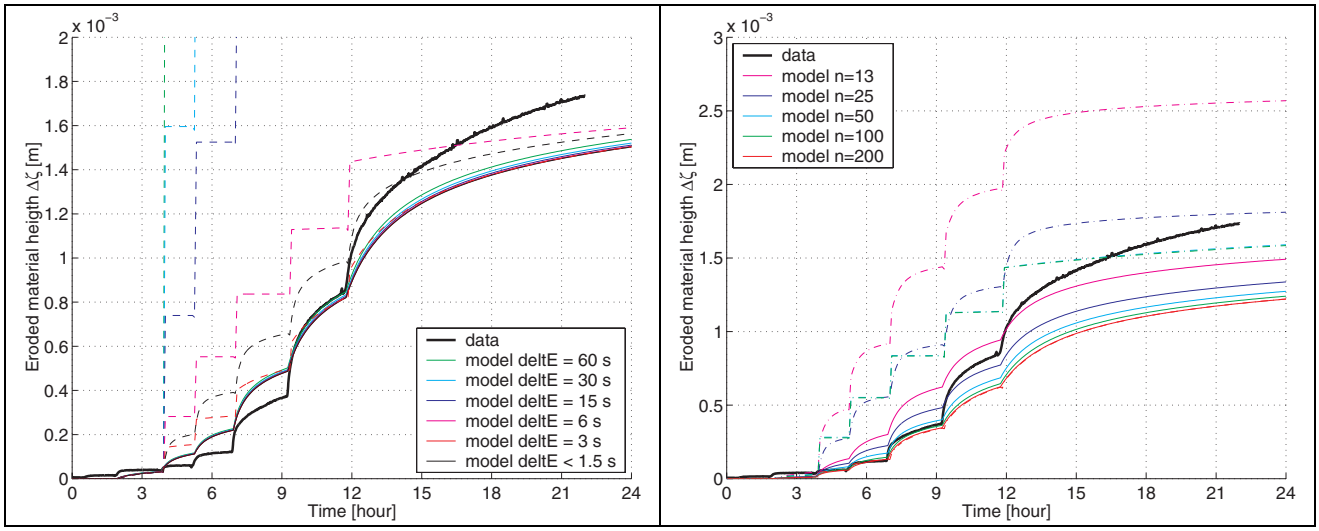

Figure 7.31 (L): Results 1-DV water bed model after 1 day of consolidation. Influence of number of sampling points *non*. (Dashed with periods of deposition (5 min.) before each successive step of the bed shear stress, solid line without deposition.)

Figure 7.32 (R): Results 1-DV water bed model after 1 day of consolidation. Influence of time step *deltE*. (Dashed with periods of deposition (5 min.) before each successive step of the bed shear stress, solid line without deposition.)

The results can be seen in figure 7.31. We see that the results without deposition (continuous erosion) are only slightly influenced by the number of sampling points. Only when the resolution is very coarse, 25 or 13 sampling points, the differences become significant. When the 5-minute periods of deposition are present, the results are already significantly different from the results without deposition. The results should be the same, irrespective if deposition occurs or not. The amount of deposition, 10^{-7} m, is very small and does not significantly influence the erosion in reality. So it is the vertical resolution that is responsible for the influence on the representation of the density near the interface. The stepwise increase in the eroded mass at n=50 & 100 is due to a too small timestep *deltE* (see next subsection). Fortunately, we also see that for 200 sampling points, deposition does not have any influence at all, since the lines with and without deposition are perfectly on top of each other. The lines with and without deposition are on top of each other. So it is possible to avoid the numerical problems of the spatial resolution. The model is quite slow though with 200 sampling points.

The results in figure 7.31 are obtained with f=3. The expectation is that the sampling resolution will affect the results more if the bed is assumed fully plastic (f=∞). The densities just below the interface will be higher then and this will lead to the highest steps and the steepest gradients. More sampling points might be required to get a stable solution with a fully plastic bed.

Influence time step deltE

The influence of the time step *deltE* can be seen in figure 7.32. Just like with the spatial resolution, the effects of *deltE* is investigated by allowing 5 minutes of deposition just before a step in the bed shear stress. When this time step is chosen too large, the behaviour of the erosion can be very strange: after each period of deposition, the erosion rate is almost infinite (vertical line), after which it immediately drops to a very low value (horizontal line). The curve looks like a staircase. When the timestep *deltE* is small enough, the erosion regains the characteristic exponential behaviour.

The results for all time steps smaller than 1.5 seconds are on the same line. So when choosing a sufficiently small time step, no numerical inaccuracies occur. The curve is still different from the curve without deposition though. This is due to a too small number of sampling points (n=50, see previous subsection). A very unexpected result is that the curve with a time step of 1.5 seconds is between the results for 6 seconds and 3 seconds. (One would expect the results for 1.5 seconds to be under the curve for 3

seconds.) We also see that if only erosion occurs, a time step of 60 seconds does not lead to any problem. So with a sufficiently small timestep *deltE* it is possible to avoid numerical problems.

Influence consolidation time step deltC

The results of the model are also dependent on the time step of the consolidation. The dependence on the time step can be attributed to the swelling behaviour. If the timestep for consolidation *deltC* is increased from 5 minutes to 30 minutes the eroded mass decreases 10 % (figure 7.33). The erosion during the first 5 minutes of the 30 minute time step is the same as when a five minute time step is used. The swelling due to this 5 minute erosion is not immediately accounted for in the 30 minute time step. Consequently the erosion during the 25 successive minutes of the time step is calculated as if the swelling behaviour of the bed were infinitely stiff. We have already seen that if the bed behaves fully plastic (figure 7.15), the erosion rate reduces. To account for the timestep dependency of the results, the values for the erosion parameters would have to be changed whenever the time step would be changed when calibrating the model.

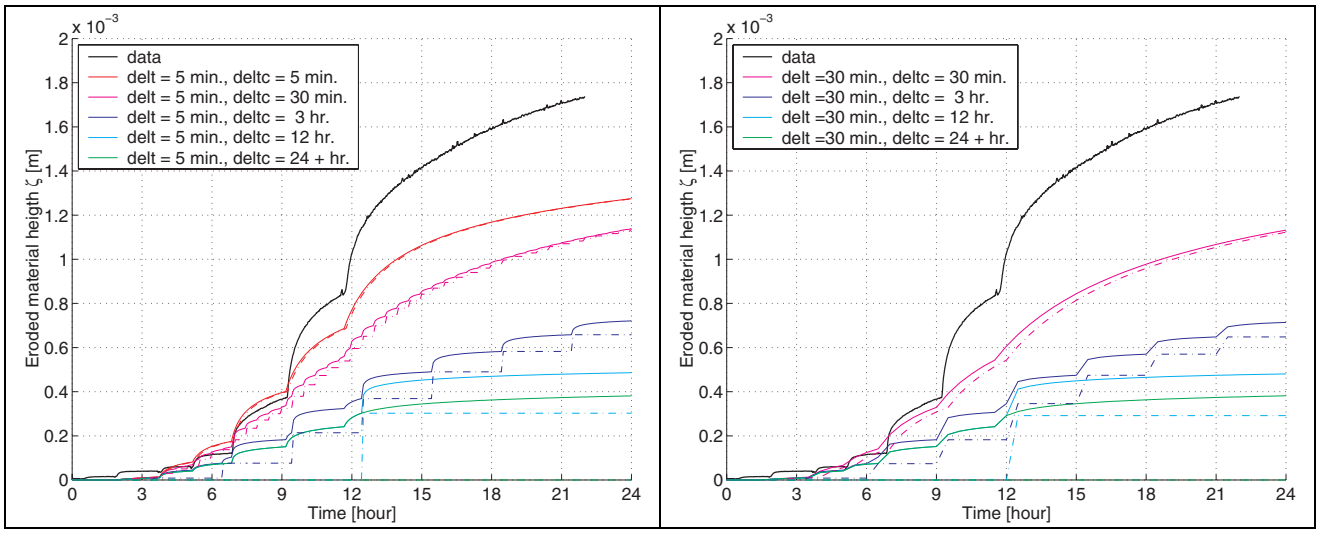

Figure 7.33 (L): Results 1-DV water bed model after 1 day of consolidation. Influence of consolidation time step *deltC*. (Dashed line eroded material height and solid line eroded material height + *ressum* - *sedsum*)

Figure 7.34 (R): Results 1-DV water bed model after 1 day of consolidation with WAQ time step *delt*=30 min. Influence of consolidation time step *deltC*. (Dashed line eroded material height and solid line eroded material height + *ressum* - *sedsum*)

The expectation was that because the time scale of the consolidation is very large, the influence of the consolidation and swelling could be neglected on time scales smaller than one hour. It turns out that the consolidation during the short time steps can certainly not be neglected. First, the small bed height in the annular flume (6 mm material height) can lead to the short time scale of the consolidation ($T::\zeta_i^2$). Furthermore, consolidation near the interface is faster than in the deeper parts of the bed. In the deeper parts the effective stress needs more time to evolve to the final equilibrium stress. Near the interface the effective stress is almost instantaneous at the equilibrium level: the boundary condition $\sigma'_v=0$ applies instantaneously to the interface and almost instantaneously to the region just below.

Using a longer time step for consolidation than the WAQ timestep, resembles modelling the bed plastic for most of the time. If for instance the WAQ time steps is 5 minutes and the consolidation time step is one hour, the bed behaves plastic for 11/12 part of the time steps. When consolidation is applied, the bed suddenly behaves non-plastic for one moment. This leads to weird artificial behaviour of the erosion. As a result the characteristic exponential decay of the erosion rate not only occurs when the bed shear stress suddenly increases, but also when the bed yield stress suddenly decreases by the swell. A fully plastic

reloading behaviour all the time can solve this anomaly. Then the bed behaves the same all the time, irrespective of the timing of the consolidation. In the validation runs however, a value of f=3 leads to acceptable results, while f=∞ leads to too little erosion. So the other erosion parameters have to be changed to make the final erosion the same as in the experiments. Hence a calibration has been performed for f=∞. The value of K_σ, which could simulate the time dependent erodibility correctly, is used. In figure 7.35 one can see that it is possible to run the model successfully with only fully plastic material. We also see that the consolidation time step still influences the erosion, even if swell is neglected. This is due to the numerical aspects of the redistribution. More sampling points can solve this. The density and effective stress profiles for *deltC*=5 min. can be seen in figures 7.36 to 7.39.

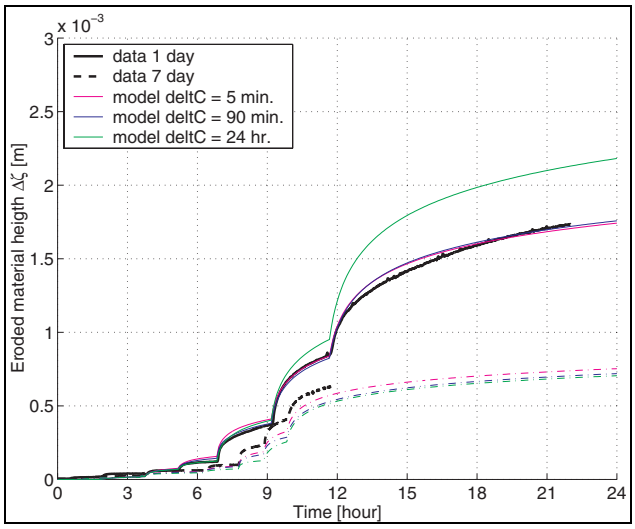

Figure 7.34: Results 1-DV water bed model after 1 day of consolidation, calibrated with f=∞, K_σ=8·10^5 Pa and φ`=3˚.

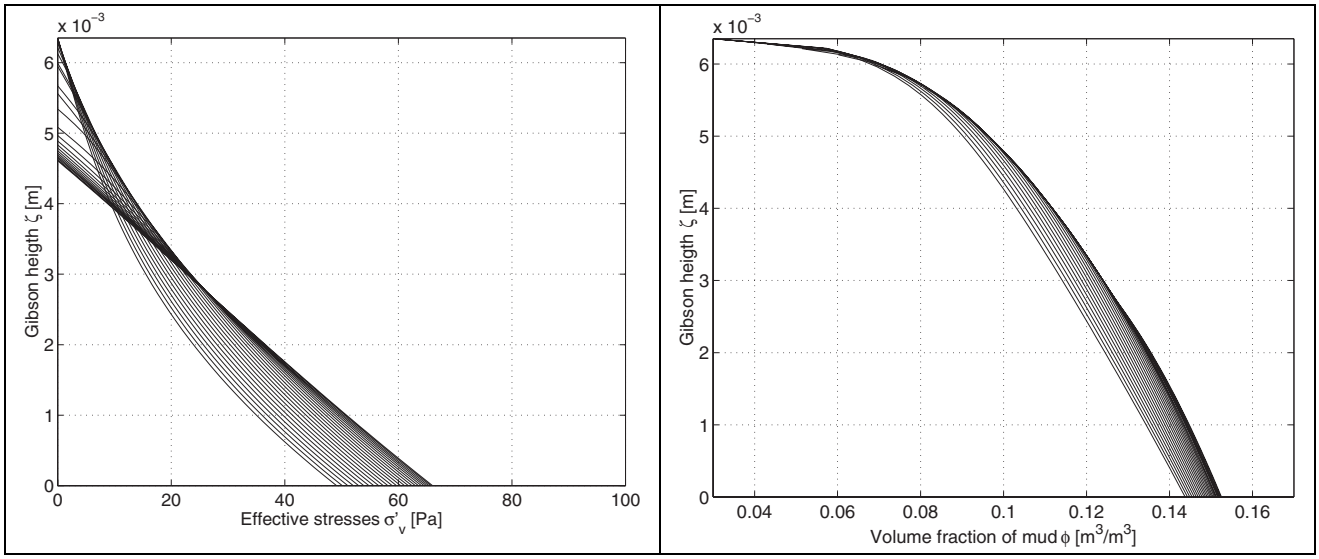

Figure 7.36 (L): Effective stress profiles at intervals of 1 hour after 1 day of consolidation, calibrated with f=∞, K_σ=8·10^5 Pa, φ`=3˚.

Figure 7.37 (R): Density profiles at intervals of one hour after 1 day of consolidation, calibrated with f=∞, K_σ=8·10^5 Pa and φ`=3˚.

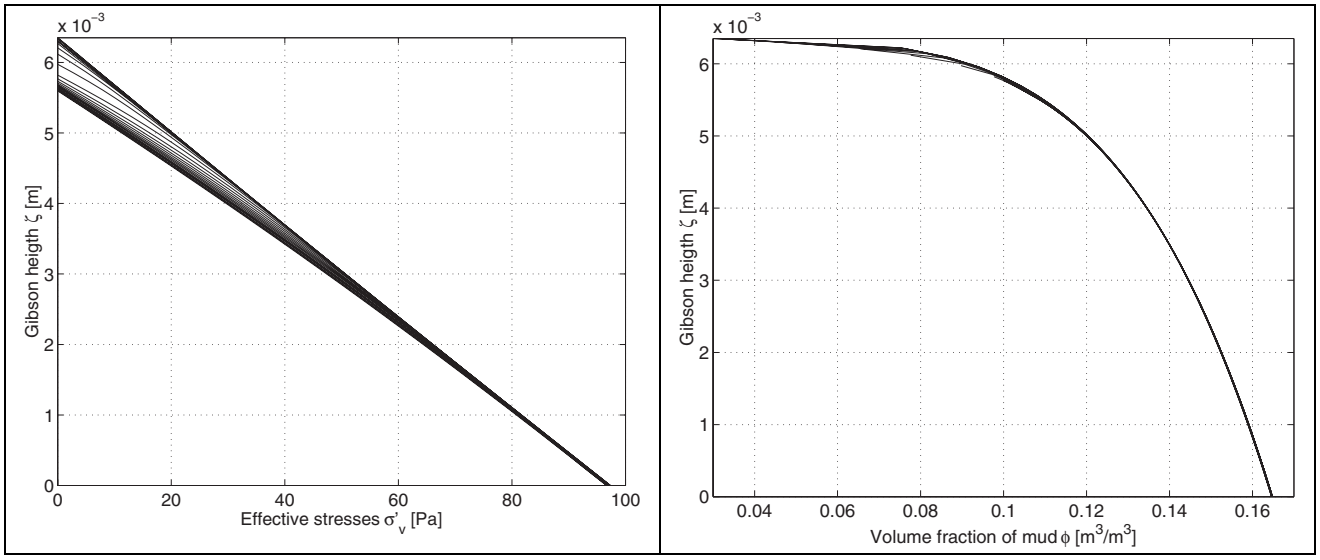

Figure 7.38 (L): Effective stress profiles at intervals of 1 hour after 1 day of consolidation, calibrated with f=∞, K_σ=8·10^5 Pa, φ`=3˚.

Figure 7.39 (R): Density profiles at intervals of one hour after 1 day of consolidation, calibrated with f=∞, K_σ=8·10^5 Pa and φ`=3˚.

Influence other numerical parameters

As we can see in figures 7.34 and 7.35 the water quality timestep *delt* of WAQ hardly influences the results. The number of Fourier components does not influence the results either. Even the use of only Fourier component (still stable according to equation 5.12 at a time step of 5 minutes) hardly influences the results.

Optimal parameter setting

Table 7.2, which contained the values of the input parameters, is repeated here with the recommended values. A fully plastic model is chosen to avoid problems with the consolidation time step. Note that other combinations of parameters could also be used to calibrate the model.

Parameter	Symbol	Values	Units
Density of sediment material	ρ_s	2600	kg/m^3
Density of pore water	ρ_w	1000	kg/m^3
Volume fraction of mud at gelling point	$\phi_{g\,el}$	0.03	m^3/m^3
Effective stress parameter	K_σ	8·10^6	N/m^2
Permeability parameter	K_k	8·10^{-12}	m/s
Fractal dimension	D	2.6	-
Ratio of swelling stiffness to virgin compression stiffness	f	∞	-
Swelling model	fully plastic		
Cohesion	$c`_a$	20	N/m^2
Angle of internal friction	φ`	3	degr
Coefficient of lateral stress	K_0	0.75	-
Entrainment rate (Erosion rate $M = w_e \cdot \phi \rho_s$)	w_e	1·10^{-3}	m/s
Scale parameter for Rayleigh distribution (with average $\mu = ½ \cdot \tau_b \cdot \sqrt{(\pi/\alpha)}$	α	0.5	-
Critical shear stress for erosion	τ_{cr}	0.1	N/m^2
Number of sampling points	*Non*	50	#
Number of Fourier components	*Nok*	50	#
Time step consolidation (=maximum timestep for consolidation *deltcmax*)	*Deltc*	5	min.
Time step for erosion and deposition (Delft3D-WAQ timestep)	*Delt*	5	min.
Time step erosion calculation	*DeltE*	6	sec.

Table 7.2 Parameters used in the runs with the consolidation- erosion model

7.6 Summary

- Different erosion models have been tested in this chapter. All of these models give results that are in the same range as the data, but all of these models have shortcomings as well.
- The models are tested with the measurements of an erosion experiment in an annular flume. A cohesive sediment bed was exposed to a series of stepwise increasing bed shear stresses. The behaviour of the measurements after application of each new bed shear stress shows the same characteristic behaviour. Immediately after the stepwise increase of the bed shear stress, the erosion rate is very high. After that the erosion rate gradually decreases to a lower and almost constant value (secondary erosion). This behaviour can roughly be described with an exponential decay function with a time scale of 1 hour. Experiments have been performed after 1 day of consolidation and after 7 days of consolidation, to assess the time dependent behaviour of the strengthening of the sediment. The erosion experiment after one day of consolidation lasted 24 hours, the one after 7 days of consolidation lasted 12 hours.
- The classical Partheniades erosion formula does not tend towards any (dynamic) equilibrium situation at all as the erosion increases. The erosion keeps on increasing at the same rate. Posing of an erosion limit can remedy this behaviour, but this leads to very unnatural behaviour. Moreover, the results are dependent on the erosion rate coefficient M. Since not much is known about M, one can conclude that the Partheniades formula is not useful for long term water quality engineering.
- The ECOMSED model uses the concept of an erosion potential: at a certain bed shear stress only a finite amount of material can resuspend. The data do not show the presence of such erosion potential, so the assumption is used that the highest occurring erosion at a certain bed shear stress is the erosion potential. This assumption leads to parameters depending on the length of the erosion experiment and to underprediction of the eroded mass at long time scales.
- A second shortcoming of ECOMSED is that it erodes the erosion potential too fast: it allows the total erosion potential to resuspend within an hour, while the exponential decay function releases the mud during three hours. ECOMSED will therefore over rate the eroded mass at short time scales and at high bed shear stresses, consequently over rating the residence times in the water and the displacements of the cohesive sediments by the currents.
- A third shortcoming of ECOMSED is that it can age material only for seven days. After 1 week all the sediment will be treated equally and the model will show the unwanted 'clean-bed' behaviour.
- An erosion model that uses a critical shear stress as a function of the density shows the characteristic exponential behaviour. The results are good when appropriate values of the parameters are chosen. The model over rates the erosion rates at small bed shear stresses and is very sensitive to the parameters.
- The new 1DV-waterbed model that takes into account the probability distribution of the bed shear stresses has also been tested. This model can simulate the characteristic behaviour of the annular flume erosion experiment well: (i) the simulations show the same characteristic exponential decay behaviour, (ii) the results can be calibrated good in a qualitative sense and (iii) the decrease in the erodibility after one and seven days of consolidation can be simulated with the consolidation as the only strengthening process. However, lower values of the effective stress parameter than found in the validation of the consolidation module are necessary. No time dependent function for the cohesion is necessary to calibrate the model. This does not imply that the cohesion parameter is not time dependent.
- We can conclude that the combination of the new parameterised consolidation module and the new erosion module in the 1-DV water bed is promising. The model does also have some minor complications however. These can be divided in physical problems and numerical problems.

- The model needs values for five physical parameters (other than the cohesion parameters) as input: cohesion parameter (constant), swelling behaviour, erosion rate coefficient *M*, the shape of the Rayleigh distribution and general geotechnical parameters. These cannot be determined from experiments as has been done in the case of the consolidation parameters. The cohesion parameter is assumed constant. With a proper choice of these parameters it is possible to achieve a good fit to the experimental data.
- The sensitivity of the 1DV-waterbed model has been investigated as well. For every parameter a mean value is estimated. Next, many simulations have been performed, changing the parameters one by one. For all the parameters (almost) the whole range of physically justifiable values has been tested. The results show that the model is also quite sensitive to the parameters, except for the erosion rate. Together with the fact that no method yet exists to determine the values of the above mentioned five input parameters, this implies that the model is not yet applicable for engineering purposes.
- If the proposed erosion formulations is physically correct, an important feature of erosion has been corroborated. This erosion formulation allows only erosion when the actual bed shear stress exceeds the actual bed shear strength. The erosion of the bed is calculated by means of an entrainment rate multiplied by the probability that the actual bed shear stress exceeds the actual bed shear strength. In all the runs this probability is in the order of 1%. That means that the erosion of the bed is actually governed by the (very) tail of the probability distribution of the bed shear stress. The turbulent bursts in the flow field control the erosion, not the average bed shear stress currently used in models.
- The numerical aspects can have a large influence on the model results as well. These parameters include the spatial resolution, the time step for consolidation *deltC* and the time step for the iterative calculation of the erosion *deltE*. The Delft3D-WAQ time step *delt* does not have an influence, nor does the number of Fourier components. The problems with the spatial resolution and the time step *deltE* can be avoided by using enough sampling points and a sufficiently small time step *deltE*. This makes the model slower however.
- The influence of the consolidation time step can be remedied as well. The time scale of the consolidation is shorter (near the interface) than expected. When large time steps for the consolidation are used, this has the same effect as neglecting the swelling behaviour during this timestep. The swelling is only accounted for at the transition from one time step to the next. During the consolidation time step the material is fully plastic. Using different time steps for consolidation and erosion will therefore result in alternating swelling and plastic behaviour. This leads to weird and artificial oscillations in the erosion. This effect can be prevented by using a fully plastic material model all the time. It is possible to calibrate the model with a fully plastic bed perfectly with one set of parameters for both the 1-day and the 7-day experiment.

8 Conclusions and recommendations

8.1 Conclusions

The aim of this study is to develop and test a one dimensional vertical (1-DV) water bed model suitable for long term water quality modelling. The model combines a new consolidation module and a new erosion module. It is implemented in the Delft3D-WAQ modelling software package, in order to make it applicable for long term water quality engineering purposes. The model should be able to simulate test cases within reasonable calculation time.

An interaction of the consolidation module and the erosion module is proposed, suitable for long term calculations at minimal calculation time. This new 1-DV water bed model has been validated against short term physical erosion experiments. These experiments consist of separate consolidation and erosion phases. With the consolidation experiment, the stand-alone consolidation module has successfully been validated, and with the erosion experiment the entire 1-DV water bed module has been successfully validated.

The new model has been validated on erosion experiments performed in a rotating annular flume in a laboratory. In this flume two experiments have been performed: one after one day of consolidation and one after seven days of consolidation. The 1-DV water bed model can simulate the results from the annular flume experiment well: (i) the simulations show the same characteristic exponential decay evolution of the eroded material height, (ii) the model can be calibrated good in a qualitative sense and (iii) the decrease in the erodibility between one and seven days of consolidation can be simulated with the consolidation as the only strengthening process. No time dependent function for the cohesion is necessary. In the erosion models used currently, a time history of the bed sediment has to be 'remembered' to determine the erodibility. In the 1-DV water bed model the history is stored in the shape of the density profile which is calculated by the consolidation module. We can conclude that the combination of the parameterised consolidation module and the erosion module in the 1-DV water bed is promising.

The model does also have some minor complications however, which can be divided in physical problems and numerical problems. In the section recommendations solutions will be proposed for these problems.

The 1-DV water bed model needs eight physical input parameters. The three consolidation parameters can be determined from standard consolidation experiments in a settling column. A method is proposed to get an objective and reproducible measure of these parameters. The other five physical parameters have to be determined by means of numerical experiments (trial and error). No standardised laboratory tests are yet available. These five parameters govern swelling, cohesion, geotechnical coefficients, erosion rate, and the scale of the probability distribution of the bed shear stress. The model results are sensitive to four of these parameters. This make the 1-DV water bed not yet fully applicable for engineering purposes.

In the short term validation simulations of the 1-DV water bed model, the erosion is governed by tail of the Rayleigh probability distribution of the actual local bed shear stress. Accordingly the stochastic nature of bed shear stress governs erosion. These findings corroborate earlier findings mentioning that turbulent bursts govern the erosion.

8.2 Recommendations

Validation on long term: Although the new 1-DV water bed model has successfully been validated on short term erosion experiments, it has not yet been applied to the long term water quality modelling

problems for which it has been developed. An important recommendation is to continue this study by applying the new model for long term water quality simulations. These simulations should (i) be compared to long term water quality field data and (ii) to results obtained with the old Delft3D-WAQ layer model. A few questions need to be answered. Does the new model lack the shortcoming of the old model: i.e. can the characteristics of the open water system be simulated with the new model? And is it possible to run the 1-DV water bed model at reasonable calculation times with a sufficient number of sampling points and with an appropriate consolidation time step.

More research swelling behaviour: The constitutive relations for swelling used in this study contain a parameter f that determines the swelling of the bed at erosion. At present f is estimated. A swelling experiment is needed to measure f, (i) to validate the 1-DV water bed model with a correct value of f, especially at densities near the gelling point, and (ii) to find an (experimental) procedure to determine f for engineering purposes. It might be considered to measure the density profiles in the annular flume immediately after the end of the erosion experiment as well as later on. These might give useful information about the (time scales of the) swelling behaviour of the bed.

More research cohesion: An experiment(al procedure) is needed to measure the cohesion parameter, which is possibly time dependent.

More research actual bed shear stress distribution: Currently a very simple Rayleigh probability distribution function is assumed for the bed shear stress. Although good results are obtained with this assumption, it has not been validated. Moreover, the parameter α, which relates the scale parameter of the Rayleigh distribution to the regularly used bed shear stress τ_b, is currently estimated. An experiment(al procedure) is needed to measure α, (i) to validate the 1-DV water bed model with the correct value of α and (ii) to formulate an method to determine α for engineering purposes.

Include stochastic nature bed strength: The effects of bioturbation, cracks and algae mats are currently omitted in the erosion formulation. I think these effects can be included in the erosion formulation. In the erosion formulation, the strength of the bed τ_y is considered a deterministic parameter at present. If this parameter would also be considered a stochastic variable, the effects of bioturbation, cracks and algae mats on the strength might be included in the statistical parameters of the probability distribution of τ_y (variance, average).

Use erosion rate parameter for calibration: The erosion rate parameter M still lacks a precise formulation in terms of for instance the entrainment and swelling of the bed. The 1-DV water bed model is not sensitive to the erosion rate parameter M (at least in case of the layered bed present in the annular flume, which is erosion type I). Therefore it is recommended to concentrate future research on the other physical parameters and use the erosion rate parameter M for calibration of the 1-DV waterbed model only.

Create numerical consolidation module for research purposes: It is recommended is to make an extended 1-DV water bed model with a fully numerical consolidation module for research purposes, instead of the parameterised consolidation model used at present. The results obtained with the full numerical water bed model have to be compared to the results obtained with the current 1-DV water bed model. The influence of the neglecting of the advection terms in the parameterised consolidation model has to be determined. Second, the numerical model can account for the swelling behaviour in a more formal way than in the current 1-DV water bed model. Third, in the long run, a full numerical model will be useful for long term water quality modelling, for in the future the computers will be faster and faster.

Implement better coordinate sampling system: The current 1-DV water bed model is not capable of dealing with alternating erosion and deposition in a reliable way with a small number of sampling points. The resolution near the interface requires more attention than in the current model. Using high resolution for the entire bed is not an option. This will make the 1-DV water bed model too slow. A recommendation is to implement an aggregated coordinate system: a second set of sampling points has to be introduced between the two highest sampling points to be able to represent the small changes in the density profile near the bed accurately. These sampling points will not necessarily be used in the Fourier transformation of the

profile. Other sampling methods, which are probably more efficient than the *sigma* coordinate system used at present, should also be explored. The option to deal with a 'clean bed' should also be implemented in the model. The current 1-DV water bed model does not allow a clean bed at present.

Implement better calculation erosion progression: Currently an iterative method is used for the calculation of the progression of the erosion. An analytical approach has also been proposed. A recommendation is to implement this second formulation and test it.

Explore best combination consolidation time step, bed thickness and number of sampling points: The 1-DV waterbed model consists of a separate consolidation and erosion module. A configuration for these two modules has been proposed, allowing larger time steps for the consolidation than for the erosion. In the validation of the short-term erosion experiment in the annular flume however, the time scale of the consolidation turned out to be very small, just as small as the erosion time scale. A hypothesis is that this is due to the very thin water bed present in the annular flume, since the time scale of the consolidation is proportional to the squared bed (material) thickness. Larger time steps for the consolidation, which lead to a reduction of the calculation time, can be used when a thicker water bed is present in the model. A thicker bed will require (i) more sampling points to gain the same resolution but (ii) less Fourier components. The required number of sampling points might be reduced when a new coordinate sampling system has been implemented (as recommended). In practical situations however, a thick water bed might not always be present. Therefore an optimal combination of the (required) bed thickness, the number of sampling points and the time step for consolidation has to be found, in order to make the new model fast enough to be suitable for long term water quality purposes.

Dealing with different sediment particle size classes by using the current Delft3D-WAQ layer model: It is recommended to use the current WAQ layer approach next to the new 1-DV water bed module. In this approach, the new model provides for the erosion rates and the old Delft3D-WAQ layer model deals with the (history of the) size distributions of the sediments.

Include wave effects: In practical situations, the resuspension of cohesive sediments during storms is to a large extent controlled by the pressure fluctuations due to the waves, not by the bed shear stresses. Currently these effects are not present in the 1-DV water bed model. These effects should be incorporated.

Dealing with spatial inhomogenity: In practical situations in open water systems, spatial segregation occurs with respect to the sediment type and the sediment size class. The new 1-DV water bed model can only be applied to areas with a muddy bed. In Delft3D-WAQ a system should be incorporated to deal with different types of water bed models at different moments in time and at different locations. It should be possible to use a separate sand erosion model next to the 1-DV water bed model.

Modify ECOM-SED: The ECOM-SED model of Hydroqual has also been tested in this thesis. The results fit the experimental data quite well in an overall sense, but they reproduce the details only to a small degree. Moreover, the 7 layers currently used in ECOM-SED are not sufficient for long term water quality modelling. A few improvements are recommended to make ECOM-SED a more powerful model. A first recommendation is to replace the current 7-day layer system by a more advanced layer system. A layer system in which each deeper layer covers a longer period should be used: 0-1, 2-4, 5-8, 9-16 days etc. Markov chains could be used to shift the material to deeper layers. A second recommendation is to modify the erosion rate formulation for the range when the erosion potential has not yet been reached. The erosion rate should be determined by dividing the remaining erosion potential by the time scale, not by dividing the total erosion potential by the time scale. A third recommendation is to make this time scale, which is currently fixed at 1 hour, editable by the user. A fourth recommendation is to adjust the model to allow for secondary erosion for the range when the erosion potential has already been reached. Currently the erosion rate is set to zero when the erosion potential has been depleted.

References

Barends, F.B.J. 1992. *Theory of consolidation.* GeoDelft.

Battjes J.A., N. Booij, M.A. Hooimeijer 1997. *Modelvorming, collegehandleiding*. TUDelft. (Dutch)

Brouwer, J. 2002. *Dynamics in extracellular carbohydrate production by marine benthic diatoms*. Netherlands Institute of Ecology. ISBN 90-9015546-5.

Gibson, R. E. , G. L. England, & M.J.L. Hussey, 1967. *The theory of one-dimensional saturated clays. I. Finite nonlinear consolidation of thin homogeneous layers.* Géotechique. J., **17**, 261-273.

Gibson, R. E. , R. L. Schiffman, & K.W. Cargill, 1981. *The theory of one-dimensional saturated clays. II. Finite nonlinear consolidation of thick homogeneous layers.* Can. Geotech. J., **18**, 280-293.

Govindaraju, R.S., S. Ramireddygari, P. Shresta, L. Roig, 1999. *Continuum bed model for estuarine sediments based on non-linear consolidation theory.* Journal of Hydraulic Engineering, March 1999, 300-3041.

HydroQual 2001, *A primer for ECOMSED, version1.2, User Manual.*HydroQual.

Jones, C. and W. Lick, may 2001. *SEDZLJ sediment transport model.* Department of mechanical and environmental engineering, University of California.

Jones, C. and W. Lick, june 2001. *Sediment erosion rates: their measurement and use in modelling*. Texas A&M Dredging Seminar WEDA, TAMU and PIANC conference.

Kesteren W.G.M. van, J.M. Cornelisse, C. Kuijper. July 1997. *Dynastar Bed model, Bed strength, liquefaction and erosion.* Cohesive sediments series report 55, Rijkswaterstaat & WL| Delft Hydraulics

Kranenburg, C. 1994. *The fractal structure of cohesive sediment aggregates*. Estuarine, Coastal and Shelf science, **39**, 451-460.

Kranenburg, C. & J.C. Winterwerp, 1997. *Erosion of fluid mud layers. I: Entrainment model*. Journal of Hydraulic Engineering, June 1997, 504-511.

Kranenburg, C. 1992. *Hindered settling and consolidation of mud - analytical results.* Techn. report no. 11-92, Delft University of Technology

Kuijper C., J.M. Cornelisse., J.C. Winterwerp. November 1990. *Erosion and deposition characteristics of natural muds. Sediments from ketelmeer*. Cohesive sediments series report 30, Rijkswaterstaat & Delft Hydraulics.

Kynch, G.J. 1951. *A theory of sedimentation*. Trans Faraday Soc., **48** , 166-176.

Lambe, T. W., R.V. Whitman, 1979. *Soil mechanics, SI version.* Series in soil engineering, John Wiley & Sons.

Lay, David C. 1993. *Linear algebra ands its applications*. Addison-Wesley Publishing Company.

Ledden M., Z. B. Wang, 2001. *Sand-mud morpho-dynamics in an estuary*. River, Coastal and Estuarine Morphodynamics Conference RCEM2001 (IAHR), Japan.

Ledden, M., W. van Kesteren 2002. *A classification for erosion behaviour of sand-mud mixtures*. In preparation for publication.

Lick, W., J. McNeil, 2001. *Effects of sediment bulk properties on erosion rates.* The Science of the Total Environment 266 (2001), 41-48.

Mehta, A. J., E. J. Hayter, R. B. Krone, & A. M. Teeter, 1989. *Cohesive sediment transport. I: Process Description.* J. Hydr. Eng., **115**(8), 1076-1093.

Merkelbach, L. 2000. *Consolidation and strength evolution of soft mud layers.* (PhD thesis) Communications on Hydraulic and Geotechnical Engineering, report 00-2, Delft University of Technology.

Merkelbach, L. 2001. *Note on parameterisation of Gibson's consolidation equation.* Internal memo WL | Delft Hydraulics.

Merkelbach, L. 1996. *Consolidation theory and rheology of mud. A literature survey.* Techn. report no. 9-96, Delft University of Technology.

Morgan, J.S, J.L. Schonfelder, 2000. *Programming in Fortran 90/95.* Computing Services Department, The University of Liverpool.

Parchure, M.T., A.J. Mehta, 1985. *Erosion of soft cohesive sediment deposits*. Journal of Hydraulic Engineering, October 1985, **111**, 1308-1326.

Partheniades, E. 1965. *Erosion and deposition of cohesive soils.* Journal of the hydraulics division, Proceedings of the ASCE, January 1965, 105-137.

Postma, L. 2001. *Note on the testing of Ecomsed from Gerben.* Internal memo WL | Delft Hydraulics.

Sanford, L. P., J. P.-Y. Maa, 2001. *A unified erosion formulation for fine sediments.* Marine Geology **179**, 9-23.

Shresta, P.L., G.T. Orlob, 1996. *Multiphase Distribution of Cohesive Sediments and heavy metals in Estuarine Systems*. Journal of Environmental Engineering, August 1996 730-740

Velleux, M., 2001. *Lower Fox River / Green bay Remedial Investigation and feasibility Study. Development and application of a PCB Transport Model for the Lower Fox River.* Wisconsin Department of Natural resources report, June 15th 2001 [from: www.dnr.state.wi.us/org/water/wm/lowerfox/rifs/modeldocs]

Voormolen S. 2001. *Suiker in de modder. Diatomeen zijn cruciaal in ecosysteem van rivierdelta's.* NRC handelsblad, katern wetenschap, 2 mrt 2001. (Dutch newspaper article)

Winterwerp, J.C. 1989. *Flow induced erosion of cohesive beds.* Cohesive sediments series report 25, Rijkswaterstaat & WL| Delft Hydraulics

Winterwerp, J.C. 2001. *Project plan, development bed model, Z2845.60.* WL | Delft Hydraulics.

Winterwerp, J.C. & C. Kranenburg, 1997. *Erosion of fluid mud layers. I: Entrainment model.* Journal of Hydraulic Engineering, June 1997, 504-512.

Winterwerp, J.C. & C. Kranenburg, 1997. *Erosion of fluid mud layers. II: Experiments and model validation.* Journal of Hydraulic Engineering, June 1997, 512-519.

Wit, P.J. 1995. Liquefaction of cohesive sediments caused by waves. (PhD thesis) Communications on Hydraulic and Geotechnical Engineering, report 95-2, Delft University of Technology.

WL | Delft Hydrualics, 1999. *Delft3D-WAQ, version 3.01. User Manual.*

Internetsites:

http://www.wldelft.nl/soft/d3d/index.html

http://woodshole.er.usgs.gov/project-pages/sediment-transport/

http://www.hydroqual.com/Hydro/ecomsed/index.htm

List of symbols

Latin symbols

Symbol	*Units*	*Description*
a_0	~	empirical erosion coefficient in ECOMSED
$c`_a$	Pa	cohesion parameter
c	Pa	cohesion
c_v	m^2/s	consolidation coefficient
C_c	-	compressibility index
C_s	-	swell index
D	-	fractal dimension
D	m/s	deposition
d_{50}	m	median diameter of aggregate
delt	s	WAQ time step
deltC	s	consolidation time step
deltcmin	s	maximum consolidation time step
deltcmax	s	minimum consolidation time step
deltE	s	erosion iteration time step
e	-	void ratio
E	m/s	erosion rate
f	-	ratio between stiffness at virgin loading and at reloading
f_k	-	amplitude of Fourier component
g	m/s^2	gravity acceleration
h	m	water depth
h	m	height of bed
$H(x)$	-	Heaviside step function: (0 if $x<0$, 1 if $x>0$)
k	m/s	permeability
k	-	Fourier number
K_k	m/s	empirical parameter in permeability relationship
K_σ	Pa	empirical parameter in effective stress relationship
$K_{\sigma,0}$	Pa	excess effective stress: overconsolidation
K_0	°	coefficient of lateral stress
m_v	m^2/N	compressibility of granular skeleton
M	$kg/m^2/s$	empirical erosion rate coefficient
$n=2/(3-D)$	-	exponent in fractal constitutive relations Merckelbach [2000]
nok	#	number of Fourier components
non	#	number of sampling points
OCR	-	ratio of maximum past consolidation stress and current stress
p	Pa	pore water pressure
p_e	Pa	excess pore water pressure
p_0	Pa	initial excess pore water pressure
P	-	probability of deposition
ressum	m	erosion cache
sedsum	m	sedimentation cache
t	s	time
t_m	s	material time
T	s	time scale of parameterised consolidation model
T_ε	s	time scale for depletion of resuspension potential in ECOMSED

u	m/s	water velocity
v_s	m/s	settling velocity
v	Pa	empirical time dependent 'cohesion'
w	Pa/Pa	empirical tangent of angle of internal friction
w_e	%	entrainment velocity
z	m	Eulerian coordinate
Z	~	empirical age coefficient in ECOMSED

Greek symbols

Symbol	*Units*	*Description*
δ	m	layer thickness
ε	kg/m^2	resuspension potential in ECOMSED
$\Delta=(\rho_s-\rho_s)/\rho_w$	-	relative density of sediment material
ζ	m	material coordinate
ζ_i	m	material coordinate of layer height
ν	m^2/s	(eddy) viscosity of water
ξ	m/m	dimensionless material coordinate
ξ_i	m/m	dimensionless layer height in material coordinate
ρ_w	kg/m^3	water density
ρ_s	kg/m^3	sediment material density
ρ_d	kg/m^3	dry density
ρ_b	kg/m^3	bulk density
$\sigma`_v$	Pa	effective stress
$\sigma`_{v,max}$	Pa	maximum past consolidation effective stress
σ_v	Pa	total stress
τ	s/s	dimensionless material time
τ_b	Pa	bed shear stress
τ_c	Pa	critical bed shear stress for erosion
τ_d	Pa	critical bed shear stress for deposition
τ_y	Pa	yield shear stress
τ_c	Pa	principal yield shear stress
φ'	deg	angle of internal friction
ϕ	m^3/m^3	volume fraction of mud
ϕ_{max}	m^3/m^3	maximum past consolidation volume fraction of mud

Acknowledgements

This thesis has been written at the WL | Delft Hydraulics offices, where I enjoyed the help of many wonderful colleagues. Jan van Beek and Leo Postma helped me very well to implement the 1-DV water bed model into the Delft3D-WAQ code. I'm also very grateful to Walther van Kesteren for enthusiastically debating with me about the physics of erosion and consolidation. And to John Cornelisse for digging into his huge digital archive of all experimental tests done at Delft Hydraulics in the past. Without the rotating annular measurements, dating back to 1990, my thesis could not have been written. I also had a great time with Lucas Merckelbach who helped me enthusiastically to learn everything about consolidation. Moreover, he also provided me with my own settling column to get a feeling for real mud, besides the digital mud I have been working on. Last but not least I would like to thank Han Winterwerp for all the knowledge and literature he provided me with and for keeping me on the main track. He also encouraged me to spend some more time on the 1-DV water bed model when it didn't work according to plan, resulting in the working and promising model present now. And last but not least I want to say I had a good time with all the other graduation students at WL | Delft Hydraulics, with whom I spent most of the time.

I would also like to thank Prof. Battjes, Prof. Barends and Julie Pietrzak for their valuable comment on my thesis, as well as for the inspiring lectures I received from them in the past years, larded with many nice experiments, movies and examples from engineering practice.

During my graduation period, I also spent a couple of weeks at the HydroQual offices in New York. I would like to thank WL | Delft Hydraulics for making this visit possible and all the magnificent people at HydroQual for the wonderful time I spent there. I would like to thank Parmeshwar Shretsa in particular for his encouraging spirit and his useful advice and Sean O'neil for our nice discussions.

I need not to say that I'm also very grateful to Gerda, Ytzen Bram, Caroline, Wouter, and other friends for supporting me.

Delft3D (http://www.wldelft.nl/soft/d3d/index.html) is a 2D/3D integrated modelling environment created by WL | Delft Hydraulics for: Hydrodynamics (FLOW), Waves (WAVE), Sediment transport (SED), Morphology (MOR), Water quality (WAQ) and Ecology (ECO). The FLOW module of Delft3D is a multi-dimensional (2D or 3D) hydrodynamic and transport simulation program which calculates non-steady flow and transport phenomena resulting from tidal and meteorological forcing on a curvilinear, boundary fitted grid. It calculates the watermotion in every gridpoint of the model, using the bathymetry and boundary/initial conditions. The resulting parameters are the velocity $\vec{u}$, the bottom shear stress $\vec{\tau}$, the water level h and the eddy viscosity eddy $\vec{\nu}$. The optional Delft3D-WAVE module calculates the wave heights and their effects on the water motion. The MOR module of Delft3D fully integrates the effects of waves, currents and sediment transport on morphological developments. It is designed to simulate the morphodynamic behaviour of rivers, estuaries and coasts on time-scales of days to years involving complex interactions between waves, currents, sediment transport and bathymetry. The Water Quality module WAQ of Delft3D is a general water quality program capable of describing a very wide range of water quality processes. It can also be used to model various organic and inorganic suspended and bed sediments and the associated substances.

The code of WAQ and large parts of D3D are still written in old Fortran formats: Fortran 90, Fortran 77 and sometimes even Fortran 66. Updating these codes to the most recent standard of Fortran 95 is a tremendous work with little direct revenues. New additions to old programs therefore have the handicap that they need to be written in old standard compatible format to prevent them from being incompatible with and uncompilable on old platforms. Special useful features from the Fortran 95 standard therefore cannot be benefited from at the link between the existing code and the new additions. These features are the run time allocation of arrays, the special array-manipulation functions and the sharing of variables/functions by means of modules. Inside the new additions these special features can be used however. A further requirement is that fixed format Fortran is used, that cannot be mixed freely with the more recent free format Fotran within one file.

In the Delft3D model, computational processor time is more scarce than memory. In order to be economical with memory, properties which remain constant or properties that can be derived from other properties, should rather be calculated once and stored in memory than be calculated every time. The computer code can be optimised by accounting for this.

Annex 2.1

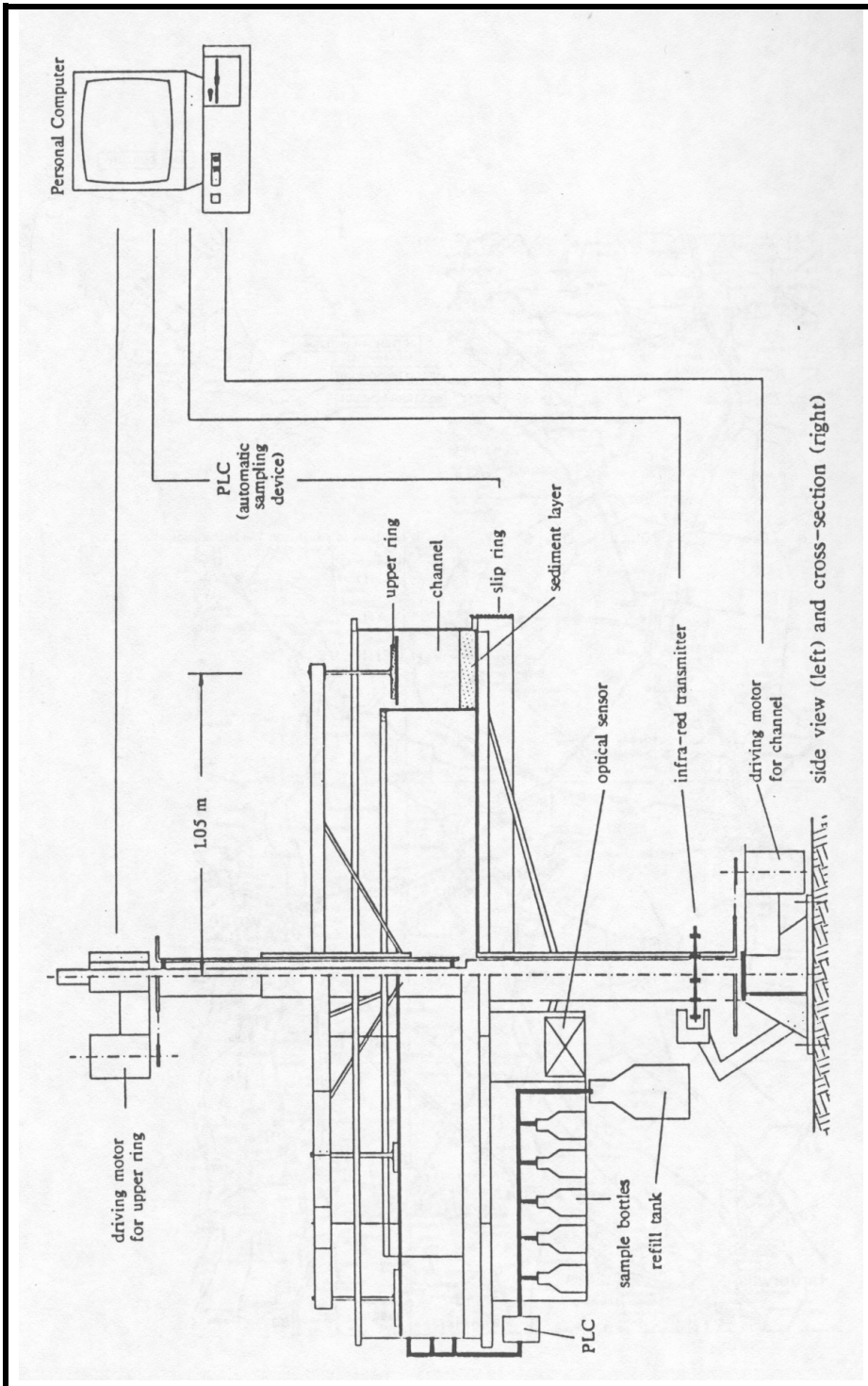

Annular flume [Kuijper, 1990]

Annex 3.1

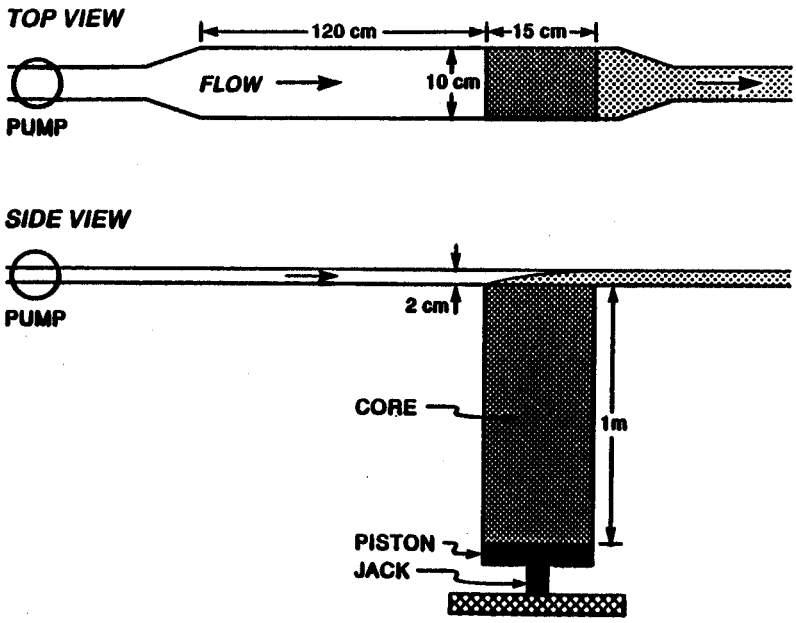

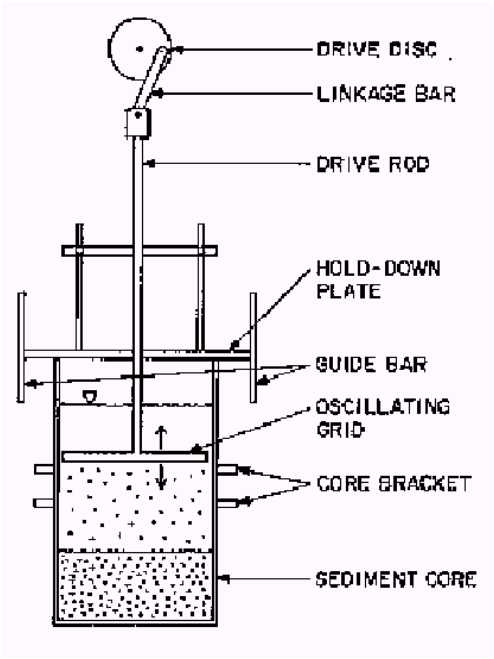

1 Sedflume [Lick, 2001]
2 Shaker [www.limno.com/pubs/Conf_present/DePinto-IAGLR01-erosion.pdf]

Annex 3.2

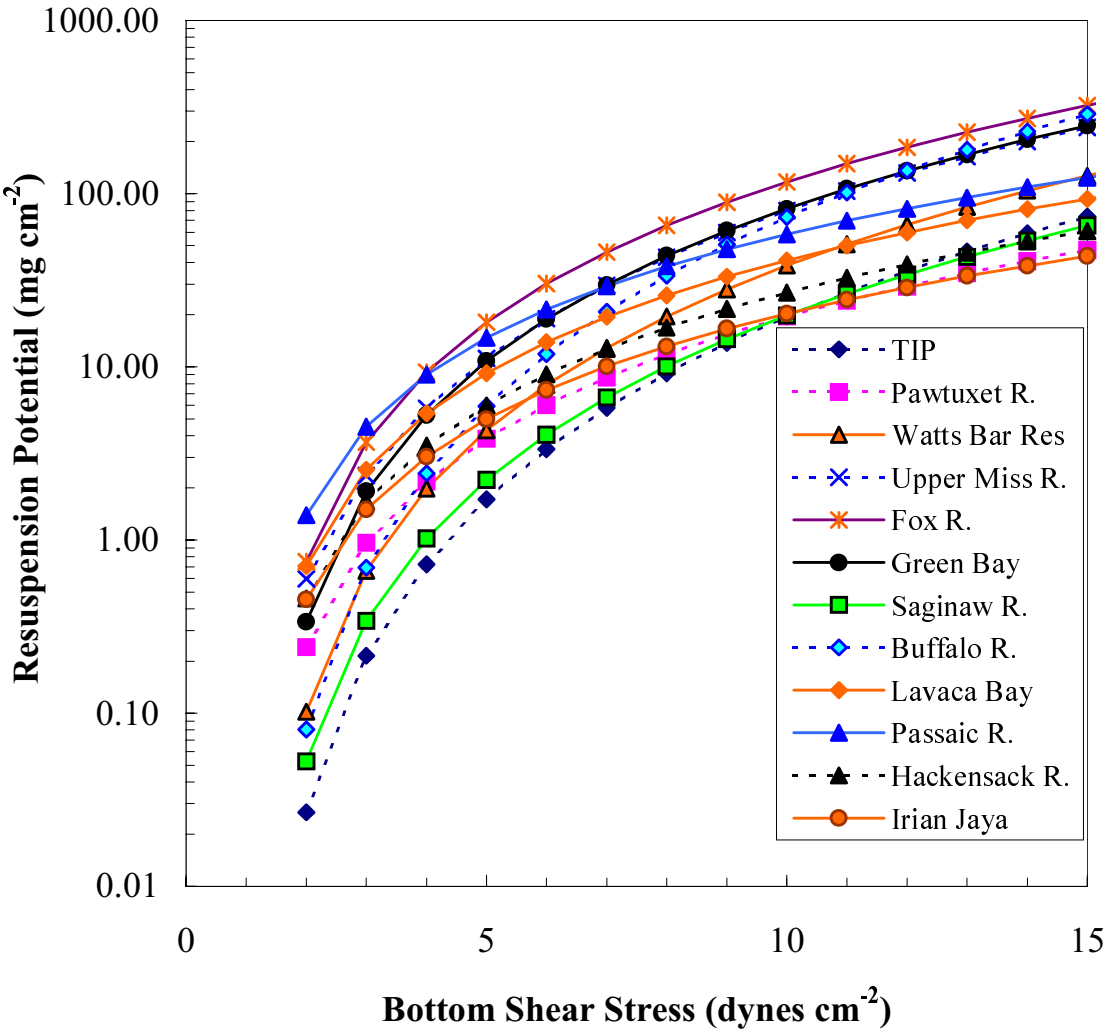

Resuspension Potential for Twelve Different Aquatic Systems determined with Sedflume. [HydroQual, 2001]

Annex 3.3

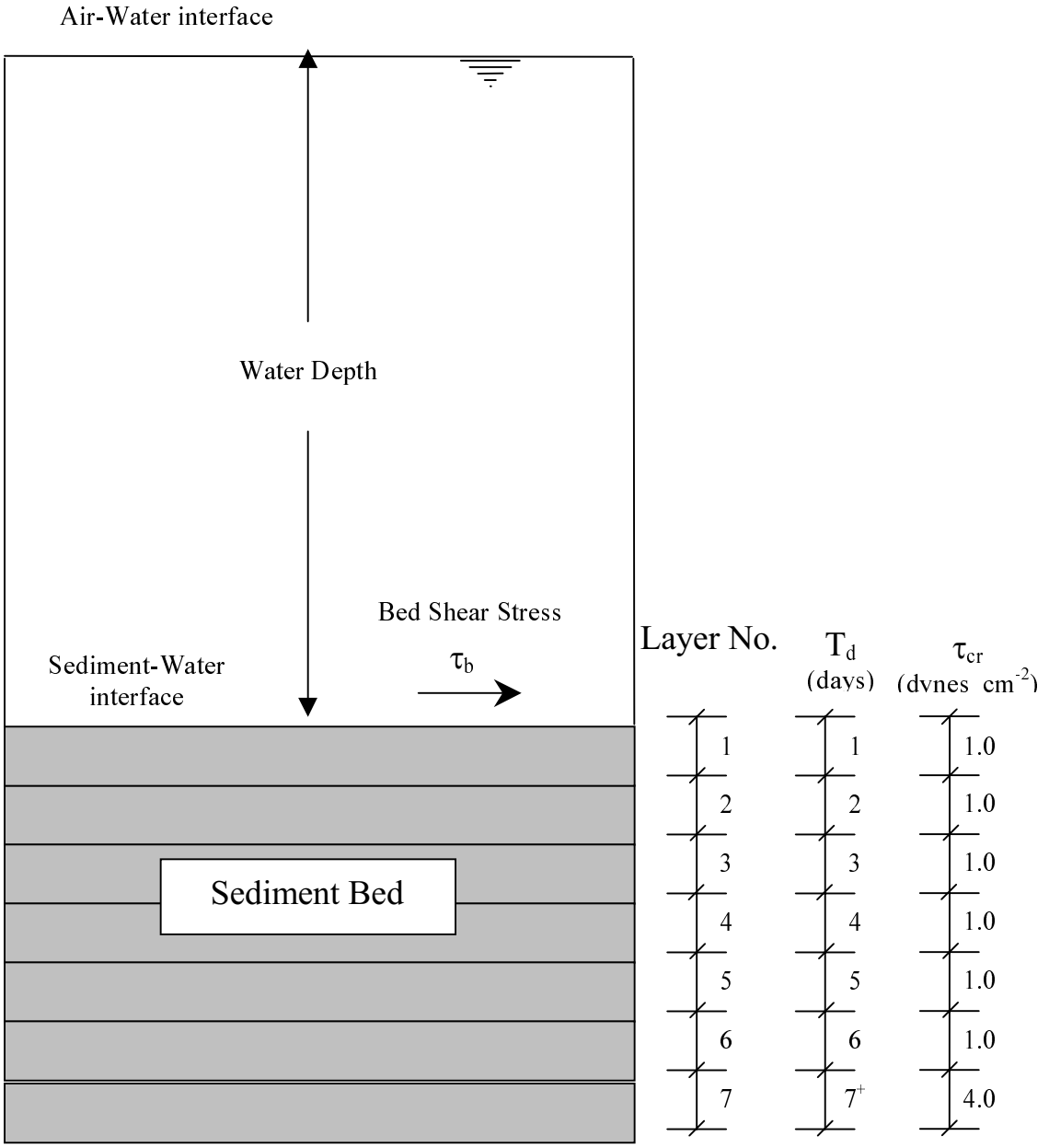

Configuration of ECOM-SED [HydroQual, 2001]

Annex 3.4

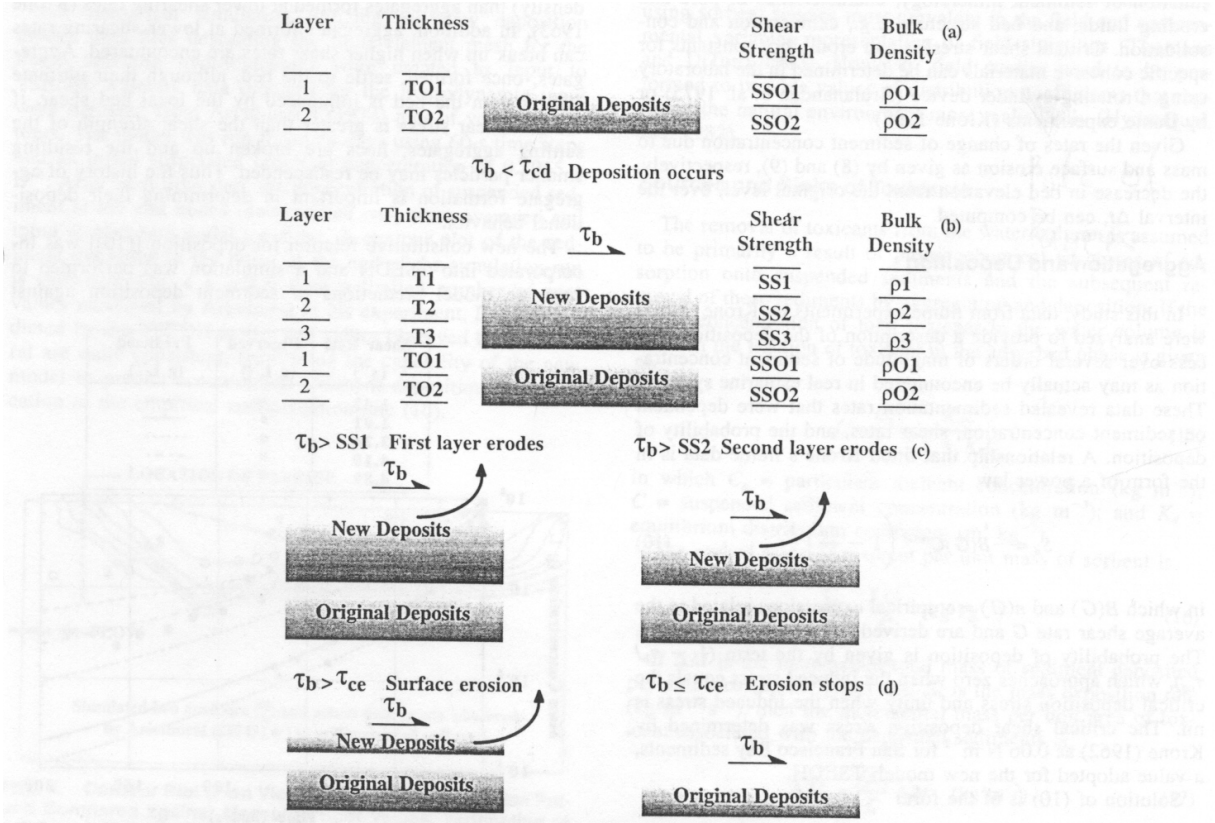

FIG. 2. Schematic View of Mass and Surface Erosion for the Case where Original Deposits Exist: (a) Initial State with Original Bed; (b) Deposition; (c) Mass Erosion; (d) Surface Erosion and Cessation of Erosion

Layer model with a layer for every single deposition event.
[Shresta, 1996]

Annex 3.5

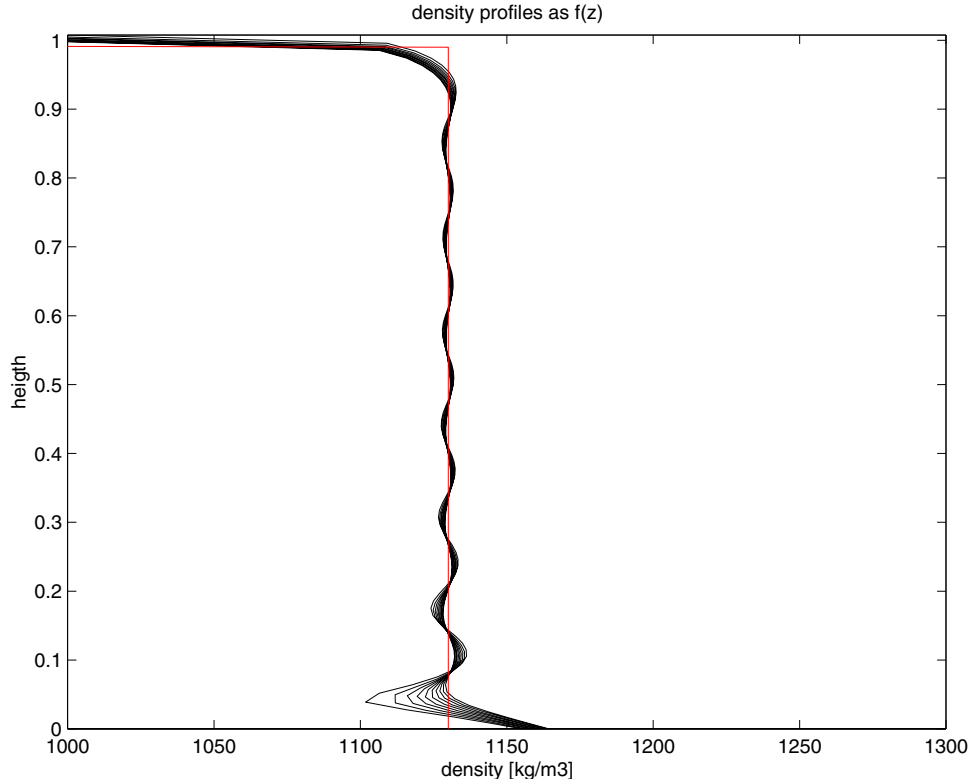

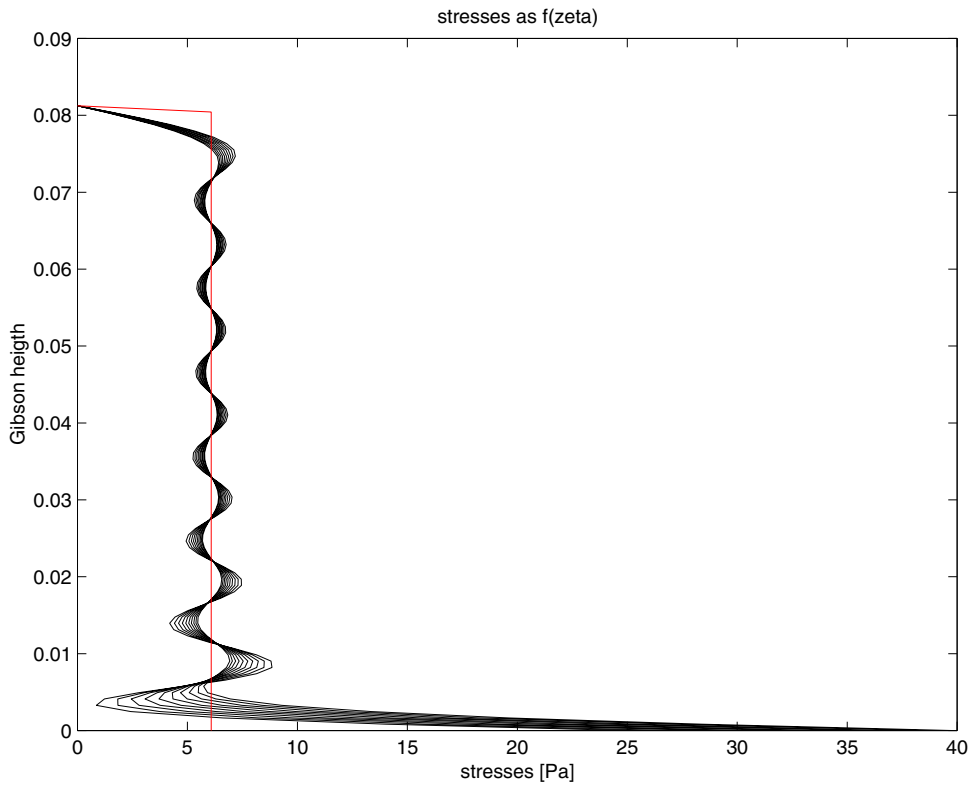

Oscillating behaviour of solution near edges:
Number of Fourier components: 15
Number of sampling points: 100
Timestep: 30 minutes

Annex 5.1

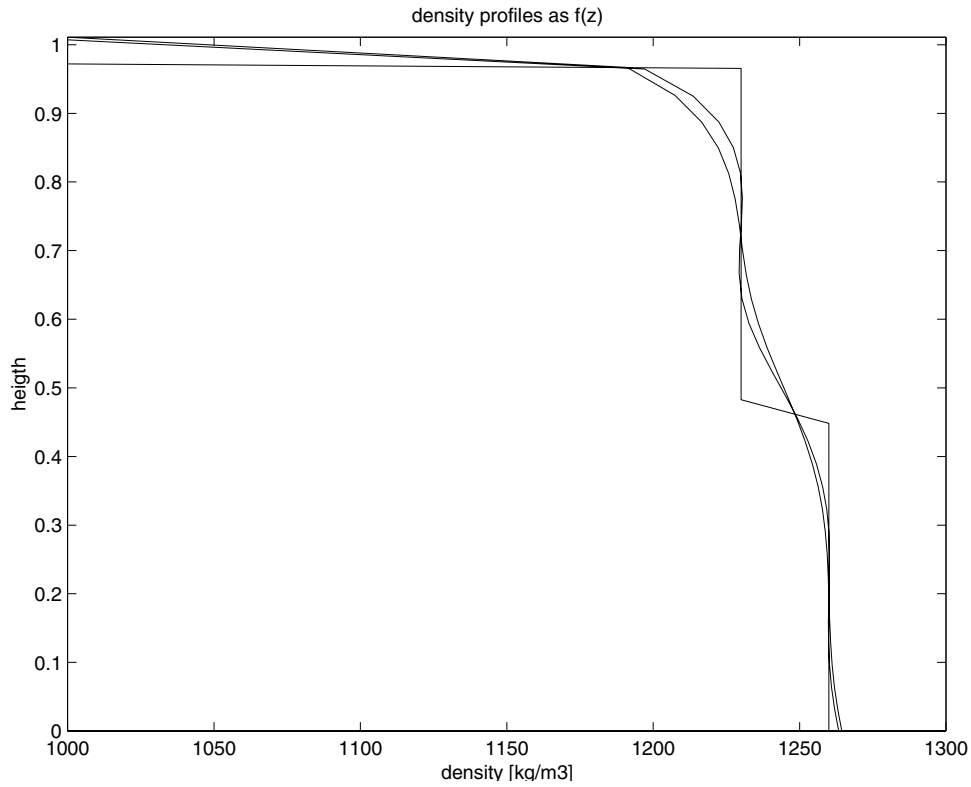

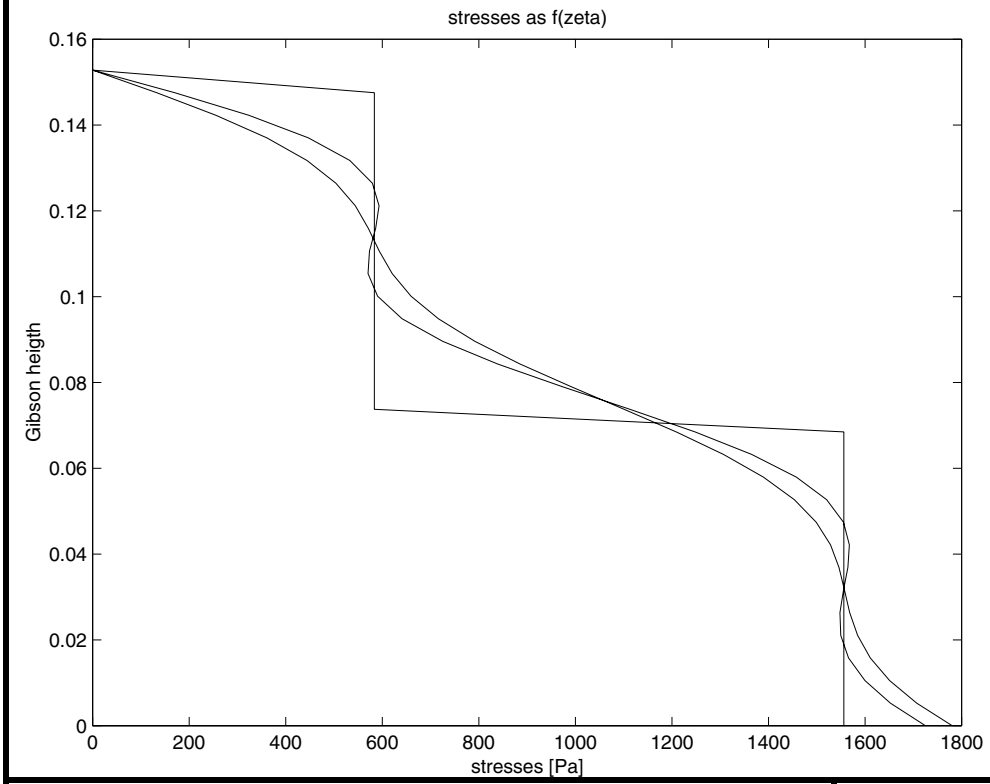

Heavy test profile on the verge of oscillation:
Number of Fourier components: 5
Number of sampling points: 30
Timestep: 100 hours
Simulation time: 200 hours

Annex 5.2

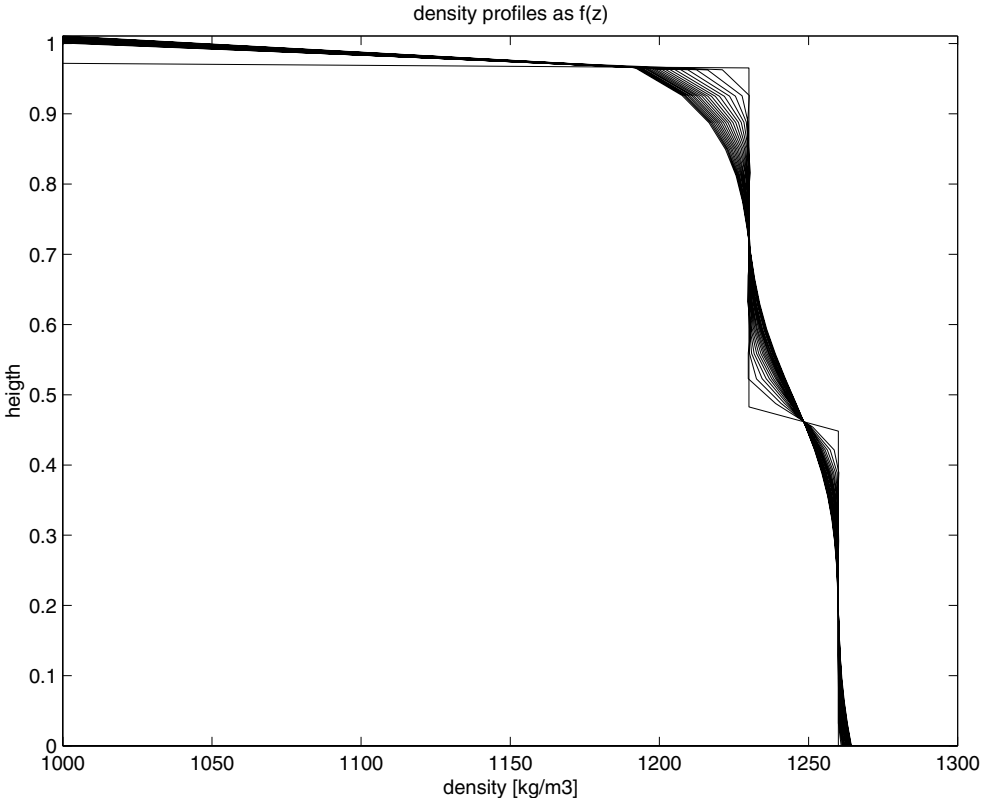

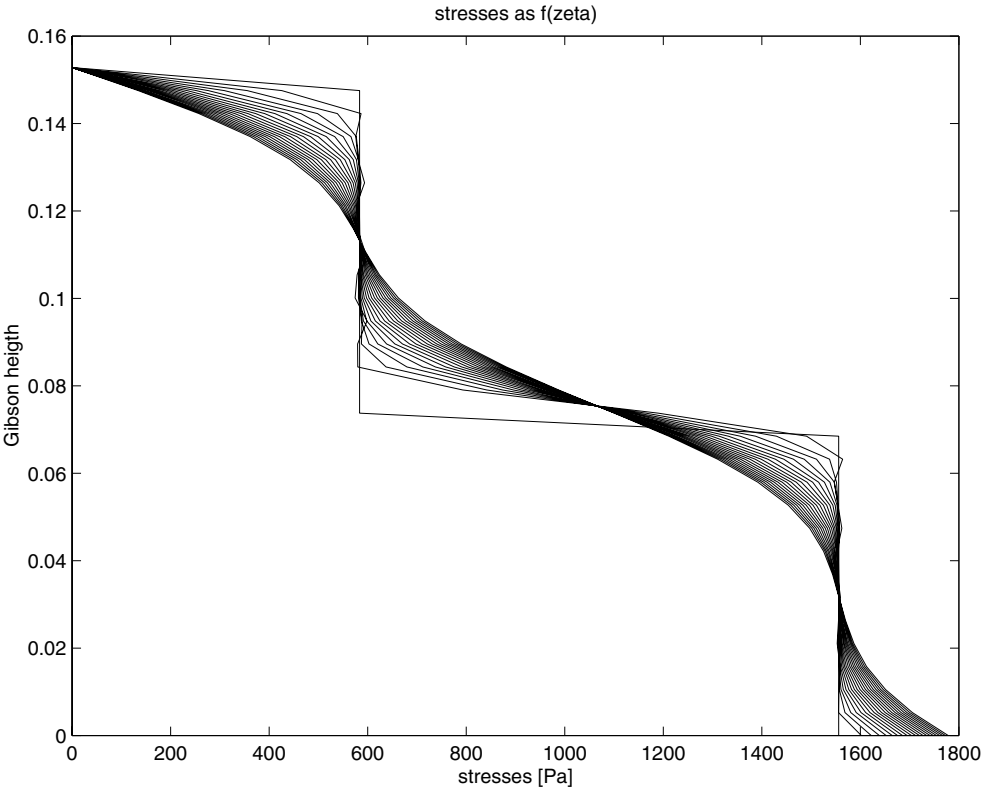

Heavy test profile on the verge of oscillation:
Number of Fourier components: 17
Number of sampling points: 30
Timestep: 10 hours
Simulation time: 200 hours

Annex 5.3

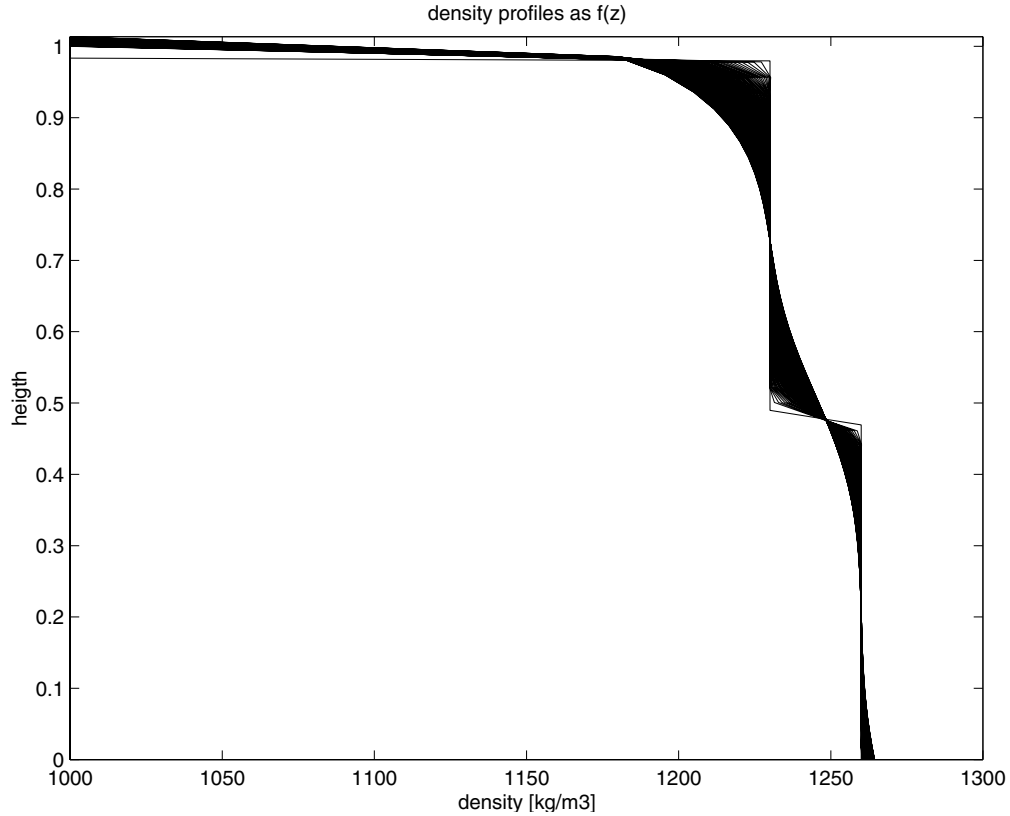

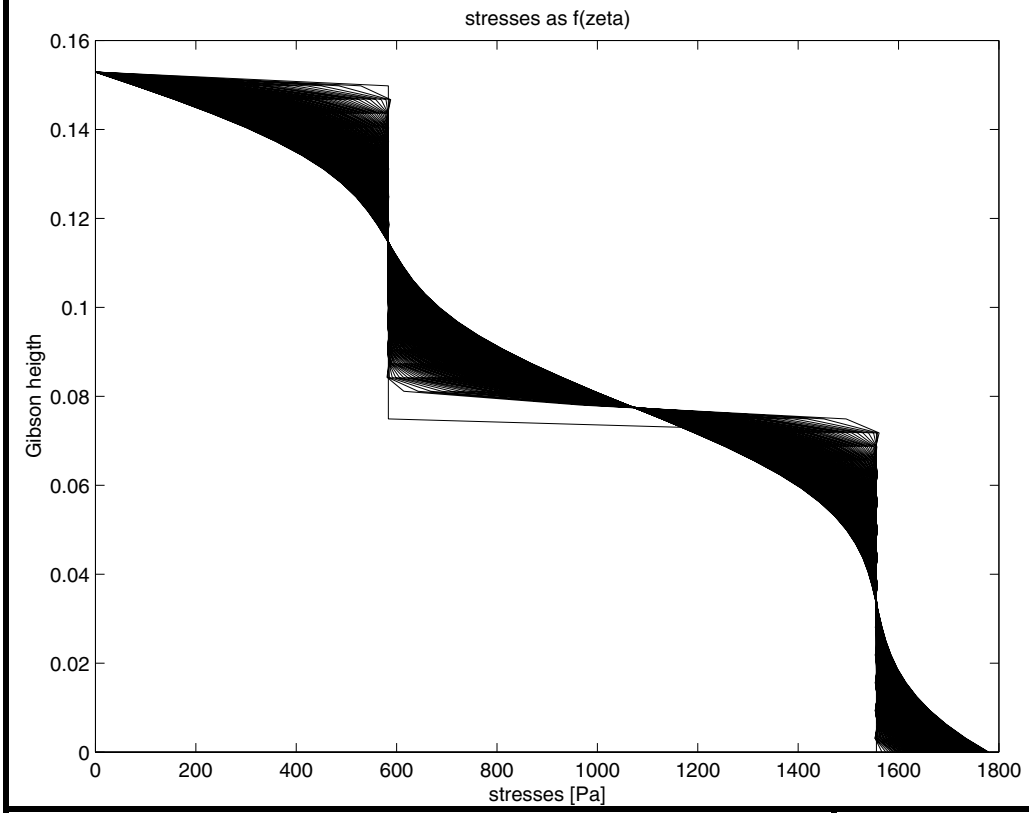

Heavy test profile on the verge of oscillation:
Number of Fourier components: 50
Number of sampling points: 50
Timestep: 1 hours
Simulation time: 200 hours

Annex 5.4

Mineral	% by weight	ρ sed [kg/m^3]	CEC	sp.area [m^2/g]
smectite	≈10			
chlorite	20	2600-2900		
illite	15	2600-2860		
kaolinite	< 5	2610-2640	40	80
quartz	30	2650	3-8	13-26
feldspar	15			
Calcite	5	2720		

Table A7.1 Mineralogical composition and properties

% <	particle diameter [μm]	Settling velocity [mm/s]
10	6	0.03
50	18	0.28
90	68	4.03

Table A7.2 Malvern measurements

Eq.part diameter	Settling velocity	% < by weight	Eq.part diameter	Settling velocity	% < by weight
2 [μm]	0.003 [mm/s]	28	16 [μm]	0.22 [mm/s]	67
4 [μm]	0.01 [mm/s]	39	30 [μm]	0.78 [mm/s]	87
6 [μm]	0.03 [mm/s]	46	38 [μm]	1.26 [mm/s]	90
8 [μm]	0.06 [mm/s]	52	53 [μm]	2.45 [mm/s]	92
10 [μm]	0.09 [mm/s]	55	63 [μm]	3.46 [mm/s]	93

Table A7.3 Sedigraph measurements

Sediment properties	**Annex 6.1**

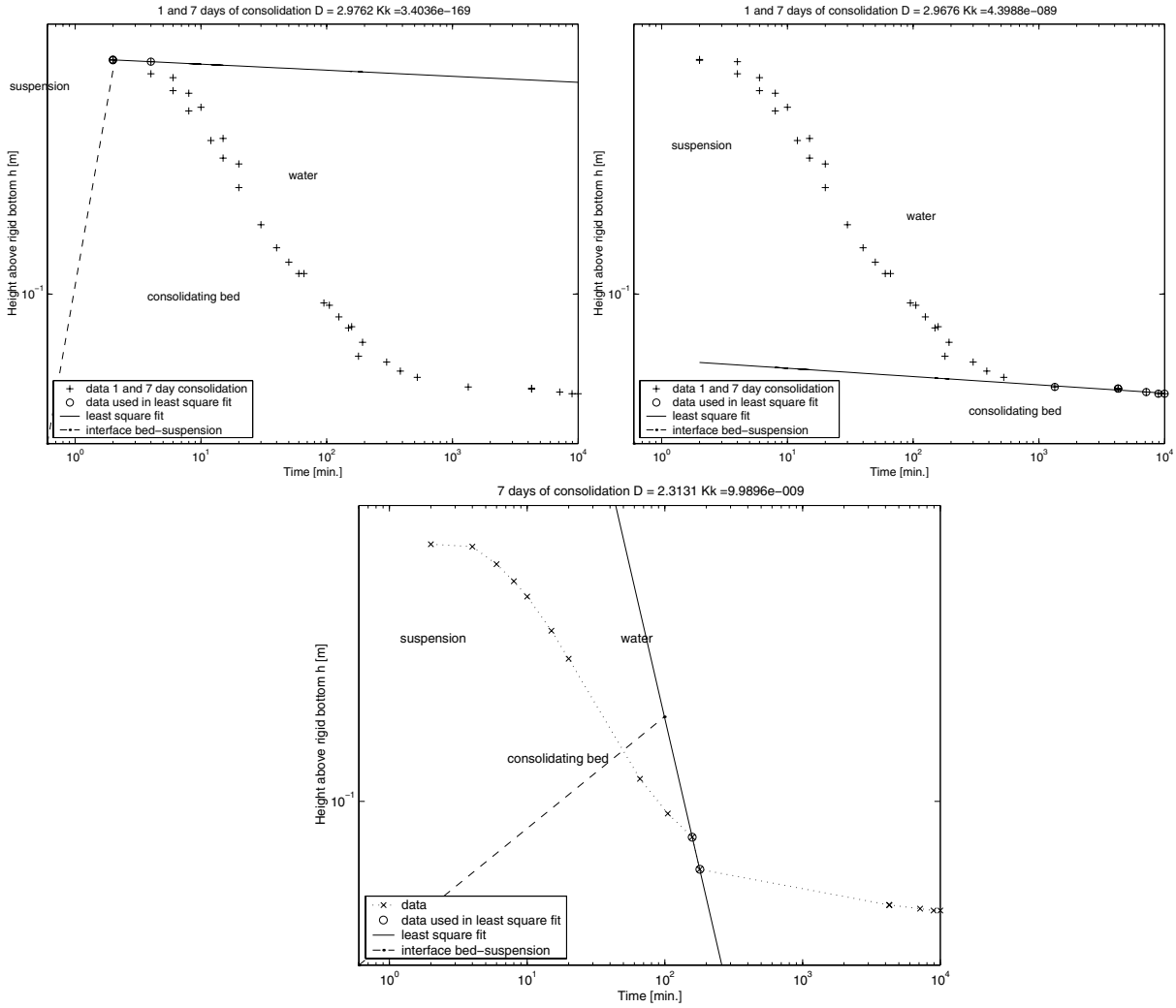

Some automatically generated least square fits lead to very odd lines. The upper two examples above show the strange lines that result from neglecting too many data points from one side of the data set. Note the extremely low values of the permeability parameter.

The third example shows the strange lines that result from neglecting too many data points. The errors in the individual data points tend to have too large an influence in the slope of the line. Note the extremely low values of the fractal dimension in the upper figure. These odd fits are filtered out by hand.

Annex 6.2

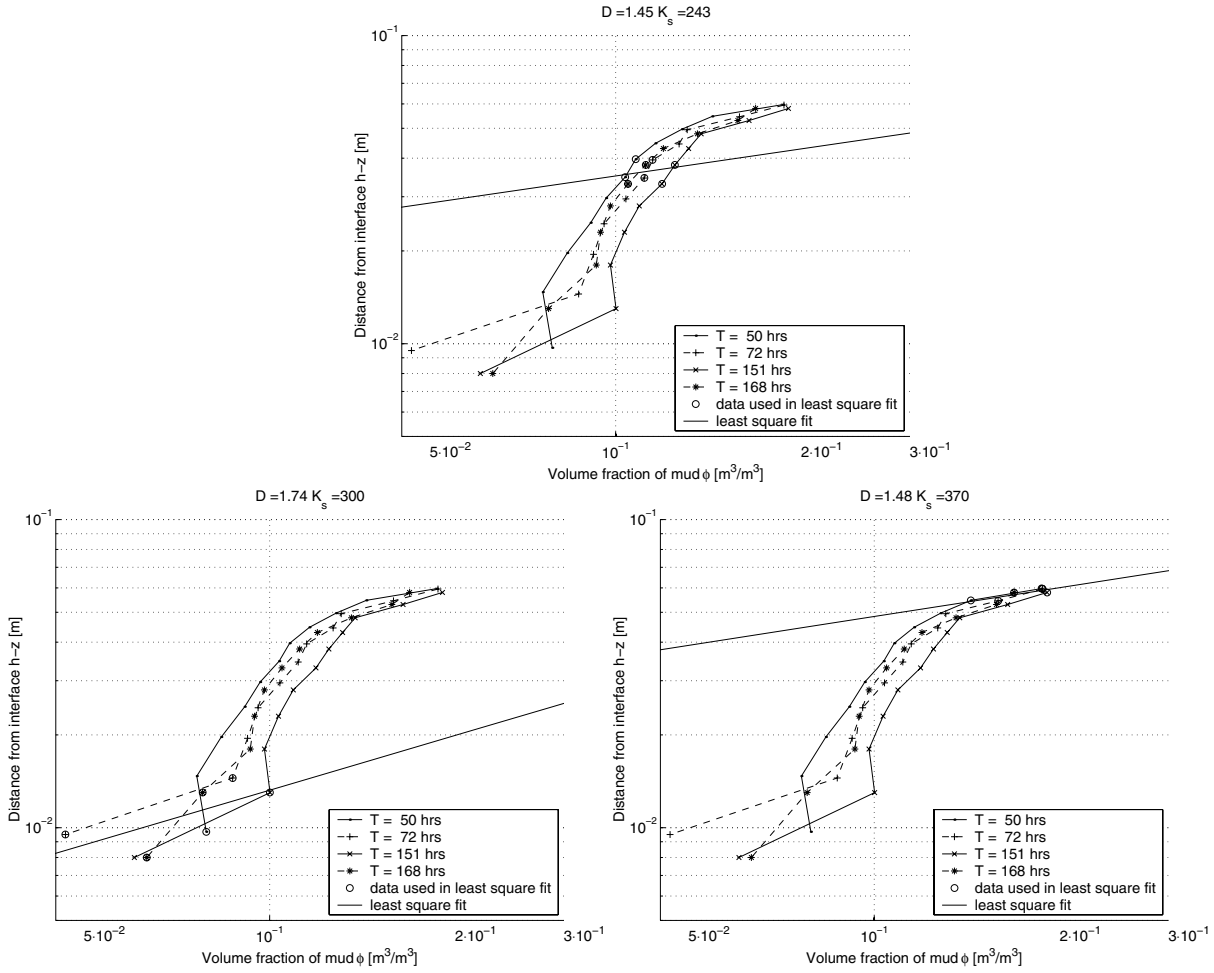

Some automatically generated least square fits lead to very odd lines. The upper examples show the strange lines that result from neglecting too many data points. The errors in the individual data points tend to have too large an influence in the slope of the line. Note the extremely low value of the effective stress parameter and the impossible fractal dimension. This odd fit is filtered out by hand.

The lower examples show the lines that result from neglecting many data points from one side of the data set. Note the very low values of the effective stress parameter. These fits however, where the largest number of data points from one side was neglected, were not considered too odd to filter them out by hand.

Annex 6.3

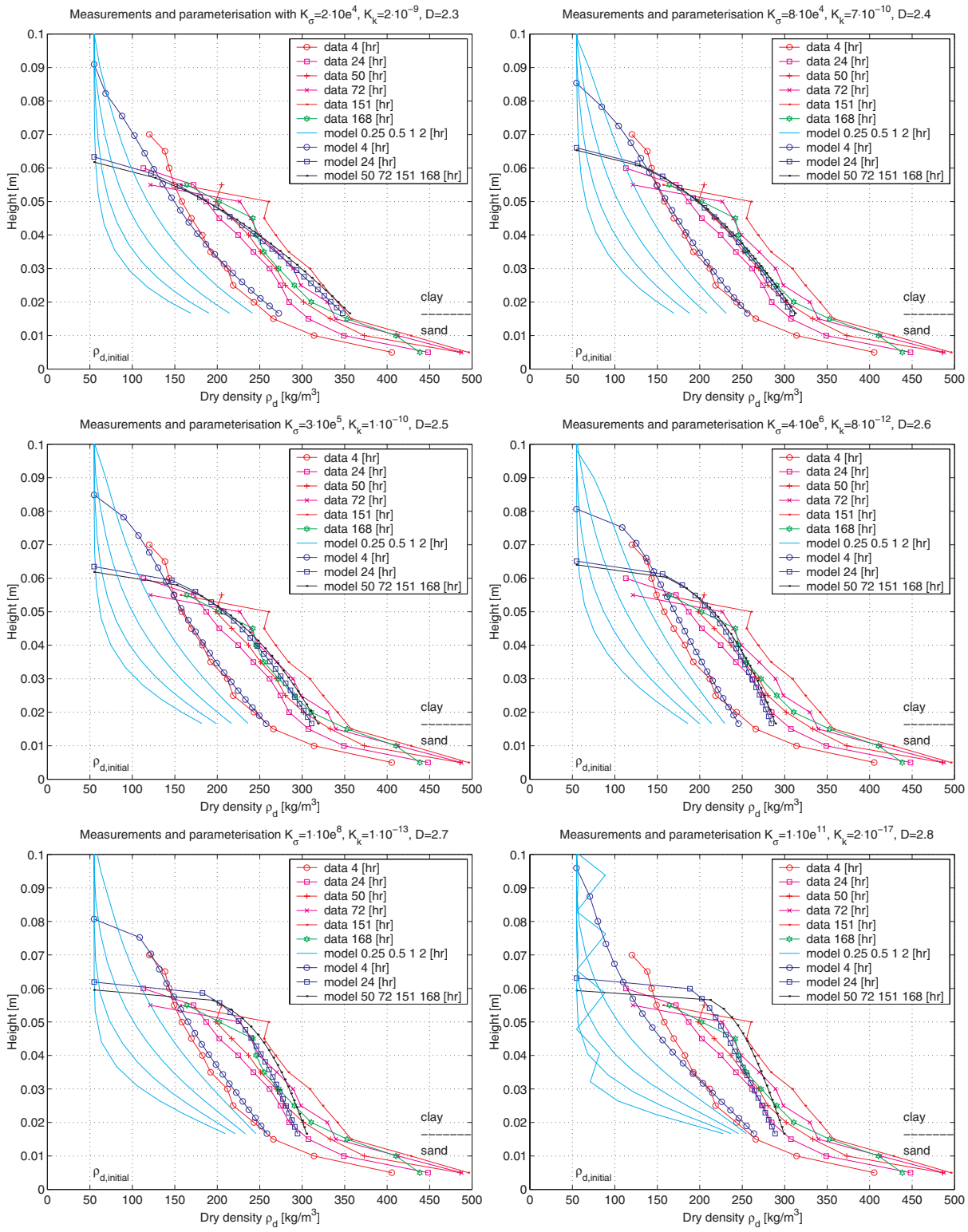

Comparison data of density profiles with parameterisation model to find the parameters of the sediment (simulations 6,5 / 4,3 / 2,1 in table 5.6). Shape mainly determined by K_σ. The profiles become steeper with increasing D and K_σ. (The oscillations for T = 0.25 hr with D = 2.8 are due to the use of a too small number of Fourier components.)

Annex 6.4

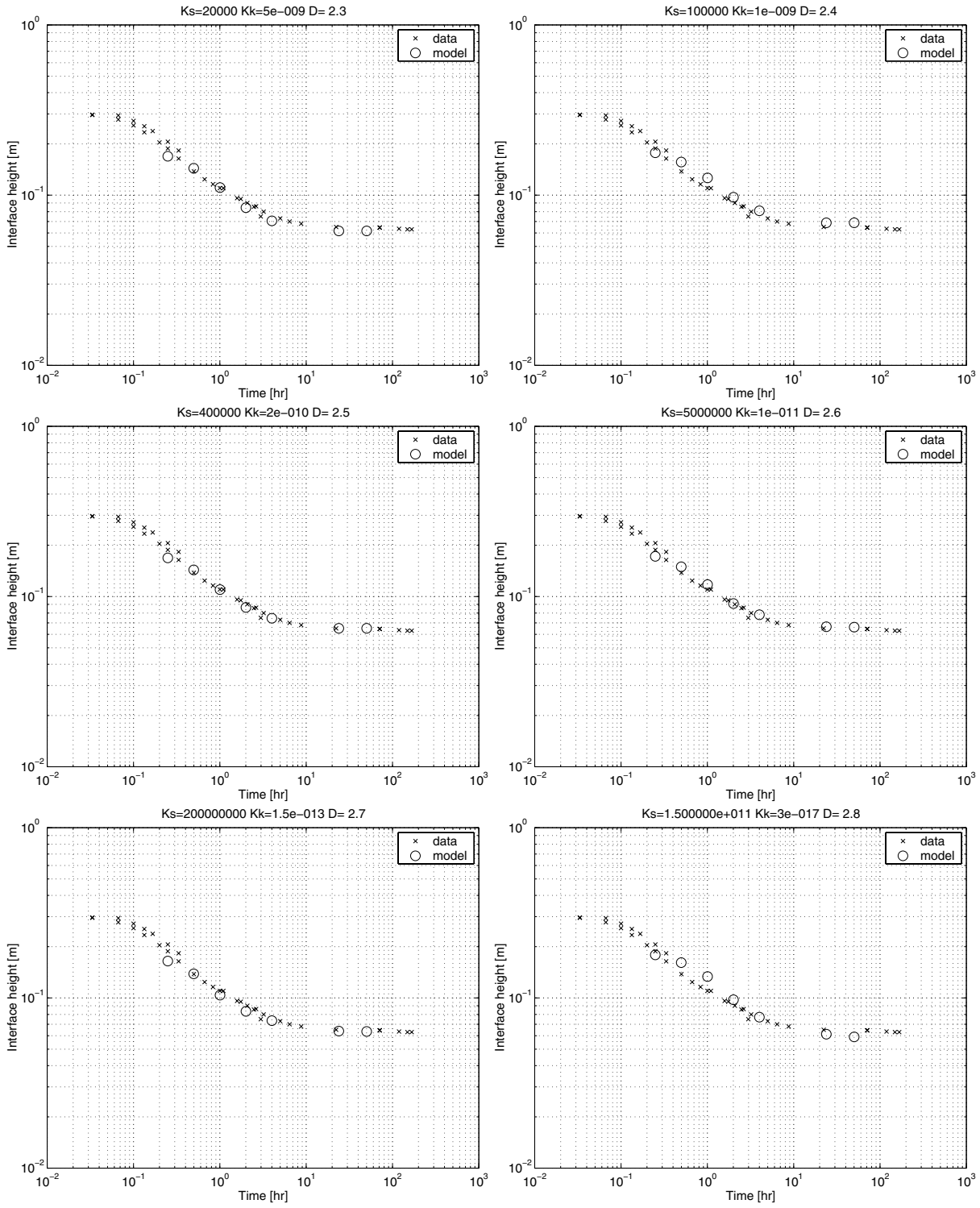

Comparison data of interface height with parameterisation model to find the parameters of the sediment (simulations 12,11 / 10,9 / 8,7 in table 5.7). Final height mainly determined by K_σ and slope and curvature mainly by K_k.

Annex 6.5

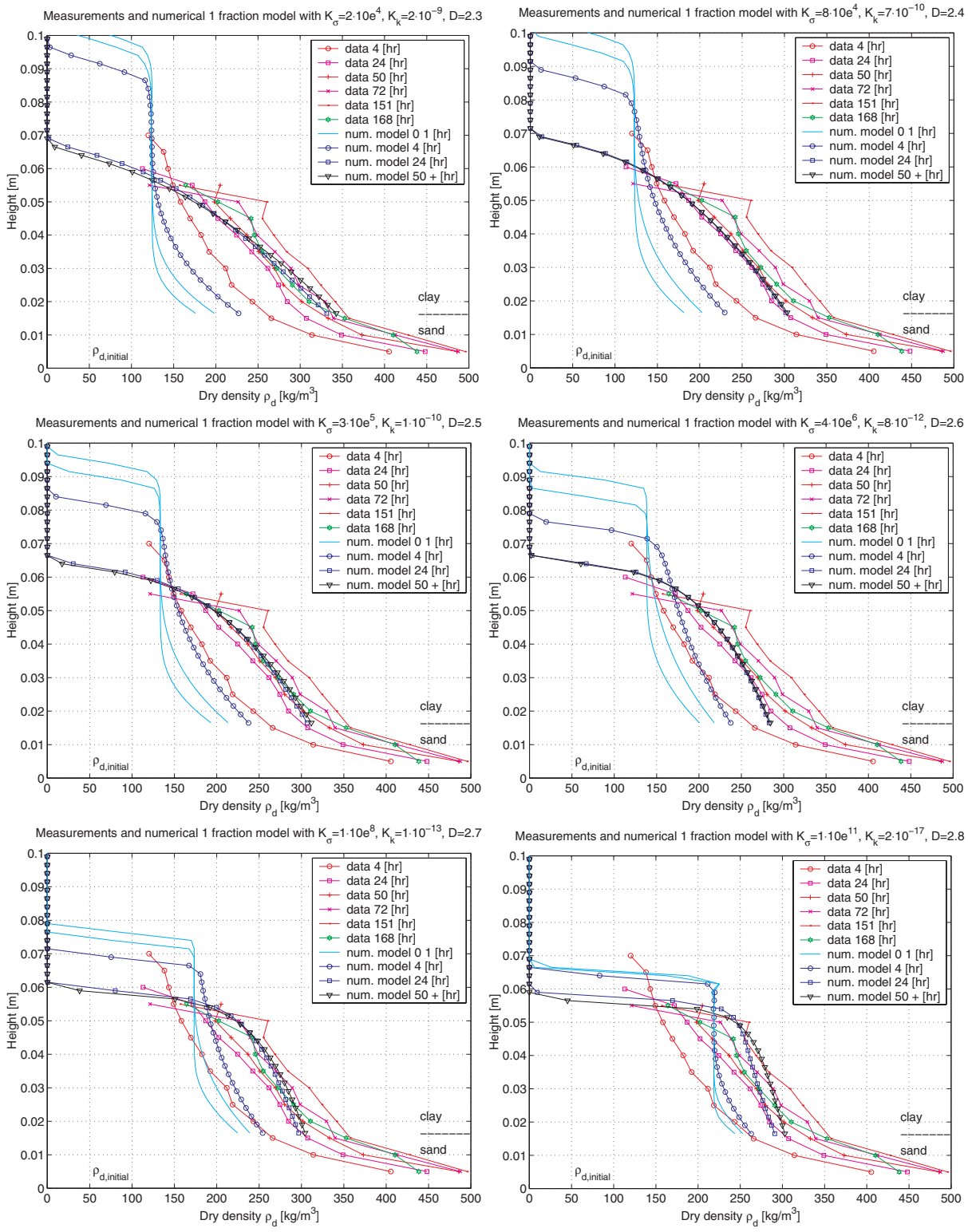

Comparison data of interface height with numerical model with one fraction. (simulations 6,5 / 4,3 / 2,1 in table 5.6)

Annex 6.6

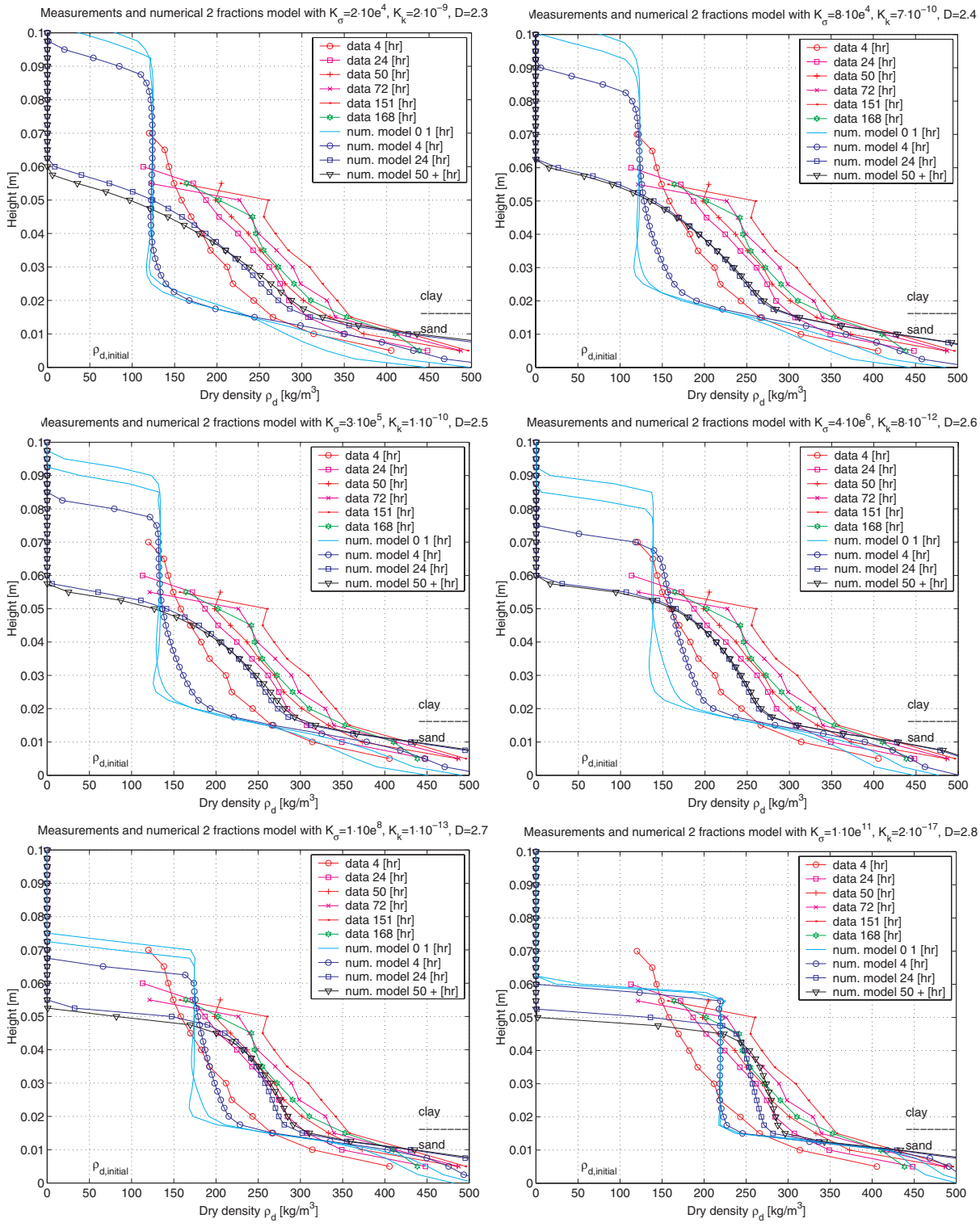

Comparison data of interface height with numerical model with two fractions. (simulations 6,5 / 4,3 / 2,1 in table 5.6)

Annex 6.7

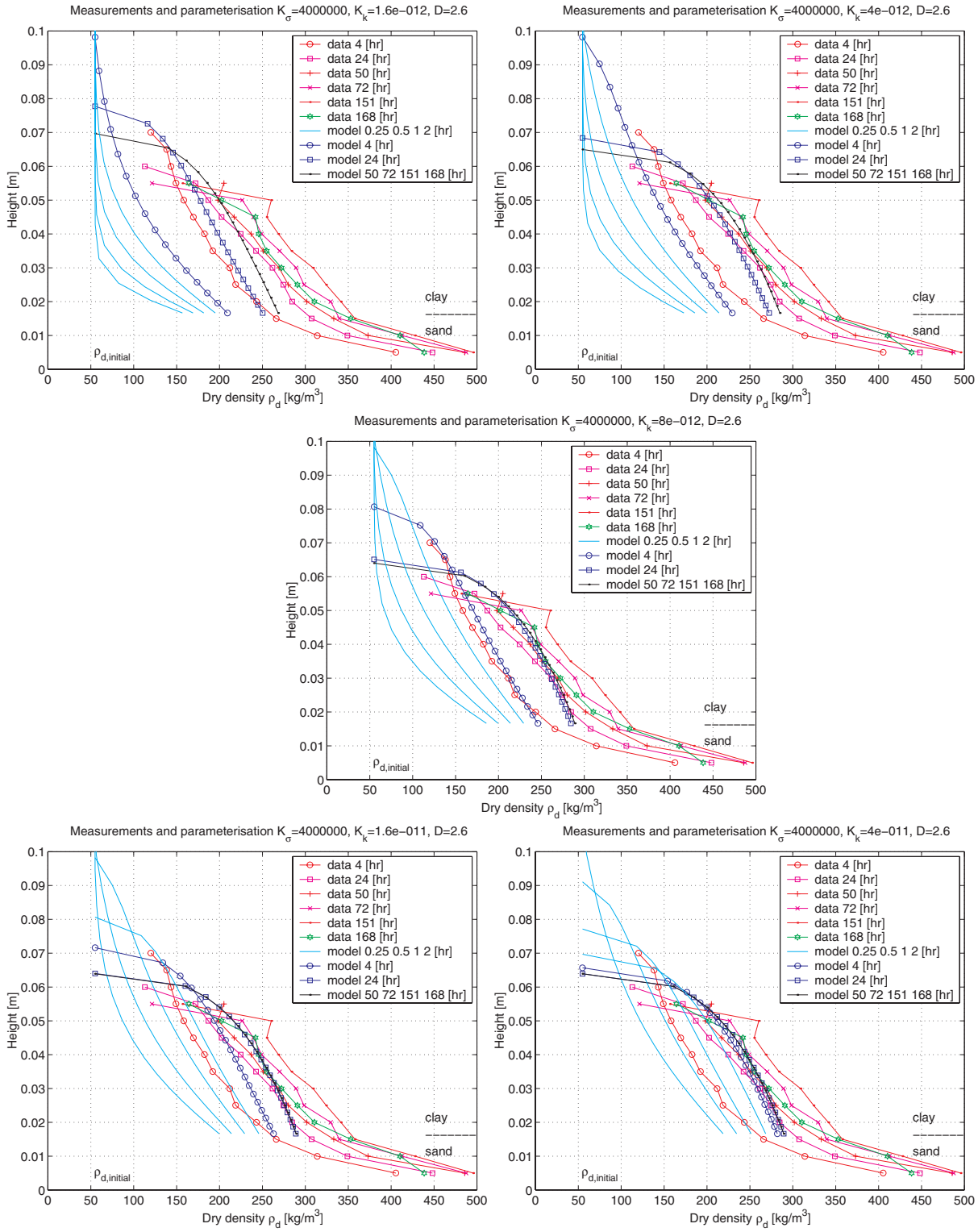

Sensitivity analysis of permeability parameter:
Upper figures: 0.2-0.5 times K_k for best fit
Upper figure: best fit K_k
Lower figures: 2.0-5.0 times K_k for best fit

Annex 6.8

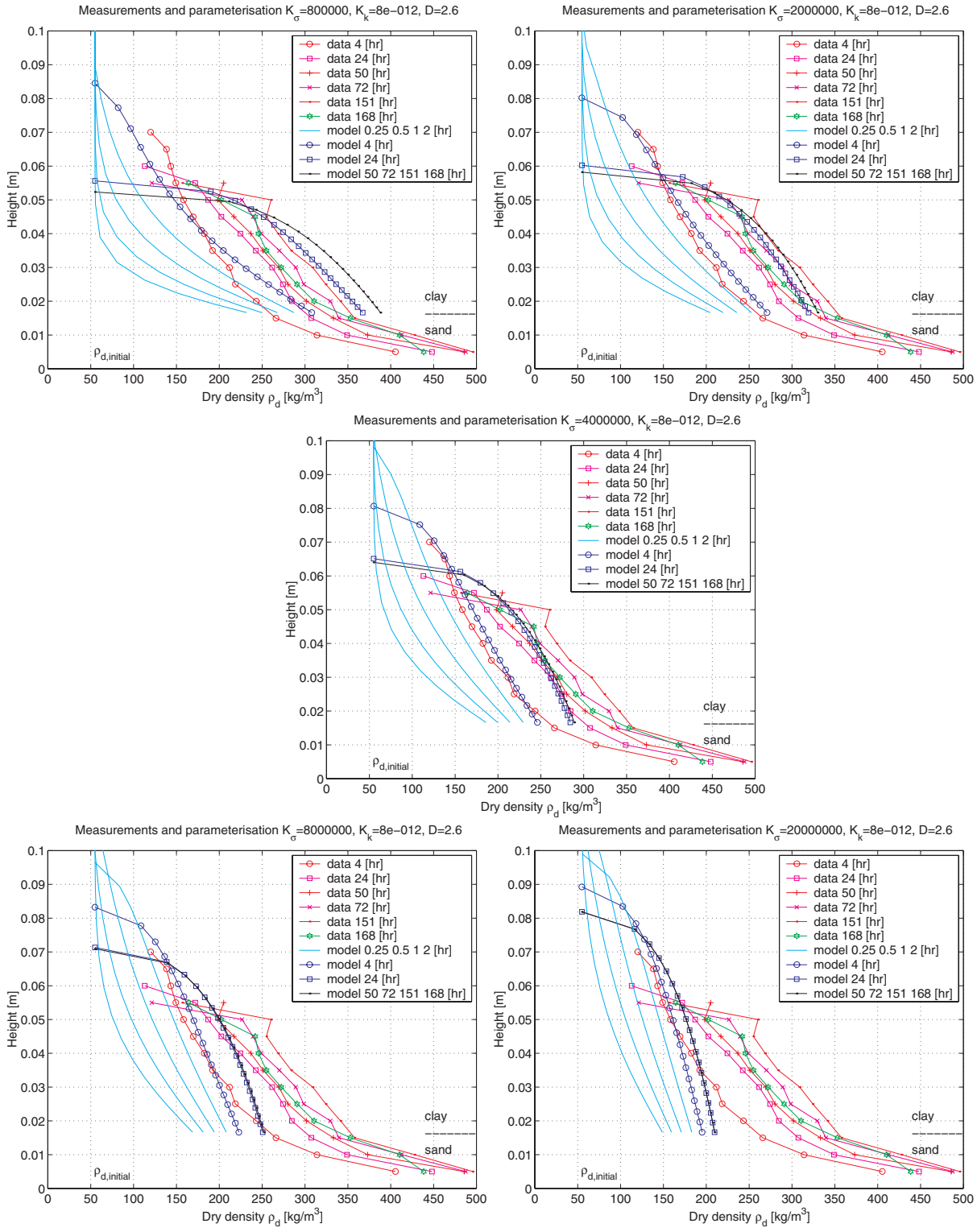

Sensitivity analysis of permeability parameter:
Upper figures: 0.2-0.5 times K_σ for best fit
Upper figure: best fit K_σ
Lower figures: 2.0-5.0 times K_σ for best fit

Annex 6.9

Testing with ECOMSED and WAQ

In order to test the bed model of ECOMSED and Delft3D-WAQ with the annular flume data, the time series of the bed shears stress have to be reproduced. It is not (hardly) possible to take the cohesive bed code out of these programs and generate this time series manually. Hence the full programs have to be used to communicate with the bed part. To create this time series, the corresponding velocity distribution has to be generated. This can be achieved by imposing the appropriate discharges at the boundaries.

A grid with circular boundary conditions, necessary for modelling an annular flume, is not present in these programs and is very hard to realise in any model. Not only the boundary conditions of the water motion would have to be circular, salinity, temperature and cohesive sediment boundary conditions would have to be met as well. Moreover, the only way to force the fluid in a circular grid is to impose an appropriate synoptic wind on top of the grid. Given all these problems, an ordinary long channel will be used. This means that any flow necessary for imposing a shear stress on the bed will result in the abduction of all the eroded sediment. Since the concentration of the sediment in the experimental annular flume does not influence the erosive behaviour of the bed, it can be neglected. Very convenient.

Even in this straight channel it proves to be very hard to reproduce a time series of the bed shear stress. The bed shear stress has to be reproduced merely by giving the right discharges at the boundaries as input. An error of say 10% in the bed shear stress can not be avoided. The bed shear stress for currents only (no waves) in, for example, ECOMSED can be calculated using the Prandtl-Von Karman logarithmic velocity profile:

$$\tau_b = \rho u_*^2 = (ku)^2 \ln^{-1}(z/z_0) \tag{A7.2}$$

where $k \approx 0.4$ is the Von Karman coefficient, u^* is the shear velocity, u is the resultant near bed velocity, z is the depth at the center of the bottommost layer and z_0 is the friction specified as input to the model. The bed shear stress in ECOMSED is calculated by using the velocity in the lowest of the 10 layers: $z = h/20$ where h is the total depth. However, in order to relate the bed shear stress to the discharge, which is imposed at the boundary condition, one has to know the relation between the average velocity in the vertical and the bed shear stress. The definition of the average velocity

$$\bar{u} = \int_{z=0}^{z=h} \frac{u}{h} dz \tag{A7.3}$$

combined with the velocity profile

$$u = \ln\left[\frac{z}{z_0}\right]\sqrt{\frac{\tau_b}{\rho}}\frac{1}{k} \tag{A7.4}$$

leads to

$$\bar{u} = \left(\ln\left[\frac{h}{z_0}\right] - 1\right)\sqrt{\frac{\tau_b}{\rho}}\frac{1}{k} \tag{A7.5}$$

	Annex 7.1

In the figure below one can see the results of an ECOMSED run. The discharges at the boundary conditions were stepwise increased in order to get a stepwise increasing bed shear stress. However, the time scale of the experiment, 15 hours, is very short with respect to the phenomena ECOMSED (and Delft3D-WAQ) has been designed for. When the discharge at the boundary condition is instantaneously increased to account for the stepwise-increasing bed shear stress, the model does not reproduce the shear stress accurately. The shear stress and the velocity show severe oscillations. These oscillations, and especially the heavy peaks, influence the erosion potential. In figure below, one can see the smooth sinus oscillations as produced by the water motion and the ones averaged out over 1 hour to deal with the sediment transport. The erosion in this graph does show the right behaviour: it increases more or less linearly until the erosion potential is reached.

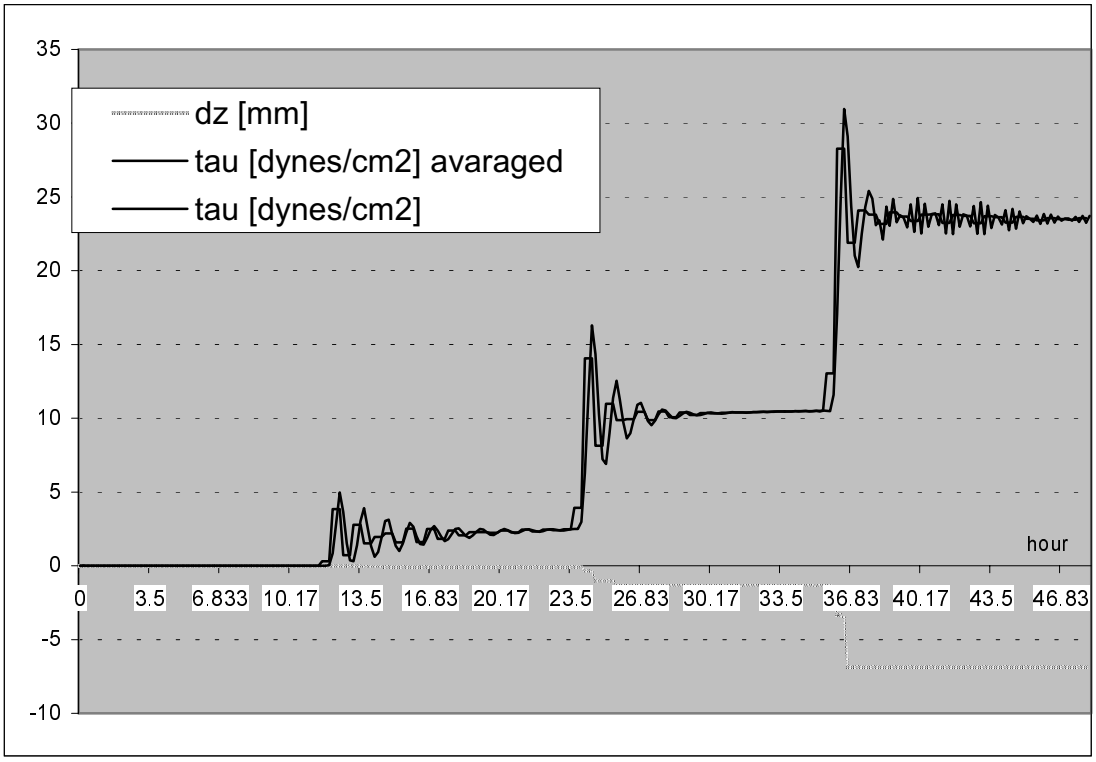

To avoid the effect of these oscillations, the ECOMSED model has been tested with a shear stress that was allowed to increase linearly over a period of one hour. In that approach the oscillations did not occur. But this approach can not be used to reproduce the time series of the experiments. It turns out however that the model gives the same values of the erosion as predicted by erosion potential equations. The equations thus have been implemented correctly, as was to be expected. The testing therefore can be carried out on the equation itself rather than in ECOMSED.

Delft3D-WAQ offers the option to impose the bed shear stresses manually, independent of the flow velocities. This option, together with stagnant water, has been used to test the 1-DV water bed model.

	Annex 7.I